Investigating DHCR24 as a protector against cellular stress: More than just a cholesterol-synthesising enzyme

Robert Kasz

Bachelor of Medical Science (Honours) (UTS)

Submitted in fulfilment of the requirements for the degree of Doctor of Philosophy at the University of Technology, Sydney

Supervisor: Dr. Kristine C. Y. McGrath

Co-supervisors: Professor Alison K. Heather and Dr. David van Reyk

Submitted February 2017

Certificate of Original Authorship

This thesis is the result of a research candidature conducted jointly with another University as part of a collaborative Doctoral degree. I certify that the work in this thesis has not previously been submitted for a degree nor has it been submitted as part of requirements for a degree except as part of the collaborative doctoral degree and/or fully acknowledged within the text.

I also certify that the thesis has been written by me. Any help that I have received in my research work and the preparation of the thesis itself has been acknowledged. In addition, I certify that all information sources and literature used are indicated in the thesis.

Robert Kasz

Date:

Acknowledgements

As I have arrived at the final destination of my PhD journey, I have numerous people to thank and acknowledge. With them this experience has not only been possible but enjoyable. I would like to begin by sincerely thanking Professor Alison Heather, who has been with me from the beginning of my research experience. I would like to extend my gratitude to her for the opportunity, for her guidance, mentorship, encouragement, and the lessons that I have learnt from not only her excellent supervision but also from her example. Her knowledge and achievements in and outside of the world of academia are inspiring.

I would like to extend my gratitude to Dr. Kristine McGrath, who contributed a package of laughter, education, support, and encouragement over the last few years. I attribute my laboratory skills to her tutelage and appreciate all of the time she offered me assistance. She created a welcoming work environment through her enthusiasm, patience, and positive attitude. Working under her guidance in the laboratory was motivating and helped me achieve my goals.

Thank you to Dr. David van Reyk, who offered valuable input and assistance with the submission of my thesis. Dr. Mike Johnson and Dr. Lynne Turnbull, for their assistance with my microscopy work, which was paired with great patience as we endured hours of troubleshooting. Dr. Lani Li for her help and advice in the laboratory. Harry Simpson for being a beacon of joy and happiness who made working in the laboratory fun, boosted morale, and importantly made sure the laboratories ran smoothly.

I cannot speak highly enough of the support and encouragement that I have received from my friends and family. Peter Irga and Martin Scott, have been with me since my first days at UTS and throughout my PhD. Their friendship is something I value highly and I am grateful that we shared the experience together.

I am fortunate enough to have also made new friendships and build upon existing ones during my time at UTS and would to thank them. Elliot Cooper has become a fantastic friend who made working in 6.01 the place to be. I thoroughly enjoyed our time together, especially the banter and nonsense that went on in that quiet lab. Thank you to Pamela Ajuyah and Rosaline Habib for the fun experiences. Samuel Brennan and Patrick Connerty – the squad life has been good to me.

Thank you to my close friends outside of university who helped me maintain a work-life balance, namely Eunji and Benjamin Blacklow, and James Tomlinson.

A special thank you to my parents, and sister Joanna, for providing me with kindness, love, support, understanding, encouragement, and for always believing in me. I love you and am forever grateful for everything that you do for me.

I would like to conclude with my gratitude to my beautiful wife, Sophie. She has stood by me throughout this tumultuous experience. She said that she got me before Honours did and now she will have me forever more. Without her, this experience would have been infinitely harder. Thank you. I love you princess.

Abstract

Atherosclerosis and insulin resistance are globally prevalent metabolic diseases, primarily driven by endothelial and hepatic inflammation, respectively. High density lipoprotein (HDL) reduces the inflammation in models of atherosclerosis and insulin sensitivity, and in doing so, improves these conditions. Our laboratory has demonstrated that in human coronary artery endothelial cells (HCAECs), HDL's suppression of the inflammatory response is a gene-regulated process and that 3β-hydroxysteroid-Δ24 reductase (DHCR24) is one of the most upregulated genes by HDL.

DHCR24 is a cholesterol biosynthesis enzyme however, recent work in various cell types shows DHCR24 emerging as a potent multifaceted protein protecting against cellular stress. This study commenced with confirming apolipoprotein I (apoA-I) rHDL increases DHCR24 expression in HCAECs, while revealing for the first time that HDL also increases DHCR24 expression in human hepatoma 7 (HuH7) cells.

This study next questioned whether DHCR24 mimics apoA-I rHDL's suppression of the inflammatory response in these cell types. The data presented provides proof-of-principle that DHCR24 replicates HDL's suppression of tumour necrosis factor-alpha (TNF-α)-induced intracellular cell adhesion molecule 1 (ICAM-1) and vascular cell adhesion molecule 1 (VCAM-1) levels in HCAECs, and interleukin 8 (IL-8) levels in HuH7 cells.

Characterising DHCR24's role was explored to learn more about how DHCR24 suppresses a TNF-α-induced inflammatory response in HCAECs and HuH7 cells. This study showed that DHCR24's oxidoreductase region mediates DHCR24's suppression of a TNF-α-induced inflammatory response in these cell types. This effect occurred without DHCR24 increasing cholesterol levels, despite the oxidoreductase site's integral role in cholesterol biosynthesis. These are exciting results as they indicate that DHCR24 is more than just a cholesterol biosynthesis enzyme in HCAECs and HuH7 cells.

Elucidating the mechanisms by which DHCR24 suppresses a TNF-α-induced inflammatory response in HCAECs and HuH7 cells highlighted a cell type-specific nature of DHCR24's activity, which is in keeping with reports in the literature. In keeping with this cell type-specificity, a TNF-α-induced inflammatory response was suppressed, in part, by a decreased endoplasmic reticulum (ER) stress response in HCAECs. Interestingly, this did not occur in HuH7 cells. The work here suggests that this is attributed to the increased cholesterol content in HuH7 cells

compared to HCAECs. DHCR24's cell type-specific effects are reinforced by the cellular response of DHCR24 levels to TNF-α-activation – in HCAECs, DHCR24 levels were modestly increased; conversely in HuH7 cells, TNF-α-activation markedly decreased DHCR24 levels. Moreover, TNF-α-activation caused DHCR24's translocation from its ER-localisation to the cytoplasm and nucleus, while in HuH7 cells, DHCR24 remained localised peri-nuclearly.

This data provides novel mechanistic insight into DHCR24's multifunctional role in two different cell types, laying the foundation for potential DHCR24-based therapeutics, and provides impetus for further investigation of DHCR24.

TABLE OF CONTENTS

List of Figures

List of Tables

List of Abbreviations

3’	Three prime
5’	Five prime
18S	18*S* ribosomal *RNA*
28S	28S ribosomal RNA
w/v	Weight per volume
Aβ	Amyloid beta
ABCA1	ATP binding cassette transporter A1
ABCG1	ATP binding cassette transporter G1
ABS	Australian bureau of statistics
ABTS	2,2'-Azinobis [3-ethylbenzothiazoline-6-sulfonic acid]-diammonium salt
ACC1	Acetyl-CoA carboxylase 1
ACC2	Acetyl-CoA carboxylase 2
ACTH	Adrenocorticotrophic hormone
AIHS	Australian Institute of Health and Welfare
ANOVA	Analysis of variance
ApoA-I	Apolipoprotein I
ApoE	Apolipoprotein E
$ApoE^{-/-}$	Apolipoprotein E homozygous knockout
ATF-4	Activating transcription factor-4
ATF-4(n)	Active nuclear form of ATF-4
ATF-6	Activating transcription factor-6
ATP	Adenosine triphosphate
ASK1	Apoptosis signal-regulating kinase 1
β2M	Beta-2 Microglobulin
BCA	Bicinchoninic acid assay
bFGF	Basic fibroblast growth factor
BSA	Bovine serum albumin
C-terminal	Carboxyl-terminal
CAM	Cell adhesion molecule
CCL2	Chemokine ligand 2
CCL5	Chemokine ligand 5
CD40L	cluster of differentiation 40L
cDNA	Complementary deoxyribonucleic acid
CETP	cholesteryl ester transfer protein
CHOP	CCAAT enhancer binding protein homologous protein
$Chop^{-/-}$	Chop homozygous knockout
CO_2	Carbon dioxide
CRP	C-reactive protein
COX	Cyclooxygenase
COX1	Cyclooxygenase 1
COX 2	Cyclooxygenase 2
CX_3CR1	CX3C chemokine receptor 1
DAB	3,3’-diaminobenzidine
DAPI	4',6-diamidino-2-phenylindole
DHCR24	3β-hydroxysteroid-Δ24 reductase
DMEM	Dulbecco’s Modified Eagle Medium

DNA	Deoxyribonucleic acid
E.coli	*Escherichia coli*
EDTA	Ethylenediaminetetraacetic acid
EGFP	Enhanced green fluorescent protein
ELISA	Enzyme linked immunosorbent assay
EIF2α	Eukaryotic initiation factor 2 alpha
eNOS	Endothelial NO synthase
ER	Endoplasmic reticulum
ERO1α	ER oxidase 1 alpha
FAD	Flavin adenine dinucleotide
FBS	Fetal bovine serum
FDA	Food and Drug Administration
FFA	Free Fatty Acid
FBG	Fasting blood glucose
FITC	Fluoroscein-Isothiocyanate
FPLC	Fast protein liquid chromatography
GAPDH	Glyceraldehyde-3-phosphate dehydrogenase
GIT	Gastrointestinal tract
GM-CSF	Granulocyte-macrophage colony stimulating factors
GRP78	Glucose-regulated protein 78
H&E	Haematoxylin and eosin
H_2O	Water
H_2O_2	Hydrogen peroxide
HbA1c	Glycated haemoglobin
HBSS	Hank's buffered salts solution
HCAECs	Human coronary artery endothelial cells
HCV	Hepatitis C virus
HDL	High-density lipoprotein
HFD	High fat diet
HO-1	Heme oxygenase-1
HRP	Horseradish peroxidase
HS	Human serum
hs-CRP	High sensitivity C-reactive protein
HuH7	Human hepatoma 7
HUVEC	Human umbilical vein endothelial cells
ICAM-1	Intracellular cell adhesion molecule 1
IFN-γ	Interferon-gamma
IGF-1	Insulin-like growth factor-1
IKK	IκB kinase
IL-1	Interleukin-1
IL-1β	interleukin 1-beta
IL-6	Interleukin-6
IL-8	Interleukin-8
ILLUMINATE	Investigation of Lipid Level Management to Understand Its Impact in Atherosclerotic Events
IRE1	Inositol 1,2,5-triphosphate-activated receptor
JNK	c-Jun amino-terminal kinase
KBr	Potassium bromide
LB	Luria broth
LDL	Low-density lipoprotein

$Ldlr^{-/-}$	LDL receptor homozygous knockout
M-CSF	Monocyte colony stimulating factor
MAPK	Mitogen-activated protein kinase
MCP-1	Monocyte chemoattractant protein-1
MEF	Mouse embryonic fibroblast
MHC	Major histocompatibility complex
MMP	Metalloproteinase
N-terminal	Amino-terminal
NaCl	Sodium chloride
NADPH	Nicotinamide adenine dinucleotide phosphate
NCBI	National Center for Biotechnology Information
NCD	Non-communicable disease
NFκB	Nuclear factor kappa B
NO	Nitric oxide
NPG	*n*-propyl gallate
OD	Optical density
OGTT	Oral glucose tolerance test
oxLDL	Oxidised low density lipoprotein
p38 MAPK	p38 mitogen-activated protein kinase
p53	Tumour suppressor p53/Protein 53/Tumour protein 53
PAGE	Polyacrylamide gel electrophoresis
PBS	Phosphate buffered saline
PC12	Pheochromocytoma
PCR	Polymerase chain reaction
PDGF	Platelet-derived growth factor
PERK	Protein kinase-like endoplasmic reticulum kinase
PI3K	Phosphatidylinositol 3-Kinase
PLPC	1-palmitoyl-2-linoleoyl-*sn*-glycero-3-phosphatidylcholine
PVDF	Polyvinylidene fluoride
qPCR	Real-time PCR
RCT	Reverse cholesterol transport
rHDL	Reconstituted high-density lipoproteins
RIPA	Radioimmunoprecipitation assay buffer
RNA	Ribonucleic Acid
ROS	Reactive oxygen species
RPM	Revolutions per minute
RPMI	Roswell Park Memorial Institute
RT-qPCR	Reverse transcription real time PCR
S1P	Site-1 protease
SAA	Serum amyloid A1
SAPK	Stress activated protein kinase
SDS	Sodium dodecyl sulfate
SEM	Standard error of the mean
SH-SY5Y	Neuroblastoma cell line
siRNA	Small interfering ribonucleic acid
SMC	Smooth muscle cell
SR-B1	Scavenger receptor class B type 1
STAT1	Signal transducer and activator of transcription-1
sXBP-1	Spliced X-box binding protein-1
TBS	Tris buffered saline

TGF-β	Transforming growth factor-beta
TNF-α	Tumour necrosis factor-alpha
TRAF2	Tumour necrosis factor receptor-associated factor 2
UPR	Unfolded Protein Response
UV	Ultraviolet
VCAM-1	Vascular cell adhesion molecule-1
WHO	World Health Organisation
XBP-1	X-box binding protein-1

Chapter 1 – Introduction

1.1 General Introduction

Chronic inflammation underlies numerous lifestyle diseases including coronary artery disease, insulin resistance, type 2 diabetes (T2D), and some cancers. Our laboratory has undertaken investigations of high-density lipoprotein (HDL) and how these particles are anti-inflammatory. A molecular dissection of signalling pathways involved suggested that the cholesterol synthesis enzyme, 3β-hydroxysteroid-Δ24 reductase (DHCR24), may be having a role in mediating HDL's protective effects [1]. Moreover, it led to the question whether DHCR24 alone can be protective.

The following sections in this chapter will introduce the lifestyle diseases, atherosclerosis and insulin resistance, and describe how the cellular stressors, inflammation and endoplasmic reticulum stress, are involved in the pathogenesis of these conditions. This review will introduce cardiovascular disease with a focus on atherosclerosis, and T2D with a focus on insulin resistance. Currently available therapies for these conditions and the aim of this project will also be discussed. The overall aim of this project was to characterise the protective effects of DHCR24 in human coronary artery endothelial cells (HCAECs) and human hepatoma (HuH7) cells against a TNF-α-induced inflammatory response.

1.2 Cardiovascular disease

Cardiovascular disease (CVD) is the name given to a group of disorders of the heart and blood vessels that includes: hypertension (high blood pressure), coronary heart disease (heart attack), cerebrovascular disease (stroke), peripheral vascular disease, heart failure, rheumatic heart disease, congenital heart disease, and cardiomyopathies (WHO). CVD is a major contributor to morbidity and mortality in Australia. CVD is attributed to approximately 40% of all deaths in Australia. This alarmingly equates to a death attributed to CVD of an Australian every 10 minutes (Heart Foundation Australia). Understandably, this is a major public concern from a heath and financial perspective where CVD inflicts an immense burden on the health care system. Additionally, beyond Australia, the WHO most recent mortality documentation (2015) reports that CVD is the leading cause of mortality globally (Figure 1.1), particularly in Western countries.

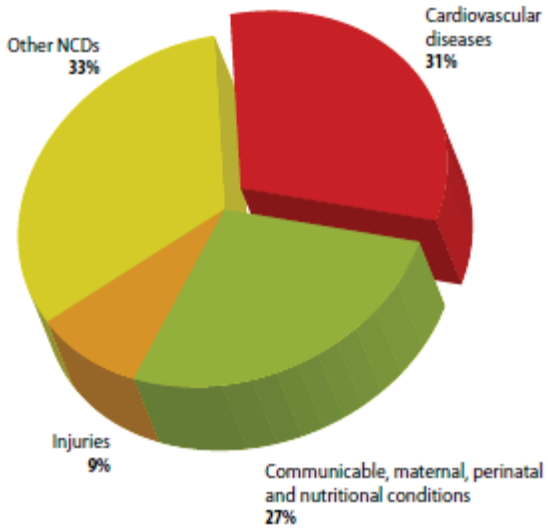

Figure 1.1 The global distribution of major causes of death (Source: Global Atlas on Cardiovascular Disease Prevention and Control - WHO 2015) NCD: Non-communicable disease

A number of risk factors associated with the development of CVD are identified in Table 1.1 and Figure 1.2 [2-12]. While some of the risk factors of CVD are non-modifiable and independent determinants, the disease can be prevented by maintaining healthy dietary and lifestyle habits. In keeping with this, the majority of atherosclerosis cases are caused by obesity. This effect of obesity, particularly sarcopenic obesity is especially apparent with increases in rates of obesity paralleled with increased CVD [13-15].

Table 1.1 Modifiable cardiovascular disease risk factors

Modifiable risk factors	Treatment
Hyperlipidaemia/ Elevated levels of low-density lipoprotein (LDL)	Dietary management Pharmaceuticals
Low levels of high-density lipoprotein (HDL)	Dietary management Pharmaceuticals
Hypertension	Dietary management Pharmaceuticals
Hyperglycaemia/Diabetes mellitus	Dietary management Pharmaceuticals
Smoking	Behaviour modification Pharmaceuticals
Depression and mental illness	Behaviour modification Pharmaceuticals
Physical inactivity	Exercise program suited to patient
Sedentary lifestyle	Exercise program suited to patient
Obesity/Elevated waist-to-hip ratio	Lower caloric intake below the amount of expended energy Exercise program suited to patient

Behavioural factors (e.g. stress)	Reduce the amount of daily stress the patient experiences daily
Excessive alcohol consumption	Reduce or eliminate alcohol consumption
Chronic methamphetamine use	Reduce or eliminate amphetamine use

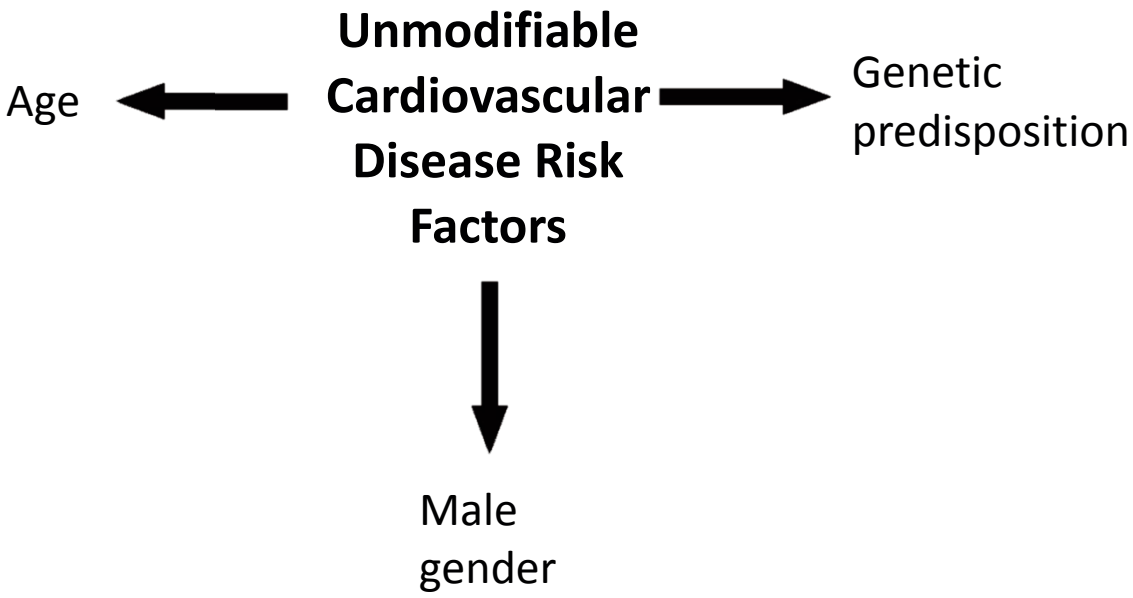

Figure 1.2 Unmodifiable cardiovascular disease risk factors

1.2.1 Atherosclerosis

Atherosclerosis is the major form of CVD in Australia and the world (AIHW, WHO). Atherosclerosis is an inflammatory disease of the arteries characterised by cholesterol-laden atherosclerotic plaques as a result of lipid and connective tissue accumulation. Atherosclerotic plaques lead to obstructions which impede blood flow, reduce arterial elasticity and the ability to contract in response to hydrodynamic stress [17]. Blood vessel occlusion may cause limb ischaemia and disruption of atherosclerotic plaques can lead to thrombus formation. Thrombi may occlude arteries, compromising oxygen supply to organs such as the heart or brain, causing a potentially fatal heart attack or stroke [18].

Atherosclerosis development is progressive, usually occurring over a period of decades and is primarily regarded as a result of vascular injury or chronic endothelial injury [19, 20]. Inflammation, endoplasmic reticulum (ER) stress, and apoptosis are causally involved in the pathogenesis of atherosclerosis and will be discussed in the following sections.

1.3 Type 2 Diabetes

Type 2 diabetes (T2D) is a condition characterised by persistent hyperglycaemia (Table 1.2), a relative lack of response to insulin in controlling blood glucose (insulin resistance), and islet β-cell dysfunction [21-23]. The lack of an insulin response is relative in T2D in contrast to the absolute lack of insulin in Type 1 diabetes (T1D).

Type 2 diabetes is a major contributor to morbidity in Australia (AIHW) and is associated with progression to conditions with a high incidence of mortality such as atherosclerosis [24, 25], pancreatic cancer [26, 27], neuropathies [28, 29], stroke [24, 30], and renal failure [31]. Diabetes by itself comprises ~10% of total deaths in Australia (AIHW 2012) and is major concern from both a health and financial perspective (WHO). In Australia, expenditure on diabetes increased by 86% between 2000–01 and 2008–09, while during the same time period, the expenditure for all diseases increased by 60%, indicating the significant financial burden attributable to the disease (AIHW 2013). While diabetes-associated and diabetes-caused deaths comprise ~10% of total deaths in Australia (AIHW 2012), the related impact of diabetes and its impact on the progression of other diseases is significant both in Australia and worldwide [32-35]. The pivotal Framingham Heart Study indicated that while the morbidity and mortality associated with CVD over the last 50 years has decreased (despite remaining the leading cause of world-wide death), the relative CVD burden caused by diabetes mellitus (DM) has significantly increased [36]. In addition, there is an increasing worldwide prevalence of T2D cases which has reached epidemic levels affecting approximately 387 million people and set to double over the next 20 years [37]. The disease is predominantly a consequence of a “modern” sedentary lifestyle coupled with chronic overeating [33, 38, 39]. While the calculated burden refers to all DM cases, it is T2D and gestational diabetes – both characterised by insulin resistance, which make up the majority of diabetes mellitus cases (>85%) and cause the majority of diabetes-associated morbidity and mortality (Diabetes Australia).

A number of risk factors associated with the development of T2D are identified in Table 1.3 and Figure 1.3 [9, 40-47]. The disease can mostly be prevented by maintaining healthy dietary and lifestyle habits. In keeping with this, the majority of T2D cases are caused by obesity. This is especially apparent with increases in rates of obesity paralleled with increased T2D [38-41, 48-56]. However, it is important to note that not all patients who develop T2D diabetes do so through obesity or insulin resistance mechanisms. For example, AKT2 mutations significantly affect insulin sensitivity and can cause T2D independent of obesity through impaired insulin

signalling, however this is rare [57]. Beta-cell failure is another mechanism through which T2D can develop independent of obesity and/or insulin resistance, although through impaired insulin secretion while maintaining normal insulin sensitivity [58, 59]. However, the experiments in this thesis focus on the investigation of the inflammatory response in hepatic cells, which is considered a primary driver of insulin resistance and subsequent T2D development [60-62].

Table 1.2 Australian diagnostic criteria for diabetes

FBG ≥7.0 mmol/L (on two separate occasions)
2 hour postprandial ≥11.0 mmol/L on OGTT (on two separate occasions)
HbA1c ≥6.5% (48 mmol/mol) (on two separate occasions)

FBG: Fasting blood glucose OGTT: Oral glucose tolerance test HbA1c: Glycated haemoglobin

Table 1.3 Modifiable insulin resistance risk factors

Modifiable risk factors	Treatment
Hyperlipidaemia/ Elevated levels of low-density lipoprotein (LDL)	Dietary management Pharmaceuticals
Low levels of high-density lipoprotein (HDL)	Dietary management Pharmaceuticals
Hypertension	Dietary management Pharmaceuticals
Hyperhomocysteinaemia	Dietary management Pharmaceuticals
Smoking	Behaviour modification Pharmaceuticals
Physical inactivity	Exercise program suited to patient
Sedentary lifestyle	Exercise program suited to patient

Obesity/Elevated waist-to-hip ratio	Lower caloric intake below the amount of expended energy Exercise program suited to patient
Sleep apnoea	Medical devices Surgery
Behavioural factors (e.g. stress)	Reduce the amount of daily stress the patient experiences daily
Environmental factors	Modify environment or change localisation

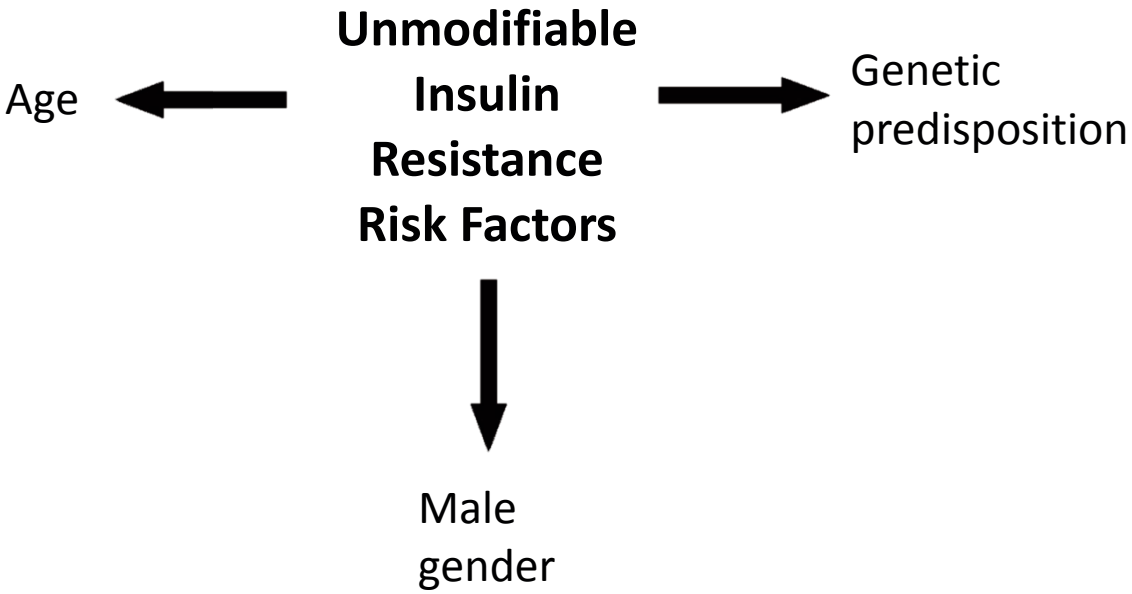

Figure 1.3 Unmodifiable insulin resistance risk factors

1.3.1 Insulin resistance

Insulin resistance is a precursor state to T2D and is classified as the body's inability to adequately respond to the secretion of insulin. One of the primary roles of insulin in the body is to control blood glucose levels. As blood glucose levels are elevated and uncontrolled by normal levels of insulin, the body attempts to restore levels to normal values through the compensatory measure of increased insulin synthesis and secretion by the pancreatic β-islet cells (termed β-cell compensation) [52, 53, 63, 64], paired with increased β-cell mass [65-67]. However, chronically increased insulin secretion can lead to hyperinsulinaemia which causes chronic pathogenic inflammation and is ineffective in the long term ~~and~~ when this state cannot be maintained. β-cell mass also decreases through a combination of β-cell apoptosis and a reduced rate of neogenesis [67]. A state of hyperinsulinaemia can also cause insulin resistance through downregulation of insulin receptors and desensitisation of post-receptor pathways [68]. Ultimately, the pancreatic β-cells producing compensatory insulin become dysfunctional [67], insulin mRNA also decreases with increasing and prolonged hyperglycaemia thereby reducing insulin secretion [69], euglycaemia cannot be persistently maintained, and consequently insulin resistance progresses to T2D (as reviewed by [70]).

The chronic hyperglycaemia associated with insulin resistance/diabetes has many deleterious effects. Chronically elevated glucose levels in the vasculature damage organs, especially the eyes, nerves, kidneys, heart, and blood vessels [21, 71-73]. The consequent damage and dysfunction of these various organs can lead to microvascular and macrovascular complications, particularly in the presence of hypertension, which are potentially fatal (Table 1.4) [74-77].

The acute and chronic effects of this disease affect both financial and health systems in both developing and developed nations (WHO). The prevalence of insulin resistance/T2D is steadily increasing with some sources estimating the total number of people with the disease reaching 366 million by 2030 [35] and 592 million by 2035 [78]. It is obvious that with the burden of T2D and its associated pathologies, management and treatment of insulin resistance is required to prevent the complications associated with the disease and to halt its progression. New approaches for the treatment of this disease state are required. Insulin resistance is a progressive metabolic disorder which is driven primarily by the cellular stressors, inflammation and ER stress [60, 62, 79, 80]. The link between these cellular stressors and the aetiology of insulin resistance will be discussed in section 1.4.2.

Table 1.4 Organ-specific complications associated with hyperglycaemia

Organ(s)	Hyperglycaemic complication
Kidneys	Diabetic nephropathy leading to renal failure
Eyes	Diabetic retinopathy leading to blindness
Nerves	Diabetic neuropathy: • Nerve entrapment • Ulceration • Diabetic amyotrophy • Amputations • Impotence
Heart	Cardiovascular disease: • Coronary heart disease • Stroke • Heart failure • Cardiomyopathy • Peripheral vascular disease • Rheumatic heart disease • Congenital heart disease
Central nervous system	Stroke
Pancreas	Pancreatic cancer

Table 1.4 Organ-specific complications associated with hyperglycaemia (continued)

Organ(s)	Hyperglycaemic complication
Muscular-skeletal system	Increased risk of fractures
	Adhesive capsulitis
	Limited joint mobility
	Dupuytren's contracture
	Carpal tunnel syndrome
	Flexor tenosynovitis
	Reflex sympathetic dystrophy
	Ankylosing hyperostosis
	Diabetic amyotrophy

1.4 The NFκB-mediated inflammatory response

Inflammation plays an important physiological role as an adaptive response reacting to harmful stressors and irritants such as infection and tissue injury. The process is characterised by the orchestrated delivery of vascular and immune products (leukocytes and plasma proteins) to the site of injury or infection [81]. The role of inflammation is usually considered to be beneficial especially when dealing with challenges such as responding to bacterial invasions or repairing damaged tissue. However, in some disease states such as gout and obesity, the role of inflammation appears to be solely deleterious. Moreover, chronic activation of inflammatory pathways causes cellular stress. Additionally, chronic inflammation, even when sub-acute, can lead to the development of diseases such as cancer [82], atherosclerosis [83], and insulin resistance [84].

The canonical NFκB pathway is implicated in inflammation (Figure 1.4). NFκB in its quiescent state resides within the cytoplasm bound to the inhibitory kinase, IκBα. Upon phosphorylation of IκBα by IKK-β, NFκB translocates to the nucleus. This occurs because phosphorylated IκBα is targeted for degradation by the proteosome, which frees NFκB. Subsequently, NFκB increases gene transcription at the promoter regions of target genes. This increases NFκB-regulated targets including proinflammatory cytokines such as TNF-α, IL-1β, IL-6 [85], and also other NFκB-regulated genes. With increases in proinflammatory cytokines, ER stress [86], and apoptosis can occur driving the pathogenesis of diseases such as atherosclerosis and insulin resistance.

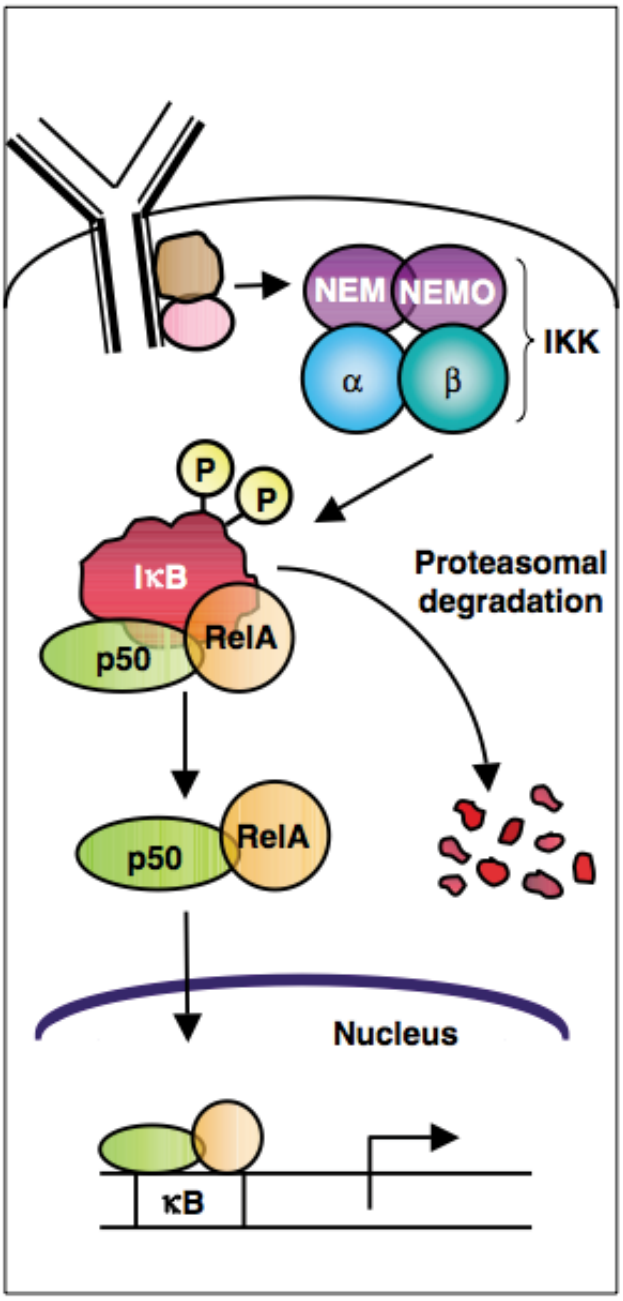

Figure 1.4 The canonical IκB kinase (IKK)/nuclear factor kappa B (NFκB) pathway

The figure above (adapted from [87]) depicts the canonical IKK/NFκB pathway. IKK-β attaches to the inhibitory kinase IκB phosphorylating it, targeting it for degradation by the proteasome. The phosphorylation of IκB liberates NFκB (depicted as the RelA/p65 heterodimer and also known as p50/p65) translocating it from the cytoplasm to the nucleus. Upon this translocation, NFκB increases gene transcription at the promoter regions of target genes, and inflammatory mediator release is increased.

1.4.1 The role of inflammation in atherosclerosis

Inflammation is primarily responsible for the progression of atherosclerotic plaques, with inflammatory processes being involved in every step of atheroma development [7]. Inflammatory stress caused by factors such as a high fat diet, hypertension, smoking, hyperglycaemia, obesity, and insulin resistance, leads to the recruitment and transformation of innate immune cells which, in turn, activate the adaptive immune system [88].

The development of atherosclerosis is understood to begin with injury to the endothelial cells lining the blood vessel wall, causing endothelial dysfunction [7]. Endothelial dysfunction or "activation" may occur in response to physical injury, such as that caused by the hydrodynamic forces of circulating blood [17], or by exposure to toxic or infectious agents such as oxidised low-density lipoproteins (oxLDL) in the intima (section 2.2.2) [89, 90]. Certain regions of the vascular endothelium, such as the branch points in the arterial tree, are more prone to dysfunction than others and are termed "lesion-prone" sites [91]. Lesion-prone sites are characterised by thickened intima, increased permeability to plasma proteins such as albumin and LDL, increased endothelial cell turnover, imbalances in thrombotic factors, growth factors and vasoactive substances, as well as increased cell adhesion molecule (CAM) expression and monocyte recruitment [17, 92-96].

Under physiological conditions, the endothelium serves as a selective permeable barrier between the intima of the blood vessel and blood, while endothelial cells provide a relatively non-adherent surface to leukocytes and monocytes (additional endothelium functions are listed in Table 1.5) [7]. Together, this provides a non-thrombogenic surface to the blood [19]. The endothelium also maintains its own basement membrane by producing collagen, proteoglycans and other matrix proteins. This facilitates the transduction of shear stress signals from the lumen to smooth muscle cells (SMCs) in the media via production of small molecules such as nitric oxide and prostacyclin (vasodilators), thromboxane, and endothelin (vasoconstrictors) [19]. However, in response to injury, endothelial cells become dysfunctional and alter their phenotype. They express CAMs on their cell surface, which allow monocyte binding and capture, part of the first identifiable stage of atherosclerotic plaque formation, the fatty streak (Figure 1.5) [97, 98]. Circulating monocytes are slowed down by selectins, such as P-selectin and E-selectin, on endothelial cells, and corresponding L-selectin on leukocytes. This causes them to roll across the endothelium via transient adhesion interactions, allowing other CAMs such as intracellular cellular adhesion molecule-1 (ICAM-1) and vascular cellular

adhesion molecule-1 (VCAM-1) to form firm bonds with the corresponding receptors, or integrins, on monocytes [99-101].

Table 1.5 Arterial endothelium functions

General Function	Functional Properties of the Endothelium
Permeability	Surface charge and presence of glycocalyx Tight junctions Basement membranes
Thrombo-resistance	Thrombomodulin content of plasma membrane Rapid metabolism of platelet aggregating agents Synthesis and secretion of prostacyclin and plasminogen activator
Mediation of vascular tone	Synthesis and section of prostacyclin, endothelium-derived relaxing factors and endothelin
Inflammatory and immune response	Expression of leukocyte adhesion molecule, leukocyte chemotactic proteins, growth factors, hematopoietic factors, major histocompatibility complex (MHC) antigens, and scavenger receptors

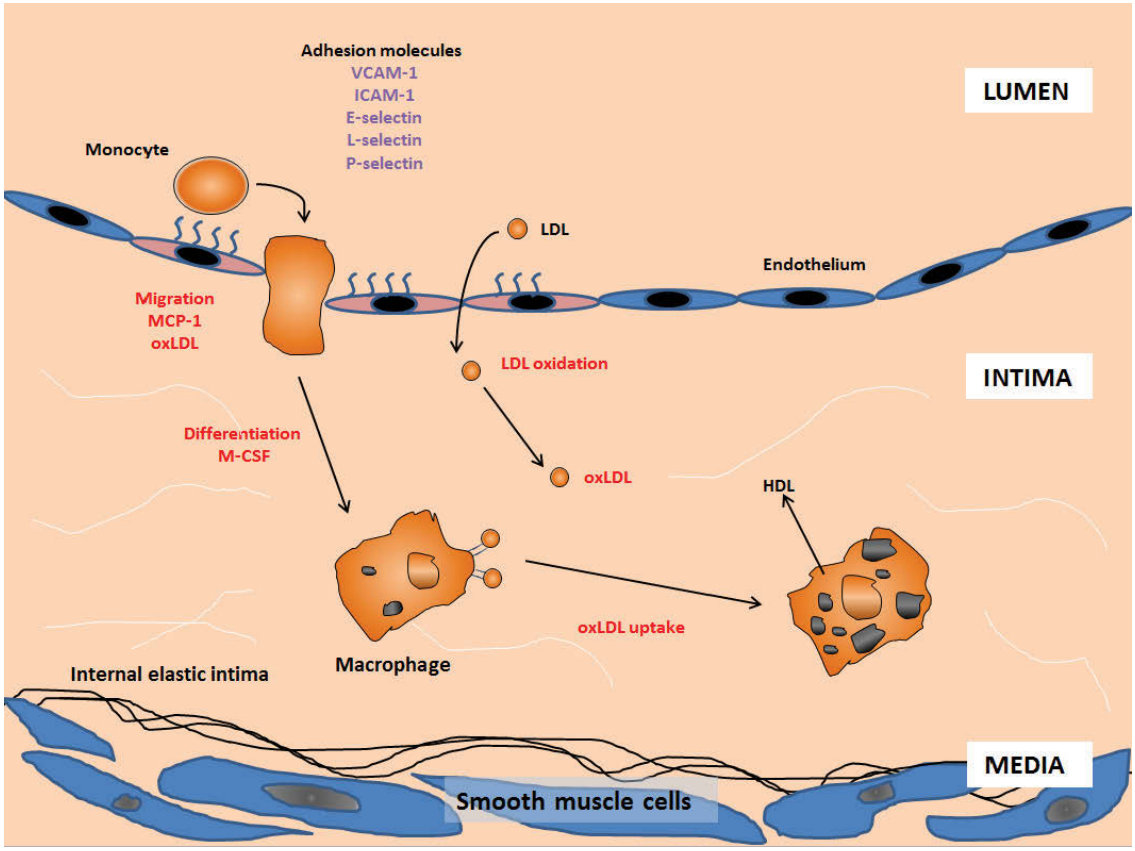

Figure 1.5 Early fatty streak/atherosclerotic plaque formation. Endothelial dysfunction, which is a response to injury, may be caused by response to physical injuries, or by exposure to toxic or infectious agents such as oxidised low-density lipoproteins (oxLDL) in the intima. The cascade of atherosclerotic events is initiated by accumulation of lipid in the intimal space and the subsequent associated influx of inflammatory cells. Migration of monocytes is facilitated by secretion of cytokines and chemoattractants in addition to induced expression molecules on endothelial cells. Monocytes differentiate into macrophages (mature form) and in an unregulated manner take up LDL that has been oxidised in the vessel wall, resulting in the formation of lipid-laden foam cells that accumulate in the intimal layer.

oxLDL: oxidised low-density lipoprotein, MCP-1: monocyte chemotactic protein, VCAM-1: vascular cell adhesion molecule-1, ICAM-1: intercellular cell adhesion molecule-1, M-CSF: monocyte colony stimulating factor

Endothelial cells are capable of secreting a range of growth factors, cytokines, chemokines, and enzymes that act on other vascular cells in the vicinity of the extracellular matrix; production of which can be upregulated in developing atherosclerotic lesions. Endothelial cells can be stimulated to produce the inflammatory cytokines, interleukin-1, -6 and -8 (IL-1, IL-6, IL-8), monocyte chemotactic protein (MCP-1) [102], as well as tumour-necrosis factor-α (TNF-α) and colony stimulating factors (GM-/M-CSF) [103]. Growth factors such as platelet-derived growth factor (PDGF), basic fibroblast growth factor (bFGF), transforming growth factor-β (TGF-β), and insulin-like growth factor-1 (IGF-1) are also produced and are responsible, to varying degrees, for the migration and proliferation of macrophages and smooth muscle cells in developing lesions [19].

Macrophage infiltration of the tissue is quintessentially an immune response to cellular stress. Macrophages also represent the dominant inflammatory cell type present in every atherogenesis phase [7]. After the rolling, the monocyte adheres to the endothelium by changing its morphology (stretching) [104], it can then undergo trans-endothelial migration into the sub-endothelial space where it differentiates into its mature form, the macrophage (Figure 1.6). Macrophages become foam cells, the principal cell type in atherosclerotic plaques after accumulating excessive amounts of modified lipoproteins via phagocytosis and various unregulated scavenger receptors [105]. The unregulated receptor expression on these macrophages causes lipid uptake to continue until the cells becomes completely lipid-laden with cholesterol esters [106].

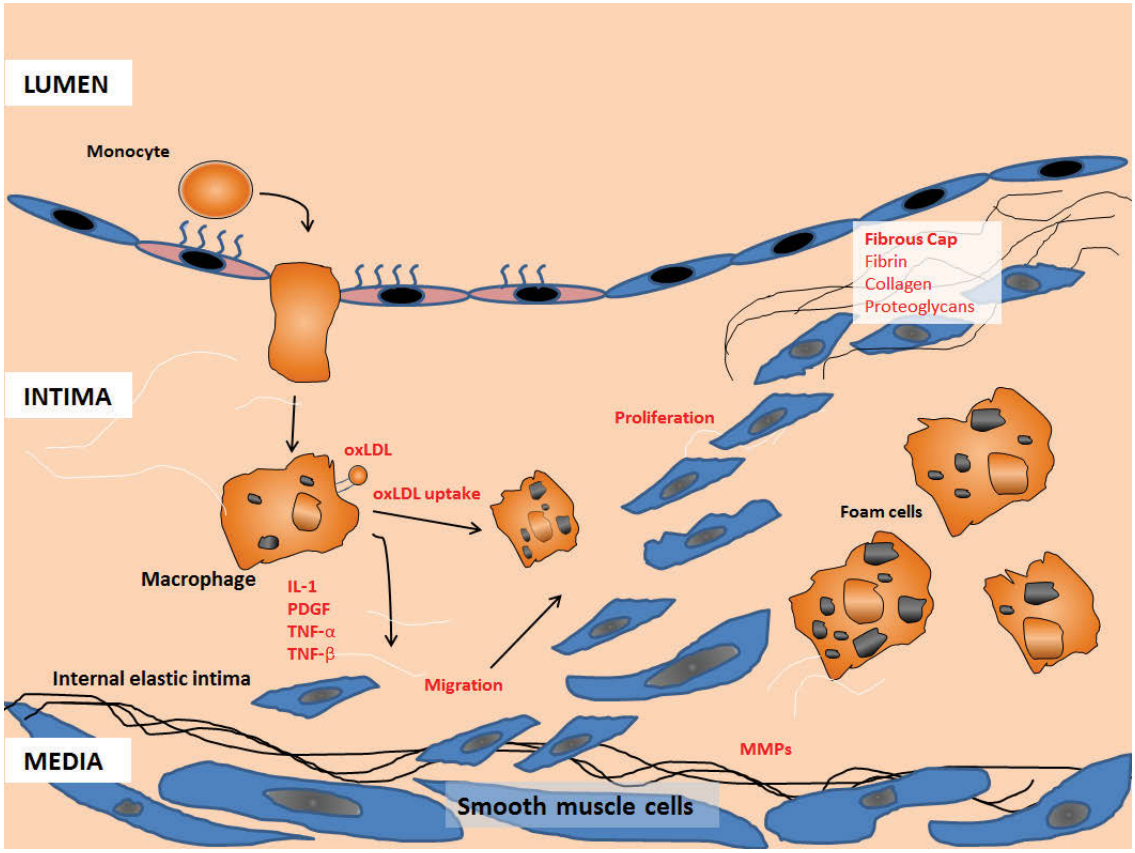

Figure 1.6 Intermediate lesion development. Foam cells and activated endothelial cells produce growth factors and cytokines that stimulate smooth muscle cells (SMCs) in the underlying medial layer. Stimulated SMCs produce matrix-degrading proteases (matrix-metalloproteinases, MMPs) that allow migration into the intima. Mitogenic factors stimulate SMC proliferation resulting in protrusion of the vessel wall into the lumen. Secretion of the extracellular matrix proteins by SMCs results in formation of a fibrous cap over the lesion. IL-1: Interleukin-1, PDGF: platelet-derived growth factor, TNF-α: tumour necrosis factor alpha, SMC: smooth muscle cell, MMP: matrix-metalloproteinases

Under normal conditions, macrophages phagocytose cell debris, apoptotic cells, or cytotoxic substances from tissue before returning to the bloodstream ensuring that the injury causing agent is cleared. In contrast, foam cells are immobilised by oxLDL in the matrix of lesion-prone sites [107, 108]. Foam cells contribute their lipid-laden contents to the necrotic core of the plaque when they die (Figure 1.7). Additionally, macrophages secrete an assortment of factors which contribute to SMC proliferation and recruitment of further inflammatory cells to the site of injury enlarging the atheroma. These factors include cytokines (e.g. IL-1), proteolytic enzymes (particularly metalloproteinases, see next section) and growth factors (e.g. platelet-derived growth factor (PDGF)) [109].

The atherosclerotic plaque becomes enlarged as the influx of macrophages, formation of foam cells, the associated migration and proliferation of SMCs, and secretion of extracellular matrix continues. This occurs in response to altered matrix components of the intima, such as a fibronectin-rich environment rather than the laminin-rich environment of the medial interstitial matrix [110]. PDGF produced by activated macrophages and endothelial cells is also a potent mitogen for SMCs [111, 112]. Rapid proliferation of SMCs results in intimal thickening characteristic of intermediate atherosclerotic lesions (Figure 1.6) [90, 113, 114]. In the more advanced lesions, production of extracellular matrix proteins such as collagen, fibrin, and proteoglycans, gives rise to the formation of a hard fibrous cap which can provide stability to a growing lesion (Figure 1.7) [7]. This process causes occlusion of the artery, leading to altered or impeded blood flow or potentially the fatal rupture of a plaque causing a myocardial infarction (heart attack) or stroke.

As the plaque develops, changes in fibrous cap thickness may occur, leading to plaque instability and rupture. Inflammatory cells in the plaque release inflammatory cytokines, including TNF-α, interferon-γ (IFN-γ) and cluster of differentiation 40L (CD40L), which induce macrophages and SMCs to release metalloproteinases, specialised enzymes which degrade elastin and collagen within the matrix [7, 19, 90, 115]. Degradation of the arterial extracellular matrix enables SMCs to penetrate through the elastic laminae and collegenous matrix of the growing plaque. This degradation of the extracellular matrix thins and subsequently weakens the fibrous cap causing it to become susceptible to rupture. Rupture of the plaque leads to spilling of the lipid core contents into the lumen, triggering thrombosis [116].

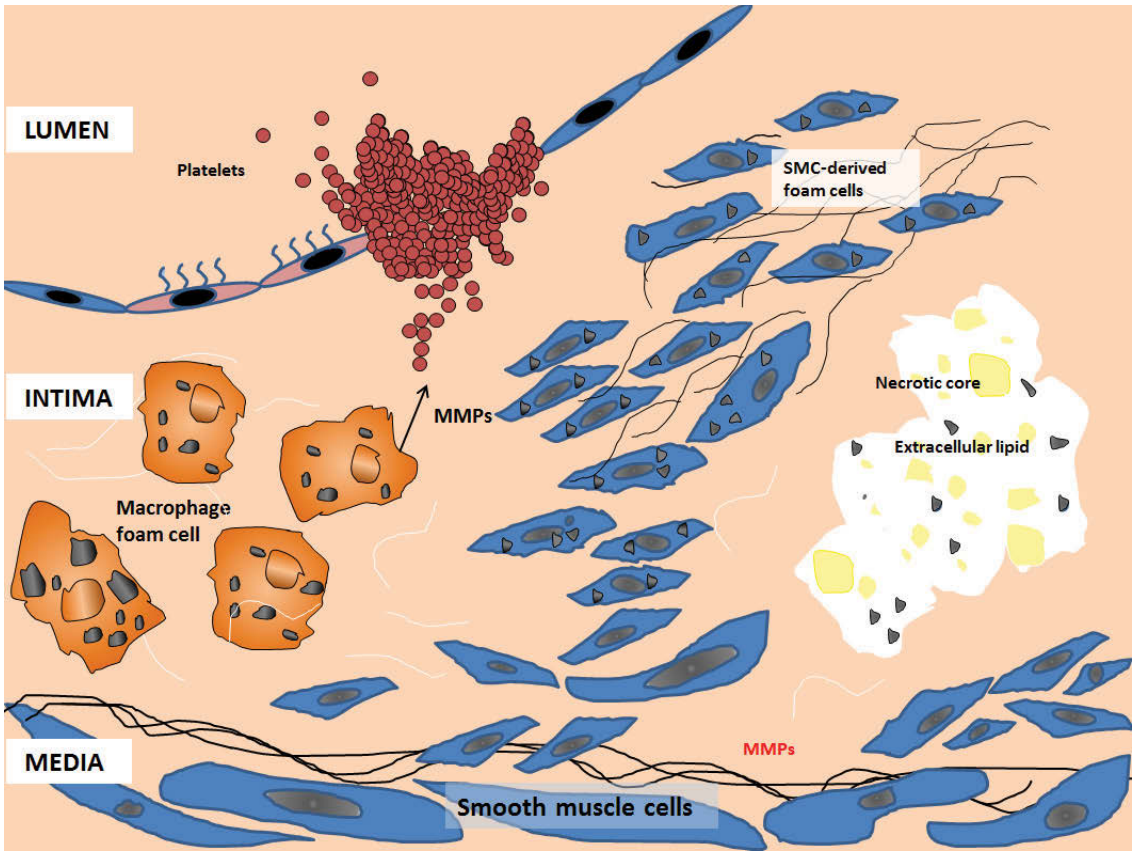

Figure 1.7 Advanced atherosclerotic plaque. Apoptosis and necrosis of both macrophages and smooth muscle cells (SMCs) results in the deposition of an unstable necrotic core of extracellular lipid and cellular debris under the fibrous cap. Decreased matrix production by remaining SMCs, combined with increased production of matrix metalloproteinases (MMPs) by macrophages, results in weakening at the shoulder regions of lesions, which can lead to rupture, exposing thrombogenic components to the blood. Advanced lesions may become increasingly complex via vascularisation, calcification, and the continued infiltration of blood components due to episodic thrombotic events. SMC: smooth muscle cell, MMP: matrix metalloproteinase

Atherosclerosis development has also been alternatively suggested to occur prior to the initiation of the inflammatory response. While the preceding mechanisms can be classified as response-to-injury, the response-to-retention hypothesis proposes contribution of proteoglycan-rich extracellular matrix [117]. Modified proteoglycans can bind and trap atherogenic lipoproteins to the vessel wall [117, 118]. The binding of atherogenic lipoproteins by proteoglycans is due to ionic interaction between the negatively-charged sulphate groups on proteoglycans and basic amino acids in lipoproteins [119]. The affinity of apoB-containing

LDL to bind to artery wall proteoglycans demonstrate that retention of lipoproteins prior to initiation of the inflammatory response may be in an early initiating step in atherogenesis [118]. Arterial retention of lipoproteins results in retarded lipoprotein egress, rather than increased LDL movement into the arterial wall [120]. LDL is consequently aggregated or modified by arterial proteoglycans before being taken up my macrophages and SMC ([121], and develop into foam cells [122, 123], the principal cell type in atherosclerotic plaques [105].

1.4.2 The role of inflammation in insulin resistance

Inflammation drives the pathogenesis of insulin resistance [84]. Consumption of a high fat diet (HFD), a sedentary lifestyle, and obesity are strongly associated with the aetiology of insulin resistance as they all lead to inflammation. A HFD diet leads to increased levels of circulating free fatty acids (FFAs). Adipose tissue possesses a role in preferably storing FFAs and triglycerides [124, 125]. When the adipocytes' threshold for lipid storage is met such as in the case of insulin resistance, the adipocytes are no longer able to perform this crucial role. The adipocytes become inflamed and release inflammatory mediators such as TNF-α, IL-6, or IL-1β. [60]. This leads to dysfunction of adipose tissue, inhibiting its storage activity. Consequentially this causes increased FFAs and glucose levels in other tissues as they attempt to compensate for this impaired storage activity of adipose tissue. The liver is one such tissue which undertakes this compensatory role, although it too can become oversaturated and inflamed. Hepatic inflammation directly participates in the onset of insulin resistance through activation of the NFκB/IKK signalling pathway [60, 61]. Fat-fed C57BL/6 mice exhibiting raised levels of circulating FFAs, triglycerides, and significantly increased hepatic NFκB activation develop insulin resistance. Moreover, NFκB activation alone results in insulin resistance development in these mice. IKK as an aetiological factor for insulin resistance is further supported by the finding that attenuation of IKK-β activity leads to improved insulin sensitivity. Heterozygous IKK-β knockout mice that were fed a HFD showed lower fasting glucose and insulin levels in addition to improved FFA levels in comparison to IKK-β positive mice littermates. This provides the link between hepatic inflammation and the onset of insulin resistance [60].

The inflammation associated with insulin resistance can also lead to the pathogenesis of other diseases. Poorly controlled blood glucose is a consequence of insulin resistance which leads to the characteristic feature of T2D – hyperglycaemia. Hyperglycaemia causes inflammation damaging tissue and organ systems leading to various pathologies. For example, endothelial cells that line blood vessels when exposed to high levels of glucose exhibit elevated expression

of CAMs (inflammatory mediators) such as intracellular adhesion molecule-1 (ICAM-1), vascular cell adhesion molecule-1 (VCAM-1), and endothelial-selectin (E-selectin) [126-131]. The combination of these CAMS can lead to the onset of atherosclerosis as described in section 1.4.1. The release of the proinflammatory cytokine TNF-α by adipose tissue has extensively demonstrated the link between obesity and IR in both experimental obesity models [132-134].

1.5 ER Stress

The endoplasmic reticulum (ER) is an organelle surrounding the nucleus which synthesises, modifies and delivers biologically active proteins to the appropriate intra- and inter-cellular sites. The ER is involved in protein folding, the storage of calcium and the synthesis and processing of cholesterol [135]. The protein folding role of the ER is crucial to ensure protein function, as unfolded proteins cannot elicit biological effects. The calcium stored in the ER is also important for protein folding as calcium enables calnexin and calreticulin to act together as molecular chaperones for protein folding [136, 137]. Additionally, ER calcium stores enable the trafficking of proteins from the ER to the Golgi apparatus for post-translational modifications [138, 139]. The other major function of the ER is the synthesis of new cholesterol and esterification of cholesterol (both newly synthesised and up-taken cholesterol). Cholesterol is generated within the ER on the cytoplasmic side of the ER membrane [140], via either the Bloch or Kandutsch-Russell cholesterol synthesis pathways (Figure 1.12), while esterification is executed in the ER by the enzyme, acyl-CoA:cholesterol acyltransferase (ACAT) [141]. Cholesterol is esterified for efflux by high-density lipoproteins (HDL) to prevent free (unesterified) cholesterol accumulation [141-143].

A state of ER stress occurs when there is an accumulation of unfolded proteins and unesterified cholesterol in the ER [135]. Within cell membranes, cholesterol serves to reduce the permeability of various molecules. However, in order for the ER to facilitate the entry of unfolded proteins, it has evolved to contain very low amounts of cholesterol [144]. ER stress occurs when the capacity of protein folding and cholesterol esterification is exceeded resulting in the accumulation of either unfolded proteins or unesterified cholesterol; both of which can trigger the unfolded protein response (UPR) [145-147].

The UPR is a cellular protective mechanism which has evolved to correct and assist ER function, particularly with impaired protein folding [135, 148]. It is the role of the UPR to eliminate misfolded/unfolded proteins to control ER stress. This is important because ER stress

will result in apoptosis if misfolded proteins or unesterified cholesterol are allowed to accumulate unchecked [149]. Therefore, the UPR has dichotomous roles in the cell, protective or apoptotic. The outcome of UPR activation, protective or apoptotic, depends on the duration of its activation or the magnitude of the ER stress. When transiently activated, the UPR improves the processing of proteins and the generation of esterified cholesterol [150]. By contrast, prolonged UPR activation is characterised by caspase-3-mediated apoptosis [151, 152].

The UPR is orchestrated by 3 quite distinct regulatory pathways called the PERK-eIF2α-ATF4 pathway [153], ATF-6 pathway [154], and IRE1-XBP-1 pathway [155].

Activation of the PERK-eIF2α-ATF4 pathway drives apoptosis [153]. This pathway is activated when the PKR-like endoplasmic reticulum kinase (PERK) responds to free cholesterol accumulation [153]. Once activated, PERK phosphorylates eukaryotic initiation factor 2α (eIF2α), which leads to the translation of activating transcription factor-4 (ATF-4). In turn, ATF-4 promotes the activity of the cell death effector, CCAAT enhancer binding protein homologous protein (CHOP), that serves as an inducer of apoptosis (Figure 1.8) [151, 156].

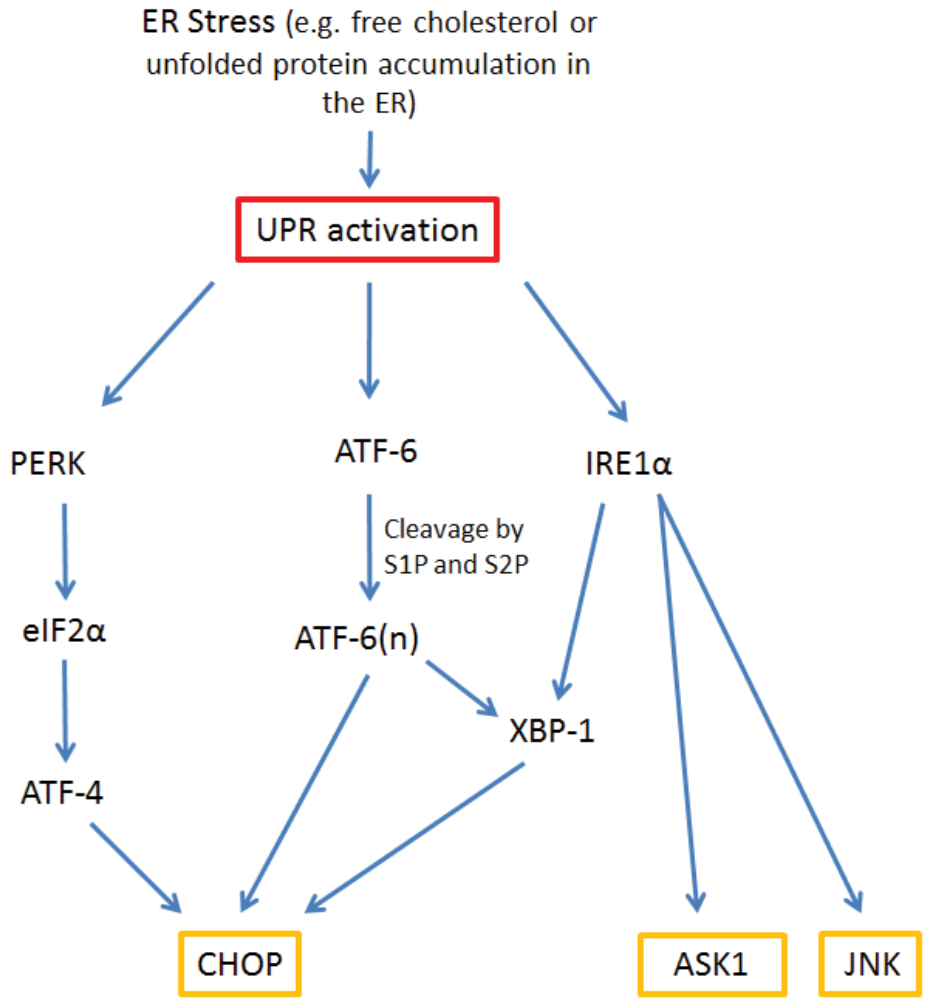

Figure 1.8 Apoptosis is activated via the unfolded protein response (UPR). Free cholesterol or unfolded protein accumulation within the ER causes activation of three UPR pathways - the PERK-eIF2α-ATF4 pathway, IRE1α-XBP-1 axis, and ATF-6 which together lead to ER stress-induced apoptosis. ER stress stimulates PERK, which phosphorylates eIF2α. Under chronic ER stress, eIF2α leads to the translation of ATF-4 and then the activation of CHOP. Once unfolded proteins/unesterified cholesterol in the ER have been accumulated, ATF-6 translocates to the Golgi apparatus. Here it is cleaved by S1P and S2P into its active nuclear form, ATF-6(n). ATF-6(n) translocates to the nucleus to activate XBP-1 and CHOP. ER stress also activates IRE1α, which triggers the IRE1 effector, XBP-1. XBP-1, in turn, activates CHOP. ER stress stimulated activation of IRE1α can also trigger the ASK1 and JNK apoptotic pathways. The PERK, ATF-6, and IRE1 pathways can each activate CHOP, leading to the induction of apoptosis.

ER: endoplasmic reticulum, PERK: PKR-like endoplasmic reticulum kinase, eIF2α: eukaryotic initiation factor 2α, ATF-4: activating transcription factor 4, ATF-4(n): active nuclear form of ATF-6, CHOP: CCAAT enhancer binding protein homologous protein, XBP-1: X-box binding protein-1, IRE1: inositol requiring enzyme 1, UPR: unfolded protein response

The second of the UPR pathways is the ATF-6 pathway. ATF-6 is an ER-resident transmembrane protein that is involved in the packaging and delivery of unfolded proteins to the Golgi apparatus [154]. Upon reaching the Golgi apparatus, ATF-6 is cleaved by site-1 protease (S1P) [157] and by site-2 protease (S2P) [158] resulting in a free N-terminal cytosolic fragment [ATF-6(n)] that translocates to the nucleus. In the nucleus, ATF-6 acts as a transcription factor that drives the expression of gene products that function in protein folding, including BiP/glucose-regulated protein 78 (GRP78) and protein disulfide isomerase [159]. If the ATF-6 pathway is chronically activated, then the active nuclear form of ATF-6 activates the apoptotic effectors, CHOP and XBP-1 [160, 161] (Figure 1.8).

The final UPR pathway is the IRE1-XBP-1 pathway. IRE1 is an ER transmembrane protein kinase, which under severe ER stress, induces apoptosis [155]. Under conditions of severe ER stress, IRE1 is phosphorylated by toll like receptor (TLR) 4 and TLR2 [162]. Following this phosphorylation, IRE1 activates the IRE1 effector X-box binding protein-1 (XBP-1). XBP-1 then leads to the synthesis of proinflammatory cytokines [163]. Under chronic ER stress, activated IRE1α also interacts with tumour necrosis factor receptor-associated factor 2 (TRAF2) and induces cell death via apoptosis signalling kinase 1 (ASK1) and c-Jun amino-terminal kinase (JNK) [164].

All three of the UPR pathways culminate in the activation of CHOP. CHOP normally functions in cholesterol transport into the ER, however under stress conditions, acts as an inducer of apoptosis. This was shown in CHOP knockout (*Chop*$^{-/-}$) mouse macrophages where cholesterol-induced apoptosis, associated with caspase-3 activation was significantly reduced [151]. Furthermore, both *Chop*$^{-/-}$ ApoE$^{-/-}$ and *Chop*$^{-/-}$ Ldlr$^{-/-}$ mice (established atherosclerosis mouse models) fed a high-fat (21.2%), high-cholesterol (0.2%) Western-type diet to promote atherogenesis, have reduced lesion sizes, plaque necrosis, and lesional apoptosis in comparison to *Chop*$^{+/+}$ ApoE$^{-/-}$ and *Chop*$^{+/+}$ Ldlr$^{-/-}$ mice controls [165]. However, knockout of *Chop* only impairs 70% of free cholesterol-mediated apoptotic processes from occurring, suggesting other pathways of cholesterol-loading ER stress-induced apoptosis exist [151]. CHOP can be induced by ATF-6 [166], ATF-4 [148, 167], or XBP-1 [168], although maximal induction occurs when all three pathways are activated [166].

Regardless of the mechanism by which CHOP is activated during ER stress, the next step is a transfer of calcium from the ER to the cytoplasm [74, 97]. Initially, CHOP stimulates ER oxidase 1α (ERO1α) to hyperoxidise the ER lumen [169]. Then once the ER lumen is in this hyperoxidised state, inositol 1,4,5-triphosphate-activated receptor (IP3R) is activated and

calcium is released from ER stores. Knockout of *Chop* in mice significantly reduces the activation of IP3-induced calcium release in comparison to wild type mice (both stressed with the UPR activator tunicamycin). However, adenovirus-mediated restoration of ERO1α in ER-stressed *Chop*$^{-/-}$ macrophages induces IP3-induced calcium release. This indicates that CHOP stimulation of ERO1α is essential to the calcium release-induced activation of apoptotic pathways. Chronically elevated cytoplasmic levels of calcium, as measured during chronic ER stress, cause the activation of calcium/calmodulin-dependent protein kinase (CaMK)II, which activates apoptotic pathways [170, 171]. These pathways include the Fas pathway, signal transducer and activator of transcription-1 (STAT1) pathway, and the inflammatory NADPH oxidase-mediated reactive oxygen species (ROS) pathway (Figure 1.9) [146, 171]. CaMK also causes the release of cytochrome c from the mitochondria [171] which in combination with BCL-2 protein imbalances, activates caspase-3.

A proteolytic cascade initiated by caspase-9 also activates caspase-3, via the classic BCL-2/BAX/BAK pathway [172-174]. Under normal conditions, pro-apoptotic BCL-2 proteins are inactivated by being bound to anti-apoptotic BCL-2 proteins. However, under conditions of ER stress this balance is disturbed and the pro-apoptotic BCL-2 proteins, Bcl-2-associated X (BAX) and Bcl-2 homologous antagonist/killer (BAK) are transcriptionally-induced. The oligomerisation of BAX and BAK and their insertion into the ER membrane causes further release of calcium, thus activating the apoptotic pathways mentioned in the previous section. Once activated, these pro-apoptotic BCL-2 proteins oligomerise and insert themselves at the mitochondrial membrane stimulating the release of cytochrome c [175, 176]. Cytochrome c released from the mitochondria (or by CaMK), APAF1 and caspase-9 then form a caspase-9 activating apoptosome, which, in turn, stimulates a proteolytic cascade that triggers caspase-3 [135].

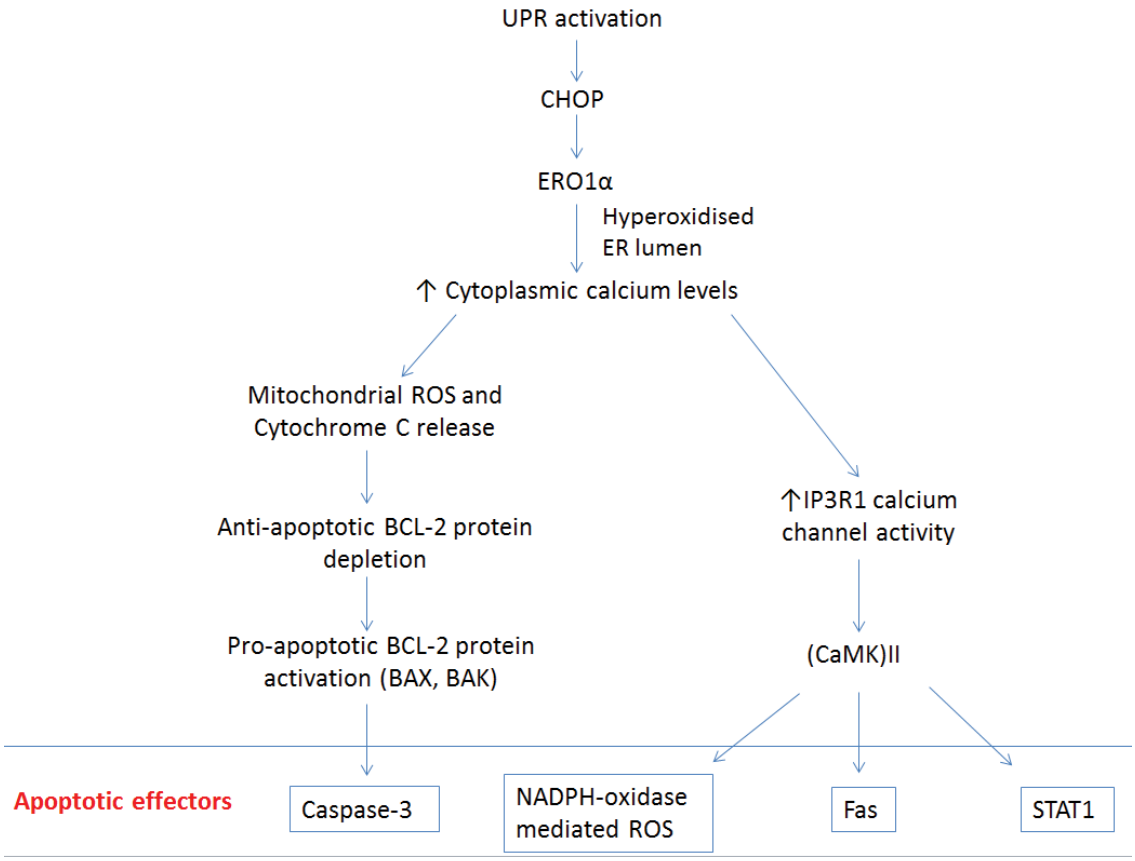

Figure 1.9 Persistent calcium release stimulates apoptotic pathways. UPR activation triggers CHOP to stimulate ERO1α release. Once the ER lumen becomes hyperoxidised by ERO1α, ERO1α upregulates the release of calcium into the cytoplasm from the ER. The calcium channel activity of IP3R1 is then activated, subsequently activating (CaMK)II, which stimulates the activation of assorted apoptotic effectors including NADPH-oxidase-mediated ROS, Fas, and STAT1. Increased cytoplasmic calcium also stimulates mitochondrial ROS production and mitochondrial cytochrome C release. The release of these factors depletes anti-apoptotic BCL-2 proteins, which induce pro-apoptotic BCL-2 proteins. Pro-apoptotic BCL-2 proteins, in turn, stimulate the caspase-3 apoptotic pathway.

UPR: unfolded protein response, CHOP: CCAAT enhancer binding protein homologous protein, ERO1α: ER oxidase 1α, IP3R1: inositol 1,4,5-triphosphate-activated receptor, CaMK(II): calcium/calmodulin-dependent protein kinase II, NADPH: nicotinamide adenine dinucleotide phosphate, ROS: reactive oxygen species, STAT1: signal transducer and activator of transcription-1 BCL-2: B-cell lymphoma 2, BAX: Bcl-2-associated X, BAK: Bcl-2 homologous antagonist/killer

1.5.1 The role of ER stress and apoptosis in atherosclerosis

ER stress and its associated inflammatory and apoptotic pathways are intricately linked with atherosclerosis [151, 177, 178]. This is evident because UPR activation is shown in models of atherosclerosis [135, 148]. For example, apoE$^{-/-}$ *Chop* knockout mice show that CHOP activation leads to increased lesion size and disturbed blood flow, a feature characteristic of the occluded arteries. In cultured endothelial cells, tunicamycin induction of the UPR leads to stress via ATF-4 and XBP-1 activation [179]. When ATF-4 and XBP-1 are inhibited, UPR activation is suppressed in human aortic endothelial cells following exposure to tunicamycin, preventing the induction of apoptotic pathways [180]. Oxidised phospholipids and cholesterol accumulation, which are common in atherosclerotic lesions, also lead to activation of the UPR [180].

The driving force behind ER stress, impaired protein folding, is associated with hyperlipidaemia, hyperglycaemia, hyperhomocysteinaemia, and inflammation. These are all established risk factors for atherosclerosis (Table 1.1) [177]. Together, with the *in vitro* and *in vivo* work outlined above, it is becoming increasingly recognised that ER stress and the UPR are significant in the aetiology of atherosclerosis.

1.5.2 The role of ER stress in insulin resistance

Similar to atherosclerosis, ER stress and its associated inflammatory pathways are intricately linked with insulin resistance [39, 79, 80, 181, 182]. Chronic overfeeding/overnutrition leads to obesity, triggering ER stress which is an early contributor to the development of insulin resistance (and inflammation). This link between a caloric surplus and ER stress leading to IR has been demonstrated in ob/ob mice that were fed a HFD. In these mice the hepatic ER stress markers including PERK and eIF2α phosphorylation, and BiP expression were increased and insulin sensitivity decreased [182]. When XBP-1 is reduced in HFD-fed mice, insulin sensitivity is impaired as ER stress cannot be alleviated [79, 182]. ER stress as marked by eIF2α phosphorylation, paired with JNK activation also increases glucose-6-phosphatase activity and glucose output in primary rat hepatocytes, a feature characteristic of insulin resistance and T2D [183]. eIF2α phosphorylation is required to maintain protein folding in the ER. PERK-mediated eIF2α phosphorylation increases ATF-4 translation to increase the folding capacity of the ER [184]. However, chronic caloric excess can overwhelm the protein folding capacity of the ER leading to persistent activation of PERK, causing inhibition of protein translation. This leads to an impaired protein folding capacity due to the uncontrolled UPR disassociating translational control of protein folding. Control of mRNA translation is essential to ensure glycaemic control. A loss of this function has been demonstrated in eIF2α mutant mice resulting in impaired glucose tolerance due to reduced insulin secretion paired with abnormal distension of the ER lumen [185].

Caloric restriction in *ob/ob* mice reduces levels of the ER stress markers, PERK, ATF-4, and eIF2α, improving hepatic insulin sensitivity through suppression of JNK-mediated IRS-1 serine-phosphorylation [186]. In keeping with this, genetically impaired protein folding capacity, the underlying cause of ER stress, leads to inflammation through JNK activation [80, 187]. In contrast, overexpressing the ER chaperone gene oxygen-regulated protein 150 (ORP150) reduces ER stress and improves insulin sensitivity in rodents [181] and in mice [188]. In obese human subjects, the ER stress markers, calnexin and sXBP-1, are increased in subcutaneous fat [189]. In addition, ATF-6 and phosphorylation eIF2α are significantly correlated with BMI and fat percentage [190]. Bariatric surgery in obese patients leads to reductions in the ER stress markers, sXBP1 and GRP78, in adipose tissue associated with improved insulin sensitivity [191]. Together, this combination of animal and human work demonstrates the relationship between obesity, ER stress, and the pathogenesis of insulin resistance.

As with atherosclerosis, the driving force behind ER stress, impaired protein folding, is associated with hyperlipidaemia, hyperglycaemia, hyperhomocysteinaemia, and inflammation. These are all established risk factors for insulin resistance (Table 1.3) [42]. Together, with the *in vitro* and *in vivo* work outlined above, it is becoming increasingly recognised that ER stress and the UPR are significant in the aetiology of insulin resistance.

1.6 Pharmacological therapies used to treat atherosclerosis and insulin resistance

This section focuses on areas of interest for therapies used to treat atherosclerosis and insulin resistance.

Inflammation, oxidative stress, and ER stress underlie the pathogenesis of atherosclerosis and insulin resistance. A range of pharmaceuticals have been developed and are being used to decrease the burden of atherosclerosis, insulin resistance, and their associated morbidities. Some of the most effective and promising therapies are discussed below.

1.6.1 Cholesterol-lowering drugs

Statins are a very successful class of cholesterol-lowering drugs used to treat atherosclerosis, providing up to 60% reductions in cardiac events [192]. The implementation of statin therapy in the last 20 years has resulted in dramatic decreases in coronary events, cardiovascular morbidity, and all-cause mortality [193].

The main mechanism of action of statins in the primary and secondary prevention of cardiovascular events is the lowering of LDL cholesterol [194-198]. Statins lower cholesterol synthesis via the inhibition of HMG-CoA reductase, the enzyme that catalyses the first step of cholesterol biosynthesis [199, 200]. Inhibition of HMG-CoA reductase occurs primarily by blocking substrate binding to the active site of the enzyme [200]. Statins were originally derived from fungal sources, however, most modern statins are fully synthetic (Table 1.6).

Table 1.6 Statin classes and origins

Class	Statin	Origin/derived from
Type 1 statins (fermentation-derived)	Mevastatin	*Penicillium citrinum*
	Lovastatin	Secondary metabolite of *Aspergillus terreus*
	Pravastatin	Biotransformation of mevastatin by *Penicillium citrinum*
Type 2 statins (fully synthetic statins)	Simvastatin	Chemical transformation of lovastatin side chain
	Fluvastatin	Fully synthetic
	Cerivastatin (withdrawn August 2001)	Fully synthetic
	Atorvastatin	Fully synthetic
	Rosuvastatin	Fully synthetic (contains sulfur)

One of the major effects of statins beside cholesterol-lowering ability are anti-inflammatory effects. For example, in human hepatocytes, inflammation was reduced by treatment with lovastatin via the reduction of high sensitivity C-reactive protein (hs-CRP). This is significant as hs-CRP is an inflammatory marker associated with CVD [201]. hs-CRP is primarily produced in the liver and predominately induces IL-6 secretion [202, 203] which indicates low-grade systemic inflammation [204]. Hs-CRP also produces an environment which promotes atherosclerotic development by down-regulating protective endothelial nitric oxide synthase (eNOS) expression [205], while increasing production of endothelin-1, a vasoconstrictor [203]. Furthermore, hs-CRP upregulates the expression of VCAM-1, ICAM-1, E-selectin [206] and MCP-1 [207], thereby augmenting monocyte adhesion and infiltration into the vessel wall. Within the wall, hs-CRP facilitates macrophage uptake of LDL [208]. Therefore, statin suppression of hs-CRP levels provides protection against numerous inflammatory events associated with the initiation and progression of atherogenesis.

Statins also improve endothelial function by increasing the production of endothelial NO through the increased expression and stabilisation of eNOS, independent of lipid lowering [209, 210]. eNOS expression can be restored by statins in the presence of hypoxia [211] and oxLDL [209], which are mediators of endothelial dysfunction. The mechanism of statin-induced eNOS upregulation is dependent on prolonging eNOS mRNA half-life [212]. This is significant as pro-atherogenic conditions such as hypoxia, oxLDL, and inflammatory cytokines such as TNF-α decrease eNOS mRNA stability and consequently reduce its expression. Abrogation of leukocyte adhesion in normocholesterolemic animals by endothelial NO production [213, 214] is also dependent on the presence of eNOS [215].

Statins can also improve endothelial function through anti-oxidant protection. ROS levels are decreased by statin treatment, enabling endothelium-dependent relaxation in the aortas of cholesterol-fed rabbits [216]. This anti-oxidant protection is provided via both lipid-lowering-dependent [217] and lipid-lowering-independent mechanisms [218]. One mechanism that is independent of lipid-lowering is statin-mediated reduction of free radicals in vascular smooth muscle cells produced by angiotensin II. This reduction occurs through the inhibition of Rac1-mediated NADPH oxidase activity and the downregulation of angiotensin I receptor expression [219].

The pro-apoptotic effect elicited by statins also contributes to their pleiotropic effects. For example, apoptosis of transformed cells may protect against the development or progression of cancer [220]. In keeping with this, statins are associated with reduced cancer risk and

cancer-related mortality [221-225]. However, paradoxically while statin treatment can prevent prostate cancer [225], statin treatment may prevent prostate cancer detection through its serum cholesterol-lowering effect and as a result a significant increase in high grade prostate cancer incidence has been reported in patients who normalised their serum cholesterol levels using statins [226]. Statin use in cancer is complicated, and affected by many external factors. Currently investigation into the link between statin use and cancer is ongoing. The pro-apoptotic effect of statins may be beneficial in cardiovascular disease by abating cardiac hypertrophy and remodelling in cardiac myocytes [227]. However, statin-induced apoptosis of healthy myocytes is associated with myopathy (discussed below).

Statins may weakly induce ER stress within cells [228]. When cells are treated with fatty acids, ER stress is significantly augmented (to a far greater extent than that induced by statins). However, the addition of statins attenuates this fatty acid-induced ER stress, providing therapeutic benefits while negating the slight increase of ER stress stimulated by the statins [228]. Statins also downregulate the ER stress mediators, CHOP and GRP78 [229].

Statins stabilise atherosclerotic plaques by reducing their size [230, 231]. The lipid-lowering effects of statins are suggested to stabilise plaques by modifying the composition of their lipid core. However, reductions in plaque size occur over an extended time of lipid-lowering, despite lipid-lowering occurring soon after the initiation of statin therapy. This indicates that other processes are at work. The reduced size and improved stability of plaques is most likely to be caused by lowered macrophage numbers and inhibition of matrix metalloproteinases from activated macrophages, in addition to reduced lipid levels [232, 233].

Administration of statins can lead to systemic increases of HMG-CoA reductase as the targeted cells and tissues attempt to restore normal regulation of the enzyme. As a consequence, inhibition of whole body cholesterol biosynthesis is attenuated [234, 235]. Atorvastatin is an exception to this compensatory response of the cells and tissues exposed to statins, as HMG-CoA reductase activity is not increased thereby facilitating a stronger cholesterol-lowering effect [236]. This effect has been attributed to atorvastatin binding more strongly to HMG-CoA reductase thereby inhibiting its recovery and activity [237, 238]. The retarded release of atorvastatin from HMG-CoA reductase exerts a more robust cholesterol-lowering effect [238]. While the compensatory response of cells to some statins occurs, this is not considered an adverse effect rather it affects these statins' efficacy. Reduced statin efficacy can be overcome with higher dosages although this increases the risk of adverse effects (as reviewed by [239]).

Statin adverse effects vary according to what statin is being used for treatment. The most frequently recorded and most robust reports of adverse effects caused by statins are myopathy and rhabdomyolysis. All statins can and have been reported to cause myopathy and rhabdomyolysis [240-243]. These effects are due, in part, to elevations in cytoplasmic calcium through depletion of isoprenoids. Isoprenoids are downstream lipid products of the HMG-CoA reductase pathway and statins prevent their formation [244]. Statin-induced elevation of calcium levels activates calpain, which leads to the translocation of Bax to the mitochondria, activating caspase-3 and caspase-9 and thereby, apoptosis [245]. Mevalonate supplementation in human skeletal muscle cells suppresses the statin-induced increase in cellular calcium levels and therefore, prevents caspase-3 activation. In turn apoptosis and myopathy-related events are blocked [244, 245]. The incidence of statin-induced myopathy and rhabdomyolysis is rare [239, 241]. However, each statin has been linked to cases of rhabdomyolysis-induced deaths [246]. A previously available statin, cerivastatin was voluntarily withdrawn from the market [240, 247], in part due to being associated with approximately 100 rhabdomyolsis-induced deaths [240]. The FDA reported a 16 to 80 times more frequent rate of fatal rhabdomyolysis for cerivastatin compared to any other statin [248]. The incidence of myopathy-related adverse effects is considered low and deaths are rare [239, 248]. The consensus is that the benefits of therapy are considered to significantly outweigh the adverse risks [249]. However, myopathy is still considered a major adverse effect of statins and its incidence is linked with (increased) statin dosage and associated with select drug interactions [241, 250].

Statins have also been associated with the onset of incident diabetes [251-254]. As previously mentioned, hyperglycaemia is a known risk factor for the development of atherosclerosis (as reviewed by [255]). Statin-induced increases in haemoglobin A1c (HbA1c) and fasting plasma glucose levels appear to dose-dependent, however, currently, to date, causality has not been demonstrated, nor have mechanisms for this association been elucidated. For a review on the potential mechanisms for statin-induced diabetes, see [256]. Despite the risk of developing diabetes as an adverse effect of statin treatment, the benefits of statin therapy outweighs this risk [251, 252].

Statin use is generally well tolerated although statin toxicity has been reported because of drug interactions. Statins are primarily metabolised by CYP450 isoenzymes, with the exception of pravastatin which undergoes sulfation [257]. CYP450 3A4 metabolises lovastatin, simvastatin, atorvastatin, and pitavastatin, while CYP450 2C9 metabolises rosuvastatin and fluvastatin [250, 258, 259]. In keeping with this, drugs which are CYP450 3A4 isozyme substrates increase the risk of myopathy by decreasing statin metabolism thereby increasing

statin plasma concentrations and increasing the risk of myopathy. CYP450 3A4 isozyme substrates and inhibitors include macrolide antibiotics, azole anti-fungals, protease inhibitors, and amiodarone [260]. Individual variation is significant as CYP3A4 levels can vary 10-fold between patients [261] due to genetic polymorphisms [262] and consequently the effect of dosage and drug interactions varies between patients. Other genetic polymorphisms that affect the pharmacokinetics of different statins leading to potential toxicity include ABCG2 polymorphisms which affect atorvastatin, rosuvastatin [263], fluvastatin, and simvastatin [264], in addition to SLCO1B1 c.521T>C single-nucleotide polymorphisms affecting simvastatin, atorvastatin, pravastatin, and rosuvastatin [265-268]. These interactions can lead to a significantly increased risk of adverse effects due to increased statin toxicity. For example, patients with the SLCO1B1 c.521T>C SNP have on average a 3.2-fold increased plasma concentration of the active acid of simvastatin, leading to a raised risk of developing statin-induced myopathy (odds ratio 16.9 at a dosage of 80 mg simvastatin) [267], as it is dose-dependent [269, 270]. Therefore, despite the generally well tolerated use of statins, drug interactions and gene polymorphisms can be deleterious when combined with statin therapy, and therefore the development of adverse effects should be monitored and contraindications considered.

1.6.2 Anti-inflammatory therapies

1.6.2.1 Salicylates

Aspirin, the acetylated form of salicylate is used to treat atherosclerosis [271, 272] and insulin resistance/T2D [273-277]. Aspirin suppresses inflammation by inhibiting the canonical IκB kinase (IKK)/nuclear factor kappa B (NFκB) signalling pathway, impairing activation of the inflammatory cascade (Figure 1.4) [278-280] and elicits anti-thrombotic effects through inhibition of thromboxane A_2 [281, 282].

Aspirin's inhibition of NFκB activation decreases monocyte adhesion to endothelial cells and smooth muscle cells [278, 279]. In keeping with this, there are fewer reports of myocardial and cerebral infarctions reported in aspirin users [272, 283-286]. Aspirin also improves insulin sensitivity through inhibition of IKK/NFκB activation [287, 288], the integral component of insulin resistance pathogenesis (section 1.4.2).

Cardiovascular outcomes are also improved by aspirin through the effect of reduced platelet aggregation which improves endothelial function [271, 289]. Aspirin inhibits production of the platelet activator thromboxane A_2 [281, 282, 290]. Thromboxane A_2 inhibition by aspirin occurs through covalent transacetylation of active site serine residues. This irreversibly inactivates the cyclooxygenase (COX) enzymes, COX 1 and COX 2, subsequently preventing thromboxane A_2 production (as reviewed by [291]). However, inhibition of COX enzymes is not the mechanism through which aspirin improves insulin sensitivity [287].

The main adverse effect associated with aspirin use is gastrointestinal tract (GIT) discomfort. In keeping with this, gastrointestinal bleeding is dose-dependent [292]. Further, aspirin use is associated with increased risk of gastrointestinal or cerebral bleeding episodes [293]. As a consequence, use of aspirin is contraindicated in some patients with high gastrointestinal risk, particularly those with peptic ulcers [294]. Hepatotoxicity can also occur with aspirin use but this adverse effect is mostly reported at higher dosages [295, 296]. Lack of aspirin efficacy in atherosclerosis or insulin resistance may also be attributed to relatively common [297-299] aspirin-resistance [300, 301]. Long-term administration of aspirin is also related to reduced efficacy of the drug [302].

1.7 Insulin sensitisation

1.7.1 Incretins

Glucagon-like peptide 1 (GLP-1) and glucose-dependent sulinotropic polypeptide (GIP) are classified as incretins. Incretins are post-prandially released enteroendocrine hormones secreted from the GIT into the bloodstream by K and L cells [303-305]. Glucose control is achieved by incretins binding to their respective receptors which via G protein, activates adenylate cyclase, stimulating increased intracellular cyclic AMP levels. Following this process, protein kinase-A is activated which enables a series of processes to occur such as enhanced exocytosis of insulin-containing granules by pancreatic β-cells [306, 307]. This increased insulin secretion through activation of β-cells occurs in a dose-response, glucose-dependent manner. Incretins also delay gastric emptying which prolongs nutrient transfer to the duodenum, reducing postprandial glycaemia [308, 309]. Incretin use for control of hyperglycaemia is beneficial as its natural release is severely dysregulated in T2D [310].

An example of a successfully used incretin is exendin-4. Exendin-4 is a GLP-1 receptor agonist/mimetic with a 53% amino-acid sequence homology to mammalian GLP-1. Exendin-4 controls hyperglycaemia through increased glucose-dependent insulin secretion, reduced postprandial secretion of glucagon, and slowed gastric emptying [311, 312]. The glucose-dependent secretion stimulated by exenatide (synthetic exendin-4) does not increase the risk of hypoglycaemia [313]. *In vitro* both exendin-4 and GLP-1 act on the GLP-1 receptor, binding with equal affinity. Exendin-4 and GLP-1 also share similar glucose-regulatory mechanisms, such as glucose-dependent enhancement of insulin secretion, glucose-dependent suppression of abnormally high glucagon secretion and reduction of hyperglycaemia (as reviewed by [314]). Additionally, in contrast to GLP-1, exendin-4 is unaffected by the enzyme that rapidly degrades GLP-1, DPP-4 [315, 316] allowing it to act longer. From *in vivo* work, exendin-4 is also able to increase β-cell proliferation and islet mass, prevent β-cell apoptosis by decreasing thioredoxin-interacting protein levels [317], enhancing islet neogenesis [318, 319], and together improving insulin secretion [313, 320]. Enhancing the proliferation and reducing the apoptosis of β-cells is significant as impaired β-cell function is characteristic of T2D [67]. Exenatide use in T2D patients leads to enhanced glycaemic control and improved cardiometabolic risk factors without hypoglycaemia or weight gain [321, 322]. Exenatide also retains the ability to stimulate insulin secretion during hyperglycaemia and euglycaemia, but not during hypoglycaemia [313, 323, 324].

The use of incretins is associated with a number of adverse effects. As incretins inhibit gastric emptying they can cause GIT discomfort and nausea after meal ingestion [325], making it unsuitable or intolerable in some patients [326]. The efficacy of incretins can be reduced due to the development of antibodies. For example anti-exanatide are particularly problematic in patients who develop a high antibody titre as they lead to diminished efficacy of the therapeutic [327]. Furthermore, the use of GLP-1 receptor agonists increases the risk of pancreatitis compared to other therapies 6-fold, and also increases the incidence of pancreatic cancer [328]. Together, this indicates that the use of incretins is limited in some patient populations, especially for long term use.

1.7.2 Metformin

Metformin belongs to the biguanide class of drugs, and is the main drug used to manage T2D and hyperglycaemia [329, 330]. Metformin improves insulin sensitivity by suppressing hepatic glucose production [331], a defect in glucose control that is increased at least two-fold in T2D patients [332]. The main mechanism of action for metformin is specific inhibition of respiratory-chain complex 1. This inhibition results in decreased cellular respiration and occurs without affecting any other mitochondrial pathways [333, 334]. This mechanism has been extensively reported in many cell lines [335-338], including rat, mouse and human primary hepatocytes [333, 334, 339], in addition to neurons [340], skeletal muscle homogenates [341], pancreatic beta cells [342], cancer cells [343, 344], and peripheral blood mononuclear cells and platelets [345]. The reduction in mitochondrial respiration causes a reduction of ATP levels and accumulation of AMP through metformin increasing AMP-activated protein kinase (AMPK) activity, [346], which in turn suppresses hepatic gluconeogenesis improving insulin sensitivity [347]. AMPK also limits hepatic fatty acid synthesis by inhibiting acetyl-CoA carboxylase 1 and 2 (ACC1 and ACC2) [348]. Thus, metformin possesses pleiotropic effects on insulin resistance.

Other hyperglycaemic control mechanisms facilitated by metformin include increased intestinal glucose utilisation, decreased fatty-acid oxidation, and increased insulin-mediated glucose disposal [349-351]. Interestingly, metformin also improves HDL functionality by inhibiting its glycation [352], increases lipoprotein particle size when combined with pioglitazone [353], reduces LDL levels when combined with sulfonylurea [354], and when apoA-I levels are attenuated, metformin's efficacy is reduced [355] demonstrating a link between metformin and HDL (discussed in the next section).

The use of metformin is successful [356-358], well tolerated [330, 359], and synergises well with other drugs used to treat hyperglycaemia [354, 360]. Metformin improves insulin sensitivity even at low doses [361], and rarely leads to hypoglycaemia [362] or weight gain [363, 364]. Moreover, when metformin is combined with other anti-hyperglycaemic or insulin sensitising drugs, additive effects are observed and in some cases synergistic effects are noted. When combined with sulfonylurea, there is an additive effect on the improvement in insulin sensitivity and inhibition of lipogenesis [360], while when combined with salicylates there are synergistic effects on the same parameters [365]. Low doses of metformin assist in reducing tumour mass and preventing relapse in a xenograft mouse model by inhibiting cellular transformation and inducing apoptosis in cancer stem cells when combined with chemotherapy [366] or 2-Deoxyglucose (2DG) [367, 368]. Additionally, cancer risk is reduced in

diabetic patients treated with metformin (as reviewed by [369]). Metformin, as with all biguanides, has the potential to induce lactic acidosis which is fatal [370, 371]. The safety of metformin use and its relationship with the development of lactic acidosis is debated [372-377] particularly in the context of its use in chronic kidney disease due to its decreased excretion which can cause metformin levels to accumulate [372, 373]. However, metformin use and the incidence of lactic acidosis in both non-diabetic and diabetic patients has been demonstrated to be extremely low when used at therapeutic dosages and rather than supratherapeutic dosages [378]. However, its use is suggested to be discontinued when serum creatinine or the estimated glomerular filtration rate reach threshold levels rather than adjusting the dosage (as reviewed by [377]). As the liver is associated with lactate processing, metformin use is contraindicated in patients with severe liver failure [379]. In keeping with this, it has been suggested that renal insufficiency merely leads to metformin accumulation, although when this occurs combined with liver failure it is dangerous [377]. Metformin-induced lactic acidosis is extremely rare ≤ 10 events per 100,000 patient-years of exposure [380] although in the reported cases, mortality rates are 30 – 50% [371, 381]. However, despite these risks the main adverse effects associated with metformin are associated with GIT discomfort as a result of metformin inhibiting gastric motility subsequently delaying gastric emptying [351, 382].

1.8 High-Density Lipoproteins (HDL)

The use of statins reduces the risk of major cardiovascular events by 21% for every 1 mM decrease in LDL [383]. However, despite intensive high-dose statin therapy being used to lower LDL levels below 2.6 mM, the risk of major cardiovascular events in patients with established CVD remains significant at a level approaching an annual risk of 9% [384, 385]. Thus, there is a need for novel treatment strategies for lowering cardiovascular risk.

Low levels of HDL are associated with an increased risk of CVD, independent of LDL levels. For every 0.026 mM increase of HDL the risk of CVD is reduced by 2-3% [386]. Epidemiological studies have reported that over a 6 year period, patients with HDL levels ≥35 mg/mL are 70% less likely to develop CVD in comparison to patients with HDL levels <0.9 mM [387]. Therefore, it is promising to use HDL as a therapeutic strategy.

Raising HDL suppresses cytokine-induced CAM expression in endothelial cells [388] and suppresses CRP-induced CAM expression in both endothelial cells *in vitro* and *in vivo* [389]. TNF-α and interleukin-1 (IL-1)-induced VCAM-1 expression is attenuated by HDL treatment in HUVECs [388]. Similarly, CRP-induced CAMs are downregulated by HDL in human umbilical vein endothelial cells (HUVEC) [389]. This inhibition of endothelial CAMs also prevents downstream monocyte recruitment into the arterial wall [389, 390]

Patients with low levels of HDL have higher levels of soluble CAMs and MCP-1 as compared to those with average or high levels HDL levels and an associated increased risk for atherosclerosis and myocardial infarction [391-394]. Raising HDL inhibits the expression of CAMs and MCP-1 expression *in vivo* [395, 396] improving atherosclerosis and therapeutic outcomes [397].

The major apoplipoprotein in HDL is apoplipoprotein A-I (apoA-I), making up 70% of all HDL protein [398]. Low levels of apoA-I are associated with strong risk of future MI [6]. Thus, treatments utilising apoA-I HDL have been investigated. ApoA-I HDL mediates anti-inflammatory protection in endothelial cells by inhibiting CAM expression [388]. Both native and reconstituted forms of HDL containing apoA-I inhibit inflammatory cytokine-induced VCAM-1, ICAM-1, and E-selectin expression in HUVECs. This effect is observed at physiological HDL levels in a dose-dependent manner [388, 399]. Furthermore, following pre-incubation of endothelial cells with rHDL this anti-inflammatory protective effect persists for several hours, even after rHDL has been removed [400].

Regulation of HDL and apoA-I levels is also important in the context of insulin resistance. An inverse correlation exists between HDL levels and insulin resistance [401, 402]. Bariatric surgery and reducing BMI have a strong effect on the blood lipid profile, increasing HDL levels, and subsequently improving insulin sensitivity [403]. A causal relationship in children between adenotonsillectomy in obstructive sleep apnoea patients (an insulin-resistance risk factor[404]) has also been reported, with insulin resistance decreasing and HDL levels increasing following surgery [405]. The presence of apoA-I is also important in regulating the effects of metformin. In apoA-I-deficient mice ($apoA^{-I-}$), the function of metformin to maintain peripheral sensitivity insulin sensitivity to effectively control glucose following glucose challenges was abrogated [355]. Moreover, apoA-I treatment suppresses hepatic inflammation in HFD-fed C57BL/6 mice improving insulin resistance [406]. Together these studies show the relationship between HDL and insulin resistance.

Work from clinical trials indicates that increasing HDL levels is not always beneficial. This lack of direct relationship between HDL raising and beneficial cardioprotective effects is clear in trials investigating the effects of cholesteryl ester transfer protein (CETP) inhibition. CETP is a hydrophobic glycoprotein, primarily synthesized in the liver [407, 408]. Once secreted into the plasma, the role of CETP is to facilitate facilitates bidirectional cholesterol ester and triglyceride transfer between lipoproteins thereby redistributing these lipids, equilibrating them between different lipoprotein fractions (as reviewed by [409]). HDL levels are increased by CETP inhibitors indirectly by precluding cholesterol ester redistribution from plasma to lipoproteins other than HDL. This increases HDL cholesterol levels while reducing cholesterol ester concentration in pro-atherogenic lipoproteins such as LDL, VLDL, and chylomicrons. While this process increases HDL the Investigation of Lipid Level Management to Understand Its Impact in Atherosclerotic Events (ILLUMINATE) trial showed that the CETP inhibitor torcetrapib, was not cardioprotective despite significantly increasing HDL levels [410]. Further torcetrapib led to increased mortality and had off-target effects especially on blood pressure [410]. The CETP inhibitors dalcetrapib and evacetrapib, while not eliciting off-target events, also do not confer cardio-protective benefits despite increasing HDL levels by 31-40% [411] and 54-129% respectively [412]. Evacetrapib also failed to improve cardiovascular outcomes, and clinical trials have since been terminated [413]. Despite increasing HDL it can still be modified, its composition altered and consequently become dysfunctional under cellular stress [414-418].

Therefore investigation into the mechanisms by which HDL facilitates its initial inhibition of atherosclerosis and insulin resistance development before becoming dysfunctional may offer new approaches to treating these disease states.

1.9 The novel discovery of DHCR24 in HCAECs - HDL upregulates DHCR24 expression

Our laboratory's investigation into the mechanisms underlying HDL's suppression of a TNF-α-induced inflammatory response in HCAECs revealed a gene-regulatory effect [1]. HCAECs pre-treated with rHDL suppressed a TNF-α-induced inflammatory response, as indicated by decreases in NFκB and VCAM-1 mRNA levels. Intriguingly, the suppressive effect was retained for up to 8 hours after HDL removal prior to TNF-α treatment. Moreover, this effect was dependent on an increase in DHCR24 levels. It was also discovered that silencing DHCR24 in HCAECs abrogates rHDL's ability to suppress a TNF-α-induced inflammatory response. Microarray data also showed that DHCR24 is one of the most upregulated genes by HDL [1].

A)

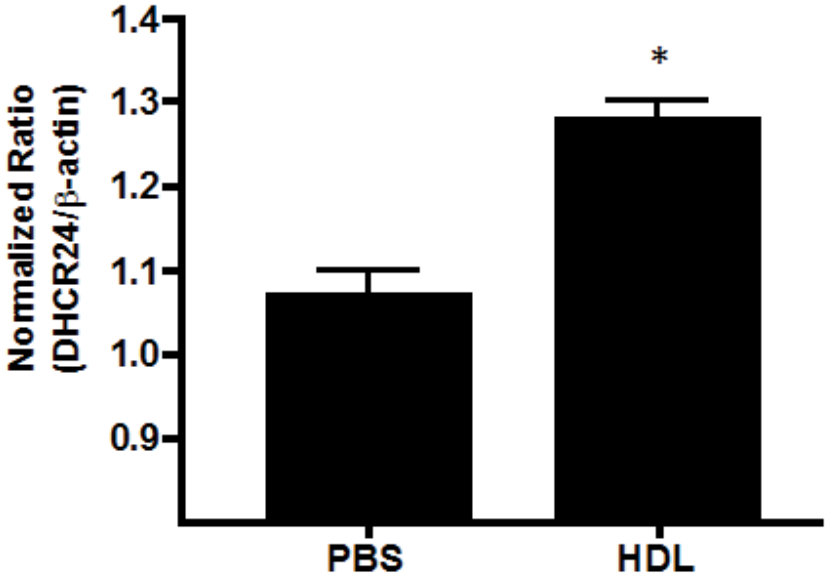

B)

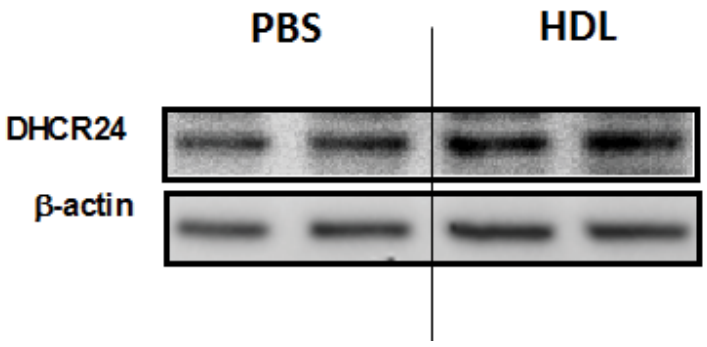

Figure 1.10 (A) DHCR24 levels were increased treated in HCAECs treated with apolipoprotein-I reconstituted high-density lipoprotein (apoA-I rHDL). HCAECs were treated with 16 µM (0.45 mg/mL) (apoA-I rHDL) for 16 hours **(B)** Western blot analysis of protein lysate extracted from HCAECs following 16 µM apoA-I rHDL treatment for 16 hours confirming the upregulation of DHCR24. * P<0.05.

1.10 What is DHCR24?

3β-hydroxysteroid-Δ24 reductase (DHCR24) is an enzyme essential for mammalian survival that has a number of key cellular roles. DHCR24 was initially discovered for its vital role in cholesterol biosynthesis, catalysing the conversion of desmosterol to cholesterol [419]. However, since then DHCR24 has also been shown to possess other roles in some cells types including protecting against oxidant [420, 421] and inflammatory insults [1, 422], and interacting with p53 [423, 424] or caspase-3 to prevent apoptosis [420, 421, 425-427].

DHCR24 is a 60.4kD flavin adenine dinucleotide (FAD)-dependent oxidoreductase [419] that is primarily localised to the ER in an N-terminal luminal/C-terminal cytoplasmic orientation [140]. The *dhcr24* gene includes 9 exons and 8 introns. The coding sequence is 1548 base pairs with an open reading frame of 516 amino acids. The *dhcr24* gene is localised to chromosome 1p31.1-p33 (Figure 1.11) [140, 419, 421, 428, 429].

The gene was identified and sequenced due to its similarity to sterol converting enzyme *diminuto-1* in the plants *Arabidopsis thaliana* and *Caenorhabditis elegans* [419, 421, 428]. *Diminuto-1* produces brassinosteriods which are plant sterols [430].

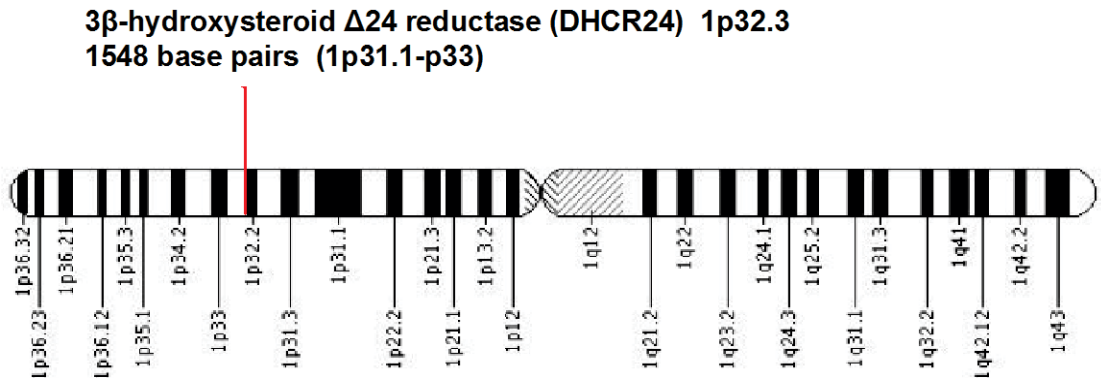

Figure 1.11 Chromosomal location of DHCR24 (1p32.3)

The encoded protein for *dhcr24* was discovered to be identical to the neuroprotective enzyme, **Sel**ective **A**lzheimer's **D**isease **In**dicator **1** (Seladin-1). This homology was based on a mutation analysis of the *dhcr24* gene, expressed in *Saccharomyces cerevisiae*, using human cDNA obtained from patients exhibiting various levels of desmosterolosis (a cholesterol deficiency syndrome resulting in accumulated desmosterol) [419].

Seladin-1 is expressed in pyramidal neurons of the brain particularly within cortical regions, the substantia nigra, caudate nucleus, hippocampus, medulla oblongata, and the spinal cord. Functional studies determined it was responsible for the biosynthesis and homeostasis of brain cholesterol [431, 432].

Low levels of seladin-1 are associated with Alzheimer's disease. Moreover, silencing of seladin-1 expression leads to the hallmark features associated with Alzheimer's disease [421, 428, 433, 434]. The discovery that *dhcr24* was identical to *seladin-1* set research into the protective functions of DHCR24 in motion [427, 428, 435].

1.10.1 The role of DHCR24 in cholesterol biosynthesis

Enzyme studies *in situ* and expression in *S. cerevisiae* showed the role of DHCR24 in catalysing the reduction of the Δ24 double bond of desmosterol to produce cholesterol [435]. DHCR24 is an important enzyme for the synthesis of cholesterol, however it is not a rate limiting enzyme. Instead, the amount of cholesterol produced is regulated by the availability of sterol precursors that enter the Bloch or Kandutsch-Russell pathway (Figure 1.12). Therefore, merely overexpressing DHCR24 is insufficient to increase cholesterol levels as DHCR24 serves as a catalyst for cholesterol production. This is consistent with observations that overexpression of DHCR24 increases cholesterol levels in some cells types while exerting no effect on others. This is attributed to varying levels of precursor molecules and differing cholesterol requirements of cells [420, 433].

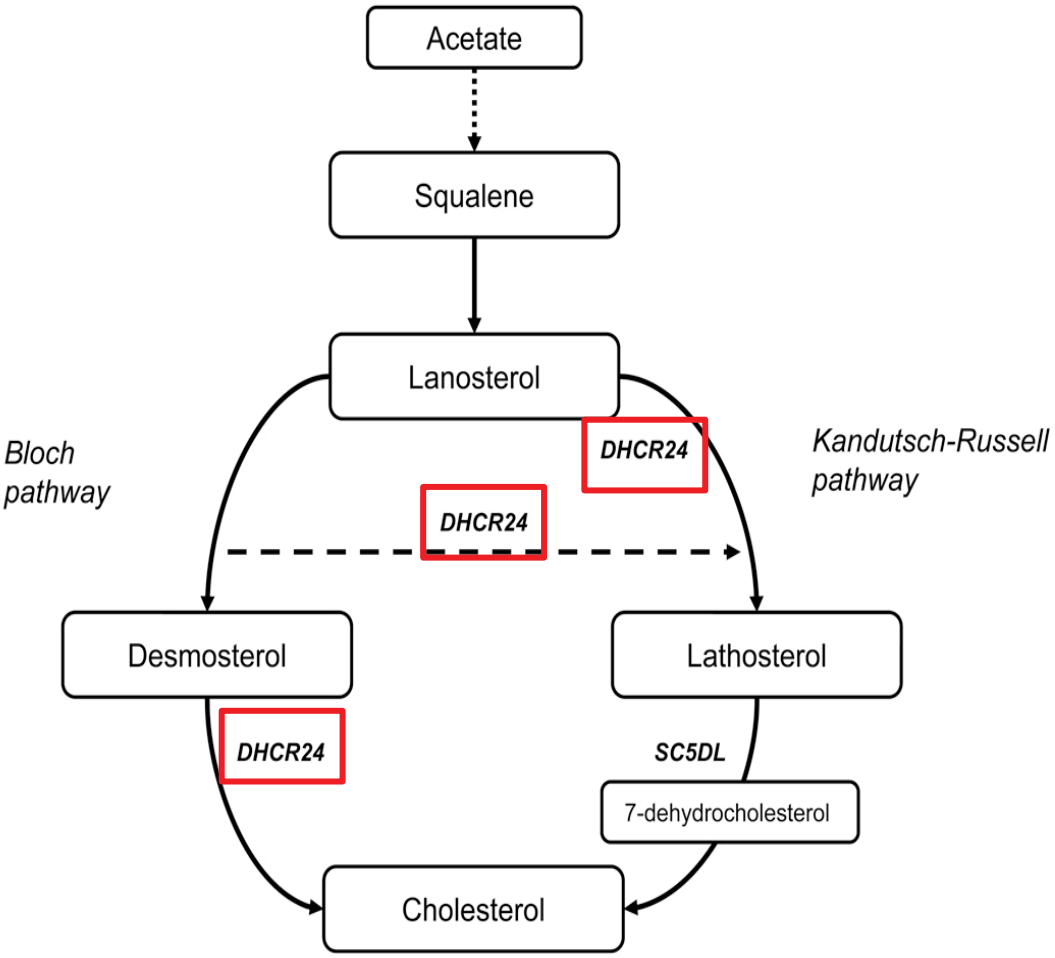

Figure 1.12 Cholesterol biosynthesis via the Bloch pathway and the Kandutsch-Russell pathway

Figure 1.12 (adapted from [436]) depicts the synthesis of cholesterol via the Bloch pathway and Kandutsch-Russell pathway. DHCR24 is identified by red boxes and is present during the conversion of desmosterol directly to cholesterol via the Bloch pathway, and during the conversion of desmosterol to lathosterol for further reactions to cholesterol.

In all cell types tested, DHCR24 is localised to the ER [140, 421, 435, 437], although it is also in the Golgi [421] and nucleus [438]. DHCR24 is located in the membrane facing the cytoplasmic side of the ER, with the N-terminal transmembrane domain being required for localisation to the ER membrane [140]. This ER localisation is in keeping with other enzymes involved in cholesterol synthesis (e.g. HMG-CoA reductase) [439] because the *de novo* pathway of cholesterol production is located on the cytoplasmic side of the ER membrane [140]. DHCR24 also possesses a FAD binding site and is a single-spanning protein [140, 429, 437], although it lacks a common consensus sequence for an NADPH binding site in its amino acid sequence despite its NADPH requirement for enzyme activity [435].

Patients demonstrating the multiple-congenital-anomaly syndrome, desmosterolosis that is caused by the accumulation of desmosterol, show mutations in the *dhcr24* gene [435, 440-445]. Desmosterolosis also leads to a deficiency in plasma membrane cholesterol. This is significant as cholesterol is essential to ensure the correct development of the human brain. Cells also require cholesterol to develop, differentiate, and function correctly [446].

Patients with desmosterolosis exhibit profound multiple congenital anomalies. The phenotypes observed in desmosterolosis patients vary yet share common features including brain malformations, facial feature abnormalities, and skeletal deformities [441-443].

A patient heterozygous for two *dhcr24* mutations who was spontaneously delivered after 34 weeks of gestation is described in the literature [441]. This patient exhibited the above-mentioned abnormalities. To investigate the role of DHCR24, the exons and flanking intronic sequences of the patient and her parent's *dhcr24* gene were sequenced. These revealed two novel heterozygous mutations in the patient, p.R94H and p.E480K amino acid substitutions. Using an evolutionary trace method, the p.R94H and p.E480K amino acid substitutions/*dhcr24* mutations were predicted to have significant effects on enzyme function. Expression of these mutants in *S. cerevisiae* confirmed this reduced enzyme activity, and showed that the p.R94H mutation is more severe than the p.E480K mutation. This may be attributed to the predicted localisation of p.R94H at the FAD binding site [441] and DHCR24 being a FAD-dependent oxidoreductase [435]. Both mutations caused DHCR24 enzyme activity to be significantly impaired resulting in lowered cholesterol levels, accumulation of desmosterol, as well as being attributed to the above-mentioned deformities [441].

In mice, complete knockout of the *dhcr24* gene, in combination with impaired maternal cholesterol transfer during embryonic development, is fatal [434]. Milder, non-lethal phenotypes of desmosterolosis in mice have also been produced. These milder phenotypes are attributed to maternal transfer of cholesterol aiding in embryonic development and reducing the severity of desmosterolosis [447]. Human Smith-Lemli-Optiz syndrome patients, while unable to synthesise cholesterol, have low levels of cholesterol in their tissues. This is attributed to maternal transfer of cholesterol. There is a correlation between maternal levels of cholesterol and fetal cholesterol levels [448, 449]. Furthermore, impaired maternal cholesterol transfer leads to more severe pathologies. For example, if a mother possesses an apo ε2 allele, which decreases the efficacy of LDL cholesterol binding to the LDL receptor, transfer is impaired and the foetus will have significantly reduced levels of maternal cholesterol transferred to it and, therefore, a more severe phenotype will be produced [450]. This demonstrates the integral role of cholesterol in the development the foetus and significance in the functions of the body.

High cholesterol levels in the membrane of DHCR24-expressing neuronal cells have been shown to protect cells against oxidative stress toxicity [438] and experimental stroke models by facilitating EAAT2's association with lipid rafts and subsequently its uptake of glutamate [451]. However, DHCR24 also facilitates directly protective effects, independent of cholesterol synthesis.

1.10.2 DHCR24 as a biomarker

The level of DHCR24 has been associated with the diagnosis of numerous diseases and as a stress marker *in vitro*. DHCR24 levels are low in the brain tissue of Huntington's disease mouse models [452] and in Huntington's disease post-mortem brain tissue [453]. DHCR24 levels are low in the CNS tissue of dementia patients [454], in hyponatremia-induced neuronal distressed in SH-SY5Y and SK-N-AS cells [455, 456] and in neuronal degeneration models. DHCR24 has been also identified as being low in Alzheimer's disease brain tissue as previously mentioned [421, 428, 433]. However, this area is contentious with some reports of DHCR24 failing to be differentially regulated in Alzheimer's disease brains [457, 458], and with DHCR24/Seladin-1 polymorphisms in Alzheimer's disease reported in some reports [459, 460] but not in all [461].

Further, reduced levels of DHCR24 in Alzheimer's disease tissues have been suggested to occur secondary to the disease and to not occur causatively [458].

DHCR24's involvement in various cancers is another area in which DHCR24 levels may be useful for diagnosis and prognosis of disease. DHCR24 is recently being considered as a molecular target for hepatitis C virus (HCV)-surface related hepatocellular carcinoma [462] and DHCR24 antibodies have been suggested as serum markers for HCV [463]. The level of DHCR24 is reflected in prostate cancer severity. DHCR24 levels are significantly reduced in metastatic castration-resistant prostate cancer in comparison to primary prostate cancer [464]. DHCR24 is increased in early and low-risk prostate cancer, yet decreased in advanced prostate cancer and metastasis [465, 466]. The decrease in DHCR24 levels in prostate cancer may be due to its involvement in proliferation. Therefore restoration of DHCR24 levels is proposed to potentially decrease cancer cell growth and steroid dependency in early and low-grade prostate cancer [466]. Increased DHCR24 levels are also prognostic for non-muscle-invasive urothelial carcinoma progression [467] while decreased DHCR24 levels have been associated with benign adenoma malignancy [468]. The heterogeneity of assorted cancers complicates the use of DHCR24 levels for diagnosis and each association between DHCR24 levels and cancer must be independently addressed.

1.10.3 DHCR24's effects against cellular stress

DHCR24 has been shown to facilitate suppression of stress responses in many cell types. Research to date has concentrated primarily on studies of neuronal or neuronal-like cells, because of its association with Alzheimer's disease.

DHCR24 facilitates reduction in oxidative stress in neuronal cells and subsequent induction of apoptosis, through the inhibition of caspase-3 [421, 425, 469]. DHCR24 (Seladin-1)-EGFP-cloned cells exposed to the oxidant H_2O_2 have significantly greater cell viability and rates of survival in comparison to control-EGFP cells. Cell death measured after 10 hours of H_2O_2 exposure was comparable between the control and DHCR24-expressing cells. However, following 16 hours of oxidant exposure, 80% of the DHCR24-expressing cells survived in comparison to only 52% of the control cells. This reduction of oxidative stress-induced apoptosis is facilitated by DHCR24 via caspase-3 inhibition. Initially both DHCR24-expressing

cells and control cells after 2 hours of H_2O_2 treatment show no caspase-3 activity in cell lysates, as measured by a caspase-3 assay kit utilising a fluorogenic substrate. However, after 4 hours of treatment, caspase-3 levels were significantly increased in control-EGFP cells in comparison to the DHCR24-expressing cells. The addition of a caspase-inhibitor lowered caspase-3 levels confirming that the observed reduction of oxidative stress-induced-apoptosis by DHCR24 expression is via caspase-3 inhibition [421]. The anti-oxidative and anti-apoptotic effects mediated by DHCR24 are also shown in neuronal cells treated with β-amyloid, the major oxidant in Alzheimer's disease implicated in the aetiology of the neurodegenerative disorder. DHCR24 is itself a substrate for caspases -3 and -6 [421], with caspase cleavage sites in its C-terminus resulting in the generation of a p40 product (Figure 1.13). This caspase-mediated cleavage releases DHCR24 into the cytoplasm, increasing free cytoplasmic DHCR24 levels which are associated with decreased levels of cellular ROS (Figure 1.13) [140]. These anti-oxidative and anti-apoptotic effects which are facilitated by DHCR24's inhibition of caspase-3 have been demonstrated in neuronal cells [421, 426, 469], human neuroblast long-term cell cultures [425], melanoma metastases [420], pituitary adenomas [427], and HUVEC [421].

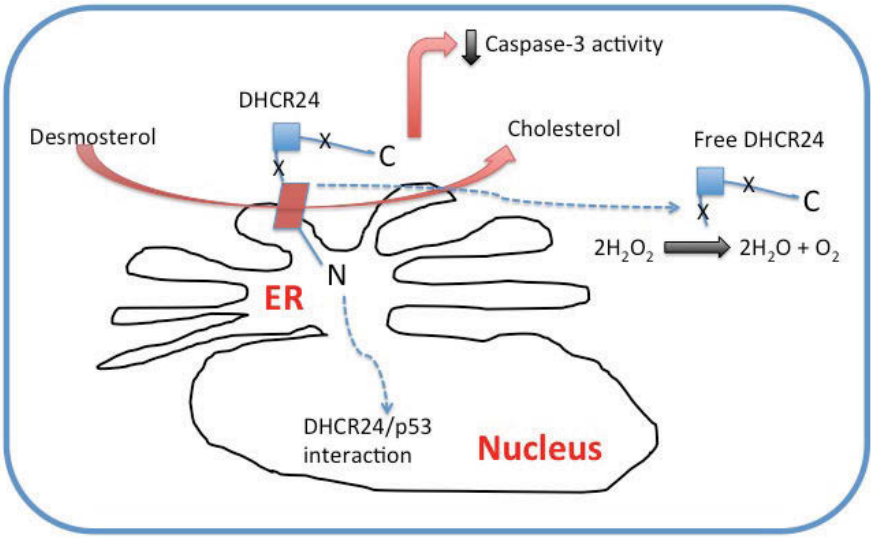

Figure 1.13 The activities of DHCR24. DHCR24 resides in the endoplasmic reticulum (ER), with the FAD binding domain (blue box) on the cytoplasmic side of the ER membrane. DHCR24 is tethered to the ER via its transmembrane region (red box). DHCR24 contains caspase cleavage sites and it may be that via caspase activity a free form of DHCR24 is generated. The membrane and free form potentially catalyse the catabolism of H_2O_2. Under oxidative stress, DHCR24 has been shown to translocate to the nucleus where it interacts with p53 and prevents apoptosis.

DHCR24 also possesses H_2O_2 scavenging ability, preventing apoptosis through the inhibition of the stress activated protein kinase (SAPK) cascade, independent of cholesterol synthesis [437]. SAPK activation can be triggered by ROS production and is characterised by augmented p38 MAPK and JNK levels, which lead to the induction of apoptosis signal regulating kinase 1 (ASK1). ASK1 is integral to the persistent activation of p38 MAPK and JNK and for the activation of apoptosis to occur in response to H_2O_2 exposure. In its quiescent form, ASK1 is bound to reduced thioredoxin. Oxidative stress causes the oxidation of thioredoxin which releases ASK1 from this bound inhibitory state. ASK1 is then activated through oligomer formation and auto-phosphorylation and apoptosis is executed [470]. DHCR24$^{-/-}$ mouse embryonic fibroblasts (MEFs) undergo apoptosis in response to H_2O_2 treatment as indicated by DNA fragmentation and confirmed by TUNEL staining. p38 MAPK, JNK and ASK1 are also strongly induced. However, wild type DHCR24-expressing MEFs resist oxidative stress-induced (H_2O_2) apoptosis, and in keeping with this, have weak activation of p38 MAPK and JNK, and barely detectable ASK1 activation. This anti-oxidative role of DHCR24 also occurs in MEF and pheochromocytoma PC12 cells (a rat adrenal medulla tumour-derived cell line) challenged with tunicamycin (an oxidative stress and ER stress inducer) [437]. Furthermore, these suppressive effects are facilitated by DHCR24 independent of cholesterol activity [437], in contrast to the hypothesis suggesting that increased cholesterol levels may suppress oxidative stress and the early stages of apoptosis [153]. The DHCR24$^{-/-}$ MEFs described above were treated with serum to prevent the influence of cholesterol depletion when exposed to H_2O_2 [437] as cholesterol withdrawal in MEFs causes susceptibility to apoptosis [471]. In the above experiments, apoptosis is prevented by treating with cholesterol, as indicated by no changes in proliferation occurring in DHCR24$^{-/-}$ MEFs as compared to wild type DHCR24$^{+/+}$ MEF [437]. This confirms that the anti-oxidant and anti-apoptotic activity facilitated by the presence of DHCR24 in these cells is cholesterol independent.

In all cell types investigated, DHCR24 is localised to the ER (Figure 1.13) [140, 421, 435, 437], although studies have shown that DHCR24 can also translocate to the nucleus in response to chronic oxidative stress stimuli in fibroblasts, suggesting a soluble isoform of the protein can be generated under appropriate conditions [472]. Furthermore, recombinant DHCR24 protein has been demonstrated to detoxify H_2O_2 with an activity approximately 7-fold less than that measured for catalase [437], providing evidence for a direct mechanism by which DHCR24 may decrease oxidative stress. In addition, the ER-localisation of DHCR24 is dependent on its N-terminal [421] while N-terminal deleted mutants of DHCR24 retain the ability to scavenge H_2O_2

in vitro [437] and H_2O_2-generated intracellular ROS *in vivo* following migration to the cytoplasm [140]. This indicates that it is the C-terminus which facilitates the anti-oxidative effects of the enzyme and provides scientific impetus in the potential to develop mimetic compounds for the treatment of oxidative stress.

Within the nucleus, DHCR24 binds to the tumour suppressor p53 and displaces the E3 ubiquitin ligase Mdm2 from p53, which allows p53 to accumulate in cells [423], serving to suppress oxidative stress and prevent cell transformation. This process of p53 accumulation occurs independently of DHCR24's oxidoreductase activity [423, 424]. In cases of chronic oxidative stress, DHCR24 levels diminish however, the suppressive effect is maintained through increased p53 ubiquitination stimulated by DHCR24 [473]. In cells exposed to oxidative and inflammatory stress, p53 activates DNA repair enzymes and induces growth arrest by holding cell cycle at G1/S so that the DNA repair enzymes can act [423]. Thus, DHCR24 through p53 can prevent cell death by activating p53-induced senescence and DNA repair (Figure 1.13). In acute responses, attenuation of DHCR24 in rat embryonic fibroblasts results in Ras-induced cell transformation as p53 accumulation is prevented. These cells exhibit condensed cellular morphology and form tumours two weeks after treatment with Ras. This demonstrates the role of DHCR24 in controlling oncogenic signalling is through control of p53. This activity is also replicated in human WI38 fibroblasts [423].

DHCR24-overexpression in HCAECs inhibits the activation of the key inflammatory mediator, nuclear factor kappa B (NFκB) [1, 422] and in a recent study it is proposed that this occurs through activation of the PI3K/Akt signal transduction pathway and induction of heme oxygenase-1 (HO-1) [422]. In addition to reproducing increased levels of DHCR24 in apoA-I-treated HCAECs, as reported during the novel discovery of DHCR24 in HCAECs [1], it was demonstrated that apoA-I increases HO-1 levels. Furthermore, when DHCR24 levels are knocked down with siDHCR24, there are significant reductions in both DHCR24 and HO-1 levels, while siHO-1 only reduces HO-1 levels following apoA-I treatment. This indicates that HO-1 induction is dependent on DHCR24. This is further supported by *in vivo* studies using New Zealand White rabbits with surgically implanted silastic carotid collars (to promote vascular inflammation). When DHCR24 levels are knocked down, apoA-I treatment is unable to increase the expression of HO-1. This upregulation of HO-1 is, at least in part, dependent on the phosphorylation of Akt by DHCR24 and the subsequent activation of PI3K [422]. Importantly activation of the PI3K/Akt prevents endothelial cell apoptosis [474]. In keeping with this, Akt

phosphorylation is also significantly attenuated in DHCR24$^{-/-}$ MEF in comparison to wild type MEFs [471].

The apoA-I upregulation of DHCR24 and HO-1 is also dependent on SR-B1 and its adaptor protein PDZK1. This is apparent as HCAECs transfected with siRNA for SR-B1 and PDZK1 before being treated with apoA-I do not have increased levels of DHCR24 or HO-1. The metabolic product, bilirubin formed by HO-1, also reduces levels of inflammation (VCAM-1, ICAM-1) and the translocation of the NFκB p65 subunit, thereby mediating the protective effects of apoA-I. However importantly, the induction of HO-1 (and therefore its metabolic products), by apoA-I treatment is dependent on increased DHCR24 expression [422]. This establishes an important interaction between DHCR24 and HO-1 in the protection against inflammatory insults.

Atherosclerosis and insulin resistance are strongly associated with the features and markers that DHCR24 has been reported to reduce – inflammation [1, 422], oxidation, ER stress and apoptosis [420, 421, 437, 471, 475]. Currently, there has been no published research on characterising DHCR24's potential role in suppressing *in vitro* cellular stress in HCAECs or HuH7 cells. Therefore, this project aims to delineate the mechanisms behind DHCR24's suppressive effects in HCAECs and HuH7 cells. This basic knowledge is essential for advancing DHCR24 as a therapeutic target and perhaps using the DHCR24 protein as the foundation for an oxidoreductase mimetic.

1.11 Summary, Aims, and Hypotheses

The work presented initially set out to examine if DHCR24 suppresses a TNF-α-induced inflammatory response in HCAECs. This investigation was based on the protective effect of HDL and its upregulation of DHCR24 levels in HCAECs [1]. This thesis shows that DHCR24 plays an important role in HCAECs replicating the effect of apoA-I rHDL. The mechanisms behind this effect were then investigated and identified. Insulin resistance is also an inflammatory condition [60, 62, 84] and can lead to the development of atherosclerosis. Arising from the positive findings in HCAECs, and the protective effect of HDL against hepatic inflammation which improves insulin sensitivity [406], DHCR24 was investigated in HuH7 cells. DHCR24 was shown to be upregulated by, and to replicate apoA-I rHDL's effects against a TNF-α-induced inflammatory response in HuH7 cells. The mechanisms underlying DHCR24's effect in HuH7 cells were investigated and are interestingly shown to be slightly different to the mechanisms in HCAECs. The differences reported may be potentially due to the higher cholesterol content of HuH7 cells. The overall aim of this project was to characterise the role of DHCR24 against a TNF-α-induced inflammatory response in HCAECs and HuH7 cells.

The encompassing hypothesis of this thesis is:

"DHCR24 coordinates suppressive mechanisms against a TNF-α-induced inflammatory response in HCAECs and HuH7 cells"

The data in Chapter 3 show that DHCR24 suppresses a TNF-α-induced inflammatory response in HCAECs. This is evidenced by reducing monocyte adhesion to HCAECs. This shows that DHCR24, at least in part, can replicate the effect of rHDL. Chapter 4 explores the mechanisms underlying DHCR24's suppressive effects against cellular stress in HCAECs. This study shows that DHCR24 suppresses TNF-α-induced VCAM-1 levels in a fashion that is independent of cholesterol biosynthesis. However, the effect does require the oxidoreductase site present in the N-terminal region of DHCR24. Interestingly, DHCR24 is an ER-associated protein and the mechanisms through which DHCR24 exerts protection involves suppressing an ER stress response, but yet under TNF-α-stimulated conditions, DHCR24 can be found in the cytoplasm and in the nucleus.

In Chapter 5, DHCR24's role in HuH7 cells was pursued. The data presented show that DHCR24 mediates HDL's suppression of TNF-α-induced IL-8 levels. Further, DHCR24 overexpression alone suppressed TNF-α-induced IL-8 expression showing that DHCR24, at least in part, can

replicate the effect of rHDL. In Chapter 6, the mechanisms through which DHCR24 mediates suppressive effects against cellular stress in HuH7 cells were pursued. DHCR24's suppression of TNF-α-induced IL-8 levels was demonstrated to be independent of cholesterol biosynthesis, yet the effect requires the oxidoreductase site present in the N-terminal region of DHCR24. Additionally, the work showed that despite DHCR24's association with the ER, its suppression of TNF-α-induced IL-8 levels was independent of DHCR24 regulating a TNF-α-induced ER stress response. Further, DHCR24 was found to move to the nucleus following cytokine activation, and a role preventing TNF-α-induced apoptosis was identified.

Finally, Chapter 7 discusses the results in the context of the wider scientific literatures and then presents a general conclusion of the results. Finally several limitations of the study are discussed, as well as potential future work and questions arising from this thesis.

Specific aims:

Chapter 3

- To determine if DHCR24 replicates the effect of apoA-I rHDL against a TNF-α-induced inflammatory response in HCAECs
- To determine whether DHCR24 overexpression reduces monocyte adhesion to HCAECs
- To determine whether DHCR24 overexpression suppresses TNF-α-induced ICAM-1 and VCAM-1 protein levels in HCAECs
- To determine whether DHCR24 overexpression suppresses TNF-α-induced VCAM-1 mRNA levels in HCAECs

Chapter 4

- To determine the mechanisms by which DHCR24 overexpression suppresses a TNF-α-induced inflammatory response in HCAECs
- To determine whether DHCR24 overexpression increases cholesterol levels in HCAECs
- To determine whether DHCR24's oxidoreductase site is required for the suppression of a TNF-α-induced inflammatory response in HCAECs
- To determine whether DHCR24 translocates from the ER to the cytoplasm and nucleus in response to TNF-α-activation in HCAECs
- To determine the effect of TNF-α treatment on DHCR24 levels in HCAECs

- To determine whether DHCR24 mediates suppression of a TNF-α-induced inflammatory response through suppression of a ER stress response in HCAECs

Chapter 5

- To determine if DHCR24 mRNA levels are increased in HuH7 cells following apoA-I rHDL treatment
- To determine if DHCR24 mediates HDL's suppression of TNF-α-induced IL-8 levels in HuH7 cells
- To determine the effect of TNF-α treatment on DHCR24 levels in HuH7 cells
- To determine whether DHCR24 can replicate the suppressive effect of rHDL against TNF-α-induced IL-8 expression in HuH7 cells

Chapter 6

- To determine the mechanisms by which DHCR24 overexpression suppresses a TNF-α-induced inflammatory response in HuH7 cells
- To determine whether DHCR24 overexpression increases cholesterol levels in HuH7 cells
- To determine whether DHCR24's oxidoreductase site is required for the suppression of a TNF-α-induced inflammatory response in HuH7 cells
- To determine DHCR24's localisation in DHCR24 following TNF-α-activation
- To determine whether DHCR24 inhibits apoptosis in HuH7 cells and if so, is its oxidoreductase region required.
- To determine if DHCR24 mediates suppression of a TNF-α-induced inflammatory response through suppression of a ER stress response in HuH7 cells.

Chapter 2 – General Methods

Table 2.1 List of reagents

Reagent	Manufacturer	Origin
18S primer (human)	GeneWorks	Thebarton, SA, Australia
1-bromo-3-chloropropane	Sigma-Aldrich	Castle Hill, NSW, Australia
1-palmitoyl-2-linoleoyl-*sn*-glycero-3-phosphatidylcholine (PLPC)	Avanti Polar Lipids	Alabaster, AL, USA
2,2'-Azinobis [3-ethylbenzothiazoline-6-sulfonic acid]-diammonium salt (ABTS)	Kirkegaard & Perry Lab (KPL)	Gaithersburg, Maryland, USA
3,3'-diaminobenzidine (DAB)	Dako	Botany, NSW, Australia
4',6-diamidino-2-phenylindole (Dapi)	Life Technologies	Carlsbad, CA, USA
ABTS solution	Kirkegaard & Perry Lab (KPL)	Gaithersburg, Maryland, USA
ABTS stop solution	Kirkegaard & Perry Lab (KPL)	Gaithersburg, Maryland, USA
Agar	Sigma-Aldrich	Castle Hill, NSW, Australia
Alexa Fluor 568 anti-GRP78 goat primary antibody	Invitrogen	Mulgrave, VIC, Australia
AlexaFluor488 Phalloidin	Life Technologies	Carlsbad, CA, USA
Amplex Red Cholesterol Assay	Life Technologies	Carlsbad, CA, USA
Anti-goat secondary antibody	Life Technologies	Carlsbad, CA, USA
Autologously donated human plasma	Gribbles Pathology	Adelaide, South Australia
BCA protein assay kit	Bio-Rad	CA, USA
Beta-2 Microglobulin (β2M) primer (human)	GeneWorks	Thebarton, SA, Australia
Bis-Tris Polyacrylamide Gel	Invitrogen	Mulgrave, VIC, Australia
Bovine anti-goat IgG conjugated to HRP	Santa Cruz Biotechnology	Dallas, Texas, US

BSA	Sigma-Aldrich	Castle Hill, NSW, Australia
Cell Death Detection ELISA PLUS	Roche	Basel, Switzerland
CellTrace™ Calcein Green-AM	Invitrogen	Mulgrave, VIC, Australia
DH5α competent *E. coli* cells	Thermo Fisher Scientific	MA, USA
DHCR24 primer (human)	GeneWorks	Thebarton, SA, Australia
DHCR24 siRNA (siDHCR24)	Santa Cruz Biotechnology	Dallas, Texas, US
DPX mountant	Merck Millipore	Carlsbad, CA, USA
Dulbecco's minimum essential medium (DMEM)	Sigma-Aldrich	Castle Hill, NSW, Australia
EDTA-Na_2	Sigma-Aldrich	Castle Hill, NSW, Australia
Experion RNA StdSens Analysis Kit	Bio-Rad	CA, USA
Falcon Tubes	Corning	Corning, NY, USA
FD3510 fluorodishes	WPI Europe	Hitchin, United Kingdom
Fetal Bovine Serum (FBS)	Sigma-Aldrich	Castle Hill, NSW, Australia
GAPDH primer (human)	GeneWorks	Thebarton, SA, Australia
GenElute Endotoxin-Free Plasmid Midi-Prep Kit	Sigma-Aldrich	Castle Hill, NSW, Australia
Goat polyclonal anti-DHCR24 IgG	Santa Cruz Biotechnology	Dallas, Texas, US
Hank's buffered salts solution (HBSS)	Sigma-Aldrich	Castle Hill, NSW, Australia
HBSS (phenol-red free)	Sigma-Aldrich	Castle Hill, NSW, Australia
HiPerfect transfection reagent	Qiagen	Hilden, Germany
HuH7 cells	Health Science Research Resources Bank	Osaka, Japan
Human coronary artery endothelial cells (HCAECs)	Cell Applications	San Diego, CA, USA
Human IL-8 ELISA kit	Invitrogen	Mulgrave, VIC, Australia

iBlot Dry Blotting System	Invitrogen	Mulgrave, VIC, Australia
ICAM-1 antibody (anti-human CD54)	BD Biosciences	North Ryde, NSW, AUSTRALIA
IL-8 primer (human)	GeneWorks	Thebarton, SA, Australia
Interferon gamma (IFN-γ)	Sigma-Aldrich	Castle Hill, NSW, Australia
Interleukin 1-beta (IL-1β)	Sigma-Aldrich	Castle Hill, NSW, Australia
iQ SYBR Green I Supermix	Bio-Rad	CA, USA
iQ SYBR Green I supermix	Bio-Rad	CA, USA
iScript cDNA Synthesis	Bio-Rad	CA, USA
Kaleidoscope Protein Ladder	Bio-Rad	CA, USA
Lab-Tek II chamber slides	Lab-Tek	Naperville, IL, USA
Loading buffer	Bio-Rad	CA, USA
Lymphoprep	Nycomed Pharma	Roskilde, Denmark
MesoEndo Cell Growth Medium	Cell Applications	San Diego, CA, USA
Mouse monoclonal anti-β-actin IgG	Amersham Biosciences	Little Chalfont, United Kingdom
NaCl	Sigma-Aldrich	Castle Hill, NSW, Australia
NH_4HCO_3	Sigma-Aldrich	Castle Hill, NSW, Australia
Nonidet P-40	Sigma-Aldrich	Castle Hill, NSW, Australia
n-propyl gallate (NPG)	Sigma-Aldrich	Castle Hill, NSW, Australia
Nuclease-free water	Bio-Rad	CA, USA
NuPAGE MES SDS Running Buffer	Invitrogen	Mulgrave, VIC, Australia
Optima LE-80K Ultracentrifuge	Beckman Coulter	Fullarton, CA,USA
PBS	Astral Scientific	Taren Point, NSW, Australia
pcDNA 3.1A(-)/myc-His	Invitrogen	Mulgrave, VIC, Australia

pEGFP-N1	Clontech–Takara Bio	Otsu, Japan
Peripheral blood	Australian Red Cross Blood Service	Sydney, NSW, Australia
Protein dye reagent	Bio-Rad	CA, USA
PureZol	Bio-Rad	CA, USA
PVDF (polyvinylidene fluoride) membrane	Invitrogen	Mulgrave, VIC, Australia
RPMI powder	Sigma-Aldrich	Castle Hill, NSW, Australia
SDS-polyacrylamide PhastGels	Amersham Biosciences	Little Chalfont, United Kingdom
Sheep anti-mouse IgG conjugated to HRP	GE Healthcare	Uppsala, Sweden
siRNA	Qiagen	Hilden, Germany
Sodium dodecyl sulfate (SDS)	Sigma-Aldrich	Castle Hill, NSW, Australia
T75 cm^2 tissue culture flasks	Corning	Corning, NY, USA
TransPass HUVEC Transfection Reagent	New England Biolabs	Ipswich, MA, USA
Trypsin-EDTA	Thermo Fisher Scientific	MA, USA
Tryptone	Sigma-Aldrich	Castle Hill, NSW, Australia
Tumour necrosis factor alpha (TNF-α)	Sigma-Aldrich	Castle Hill, NSW, Australia
Tween 20	Sigma-Aldrich	Castle Hill, NSW, Australia
VCAM-1 antibody (anti-human CD106)	BD Biosciences	North Ryde, NSW, Australia
VCAM-1 primer (human)	GeneWorks	Thebarton, SA, Australia
Western blot stripping buffer	Thermo Fisher Scientific	MA, USA
Western Lightning Plus – ECL (Enhanced Chemiluminescence) Substrate	Perkin Elmer	Rowville, VIC, Australia

White blood cell concentrates	Australian Red Cross Blood Service	Sydney, NSW, Australia
Wright's stain	Diff-Quik, Laboratory Aids	NSW, Australia
Yeast Extract	Sigma-Aldrich	Castle Hill, NSW, Australia
β2-mercaptoethanol	Bio-Rad	CA, USA

2.1 Cell culture

2.1.1 Cell culture conditions and cell maintenance

Human coronary artery endothelial cells (HCAECs) purchased from Cell Applications were cultured in MesoEndo Cell Growth Medium (Cell Applications) at 37 ^{o}C and 5% CO_2 humidity. For HCAECs, cell passages used were limited between 4 and 7 as HCAECs are primary cells.

Human hepatoma (HuH7) cells obtained from the Health Science Research Resources Bank, Osaka, Japan were cultured in Dulbecco's minimum essential medium (DMEM) (Sigma-Aldrich) supplemented with 10% (v/v) FBS (Sigma-Aldrich) at 37 ^{o}C and 5% CO_2 humidity. For HuH7 cells, cell passages used were limited between 20 and 25 (cell line).

Cells were grown in T75 cm^2 flasks to a confluency of 80-90% before being passaged into fresh flasks. Passaging the cells involved removing the existing media and performing a brief wash using phosphate buffered saline (PBS). This was followed by a 5 minute incubation with trypsin-EDTA (Thermo Fisher Scientific) (enough to cover the flask surface) at 37 ^{o}C and 5% CO_2 in order to dislodge the cells from the flask surface. The trypsin-EDTA was then inactivated by the addition of an equal or greater amount of serum-containing media. The detached cells were then transferred to 50 mL centrifuge tubes and centrifuged at 2500 RPM over 5 minutes into a pellet. The supernatant was aspirated while the retained cell pellet was carefully resuspended using media. The cells were either passaged or adjusted to an appropriate concentration before seeding onto plates (section 2.1.2) for RT-qPCR, ELISA, western blot, flow cytometry, cholesterol quantitation, and microscopy experiments.

2.1.2 Cell counting

Cells were counted for the purposes of seeding appropriate cell amounts into wells. HCAECs cells were adjusted to a concentration of $1x10^5$ cells/mL (using MesoEndo Cell Growth Medium) 24 hours prior to being transfected or treated. HuH7 cells were adjusted to a concentration of $1.5x10^5$ cells/mL (using DMEM + 10% (v/v) FBS) 24 hours prior to being transfected or treated.

Cell suspensions were seeded into 6-well, 12-well, or 96-well plates dependent on the experiment (detailed in subsections). For microscopy, cell suspensions were seeded onto 4-well Lab-Tek II chamber slides (Lab-Tek) or FD3510 fluorodishes (WPI Europe). Cells were maintained at the cell culture conditions described in section 2.1.1 (37 ^oC at 5% CO_2 humidity). Cell counting was undertaken using a Neubauer haemocytometer (Figure 2.1).

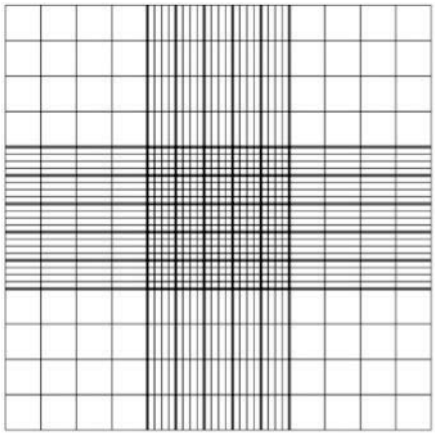

Number of cells per mL = Average number of cells counted from 4 corners (grey area) of the counting chamber X 10^4

E.g. If an average of 10 cells were present in all 4 squares, the number of cells would then be $1.0x10^5$ cells/mL.

Figure 2.1. Counting cells using the Neubauer haemocytometer. The shaded regions in the figure above represent the boxes that were counted and averaged out to calculate the concentration of the cells.

2.2 Plasmids

2.2.1 Wild type DHCR24

To overexpress DHCR24, DHCR24 cDNA (1.55 kb) was cloned into pcDNA 3.1A(-)/myc-His (pcDNA3.1A) (Invitrogen) plasmid vector at restriction sites EcoRI and XhoI and transformed into DH5α competent *E. coli* cells (Figure 2.2) (Thermo Fisher Scientific). The entire coding sequence of human DHCR24 cDNA was amplified by PCR using sense primer 5'-GAATTCGCCACCATGGAGCCCGCCGTGTCGCTGGCC-3' and antisense primer 5'-CTCGAGGTGCCTGGCGGCCTTGCAGATCTTGTC-3' (*Eco*RI site, translation start site, and *Xho*I site are *underlined*). A Kozak sequence was introduced in the sense primer. The stop codon was deleted in the antisense primer. The amplified cDNA was cloned into the *Eco*RI-*Xho*I site of pcDNA3.1A plasmid.

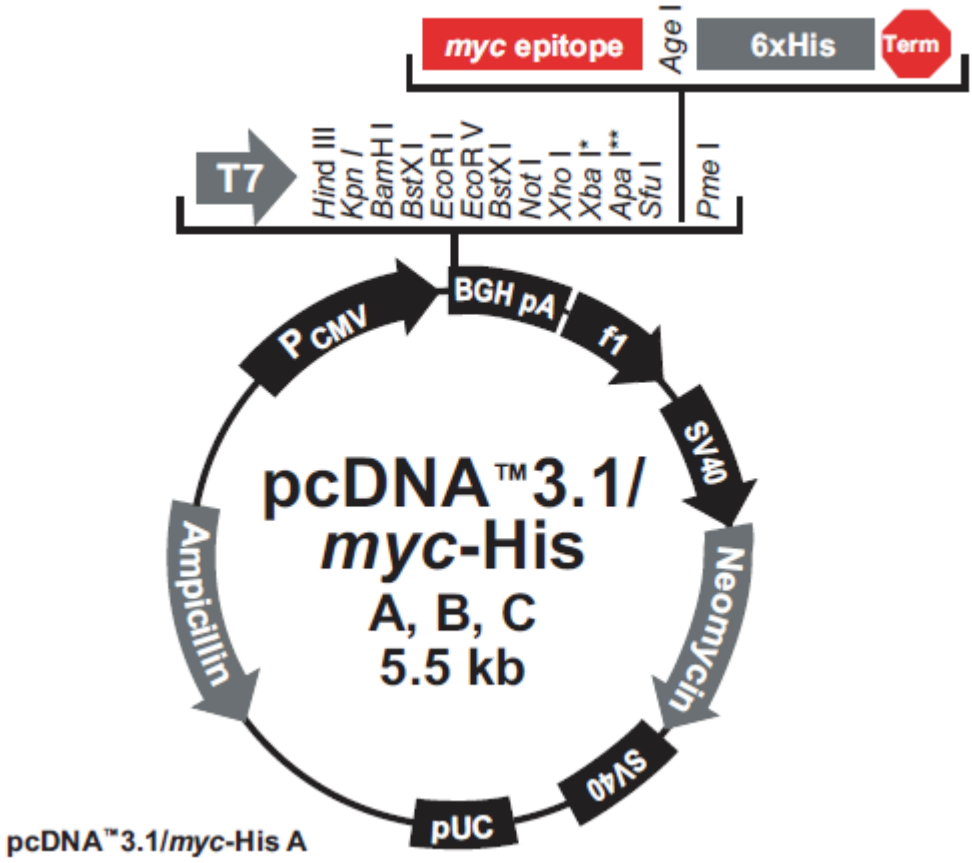

Figure 2.2 pcDNA 3.1A(-)/myc-His plasmid vector. DHCR24 cDNA (1.55 kb) was cloned into pcDNA 3.1A(-)/myc-His vector at restriction sites EcoRI and XhoI and transformed into DH5α competent *E. coli* cells. (Figure adapted from Invitrogen pcDNA™ user manual, catalog no. V800-20, page 3.)

2.2.2 DHCR24-EGFP

For fluorescent microscopy, a DHCR24-EGFP fusion plasmid was produced by Genscript based on [140]. Briefly, the entire cloning sequence of human DHCR24 cDNA was amplified and cloned into the XhoI-EcoRI site of plasmid pEGFP-N1 (Clontech–Takara Bio) (Figure 2.3) using:

PCR sense primer 5'-CTCGAGGCCACCATGGAGCCCGCCGTGTCGCTGGCC-3'

Antisense primer 5'-GAATTCGGTGCCTGGCGGCCTTGCAGATCTTGTC-3'

Additionally, a KOZAK sequence was introduced in the sense primer, and stop codon deleted in the anti-sense primer.

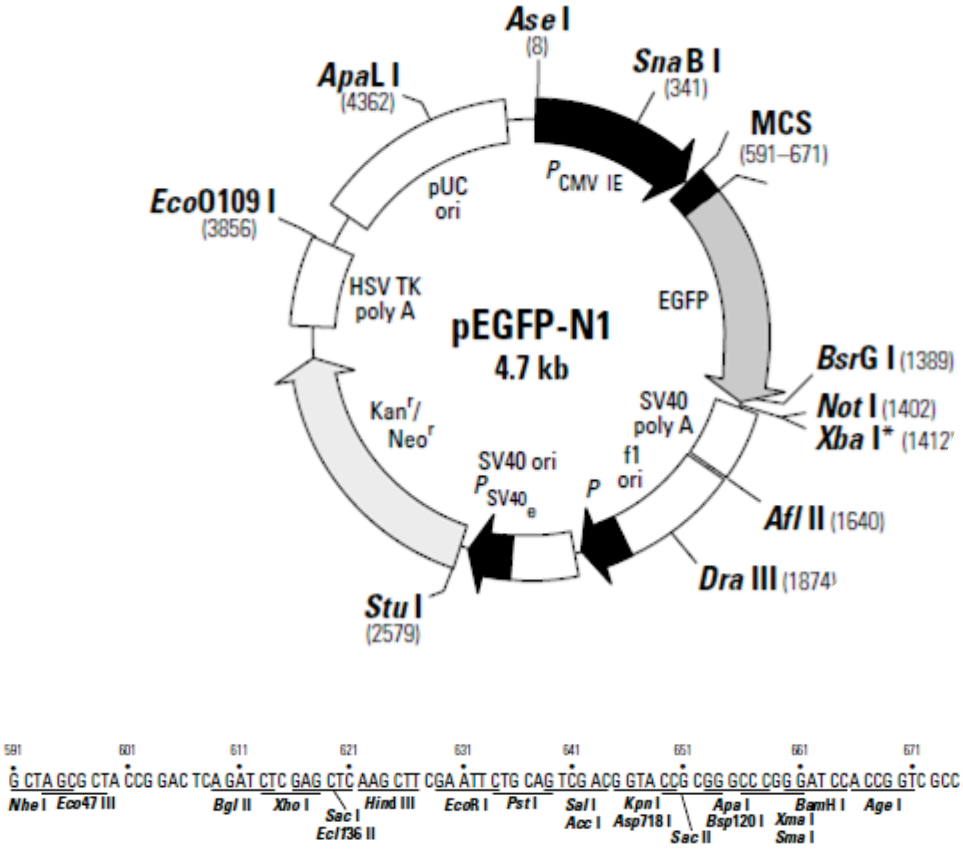

Figure 2.3 pEGFP-N1 plasmid vector. DHCR24 cDNA (1.55 kb) was cloned into pEGFP-N1 plasmid vector at restriction sites EcoRI and XhoI and transformed into DH5α competent *E. coli* cells. (Figure adapted from CLONTECH Laboratories, Inc user manual, version PR93631, page 1.)

2.2.3 DHCR24 oxidoreductase mutant

From the pcDNA3.1A-DHCR24 clone, a double mutant (N294T/K306N) was generated by Genscript from the wild type DHCR24 template using site-directed mutagenesis and cloned into the pcDNA 3.1A(-)/myc-His plasmid vector (Figure 2.4) based on [435]. The coding strand primer sequences to generate the mutant are:

N294T: 5'-GAGCCCAGCAAGCTGACTAGCATTGGCAATTAC-3'

K306N: 5'-GCCGTGGTTCTTTAACCATGTGGAGAACTATCTG-3'

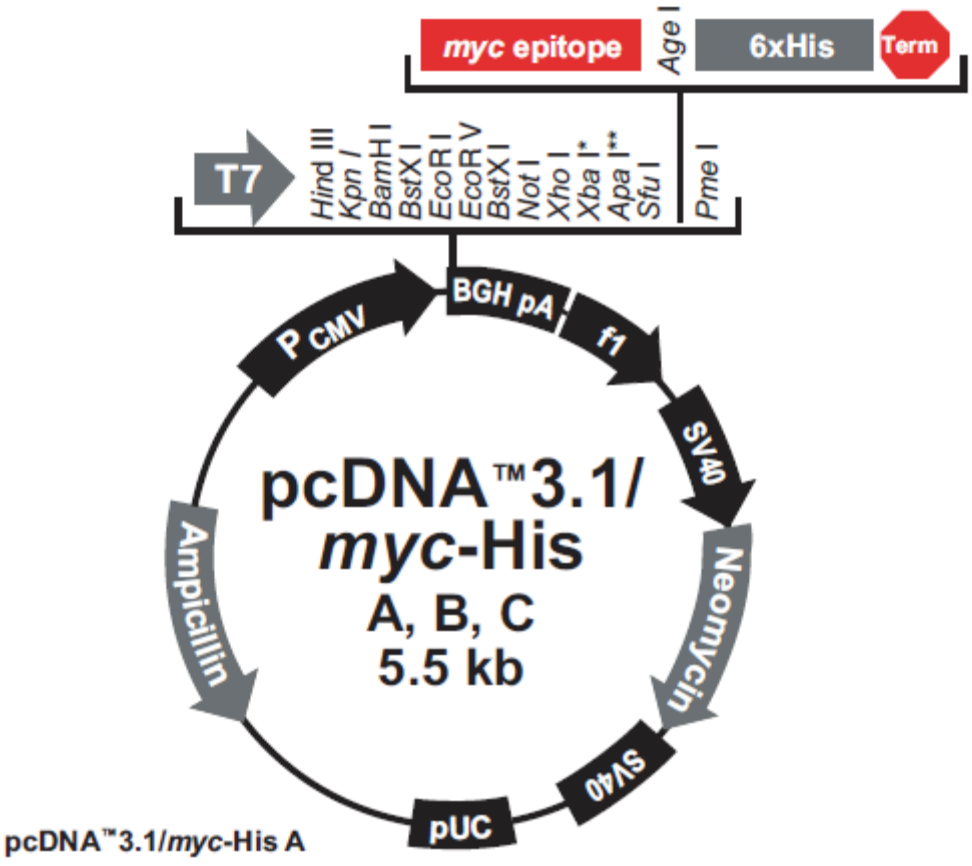

Figure 2.4 pcDNA 3.1A(-)/myc-His plasmid vector. Using site-directed mutagenesis DHCR24-double mutant (N294T/K306N) cDNA (1.55 kb) was generated, cloned into pcDNA 3.1A(-)/myc-His vector at restriction sites EcoRI and XhoI and transformed into DH5α competent *E. coli* cells. (Figure adapted from Invitrogen pcDNA™ user manual, catalog no. V800-20, page 3.)

2.3 Plasmid purification for transfection

2.3.1 Materials

LB-medium (ampicillin/kanamycin)

NaCl	10 g
Tryptone	10 g
Yeast extract	5 g

Dissolved in 1 L deionised water, autoclaved, and cooled to 55 ^{o}C before adding ampicillin (100 µg/mL) or kanamycin (50 µg/mL) and left to cool at room temperature.

LB-agar (ampicillin/kanamycin)

NaCl	10 g
Tryptone	10 g
Yeast extract	5 g
Agar	15 g

Dissolved in 1 L deionised water, autoclaved, and cooled to 55 ^{o}C before adding ampicillin (100 µg/mL)) or kanamycin (50 µg/mL) and left to cool at room temperature.

2.3.2 Plasmid preparation

All of the vectors were purified using the GenElute Endotoxin-Free Plasmid Midi-Prep Kit (Sigma-Aldrich), following the manufacturer's instructions. Briefly, transformed DH5α competent *E. coli* cells were grown on LB agar with ampicillin (100 µg/mL) (wild type DHCR24 and DHCR24 oxidoreductase mutant) or kanamycin (50 µg/mL) (DHCR24-EGFP). Single colonies were grown for 16 hours in 50 mL of LB broth at 37 ^{o}C, 225 RPM. The next morning cells were pelleted at 3000 RPM for 10 minutes. Supernatant was discarded and the cell pellet resuspended with resuspension solution (1.2 mL) before being incubated in lysis solution (1.2 mL) for 5 minutes. Following the lysis step, neutralization solution (0.8 mL) was added and mixed by gentle inversion, before pelleting debris at 15000 RPM for 15 minutes. Cleared lysate was transferred to a clean tube and endotoxin removal solution (300 µL) was added, mixed, and chilled on ice for 5 minutes to remove endotoxins. The solution was then incubated in a 37 ^{o}C water bath for 5 minutes, and centrifuged at 5000 RPM for 5 minutes. The separated clear upper phase was transferred to a clean tube and the endotoxin removal step was repeated. The resulting solution was then mixed with DNA binding solution (800 µL), transferred into a midi binding column inserted in a collection tube, and centrifuged at 5000 RPM for 2 minutes to bind plasmid DNA to the column. To remove contaminants from the plasmid preparation, flow through was discarded and the optional wash solution (2 mL) added to the column before being centrifuged at 5000 RPM for 5 minutes, and discarding flow through. Following the optional wash, wash solution (3 mL) was added to the column and centrifuged at 5000 RPM for 5 minutes. Flow through was discarded and the column transferred to a new collection tube. Endotoxin-free water was added to the column and centrifuged at 5000 RPM for 5 minutes to elute purified plasmid DNA. Plasmid DNA concentration was then quantified and quality assessed using a UV spectrophotometer at A_{260}/A_{280} nm (Nanodrop 1000, Thermo Scientific). A 260/280 ratio of approximately 1.8 was accepted for downstream applications of the purified plasmid. qPCR was used to confirm successful plasmid DNA purification.

2.4 Transfection

2.4.1 Overexpression of DHCR24 by transient transfection using TransPass HUVEC Transfection Reagent

Twenty-four hours prior to transfection, cells were seeded at a cell density of $1x10^5$ cells/mL in MesoEndo Growth Medium for HCAECs, and $1.5x10^5$ cells/mL in DMEM + 10% (v/v) FBS for HuH7 cells (section 2.1.2). Before each transfection was performed, a qualitative assessment of the seeded cells using a light microscope was performed, ensuring the cells displayed normal morphology. According to the manufacturer's protocol (New England Biolabs), cells were transiently transfected with pDHCR24 (inserted into pcDNA3.1A), pControl (empty pcDNA3.1A vector), pDHCR24-N294T/K306N, or pDHCR24-EGFP expression vectors using TransPass HUVEC Transfection Reagent (New England Biolabs). A mixture of plasmid DNA and TransPass reagents were prepared in serum-free medium in accordance with the manufacturer's protocol in Table 2.2. This mixture was added drop-wise onto the cells and incubated for 24 hours (37 ^{o}C and 5% CO_2 humidity). Following this incubation period, the culture medium was changed and the cells were allowed to recover for a further 24 hours in which time DHCR24/*dhcr24* expression is increased.

Table 2.2 Transfection with pDHCR24 using TransPass HUVEC Transfection Reagent

Components	Amount in 1 mL of growth medium
Plasmid DNA	**1.6 µg**
Serum-free DMEM	**150 µL**
HUVEC Reagent Component	**1 µL**
TransPass V	**2 µL**
Total transfection volume	**153 µL**

2.4.2 Suppression of DHCR24 by transient transfection using siRNA HiPerfect transfection reagent

DHCR24 knockdown using HiPerfect transfection reagent (Qiagen) involved creating separate mixtures of the silencing DHCR24 siRNA (siDHCR24) (Santa Cruz Biotechnology) or silencing control siRNA (siControl) (Qiagen) and adding them to serum-free DMEM (Table 2.3). To knockdown DHCR24, siDHCR24 consisting of a 10 μmol siRNA pool of 19-25 nucleotides targeted against 3-5 targets specific to DHCR24 was purchased from Qiagen. Knockdown of DHCR24 was then achieved using HiPerfect transfection reagent (Qiagen). A silencing control siRNA (siControl) of a 10 μmol siRNA pool of 20-25 mixed nucleotides consisting of scrambled sequences which do not lead to specific degradation was used for sham transfection. HiPerfect transfection reagent was added and following vortexing, the transfection mix was incubated for 10 minutes. The transfection mix was then added onto cells drop-wise. After a 6 hour incubation, cells were rinsed with PBS, before the addition of fresh growth medium. Cells were incubated for a further 24 hours in which time DHCR24 expression is decreased.

Table 2.3 siDHCR24 in HuH7 cells using HiPerfect Transfection Reagent

Components	Amount in 1 mL of growth medium
siRNA	**20 μL**
Serum-free DMEM	**80 μL**
HiPerfect	**9 μL**
Total transfection volume	**109 μL**

2.5 Treatments

2.5.1 Preparation of Bovine Serum Albumin (BSA)-conjugated free fatty acids (FFA)

Free fatty acids (FFA) (oleic acid, palmitic acid, stearic acid) were dissolved using appropriate solvents (Table 2.4) and conjugated to 10% (w/v) bovine serum albumin (BSA) (Sigma-Aldrich) in DMEM. Each FFA was first prepared to a working stock concentration of 100 mM. The FFAs were alternated between vortexing and heating the solutions to 55 ^{o}C in a water bath until they were completely dissolved. A 10% (w/v) solution of BSA was prepared in DMEM and syringe filtered through 0.4 μm filter. The FFAs were then conjugated to 10% (v/v) BSA in DMEM making up a working stock concentration of 10 mM using the heating and vortexing methodology described above and syringe filtration was repeated (0.4 μm).

Table 2.4 FFA diluents

Free Fatty Acid (FFA)	Solvent
Oleic acid	Isopropanol
Palmitic acid	Water
Stearic acid	Ethanol

2.5.2 Cytokine cocktail preparation

Working stocks of tumour necrosis factor alpha (TNF-α), interferon gamma (IFN-γ) and interleukin 1-beta (IL-1β) (Sigma-Aldrich) were freshly prepared in nuclease free water (Bio-Rad) before each treatment. The cytokine stocks were diluted to 0.1 ng/mL (working stock concentration). Table 2.5 shows the dilutions carried out for each cytokine.

Table 2.5 Cytokine dilutions

Cytokine	Stock conc (ng/mL)	Dilution
TNF-α	10	1:10
IL-1β	10	1:10
IFN-γ	200	1:2000

2.5.3 Preparation of apolipoprotein I (apoA-I) reconstituted high-density lipoproteins (rHDL)

Using pooled samples of autologously donated human plasma (Gribbles Pathology) apoA-I was isolated and purified through sequential isopycnic ultracentrifugation (Beckman Coulter), and anion exchange chromatography as described by [476]. Plasma density was adjusted using KBr and sequential isopycnic ultracentrifugation at the upper limit density range was performed at 55000 RPM at 4 ^{o}C in a 55.2Ti rotor (Optima LE-80K Ultracentrifuge) (Beckman Coulter) to ensure the dissociation of higher density proteins. The collected d<1.21 g/mL fraction was dialysed against 5 mM NH_4HCO_3/1 mM EDTA-Na_2 (Sigma-Aldrich) before being lyophilised for 5 hours. The HDL was then dried in N_2, dissolved in 20 mM Tris (pH 8.2), pooled, and lyophilised.

ApoA-I was isolated using the Q-Sepharose Fast Flow column (GE Healthcare) attached to a FPLC/AKTA system (Amersham Biosciences). ApoA-I was reconstituted in 20 mM Tris/6 M Urea (pH 8.5, Buffer A) and loaded into the Buffer A pre-equilibrated column. The apolipoproteins were eluted at a flow rate 3 mL/min using a continuous gradient of Buffer B (20 mM Tris/6 M Urea/0.2 M NaCl; 0.40% Buffer B over 5 min, 40-48% Buffer B over 70 min, 48-70% Buffer B over 110 min). Following on, the collected fractions were electrophoresed on homogenous 20% (w/v) SDS-polyacrylamide PhastGels (Amersham Biosciences). ApoA-I and apoA-II showed a single band after Coomassie R-350 staining (Amersham Biosciences). Purified apoA-I and apoA-II were dialysed against 20 mM NH_4HCO_3, and then again in endotoxin-free PBS for 2 days ensuring that the reconstituted apolipoproteins were endotoxin-free. ApoA-I was then lyophilised and stored at -20 ^{o}C until needed.

Prior to use, apoA-I was reconstituted in 10 mM Tris-HCl, 3.0 M guanidine-HCl, 0.01% (w/v) EDTA-Na_2 (pH 8.2) and dialysed against Tris Buffered saline (TBS), pH 7.4 (5 x 1 L), containing 10 mM Tris HCl, 150 mM NaCl, 0.006% (w/v) NaN_3, and 0.0005% (w/v) EDTA-Na_2.

Discoidal rHDL containing apoA-I was complexed to 1-palmitoyl-2-linoleoyl-*sn*-glycero-3-phosphatidylcholine (PLPC) (Avanti Polar Lipids) using the cholate dialysis method [477]. Briefly, PLPC was reconstituted in chloroform:methanol (2:1 v/v) before being dried in glass test tubes under N_2 and lyophilised overnight. Following lyophilisation, the PLPC was dissolved in sodium cholate (30 mg/mL in TBS, pH 7.4) and made up to a volume of 500 µL using TBS. The dissolved solution was subsequently vortexed (every 15 minutes) and kept on ice until the solution became clear. ApoA-I was then added to the PLPC:cholate tubes at a 100:1 molar ratio

of PLPC:apoA-I and then left on ice for 2 hours before being pooled and dialysed against TBS (5 x 1 L) over 5 days to remove the cholate. Prior to use in experiments, rHDL preparations were dialysed extensively against endotoxin-free PBS (pH 7.4) (Sigma-Aldrich).

2.6 Cell treatment conditions

2.6.1 Treatment conditions in HCAECs

Following transient transfection of HCAECs with pcDNA3.1A (pControl), pcDNA3.1A-DHCR24 (pDHCR24), or pDHCR24-N294T/K306N (pN294T/K306N) using TransPass HUVEC reagent, cells were activated with TNF-α 2.5 ng/mL for 4 hours for protein analysis using ELISA (section 2.8), and mRNA analysis using RT-qPCR (section 2.10 – 2.14).

To assess the effect of DHCR24 on monocyte adhesion (section 2.7), pControl or pDHCR24-transfected HCAECs were treated with H_2O_2 (100 µM) or TNF-α (1 ng/mL) for 4 hours.

To analyse DHCR24 localisation using immunocytochemistry (section 2.16), HCAECs were treated with PBS (control) or TNF-α (1 ng/mL) for 4 hours, and apoA-I rHDL (16 µM/0.45 mg/mL) for 16 hours.

For DHCR24 localisation experiments using fluorescent microscopy (section 2.17), HCAECs were transfected with pDHCR24-EGFP and treated with TNF-α (2.5 ng/mL).

Cells treated with PBS or no treatment were also included for each experiment as vehicle controls for comparison with the treatment groups. Cells were incubated with treatments at 37 ^{o}C under 5% CO_2 for 4 hours before analysis as described in section 2.1.1.

2.6.2 Treatment conditions in HuH7 cells

Following transient transfection of HuH7 cells with pcDNA3.1A (pControl), pcDNA3.1A-DHCR24 (pDHCR24), or pDHCR24-N294T/K306N (pN294T/K306N) using TransPass HUVEC reagent, cells were activated with TNF-α 5 ng/mL for 4 hours for protein analysis using ELISA (section 2.8), and mRNA analysis using RT-qPCR (section 2.10 – 2.14).

To analyse DHCR24 localisation using immunocytochemistry (section 2.16), HuH7 cells were treated with PBS (control) or TNF-α (5 ng/mL) for 4 hours.

Apoptosis was induced in HuH7 cells transfected with pControl, pDHCR24, or pDHCR24-N294T/K306N by treating with TNF-α (15 ng/mL) for 18 hours (section 2.18).

Cells treated with PBS or no treatment were also included for each experiment as vehicle controls for comparison with the treatment groups. Cells were incubated with treatments at 37 ^{o}C under 5% CO_2 for 4 hours before analysis as described in section 2.1.1.

2.6.2.3 Treatment of DHCR24 knocked down HuH7 cells

To elucidate whether DHCR24 mediates the anti-inflammatory effects of apoA-I rHDL in HuH7 cells, knockdown of DHCR24 expression was carried out. siDHCR24 HuH7 (HiPerfect) were treated for 3 hours with FFAs and the cytokine cocktail (TNF-α, IFN-γ, IL-1β) (1 ng/mL) and with FFAs and TNF-α (5 ng/mL). Cells were treated with A-I rHDL at half-physiological concentrations (16 µM) 16 hours prior to the addition of the inflammatory stimuli.

2.6.2.4 ApoA-I rHDL treatment of HuH7 cells

HuH7 cells were treated with 16 µM apoA-I rHDL (half-physiological concentrations) for 16 hours. PBS was used as vehicle control.

2.6.2.5 Cell treatment of transfected HuH7 cells using cytokine cocktail and FFA

Following transient transfection of HuH7s with pcDNA3.1A-DHCR24 (pDHCR24) or pcDNA3.1A (pControl) using TransPass HUVEC reagent, cells were exposed to inflammatory conditions. Free fatty acids (FFA) (oleic, palmitic, stearic) at lipid loading ratios/concentrations (3:1:1) (300 mM, 100 mM, 100 mM) were used to treat the cells with a cytokine cocktail (TNF-α, IFN-γ, IL-1β) (1 ng/mL) or FFAs were used with TNF-α (5 ng/mL) over 3 hours in 12-well plates. Total RNA was subsequently extracted using PureZol (Bio-Rad) (section 2.10). To assess DHCR24 mRNA levels, reverse transcription real time PCR (RT-qPCR) was used (section 2.11 – 2.14). Cells transfected with pControl acted as the control.

2.7 Monocyte adhesion assay

2.7.1 Materials

Phenol-red free RPMI Medium (pH 7.5)

Modified RPMI powder (Sigma-Aldrich)	10.4 g
$NaHCO_3$	2 g

Dissolved in 1 L of Baxter water and filtered through a VacuCap 90 Filter with a 0.22 µm Supor Membrane (Pall Corporation).

2.7.2 Method

2.7.2.1 Isolation and labelling of human monocytes with Calcein Green-AM

Peripheral blood from healthy donors from the Australian Red Cross Blood Service was used to obtain white blood cell concentrates. Monocytes were isolated by density gradient ultracentrifugation using Lymphoprep (Nycomed Pharma), followed by counterflow centrifugation elutriation at 20 ^{o}C using a centrifuge equipped with an elutriation chamber (Beckman Instruments) within 24 hours of obtaining peripheral blood. Elutriation tubes and the rotor were both rinsed with 250 mL each of 70% (v/v) ethanol, 6% (w/v) hydrogen peroxide, elutriation buffer, and endotoxin-free water. The elutriation buffer contained Hank's buffered salts solution (HBSS) (Sigma-Aldrich) supplemented with EDTA (0.1 g/L) and 1% (w/v) heat-inactivated human serum.

The separated mononuclear cell fraction was subsequently loaded into the elutriation chamber before being centrifuged at 2000 RPM at 20 ^{o}C, with the tubing flow rate set at 9 mL/min. Every 10 minutes, the flow rate was increased by 1 mL/min. The effluent was then collected between 15-18 mL/min in separate fractions. Wright's stain-Diff Quik (Laboratory Aids) and Cytospin system was used to examine the collected monocyte fractions for purity. Monocyte fractions with purity >90% were considered as acceptable provided that cell viability exceeded 95% as assessed by Trypan blue exclusion. Monocytes were resuspended in phenol

red-free RPMI and ready for adhesion assay. Prior to use in the monocyte adhesion assay, monocytes were loaded with CellTrace™ Calcein Green-AM (5 µM) (Invitrogen) for 30 minutes at 37 ^{o}C. Following incubation, cells were washed with PBS to remove excess compound and resuspended using RPMI medium to cell density of 3x10^{6} cells/mL.

2.7.2.2 Monocyte adhesion assay procedure

HCAECs were seeded (1x10^{5} cells/mL) as per the conditions described in section 2.1.2 24 hours prior to transfection. The cells were then transfected as per section 2.4.1 with pcDNA3.1A (pControl), pcDNA3.1A-DHCR24 (pDHCR24), or pDHCR24-N294T/K306N (pDHCR24-N294T/K306N) expression plasmids. Transfectants were then stimulated with TNF-α (2.5 ng/mL) or H_2O_2 (100 µM) for 4 hours. Following incubation, media was removed and the cells were washed twice with PBS. Monocytes (1 mL) loaded with Calcein Green were then to each well containing a HCAECs monolayer and incubated for 1 hour at 37 ^{o}C. After incubation, the cells were gently washed using the medium contained in each well to remove unattached monocytes. Then the medium containing unattached monocytes was then aspirated before the addition of fresh RPMI medium (1 mL). Plates were read at an excitation wavelength of 494 nm and an emission wavelength of 517 nm using Flexstation 3 plate reader (Molecular Devices). The amount of fluorescence emitted from each well was proportional to the amount of monocytes adhered to the endothelial cell layer.

2.8 Enzyme-linked immunosorbent assay (ELISA)

2.8.1 Materials

Hank's buffered salts solution (HBSS)

HBSS (phenol-red free) (Sigma-Aldrich) was mixed additionally with:

Na_2CO_3	0.35 g
EDTA	0.10 g

Dissolved in a total volume of 1 L deionised water (pH 7) and filtered through a VacuCap 90 (Pall Corporation) and filtered with a 0.22 µm Supor Membrane (Pall Corporation).

HBSS/0.05% (v/v) Tween 20 (for washing)

HBSS	100 mL
Tween 20	50 µL

HBSS/10% (v/v) Human Serum (HS) (Primary antibody diluent)

HBSS	9 mL
Human serum (HS)	1 mL

HBSS/10% (v/v) Human Serum/0.05% (v/v) Tween 20 (Secondary antibody diluent)

HBSS	9 mL
Human serum (HS)	1 mL
Tween 20	50 µL

2.8.2 Method

2.8.2.1 VCAM-1, ICAM-1 ELISA protocol

HCAECs were seeded as per the conditions described in section 2.1.2 24 hours prior to transfection. The cells were then transfected as per section 2.4.1 with pcDNA3.1A (pControl), pcDNA3.1A-DHCR24 (pDHCR24), or pDHCR24-N294T/K306N (pDHCR24-N294T/K306N) expression plasmids. Transfectants were then stimulated with TNF-α (5 ng/mL) for 4 hours. Following cell treatment, media was removed and cells were washed three times with HBSS (Sigma-Aldrich). VCAM-1 antibody (anti-human CD106) (BD Biosciences)/ICAM-1 antibody (anti-human CD54) (BD Biosciences) was diluted in HBSS/10% (v/v) HS (1:500) and added to cells (100 µL per well). IgG control was diluted with HBSS/10% (v/v) HS and added to separate wells (100 µL). Cells were next incubated on ice for 30 minutes. Following incubation cells were washed with HBSS/0.05% (v/v) Tween 20 three times before adding the secondary antibody (sheep anti-mouse-HRP (GE Healthcare) (diluted 1:500 in HBSS/10% HS (v/v)/Tween 20; 100 µL), and incubating on ice for a further 30 minutes. Following incubation with the secondary antibody, cells were washed with HBSS/0.05% (v/v) Tween 20 three times. Finally, 2,2'-Azinobis [3-ethylbenzothiazoline-6-sulfonic acid]-diammonium salt (ABTS) (KPL) (150 µL) was added and cells incubated at room temperature for approximately 10-15 minutes for colour to develop. The reaction was stopped by the addition of 10% (v/v) acetic acid (50 µL). Absorbance was measured using with a Tecan Infinite 200 plate reader (Tecan) at wavelength of 405 nm.

2.8.2.2 IL-8 ELISA protocol

HCAECs were seeded as per the conditions described in section 2.1.2 24 hours prior to transfection. The cells were then transfected as per section 2.4.1 with pcDNA3.1A (pControl), pcDNA3.1A-DHCR24 (pDHCR24), or pDHCR24-N294T/K306N (pDHCR24-N294T/K306N) expression plasmids. Transfectants were then stimulated with TNF-α (5 ng/mL) for 4 hours.) Following completion of cell treatment, supernatant was collected from HuH7 cells, and IL-8 protein levels were measured using the Human IL-8 ELISA kit (Invitrogen) following manufacturer's instructions (Invitrogen). Briefly, 50 µL of collected sample supernatant (diluted 1:4), IL-8 standards (for a standard curve), and chromogen control were added to microtitre wells. Biotinylated anti-IL-8 solution (50 µL) was then added to each of the wells (except the chromogen). The plate was tapped gently to mix the solutions, covered with a plate cover and incubated for 1 hour and 30 minutes at room temperature. Following the incubation period, solution was removed and the wells washed four times with wash buffer before addition of streptavidin-HRP working solution (100 µL) to each of the wells (except the chromogen). The plate was then covered and incubated for a further 30 minutes at room temperature. After the streptavidin-HRP working solution incubation, solution was removed and the wells washed four times with wash buffer before stabilised chromogen (100 µL) was added to each of the cells. The plate was incubated at room temperature in the dark for 30 minutes for colour to develop. Once colour was developed, stop solution (100 µL) was added to the wells and gently mixed by tapping. Absorbance was measured with a Tecan Infinite 200 plate reader (Tecan) at wavelength of 450 nm. Background absorbance was subtracted from the obtained O.D. values, and IL-8 protein levels were determined using the IL-8 standard curve.

2.9 Protein extraction

2.9.1 Materials

RIPA lysis buffer

Nonidet P-40	1% (w/v)
Sodium dodecyl sulfate (SDS)	0.1% (w/v)
Deoxycholate	0.5% (w/v)
NaCl	150 mM
Tris (pH 8)	50 mM

Dissolved in a total volume of 1 L deionised water (pH 7) and stored at 4 ^{o}C. Protease inhibitor (1 µg/mL) (Sigma-Aldrich) was added to the buffer at 1:100 dilution prior to use.

5x Protein loading buffer

Tris-HCl (pH 6.8)	62.5 mM
SDS	2% (w/v)
β2-mercaptoethanol	5% (w/v)
Glycerol	20% (w/v)
Bromophenol blue	0.05% (w/v)

Dissolved in a total volume of 1 L deionised water (pH 7).

1x Protein electrophoresis buffer

Tris	3 g
Glycine	14.4 g
SDS	1 g

Dissolved in a total volume of 1 L deionised water (pH 7).

2.9.2 Method

2.9.2.1 Protein extraction

Whole cell protein lysate was extracted using RIPA lysis buffer (Sigma-Aldrich). Briefly, the culture medium was aspirated, the wells were washed twice with cold PBS and an appropriate volume of RIPA lysis buffer (200 µL per well for a 12-well plate) was added to the wells. Cells were scraped into a lysate using sterile scrapers and transferred into sterile polypropylene tubes. Following a 30 minute incubation on ice, the cell lysates were briefly vortexed and then the tubes were centrifuged at 14000 RPM at 4 ^{o}C for 10 minutes. After centrifugation, the protein retained in the supernatant was collected and transferred into new sterile polypropylene tubes for protein quantification or stored at -80 ^{o}C for downstream applications.

2.9.2.2 Protein quantification

Protein concentrations were quantified using the BCA protein assay kit (Bio-Rad). A standard curve was formed using 1:2 serial dilutions of 10 mg/mL BSA (Sigma-Aldrich). Aliquots (10 µL) of each BSA standard and protein lysate sample were then pipetted into the individual wells of a clear 96-well plate. Protein dye reagent (Bio-Rad) was prepared by diluting 1 part dye concentrate with 4 parts deionised water. The dye was added into each well (190 µL/well), followed by incubation at room temperature for 5 minutes for the colour to develop. Absorbance was measured with a Tecan infinite 200 plate reader at a wavelength of 595 nm.
To determine the protein concentrations of the samples, a standard curve was produced using the absorbance of the samples against the BSA standards.

2.9.2.3 Polyacrylamide gel electrophoresis (PAGE)

After quantifying the protein samples, 10 µg of total protein lysates were run in polyacrylamide gel electrophoresis (PAGE). Each protein sample was diluted with 5x protein sample loading buffer before being denatured by heating at 95 ^{o}C for 5 minutes and immediately after placed onto ice. Proteins were then separated by molecular weight by loading sample into separate wells of a 10% w/v Bis-Tris Polyacrylamide Gel (Invitrogen). The

gel was used to separate proteins between 30 to 100 kDa. Kaleidoscope Protein Ladder (10 µL) of (Bio-Rad) was also added into one of the wells. Finally, gels were run by electrophoresis loaded with 11x NuPAGE MES SDS Running Buffer (Invitrogen) for 1 hour at ~120-150V until separation of the ladder was observed.

2.9.2.4 Western blot analysis

Following PAGE, proteins were transferred onto a PVDF (polyvinylidene fluoride) membrane (Invitrogen) using the iBlot™ Dry Blotting System (Invitrogen) for 7-minute transfers according to the manufacturer's instructions. After transferring to the membrane, non-specific sites on the membrane were blocked using 5% (w/v) skim milk solution for 1 hour at room temperature. After blocking, skim milk solution was removed and the membrane washed three times with 1x TBST (5 minutes each wash). The membrane was then incubated overnight with primary antibody at 4 ^{o}C (see Table 2.6 for antibody dilutions). Following the incubation period, the primary antibody was removed and then the membrane was washed three times with 1x TBST (5 minutes each wash). After washing, the membrane was then incubated with the secondary antibody conjugated to horseradish peroxidase (HRP) for 2 hours at room temperature. The membrane was washed again three times with 1x TBST (5 minutes each wash) and then incubated with Western Lightning Plus – ECL (Enhanced Chemiluminescence) Substrate (Perkin Elmer) protected from light for 1 minute. Excess ECL reagent was drained and placed into a sample bag.

Protein bands were detected and their densities quantified using a ChemiDoc XRS (Bio-Rad) imaging system using the Quantity One™ software (Bio-Rad). The membrane was re-probed for β-actin expression to control for protein loading. Briefly, the membrane was incubated in Western Blot Stripping Buffer (Thermo Fisher Scientific) for 30 minutes at room temperature while rocking and then washed three times in 1x TBST (5 minutes each wash). The membrane was then blocked with 5% (w/v) skim milk. Immunoblotting was performed as described above.

Table 2.6 Primary and secondary antibody dilutions used for Western blotting

Primary Antibody	Size (kDa)	Dilution	Secondary Antibody	Dilution
Goat polyclonal anti-DHCR24 IgG (Santa Cruz Biotechnology)	60	1:500	Bovine anti-goat IgG conjugated to HRP (Santa Cruz Biotechnology)	1:10000
Mouse monoclonal anti-β-actin IgG (Amersham Life Sciences)	43	1:1000	Sheep anti-mouse IgG conjugated to HRP (GE Healthcare)	1:10000

2.10 Total RNA isolation

Total RNA was isolated using PureZol (Bio-Rad). Briefly, the medium was aspirated and an appropriate volume of PureZol was added to the wells (1 mL for a 6-well plate or 0.5 mL for a 12-well plate). Cells were scraped into a lysate using sterile scrapers and transferred into sterile polypropylene tubes. Following a 5-minute incubation at room temperature (to allow complete dissolution of nucleoprotein complexes), 1/10 volume (100 μL for 6-well plates, 50 μL for 12-well plates) of 1-bromo-3-chloropropane (Sigma-Aldrich) was added to each tube and then vortexed for at least 15 seconds. The mixture was incubated for 5 minutes at room temperature with vigorous vortexing every 2-3 minutes. The tubes were then centrifuged at 14000 RPM at 4 ^{o}C for 15 minutes. Centrifugation separated out the RNA into the aqueous top phase, DNA into the interphase (middle phase) and protein into the organic bottom phase. The aqueous top phase was immediately transferred into fresh tubes and 0.5 volume of isopropanol added (500 μL for 1 mL PureZol used – 6-well plate, 250 μL for 0.5 mL PureZol used – 12-well plate). Each tube was vigorously vortexed for at least 15 seconds and stored overnight at -20 ^{o}C to allow precipitation of the RNA. After the overnight precipitation step, the tubes were centrifuged at 14000 RPM at 4 ^{o}C for 10 minutes. The supernatant was then removed and the pellet was washed with 0.5 volume of ice-cold 75% (v/v) ethanol. The pellet was then vortexed and centrifuged again at 14000 RPM at 4 ^{o}C for 5 minutes. The supernatant was discarded and the RNA pellet briefly air-dried (5-10 minutes). The RNA pellet was then resuspended in 25 μL of nuclease-free water (Bio-Rad). RNA was quantified using a UV spectrophotometer at A_{230}/A_{260} nm (Nanodrop 1000, Thermo Scientific). The RNA was then stored at -80 ^{o}C for downstream applications.

2.11 RNA quality check using the Experion System

Total RNA quality was assessed prior to further analysis using the Experion RNA StdSens Analysis Kit (Bio-Rad) (an automated electrophoresis system) according to the manufacturer's instructions. Briefly, an aliquot of RNA ladder (Bio-Rad) or RNA sample (3 μL) was denatured by heating at 70 ^{o}C for 3 minutes and then an immediate 5-minute incubation on an ice block. The Experion RNA StdSens Chip (Bio-Rad) was primed by loading 9 μL of filtered gel-strain into the appropriately labeled gel priming well on a StDSens Chip and placed into a priming station at setting 1B for thirty seconds. After this priming step, gel stain was added to another gel stain well and then each remaining well was loaded with 5 μL of loading buffer (Bio-Rad). After adding the loading buffer, 1 μL of denatured RNA ladder and each RNA sample was added into the marked wells. The loaded chip was placed onto an automated vortex station (Bio-Rad) for 1 minute and then transferred onto the electrophoresis station (Bio-Rad) for analysis.

Results from this analysis are represented as a virtual gel and an electropherogram showing the bands and peaks of the RNA ladder and samples (Figure 2.5). The electropherogram of the RNA ladder generates nine individual peaks, each indicative of the various sizes of the RNA ladder. The first peak represents 18S ribosomal RNA and the second (higher peak) represents 28S ribosomal RNA. A peak with two separate individual peaks and a low baseline is characteristic of a good quality RNA sample. The virtual gel will also have two bands, with the 18S band being double the thickness of the 28S band when RNA quality is good.

a)

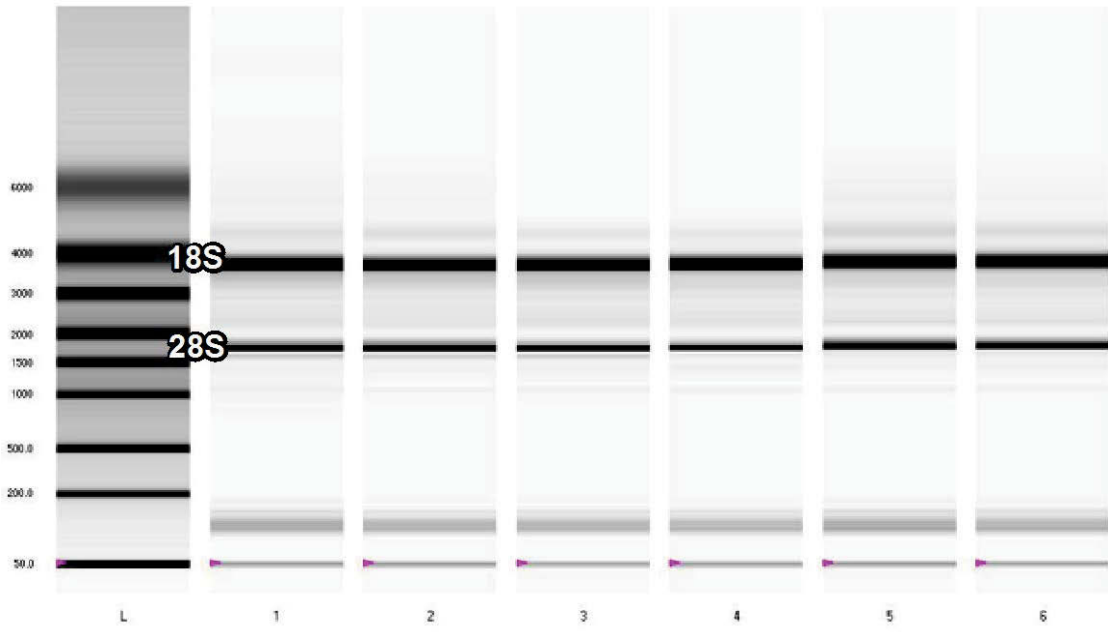

b)

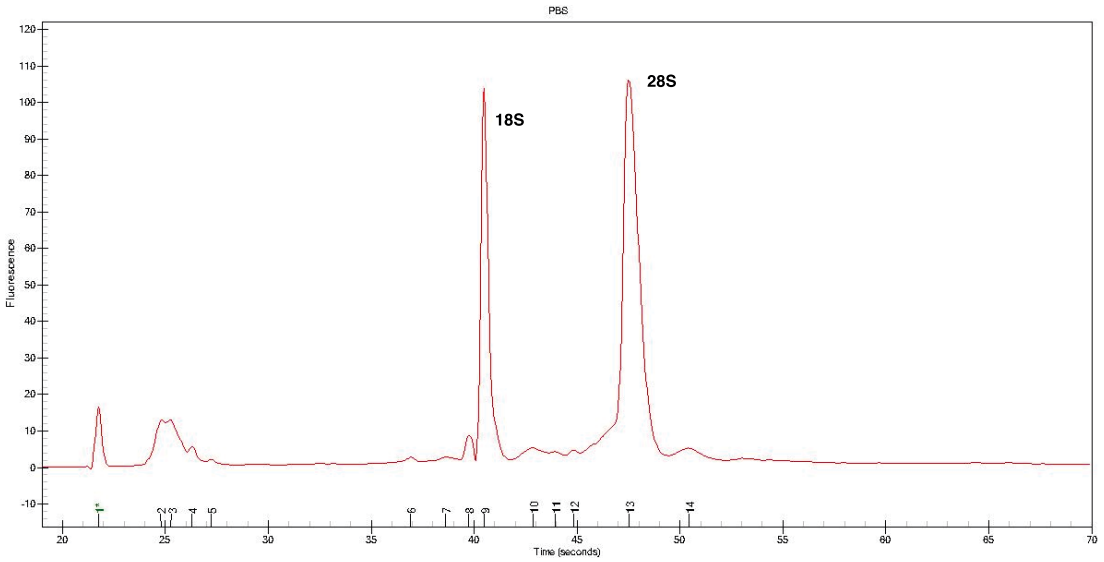

Figure 2.5. An Experion generated virtual gel of a total RNA sample. a) The representative virtual gel generated by the Experion software analysis system shown above, depicts the sizes of total RNA and qualitatively indicates the condition of the extracted RNA. **b)** Electropherogram showing two distinct peaks representing good quality 28S and 18S ribosomal RNA.

2.12 Reverse transcription

All RNA samples were normalised to 200 ng/µL ±10 ng prior to reverse transcription to cDNA. RNA samples were reverse transcribed into cDNA in triplicate using the iScript cDNA Synthesis Kit (Bio-Rad). Table 2.7 outlines the components and quantities used for the reaction. In order to prevent dilution errors, a master mix was made. Following the manufacturer's protocol, the reaction mix (Table 2.7) was incubated for 5 minutes at 25 ^{o}C, 30 minutes at 42 ^{o}C, 5 minutes at 85 ^{o}C, and then held at 4 ^{o}C. The cDNA was then diluted 1:3 using nuclease-free water (Bio-Rad) before amplification by real-time PCR (qPCR) (section 2.13).

Table 2.7 Reagents and volumes used for the iScript cDNA Synthesis Kit

Components	Volume Per Reaction (1x)
5x iScript reaction mix	**0.5 µL**
iScript reverse transcriptase	**2 µL**
Nuclease-free water	**7.5 µL – (RNA template volume)**
RNA template (200 ng/uL)	**1 µL**
Total volume	**10 µL**

2.13 Real time PCR

PCR amplification of cDNA was performed in triplicate using iQ SYBR Green I supermix (Bio-Rad) and target gene specific primers as shown in Table 2.8. (All primers used were designed against human sequences using the NCBI database.)

Table 2.8 Primer sequences

Primer	Forward/Reverse primer	Primer Sequence
Human DHCR24	F	5'-CTCCTGCCGCTCTCGCTTATC-3'
	R	5'-GTCCTGCTACCCTGCTCCTTCC-3'
Glyceraldehyde-3-phosphate dehydrogenase (GAPDH)	F	5'-TTCAACAGCGACACCCSCT-3'
	R	5'-TTCCTCTTGTGCTCTTGCT-3'
Beta-2 Microglobulin (β2M)	F	5'-CATCCAGCGTACTCCAAAGA-3'
	R	5'-GACAAGTCTGAATGCTCCAC-3'
18S	F	5'-CCAATCACTTCCGACCTGCTG-3'
	R	5'-GCTTTGTATCCCTGCCCTGAG-3'
Vascular cell adhesion molecule-1 (VCAM-1)	F	5'-ATGTAGTGTCATGGGCTGTG-3'
	R	5'-GGAATGAGTAGAGCTCCACC-3'
Interleukin 8 (IL-8)	F	5'-GCAGCTCTGTGTGAAGGTGCAGTTT-3'
	R	5'-GTTGGCGCAGTGTGGTCCACTC-3'

The components of the iQ SYBR Green I Supermix (Bio-Rad) are listed in Table 2.9. A master mix was made and the appropriate amounts of master mix and cDNA were pipetted into the individual wells in the PCR plate. The protocol for PCR reaction cycling settings used was an initial 3 minute denaturation step; 30 seconds at 95 ^{o}C, 30 seconds at 60 ^{o}C, 30 seconds incubation at 72 ^{o}C. A melt curve was then generated by 1 minute incubation at 95 ^{o}C for 1 cycle; 1 minute incubation at 55 ^{o}C for 1 cycle; and finally 10 seconds incubation at 60-94.5 ^{o}C for 70 cycles. Relative quantification of gene expression was relative to the reference genes GAPDH, 18S, and β2M.

Table 2.9 iQ SYBR Green Supermix reagents for Real-Time PCR

Components	Volume (µL)
iQ SYBR Green Mix	**7.5**
Sense primer (20 pmol/µL)	**0.6**
Anti-sense primer (20 pmol/µL)	**0.6**
Nuclease-free water	**3.3**
cDNA (diluted)	**3.0**
Total volume	**15**

2.14 PCR data analysis

RT-qPCR data was analysed using the $\Delta\Delta C_T$ method [478]. The threshold value (C_T) refers to the first point that significant gene expression is detected. The difference between threshold values (ΔC_T) for the gene of interest (GOI) and reference gene was used. The average C_T value observed for the reference gene (β2M, 18S, GAPDH) was then subtracted from the average C_T value of the gene of interest (GOI) (e.g. DHCR24, VCAM-1, IL-8). This average result was then set as the baseline ΔC_T. The comparative expression level of the GOI was then assessed using the formula $2^{-\Delta\Delta CT}$. mRNA levels were then expressed as a percentage of the control treatment group.

2.15 Quantifying cellular cholesterol levels

2.15.1 Delipidation of cells

Cells were seeded as per the conditions described (section 2.1), 24 hours prior to transfection. The cells were then transfected as per section 2.4.1 with pcDNA3.1A (pControl) or pcDNA3.1A-DHCR24 (pDHCR24) expression plasmids. After 24 hours of transfection, media was changed and the cells were rested for a further 24 hours (in which time DHCR24 expression is increased). After this rest period, cells were delipidated for cholesterol content analysis by adding a mixture of hexane:isopropanol (3:2) to the cells incubating on ice. Following incubation with hexane:isopropanol, the solvent was added to glass tubes and evaporated overnight. The desiccant was resuspended in 80% (v/v) ethanol.

To confirm DHCR24 overexpression, RNA was extracted from the delipidated cells. Cells were first washed with PBS three times and then the RNA isolation protocol described in 2.10 was followed.

2.15.2 Amplex Red Cholesterol Assay

Cholesterol extracted from transfectants was quantified using an Amplex Red Cholesterol Assay following the manufacturer's instructions (Life Technologies). Briefly, samples were diluted 1:4 with 1x reaction buffer for a final volume of 50 µL. Samples were then transferred to separate wells of a 96-well plate before 50 µL of a reaction mix containing Amplex Red reagent, HRP, cholesterol oxidase, cholesterol esterase, and reaction buffer was added. The microplate was then incubated covered for 30 minutes at 37 ^{o}C before fluorescence was measured with a Tecan infinite 200 plate reader at an excitation wavelength of 530 nm and emission detection wavelength of 590 nm.

A resorufin standard curve was prepared to ensure that the reaction took place. A 10 µM H_2O_2 positive control and no-cholesterol control were also used. Cellular cholesterol levels were quantified against a prepared cholesterol standard curve standard. For each point, values were corrected for background fluorescence by subtracting the measured values from the no-cholesterol control.

2.16 Immunocytochemistry

2.16.1 Materials

TBST

Tris Base	13.9 g
Tris HCL	60.6 g
NaCl	60.6 g
Tween 20	5 mL

A 10x stock solution was made up to 1 L with deionised H_2O.

0.3 % (w/v) Hydrogen peroxide solution

30% (w/v) Hydrogen peroxide	0.05 mL
Methanol	50 mL

2.16.2 Staining method

HCAECs were seeded into 4-well Lab-Tek II chamber slides (Lab-Tek) in 1 mL of MesoEndo growth media as per section 2.1. 24 hours prior to being treated. HCAECs were treated with PBS (control) or TNF-α (1 ng/mL) for 4 hours, and apoA-I rHDL (16 µM/0.45 mg/mL) for 16 hours.

HuH7 cells were seeded into 12-well plates in 1 mL of DMEM + 10% (v/v) FBS media per well as per section 2.1.2, 24 hours prior to being treated. HuH7 cells were treated with PBS (control) and TNF-α for 4 hours

Following treatment, cells were fixed in 4% (w/v) paraformaldehyde, blocked with a 0.3% (w/v) hydrogen peroxide solution (made up in methanol) for 20 minutes and incubated with anti-DHCR24 rabbit monoclonal IgG (1:200 dilution in 5% (w/v) goat serum) (Cell Signalling Technology) overnight and then with goat anti-rabbit IgG conjugated to horseradish peroxidase (HRP) (1:200 dilution in 5% (w/v) goat serum) (Cell Signalling Technology) for 30

minutes. To visualise the cells, cells were stained with 3,3'-diaminobenzidine (DAB) (Dako) for 5 minutes, counterstained in haemotoxylin, mounted with DPX mountant (Merck Millipore), and then cover-slipped. Cell images were obtained using a BH-2 Olympus microscope at 20x magnification (HCAECs) and 40x magnification (HuH7 cells).

2.17 Fluorescent microscopy

HCAECs seeded in FD3510 fluorodishes (WPI Europe) and transiently transfected with pDHCR24-EGFP as per section 2.4.1 were treated with 2.5 ng/mL TNF-α, following treatment were fixed with 4% (w/v) paraformaldehyde (20 minutes, room temperature), blocked with 1% (w/v) BSA, 2% (w/v) FBS before being washed with TBST. The endoplasmic reticulum was stained by incubating cells with anti-GRP78 goat primary antibody (1:1000 dilution in 1% (w/v) BSA, 2% (w/v) FBS) (Invitrogen) for 1 hour and then with anti-goat secondary antibody (1:200 in 1% (w/v) BSA, 2% (w/v) FBS) (Life Technologies) for 1 hour. The nucleus was stained with 4',6-diamidino-2-phenylindole (Dapi) (1:1000 dilution in PBS) (Life Technologies), and actin with AlexaFluor488 Phalloidin (1:200 dilution in 1% (w/v) BSA, 2% (w/v) FBS) (Life Technologies) (20 minutes each). Cells were covered in glycerol/*n*-propyl gallate (NPG) mounting media (Sigma-Aldrich) and imaged at 60x magnification under oil immersion with a Nikon Ti inverted epifluorescent microscope. NIS elements software (Nikon) was used to collect cell images.

2.18 Apoptosis Assay

HuH7 cells were seeded a cell density of $1x10^5$ cells per mL in 12-well plates and transfected as per section 2.2.1. Following transfection, apoptosis was induced by treating cells with TNF-α (15 ng/mL) for 18 hours. Apoptosis was measured using Cell Death Detection ELISA PLUS (Roche) following the manufacturer's instructions. Briefly, cells were lifted from the plate using trypsin, centrifuged at 10000 RPM for 10 minutes, and then the supernatant was removed. The cell pellet was resuspended using 200 µL cell lysis buffer and incubated for 30 minutes at room temperature allowing lysis to occur. After the lysate was centrifuged for 10 minutes at 10000 RPM, the supernatant (20 µL) was added to streptavidin-coated microplates. Next, 80 µL of immunoreagent was added to each well and then the plate was covered with adhesive foil before incubating on a plate shaker for 2 hours at room temperature and 250 RPM. Following incubation, the solution was removed and the plate was rinsed three times using 300 µL of incubation buffer. After rinsing, 100 µL ABTS solution (KPL) was added to each well and incubated on a plate shaker at room temperature and at 250 RPM until colour developed. The reaction was terminated by adding 100 µL ABTS stop solution (KPL) to each well. Absorbance was measured with a Tecan infinite 200 plate reader at a wavelength of 405 nm against ABTS solution + 100 µL ABTS stop solution as a blank (reference wavelength ~490nm).

Apoptosis was measured as the specific enrichment of mono- and oligonucleosomes released into the cytoplasm using the formula:

$$Enrichment\ factor = \frac{mU\ of\ sample}{mU\ of\ corresponding\ negative\ control}$$

mU = absorbance [10^{-3}]

2.19 Statistical Analysis

Data are expressed as mean ± SEM. Direct comparisons between two treatments were performed using unpaired t-test, while significant differences between multiple treatments were determined by one-way ANOVA with Sidak's *post hoc* test analysis. GraphPad Prism 6.0 was used for analysis. Significance was set at $P<0.05$. To show the effect size, P values lower than $P <0.05$ were specified.

Chapter 3 – DHCR24 replicates apoA-I rHDL's suppression of a TNF-α-induced inflammatory response in HCAEC

3.1 Introduction

Cardiovascular disease (CVD) is the primary cause of death worldwide [479]. The main form of CVD is atherosclerosis due to the accumulation of lipids and connective tissue producing cholesterol-laden atherosclerotic plaques. Atherosclerotic plaques formation affects arteries, reducing their elasticity, leads to obstructions which impede blood flow, and diminishes their ability to contract in response to hydrodynamic stress [17]. Disruption of the plaques leads to thrombus formation. Thrombi may occlude arteries, compromising oxygen supply to organs such as the heart or brain, causing potentially fatal heart attack or stroke [18].

Atherosclerosis is considered an inflammatory disease [83, 88, 480]. Obesity caused by a sedentary lifestyle and chronic overfeeding is one of the main drivers of inflammation. Increased adiposity causes secretions of numerous proinflammatory cytokines such as TNF-α, IL-6, IL-β, CRP, and IL-8, that drive inflammation [481-486]. In the context of atherosclerosis, inflammation causes endothelial cells to increase levels of cell adhesion molecules (CAMs) such as vascular cellular adhesion molecule-1 (VCAM-1) and intracellular cellular adhesion molecule-1 (ICAM-1) [487]. Increased CAMs allow circulating monocytes to bind to the endothelium, contributing to the first identifiable stage of atherosclerotic plaque formation, the fatty streak (Figure 1.5) [97, 98]. Selectins, such as P-selectin and E-selectin, on endothelial cells slow down circulating monocytes allowing them to roll across the endothelium via transient adhesion interactions. This process allows CAMs such as ICAM-1 and VCAM-1 to form firm bonds with the corresponding receptors, or integrins, on monocytes [99, 488, 489]. The tethered monocytes then differentiate into macrophages, take up cholesterol, become lipid-laden and develop into foam cells [105]. These foam cells undergo apoptosis leading to tissue injury and increase the risk of plaque rupture.

Extensive evidence indicates that high-density lipoprotein (HDL) levels are inversely related to development and progression of atherosclerosis, independent of LDL levels [490-493]. For every 1 mg/dL increase of HDL, the risk of CVD is reduced by 2-3% [490]. Epidemiological studies have reported that over a 6 year period, patients with HDL levels ≥35 mg/mL are 70% less likely to develop CVD in comparison to patients with HDL levels <35 mg/dL [491].

Raising HDL levels through HDL infusions has been successful in many studies. The positive effects of HDL infusion against atherosclerosis include reducing C-C chemokine receptor type 2 (CCR2) and CX3C chemokine receptor 1 (CX_3CR1) expression in plaques, in addition to

chemokine ligand 2 (CCL2)/MCP-1) and chemokine ligand 5 (CCL5) in the plasma [494], reducing aortic ICAM-1 and VCAM-1 mRNA levels [495, 496], removing lipid from fatty streaks [497], and reducing atherosclerotic lesion size [498-500]. HDL infusions of reconstituted and recombinant forms of apolipoprotein A-I (apoA-I) rHDL both elicit the abovementioned protective effects following even single HDL infusions [495, 496, 499, 501, 502]. Additionally, pharmaceutical approaches for raising HDL have presented positive effects against atherosclerotic plaque formation and facilitated plaque regression. ApoA-I mimetic peptides attenuate ICAM-1, VCAM-1, p65 [496, 503, 504], NOX4 [496], O_2^- [496, 505] and reduce plaque size [504, 506-509] and atheroma progression [510] some without alterations to total plasma or HDL cholesterol [511]. Thus it is promising to use HDL as a therapeutic strategy. The link between HDL levels and the prevention of cardiovascular disease is referred to as the HDL cholesterol hypothesis [512].

HDL improves cardiovascular outcomes/atherosclerotic risk through a number of mechanisms. These mechanisms include: cholesterol efflux/reverse cholesterol transport (RCT) by increasing expression of ATP binding cassette transporter A1 (ABCA1) [513-515], ATP binding cassette transporter G1 (ABCG1) [515, 516], and scavenger receptor class B type 1 (SR-B1) [517-519]; decreasing inflammation via modulation of inflammatory mediators particularly CAMs (such as VCAM-1 and ICAM-1) through suppression of nuclear factor transcription factor (NFκB) levels [1]; anti-thrombotic mechanisms by increasing levels of the vasodilator nitric oxide (NO) via increased activity of eNOS as a result of HDL binding to SR-B1 and activating the PI3-kinase-Akt kinase pathway and MAP kinase; inhibition of factor X activation, tissue factor expression, and plasminogen activator inhibitor secretion [492]; anti-oxidative effects by inhibiting low-density lipoprotein (LDL) oxidation through transferring oxidation products from LDL to HDL, which in turn prevents free radical production [520], and reactive oxygen species (ROS) scavenging; anti-apoptotic effects by increasing endothelial cell proliferation and migration [521], and inhibiting oxLDL-induced apoptosis by making contact with the particles leading to inhibition of its associated cytotoxic Ca^{2+} peak [522] and scavenging oxidised LDL-released ROS [523], preventing TNF-α-induced CPP32-like protease activity [524], activation of phosphoinositide 3-kinase (PI3K)/Akt, and upregulation of Bcl-2-like protein 1 [525].

Despite the link between high levels of HDL and decreased atherosclerosis/CVD, HDL molecules are a heterogeneous mix of particles and function differently leading to varying clinical outcomes [526]. The relationship between HDL particle size and composition, with cholesterol transfer is particularly relevant. Treatment for atherosclerosis focuses on altering

the lipid profile by lowering LDL and increasing HDL. Two of the main pharmaceuticals developed with these goals of improving the lipid profile are statins and CETP inhibitors.

Statins are a very successful class of cholesterol-lowering drugs used to treat atherosclerosis and are considered a frontline therapy, providing up to 60% reductions in cardiac events [527]. Dramatic decreases in coronary events, cardiovascular morbidity, and all-cause mortality have occurred as a result of the implementation of statin therapy in the last 20 years [193].

The lowering of LDL cholesterol is the main mechanism of action of statins in the primary and secondary prevention of cardiovascular events [194-198]. Statins lower cholesterol synthesis via the inhibition of HMG-CoA reductase, the enzyme associated with the first step of cholesterol biosynthesis inhibition of HMG-CoA occurs primarily by blocking substrate binding to the active site of the enzyme [200]. Statins also modestly increase HDL levels while reducing LDL [528].

Besides the cholesterol-lowering function of statins, another major effect is anti-inflammatory function. It is well established that statins reduce inflammation. For example, in human hepatocytes, inflammation was reduced by treatment with lovastatin via the reduction of high sensitivity C-reactive protein (hs-CRP) levels. Highlighting this effect as pleotropic and specifically independent of cholesterol-lowering, monotherapy with ezetimibe, a non-statin lipid-lowering drug, reduces LDL levels, however does not elicit any effects on CRP levels [529]. This pleiotropic effect is significant as hs-CRP is an inflammatory marker associated with CVD [201]. hs-CRP is primarily produced in the liver and predominately induces IL-6 [202, 203] which indicates low-grade systemic inflammation [204]. CRP also produces an environment which promotes atherosclerotic development by down-regulating protective eNOS expression [205], while increasing production of endothelin-1, a vasoconstrictor [203]. Furthermore, CRP upregulates the expression of VCAM-1, ICAM-1, E-selectin [206], and MCP-1 [207], thereby augmenting monocyte adhesion and infiltration into the vessel wall. Within the wall, CRP facilitates macrophage uptake of LDL [208]. Therefore, statin suppression of CRP levels provides protection against numerous inflammatory events associated with the initiation and progression of atherosclerosis. Despite the cholesterol-lowering and anti-inflammatory effects, patients on statins still have residual risk of atherosclerotic-associated cardiovascular events [383, 530-535]. Therefore, other therapies and targets are required.

A therapeutic avenue for improving HDL levels indirectly is cholesteryl ester transfer protein (CETP) inhibition. CETP is a hydrophobic glycoprotein, primarily synthesized in the liver [407, 408]. Following secretion into the plasma, circulating CETP facilitates bidirectional cholesterol ester and triglyceride transfer between lipoproteins. This process redistributes these lipids, equilibrating them between different lipoprotein fractions (as reviewed by [409]). Cholesterol esters predominately originate in HDL and are transferred into the plasma. The cholesterol esters in a mass net transfer, move from the non-atherogenic HDL to potentially pro-atherogenic lipoproteins such as LDL, VLDL, and chylomicrons.

Genetic CETP inhibition alters plasma lipoprotein levels in humans. CETP-deficient subjects have increased HDL cholesterol and lower cholesterol concentrations in non-HDL lipoprotein fractions [536-539]. Moreover, humans treated with CETP inhibitors exhibit increased HDL cholesterol and apoA-I concentrations [412, 540-542]. The goal of therapeutic CETP inhibition is prevention of cholesterol ester redistribution from plasma to lipoproteins other than HDL. This increases HDL cholesterol levels while reducing cholesterol ester concentration in non-HDL.

The effectiveness of CETP inhibitors for atherosclerosis treatment is under investigation. The Investigation of Lipid Level Management to Understand Its Impact in Atherosclerotic Events (ILLUMINATE) trial showed that torcetrapib, the first CETP inhibitor used in a large-scale clinical trial, was not cardioprotective [410]. Moreover, the trial was stopped following increased mortality in patients administered torcetrapib. The increased mortality associated with torcetrapib administration is suggested to be a result of off-target effects, particularly on blood pressure [410]. The CETP inhibitors dalcetrapib and evacetrapib do not exhibit off-target effects but also do not confer cardio-protective benefits despite increasing HDL levels by 31-40% [411] and 54-129% respectively [412]. Evacetrapib also failed to improve cardiovascular outcomes, and clinical trials have since been terminated [413]. However, despite these results it is argued that even if increased HDL concentration is not protective against atherosclerosis, the reduction in levels of non-HDL lipoproteins may reduce atherosclerosis risk [543].

New approaches are required to address atherosclerosis to provide more clinical options for treating a variety of patients. In the pursuit of investigating new approaches to treat atherosclerosis our laboratory investigated how HDL regulates genes associated with inflammation. Our laboratory led an investigation into the ability of HDL to upregulate genes with the potential to protect against mediators of inflammation in human coronary artery

endothelial cells (HCAECs) [1]. The study revealed that HDL protects against increases in VCAM-1 mRNA expression, and NFκB activity via suppression of the classical IKK/IκBα/NFκB signalling pathway by increasing IκBα levels and decreasing NFκB regulated transcription in HCAECs treated with TNF-α (5 hours). This effect was sustained even when the HDL was removed from the cells several hours prior to the TNF-α treatment. This is in keeping with *in vivo* observations; with the anti-inflammatory effect of HDL persisting after injected HDL had been removed by the circulation [501]. Using a microarray approach the mRNA of HCAECs pre-incubated with rHDL for 16 hours was analysed revealing 3β-hydroxysteroid-Δ24 reductase (DHCR24) as one of the most upregulated genes [1].

3β-hydroxysteroid-Δ24 reductase (DHCR24) is an enzyme essential for mammalian survival that has now been shown to have a number of key cellular roles. DHCR24 was initially discovered for its vital role in cholesterol biosynthesis, catalysing the conversion of desmosterol to cholesterol [435]. However, since then DHCR24 has also been shown to possess other roles in some cells types including protecting against oxidant [420, 421] and inflammatory insults [1, 544] and interacting with p53 [423, 424] or caspase-3 to prevent apoptosis [420, 421, 425-427].

The encoded protein for *dhcr24* was discovered to be identical to the neuroprotective enzyme, **Sel**ective **A**lzheimer's **D**isease **In**dicator **1** (Seladin-1). This homology was based on a mutation analysis of the *dhcr24* gene, expressed in *Saccharomyces cerevisiae*, using human cDNA obtained from patients exhibiting various levels of desmosterolosis (a cholesterol deficiency syndrome resulting in accumulated desmosterol [419].

Seladin-1 is expressed in pyramidal neurons of the brain particularly within cortical regions, the substantia nigra, caudate nucleus, hippocampus, medulla oblongata, and the spinal cord. Functional studies determined it was responsible for the biosynthesis and homeostasis of brain cholesterol [431, 432].

Low levels of seladin-1 are associated with Alzheimer's disease. Further, silencing of seladin-1 expression causes the hallmark features associated with Alzheimer's disease to develop [421, 433, 434, 545]. The discovery that *dhcr24* was identical to *seladin-1* set research into the protective functions of DHCR24 in motion [419, 426, 545].

High levels of functional HDL have been demonstrated to protect against atherosclerosis [546]. Our laboratory has focused on determining the mechanisms by which HDL suppresses markers

of inflammation in HCAECs. From this work our laboratory revealed that HDL's protective effects are through gene regulation and that DHCR24 is one of the most upregulated genes in HCAECs by HDL. Moreover, it was discovered that silencing DHCR24 in HCAECs results in an abrogation of HDL's ability to suppress TNF-α-induced inflammation [1]. Consequently, this work aims to determine whether increased DHCR24 can mimic HDL's protective effects in HCAECs. The first aim of this work was to ascertain if increased DHCR24 reduces monocyte to HCAEC adhesion stimulated by TNF-α and H_2O_2. The second aim was to elucidate if increased DHCR24 levels result in the suppression of ICAM-1 and VCAM-1 levels following inflammatory activation by TNF-α. The overall hypothesis for this work is that increased DHCR24 can replicate, in part, the protective effect of HDL in HCAECs.

3.2. Methods

3.2.1 Transient transfection using TransPass HUVEC Transfection Reagent

HCAECs were seeded at a cell density of $1x10^5$ cells/mL in EGM + 10% (v/v) FBS (section 2.1). According to the manufacturer's protocol (New England Biolabs), HCAECs were transiently transfected with pDHCR24 (inserted into pcDNA3.1A) or pControl (empty pcDNA3.1A) expression vectors using TransPass HUVEC Transfection Reagent (New England Biolabs) as described in section 2.4.1. Following a 24-hour incubation period, the culture medium was changed and the cells were allowed to recover for a further 24 hours.

3.2.2 Monocyte-to-endothelial cell adhesion assay

HCAECs were cultured in 12-well plates ($1x10^5$ cells/mL) and transfected with pControl or pDHCR24 as described in section 2.1. Following transfection, the transfectants were left for 24 hours before activation with TNF-α (2.5 ng/mL) or H_2O_2 (100 μM) for 4 hours prior to measuring the amount of fluorescently labelled monocytes adhered to endothelial cells by performing a monocyte adhesion assay as described in section 2.7.

3.2.3 ELISA

HCAECs were cultured in 96-well plates ($1x10^5$ cells/mL) and transfected with pControl or pDHCR24 as described in section 2.1. Following transfection, the transfectants were left for 24 hours before the cells were treated with TNF-α (2.5 ng/mL, 4 hours). Following TNF-α activation, ICAM-1 and VCAM-1 protein levels were measured using ELISA as described in section 2.8.

3.2.4 Western Blot

HCAECs were cultured in 12-well plates ($1x10^5$ cells/mL) (section 2.1) and transfected with pcDNA3.1A (pControl) or pcDNA3.1A-DHCR24 (pDHCR24) as described in section 2.4. Following transfection, the transfectants were left for 24 hours before protein was extracted (section 2.9.2.1), quantified (section 2.9.2.2), and subjected to western blot analysis as described in section 2.9.2.4.

3.2.5 Real Time PCR

HCAECs were cultured in 12-well plates ($1x10^5$ cells/mL) (section 2.1) and transfected with pcDNA3.1A (pControl) or pcDNA3.1A-DHCR24 (pDHCR24) as described in section 2.4. Following transfection, the transfectants were left for 24 hours before being treated. Total RNA extracted from HCAECs using PureZol (Bio-Rad) was normalised to 200 ng/µL using a UV spectrophotometer at 260/280nm (Nanodrop 1000, Thermo Scientific) (section 2.10). Normalised mRNA was reverse transcribed into cDNA using the iScript cDNA Synthesis Kit (Bio-Rad) (section 2.12). iSCRIPT/iQ SYBR Green Supermix was used to perform RT-PCR in a Bio-Rad iQ5 thermocycler (section 2.13). Relative changes in mRNA levels were determined by the $\Delta\Delta C_T$ method [478], using β2-microglobulin (β2M) and 18S levels as reference genes (section 2.14). Primer pair sequences are listed in Table 3.1.

Table 3.1. Primer sequences

Primer	Forward/Reverse primer	Primer Sequence
Human DHCR24	F	5'-CTCGCCGCTCTCGCTTATC-3'
	R	5'-GTCTTGGCTACCCTGCTCCTTCC-3'
VCAM-1	F	5'-GGGACCACATCTACGCTGACA-3'
	R	5'CCTGTCTGCATCCTCCAGAAA-3'
Beta-2 Microglobulin (β2M)	F	5'-CATCCAGCGTACTCCAAAGA-3'
	R	5'-GACAAGTCTGAATGCTCCAC-3'
18S	F	5'-CCAATCACTTCCGACCTGCTG-3'
	R	5'-GCTTTGTATCCCTGCCCTGAG-3'

3.2.6 Statistical analysis

Data are expressed as mean ± SEM. Direct comparisons between two treatments were performed using unpaired t-test, while significant differences between multiple treatments were determined by one-way ANOVA with Sidak's *post hoc* test analysis. GraphPad Prism 6.0 was used for analysis. Significance was set at $P<0.05$. To show the effect size, P values lower than $P <0.05$ were specified.

3.3 Results

3.3.1 Transient transfection of pcDNA3.1A-DHCR24 increases DHCR24 levels in human coronary artery endothelial cells (HCAECs)

To confirm that transient transfection of pcDNA3.1A-DHCR24 (pDHCR24) increased DHCR24 levels in HCAECs, cultured HCAECs were transfected with pcDNA3.1A (pControl) or pDHCR24 expression vectors using TransPass V reagent (New England Biolabs) with the optimised conditions described in section 2.4.1. pcDNA3.1A vector (pControl) was the vehicle control for transfection because DHCR24 was cloned into pcDNA3.1A vector for overexpression analysis. Following transfection, cells were left for 24 hours prior to extraction of total RNA and subsequent analysis of DHCR24 mRNA levels by real-time RT-qPCR and protein levels by Western blotting.

From the RT-qPCR results shown in Figure 3.1 (A), transfection using TransPass V (New England Biolabs) was successful with DHCR24 mRNA levels significantly increased by 1760-fold ($P<0.0001$ vs pControl), compared to the empty vector control. The increased mRNA level also led to increased DHCR24 protein levels as shown in Figure 3.1 (B).

(A)

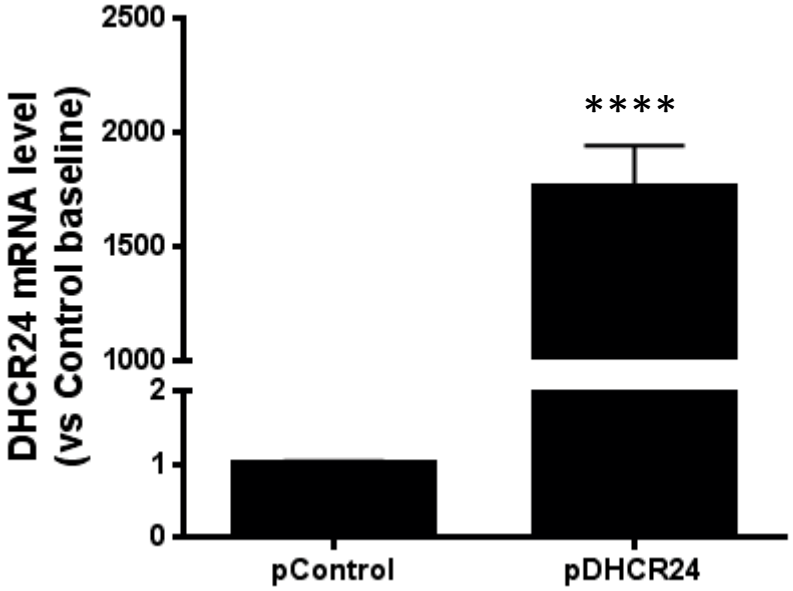

(B)

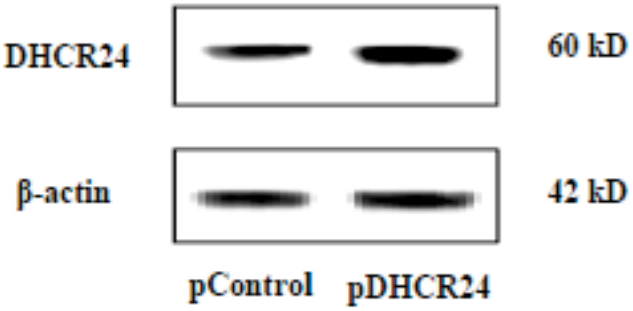

Figure 3.1 Transient transfection of HCAECs with pcDNA3.1A-DHCR24 successfully increased DHCR24 levels. HCAECs cells were transfected with pcDNA3.1A (pControl) or pcDNA3.1A-DHCR24 (pDHCR24) for 24 hours. (A) Total RNA was isolated and RT-qPCR used to measure DHCR24 mRNA levels. (B) Protein was isolated and western blot was used to determine protein levels (representative of 3 replicates) **** $P<0.0001$ ($n = 4$).

3.3.2 Increased DHCR24 levels suppresses TNF-α-activated monocyte adhesion to HCAECs

Increased monocyte adhesion to the endothelium is one of the first detectable stages of atherosclerotic plaque formation [97, 98]. HDL inhibits monocyte adhesion to endothelial cells preventing atheroma development [547, 548]. To ascertain whether DHCR24 is able to similarly prevent monocyte adhesion to HCAECs, cells were transfected with pcDNA3.1A vector (pControl) or pcDNA3.1A-DHCR24 (pDHCR24). After 24 hours during which DHCR24 levels increase (Figure 3.1), transfected cells were activated with (2.5 ng/mL) TNF-α or H_2O_2 (100µM) for 4 hours. Fluorescent-labelled monocytes were added to HCAECs after activation by TNF-α and incubated for 1 hour. Non-adhered monocytes were removed and the total fluorescence emitted by the adhered monocytes was measured using a Flexstation 3 plate reader.

Figure 3.2 shows that inflammatory activation with TNF-α at 2.5 ng/mL significantly increased monocyte adhesion to HCAECs by 13% ($P<0.001$) compared to empty vehicle treated cells. Increased DHCR24 reduced monocyte adhesion to HCAECs by 16% below baseline when treated with 2.5 ng/mL TNF-α ($P<0.05$) (Figure 3.2).

Hydrogen peroxide (H_2O_2) is another active player in the inflammatory milieu, associated with the activation of endothelial cells in an atherosclerotic environment. Therefore it was investigated whether DHCR24 could suppress H_2O_2-induced monocyte adhesion. To investigate whether overexpression of DHCR24 in HCAECs also suppressed H_2O_2-induced monocyte adhesion, cells were exposed to H_2O_2 at 100 µM for 4 hours before monocytes were exposed to the activated HCAECs. H_2O_2 markedly increased the level of adhered monocytes by 41% above the baseline control ($P<0.0001$) (Figure 3.3). By contrast, overexpression of DHCR24 protected against monocyte binding by 9% below baseline control and by 50% compared to H_2O_2-activated pControl-transfected cells ($P<0.0001$) (Figure 3.3).

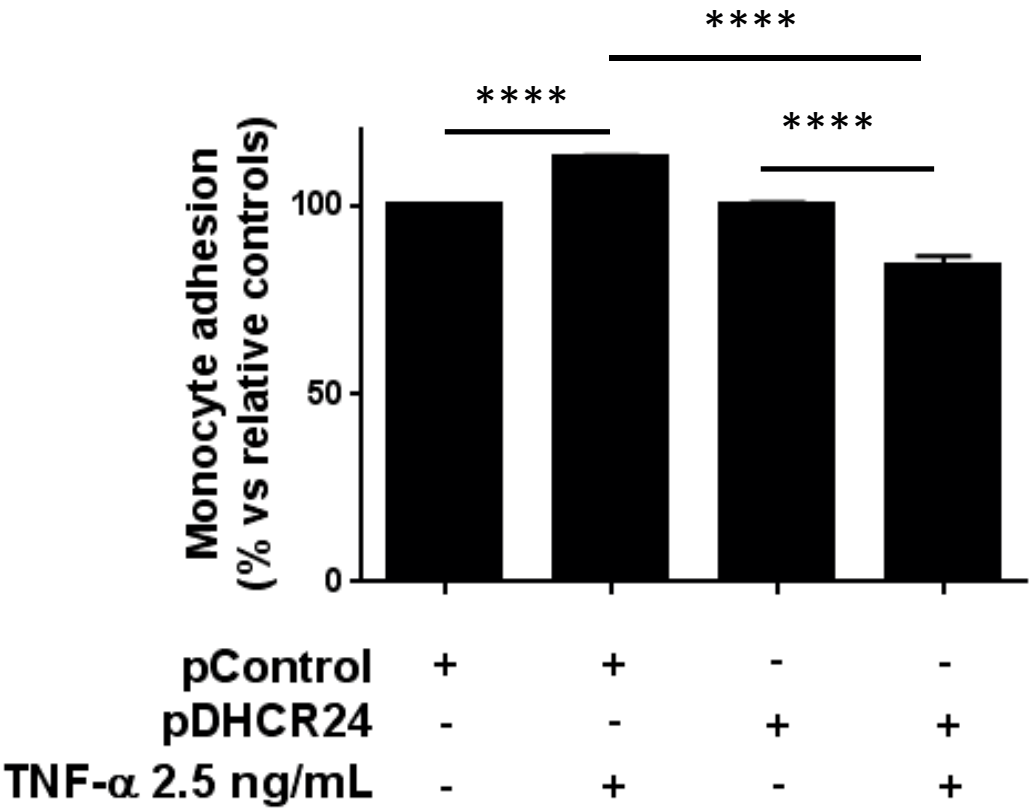

Figure 3.2 DHCR24-overexpression reduced monocyte to HCAECs adhesion in TNF-α-activated HCAECs. HCAECs were transfected with pcDNA3.1A (pControl) or pcDNA3.1A-DHCR24 (pDHCR24) before activation with 2.5 ng/mL for 4 hours. Fluorescent-labelled monocytes were added to HCAECs after activation by TNF-α and incubated for 1 hour. Non-adhered monocytes were removed and the total fluorescence emitted by the adhered monocytes was measured using a Flexstation 3 plate reader. pControl and pDHCR24 were set as vector controls at 100%. All data are shown as mean ± SEM (n = 3) **** P<0.001.

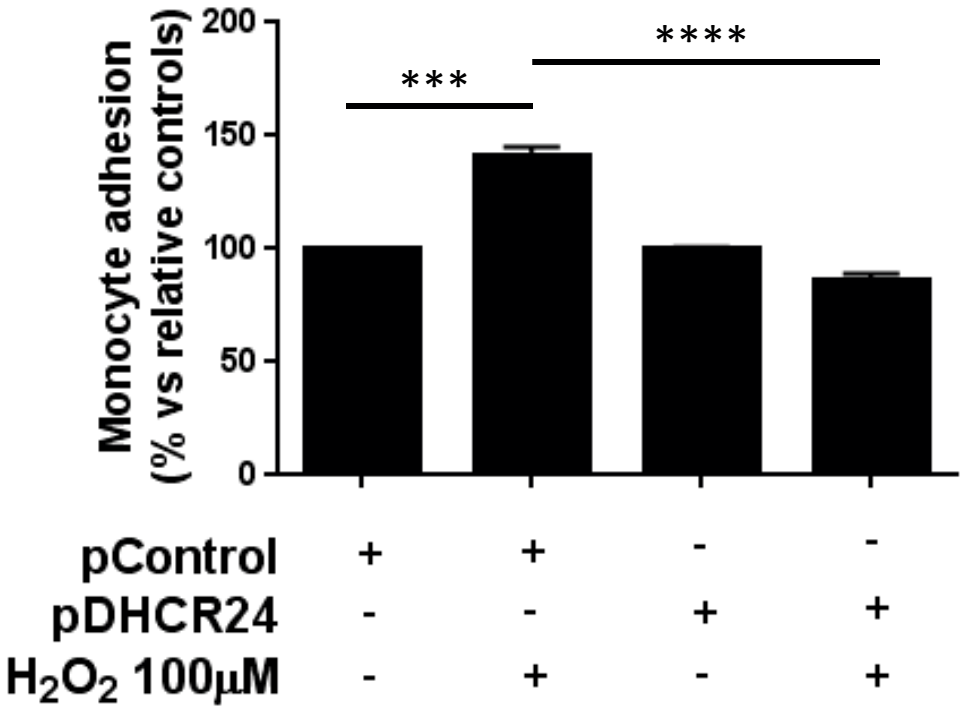

Figure 3.3 DHCR24-overexpression reduced monocyte to HCAECs adhesion in H_2O_2-activated HCAECs. HCAECs were transfected with pcDNA3.1A (pControl) or pcDNA3.1A-DHCR24 (pDHCR24) before activation with 100 µM in H_2O_2 for 4 hours. Fluorescent-labelled monocytes were added to HCAECs after activation by H_2O_2 and incubated for 1 hour. Non-adhered monocytes were removed and the total fluorescence emitted by the adhered monocytes was measured using a Flexstation 3 plate reader. pControl and pDHCR24 were set as vector controls at 100%. All data are shown as mean ± SEM (n = 4) *** P<0.001, **** P<0.0001.

3.3.3 Increased DHCR24 suppresses TNF-α-activated ICAM-1 and VCAM-1 levels

Expression of cell adhesion molecules (CAMs) is intricately associated with atherosclerosis risk and development [549, 550]. As monocytes roll across the endothelium, CAMs form firm bonds with integrins on monocytes causing attachment to the endothelium. HDL reduces the expression of CAMs both *in vivo* and *in vitro* [1, 501, 551-554]. The effect of increased DHCR24 levels on expression of the two major CAMs associated with atherosclerosis, intracellular cell adhesion molecule-1 (ICAM-1) and vascular cell adhesion molecule-1 (VCAM-1) was investigated. It was hypothesised that increasing DHCR24 levels would mimic the effects of HDL.

HCAECs were transfected with pcDNA3.1A (pControl) or pcDNA3.1A-DHCR24 prior to TNF-α (2.5 ng/mL) treatment for 4 hours. ICAM-1 and VCAM-1 protein levels were measured using ELISA. TNF-α treatment increased ICAM-1 protein levels by 18.6% compared to vehicle control ($P<0.01$), a result that was abrogated in pDHCR24-transfected HCAECs (19.6% reduction) ($P<0.01$) (Figure 3.4). TNF-α treatment increased VCAM-1 protein levels by 114% compared to vehicle control ($P<0.0001$), while pcDNA3.1A-DHCR24-transfectants showed a 33% suppression of VCAM-1 protein levels ($P<0.05$) (Figure 3.5).

Previously, our laboratory has shown that HDL mediates its effects on VCAM-1 expression at the level of gene transcription. Therefore, investigation as to whether the effect of increased DHCR24 levels affected VCAM-1 mRNA levels was undertaken. HCAECs were transfected with pcDNA3.1A (pControl) or pcDNA3.1A-DHCR24 prior to TNF-α (2.5 ng/mL) treatment for 4 hours. VCAM-1 mRNA levels were measured using RT-qPCR using β2M as a reference gene. TNF-α treatment increased VCAM-1 mRNA levels by 59-fold compared to vehicle control ($P<0.001$), and HCAECs transfected with pcDNA3.1A-DHCR24 suppressed VCAM-1 mRNA levels compared to TNF-α-activated pcDNA3.1A HCAECs by 35-fold ($P<0.05$) (Figure 3.6).

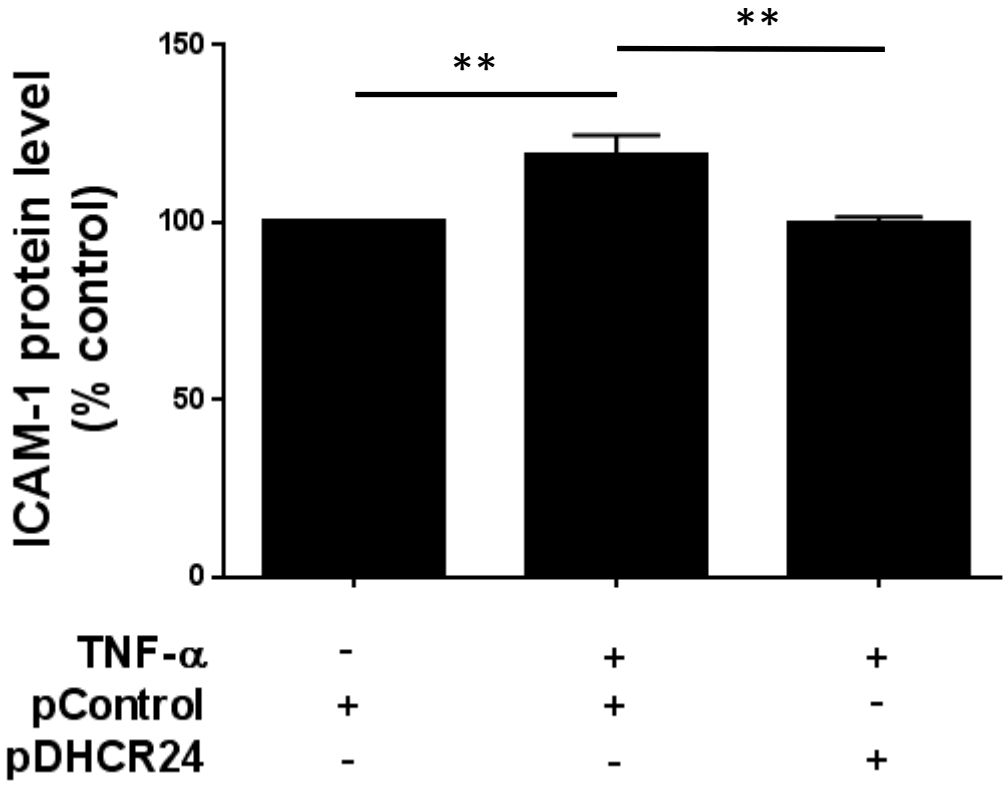

Figure 3.4 DHCR24-overexpression suppressed TNF-α-activated ICAM-1 protein levels in HCAECs. HCAECs were transfected with pcDNA3.1A (pControl) or pcDNA3.1A-DHCR24 (pDHCR24) before activation with 2.5 ng/mL TNF-α for 4 hours. ICAM-1 protein levels were measured using the ELISA. Data are shown as mean ± SEM (n = 3) ** P<0.01.

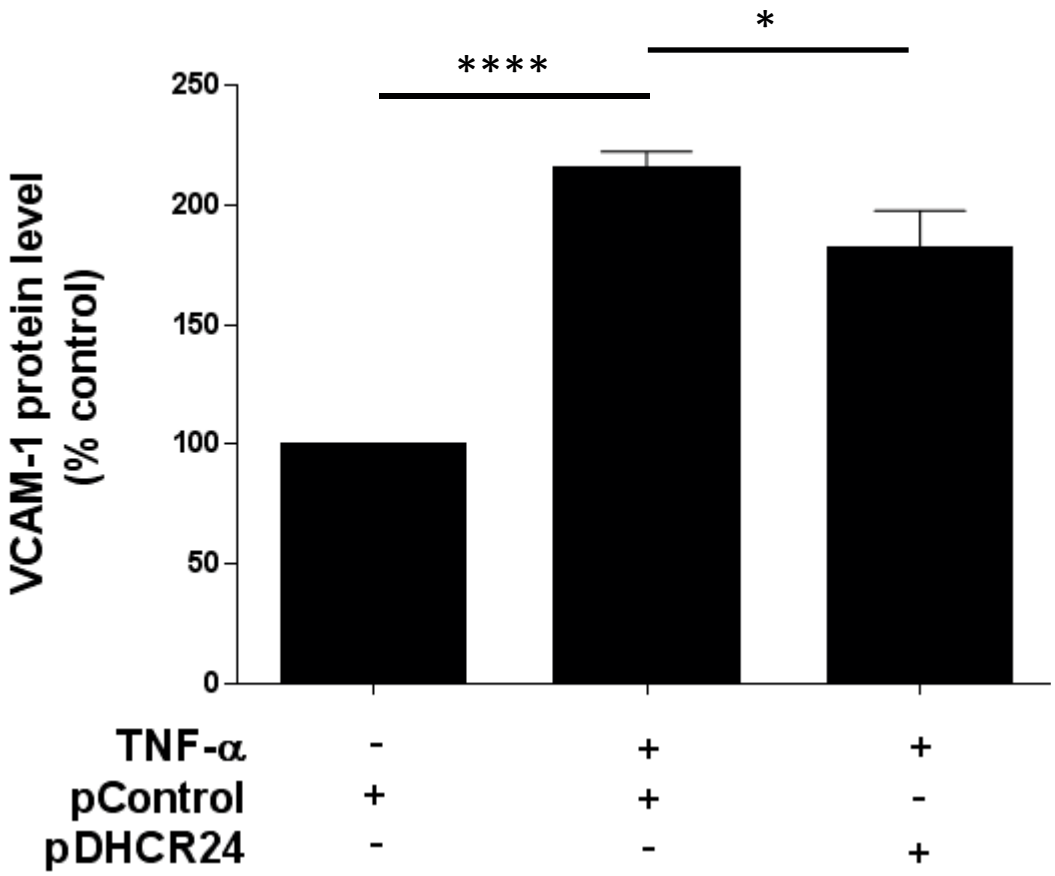

Figure 3.5 DHCR24-overexpression suppressed TNF-α-activated VCAM-1 protein levels in HCAECs. HCAECs were transfected with pControl or pDHCR24 before activation with 2.5 ng/mL TNF-α for 4 hours. VCAM-1 protein levels were measured using the ELISA. Data are shown as mean ± SEM (n = 5) * P<0.05, **** P<0.0001.

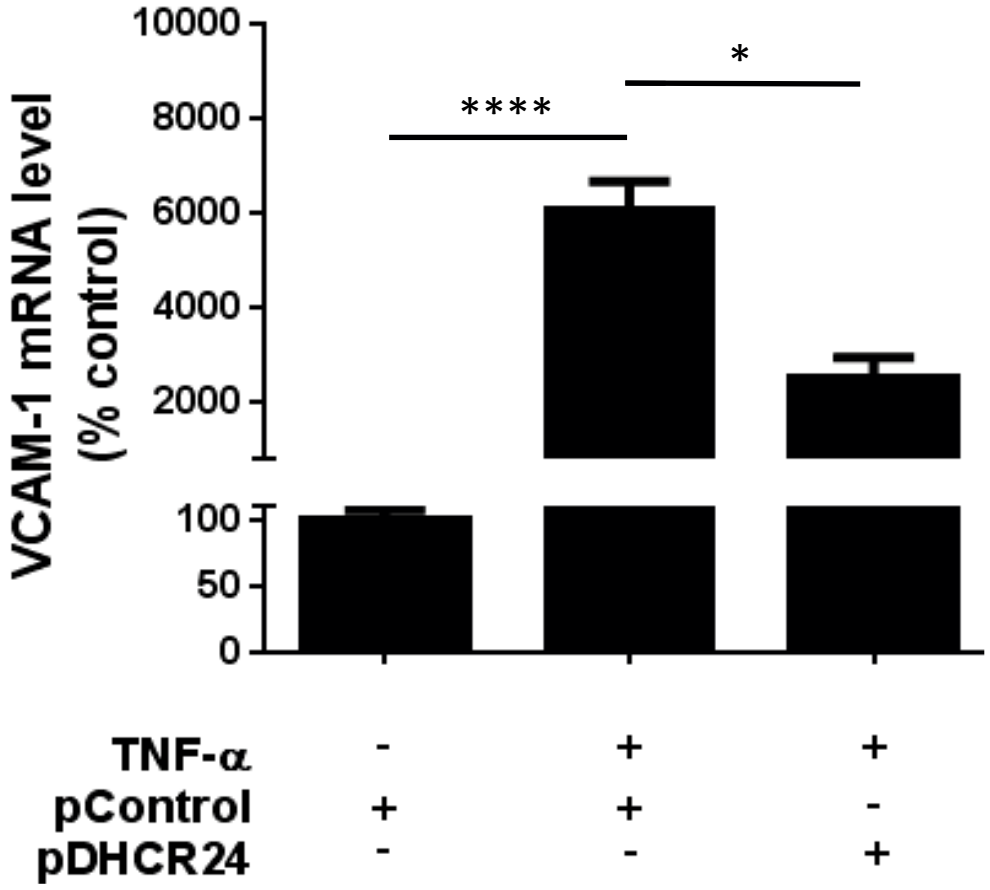

Figure 3.6 DHCR24-overexpression suppressed TNF-α-activated VCAM-1 mRNA levels in HCAECs. HCAECs were transfected with pcDNA3.1A (pControl) or pcDNA3.1-DHCR24 (pDHCR24) before activation with 2.5 ng/mL TNF-α for 4 hours. VCAM-1 mRNA levels were measured using RT-qPCR with β2M as a reference gene. Data are shown as mean ± SEM (n = 3) * P<0.05, *** P<0.001.

3.4 Discussion

The work presented in this chapter provides for the first time, proof-of-principle that DHCR24 replicates HDL's ability in HCAECs to reduce monocyte adhesion (to endothelial cells) and its ability to suppress levels of the inflammatory mediators ICAM-1 and VCAM-1 following stimulation by TNF-α and H_2O_2. HDL has been extensively reported to reduce monocyte-endothelial cell adhesion [547, 548, 555, 556] and to attenuate inflammatory marker levels, specifically ICAM-1 and VCAM-1, both *in vitro* and *in vivo*, events integral to the development of early atherosclerosis [1, 501, 551-554, 557].

Impetus into investigating the ability of DHCR24 to replicate the effects of HDL was provided following work from our laboratory. The work showed that HCAECs pre-incubated with HDL (16 µM/0.45 mg/mL, half-physiological concentration) for 16 hours before activation with the inflammatory cytokine TNF-α (0.1 ng/µL) for 5 hours decreased levels of NFκB-regulated inflammatory mediators and that this effect was retained even when HDL was removed prior to TNF-α exposure. This indicated a gene regulatory effect as HDL was not present to directly interact with TNF-α. Using a microarray approach, it was determined that one of the most upregulated genes by HDL treatment (16 µM, 16 hours) in HCAECs was *dhcr24* [1]. Subsequently it was shown that silencing DHCR24 abrogated the ability of HDL to suppress TNF-α-induced ICAM-1 and VCAM-1 expression, key atherosclerotic inflammatory mediators. This suggested that DHCR24, at least in part, plays a role in HDL's ability to decrease inflammatory mediator levels [1]. DHCR24 was of major interest because in addition to its known role as a cholesterol biosynthesis enzyme, DHCR24 also facilitates suppressive or inhibitory effects against cellular stress. DHCR24 elicits anti-apoptotic [425, 437, 471] and anti-oxidative [421, 423, 438] functions in a variety of cells including fibroblasts and neuronal cells. Therefore, it was hypothesised that DHCR24 would be responsible for performing some of the anti-inflammatory effects of HDL in HCAECs.

The effect of increased DHCR24 on monocyte adhesion to HCAECs was investigated first, elucidating the effect of DHCR24 and determining whether it replicates this well-established HDL function [547, 548, 555, 556]. Monocyte adhesion to the endothelium is a critical component of atherosclerotic plaque formation [2, 88, 558]. In response to injury and inflammatory conditions, endothelial cells are activated thus altering their phenotype. The endothelial cells express cell adhesion molecules (CAMs) on their cell surface, allowing

monocyte binding and capture, the first identifiable stage of atherosclerotic plaque formation [97, 98]. Preventing monocyte adhesion significantly decreases the formation of atherosclerosis [559, 560] and this protective effect is facilitated by HDL [547, 548, 555]. In this chapter the effect of DHCR24 on monocyte to endothelial cell (HCAECs) adhesion was investigated against challenges using TNF-α and H_2O_2. Monocyte to endothelial cell adhesion was significantly reduced by increased DHCR24 expression (Figure 3.2). Our laboratory has previously shown that both native and reconstituted forms of HDL upregulate DHCR24 mRNA levels and that this effect is sustained for hours after HDL are removed [1]. Further, independent of HDL exposure, increased DHCR24 levels in HCAECs reduce monocyte to endothelial cell adhesion. Therefore, DHCR24 may be a central player in mediating the protective effects of HDL.

Showing that increased DHCR24 expression alone can elicit this effect of reduced monocyte to endothelial cell adhesion is important not only because it shows that it occurs independent of HDL, but because HDL loses this ability under pathogenic conditions [561]. In keeping with this, HDL from CVD patients has a reduced effect on inhibiting monocyte migration *in vitro* [562]. The next experiments sought to investigate whether the reduced monocyte binding to HCAECs facilitated by DHCR24 overexpression was attributed to reductions in the levels of the cell adhesion molecules (CAMs) ICAM-1 and VCAM-1.

As mentioned, TNF-α is a major player involved in atherosclerosis [563-566], driving expression of inflammatory markers particularly ICAM-1 and VCAM-1 – the main inflammatory markers associated with atherosclerosis [549, 567-571]. Increased DHCR24 levels caused attenuation of these markers indicating there may be merit in pursuing DHCR24 as a therapeutic target for the treatment of atherosclerosis. Human epidemiological studies indicate that increased HDL levels are associated with a decreased risk of developing atherosclerosis [490], however this relationship may not be causal. In keeping with this, HDL can be modified, its composition altered and consequently become dysfunctional under cellular stress [414-418]. Therefore, increasing HDL levels may not necessarily reflect their protective properties for supporting cardiac function [572]. DHCR24 can perform some of the anti-inflammatory effects of HDL in HCAECs and could be used as a therapeutic to replicate 'healthy HDL'. DHCR24's ability to inhibit monocyte adhesion to HCAECs and to suppress ICAM-1 and VCAM-1 levels in HCAECs activated by TNF-α, provides impetus into its investigation as a therapeutic target and also indicates that DHCR24 serves a multifaceted role in HCAECs, being involved in more than just cholesterol biosynthesis.

DHCR24's multifaceted role in HCAECs is in keeping with its effects in other cell types. DHCR24's facilitation of cellular stress suppression has been predominately reported in neuronal cells [421, 423, 438, 573] and MEF [140, 437, 471]. The effects DHCR24 has displayed in these cells have been anti-apoptotic and anti-oxidative. However, DHCR24's ability to directly suppress inflammatory markers has not been previously reported in the literature in any cell type to date and no work exists for the role of increased DHCR24 in HCAECs.

The data presented in this chapter show for the first time, that DHCR24 overexpression alone can prevent monocyte to endothelial cell adhesion, and reduces ICAM-1 (protein) and VCAM-1 (protein and mRNA) levels in HCAECs. This work provides proof-of-principle that DHCR24 replicates, in part, the protective effect of HDL in HCAECs and builds upon the current reported knowledge of DHCR24's potentially protective abilities (anti-oxidative [421, 423, 438] and anti-apoptotic effects [421, 425, 437, 471]) adding inflammatory mediator modulation to its repertoire. Building upon this proof-of-principle study, the next chapter focuses on investigating the mechanisms involved in DHCR24's ability to modulate levels of inflammatory mediators in HCAECs.

Chapter 4 – Characterisation of the mechanisms mediating DHCR24's protective effects in HCAEC

4.1 Introduction

In the previous chapter, it was established for the first time, that increasing DHCR24 levels in human coronary artery endothelial cells (HCAECs) mimics HDL's protective effect of suppressing TNF-α-induced ICAM-1 and VCAM-1 levels. The decrease in TNF-α-induced ICAM-1 and VCAM-1 levels facilitated by DHCR24, was associated with reduced monocyte to endothelial cell adhesion. These observations are significant although they do not point to the mechanism by which DHCR24 mediates these effects. DHCR24 is reported to have multiple roles in various cell types however, it is unknown which of these roles, DHCR24 plays in HCAECs. This study focuses on investigating the mechanisms by which DHCR24 mediates the effect of suppressing TNF-α-induced ICAM-1 and VCAM-1 levels in HCAECs, building upon the novel discoveries of the work in the previous chapter. This study set out to characterise in HCAECs, DHCR24's cholesterol biosynthesis role, the significance of its oxidoreductase site, and its potential ability to translocate throughout the cell following TNF-α-activation.

DHCR24 was initially discovered and is primarily known as a cholesterol biosynthesis enzyme. DHCR24 catalyses the final step of cholesterol biosynthesis – the conversion of desmosterol to cholesterol, via the oxidoreductase site [419]. The presence of cholesterol is essential to all mammalian organisms, with an absence of cholesterol being fatal [419, 440, 443]. In keeping with this, patients demonstrating the multiple-congenital-anomaly syndrome desmosterolosis, that is caused by the accumulation of desmosterol, show mutations in the *dhcr24* gene [419, 440-443, 574]. Desmosterolosis also leads to a deficiency in plasma membrane cholesterol. This leads to death shortly after birth in humans [443] and in mice [434, 575, 576]. Patients with milder forms of the disease, where DHCR24 is partially functional and produces small amounts of cholesterol, exhibit profound disability with impaired learning ability and multiple physical anomalies. The phenotypes observed in desmosterolosis patients vary yet share common features including, brain malformations, facial feature abnormalities, and skeletal deformities [419, 440-442, 574]. DHCR24's cholesterol biosynthesis role is integral to the correct development and functioning of the body but also facilitates protection against cellular stressors. For example, the protection brought on by DHCR24 occurs in a cholesterol-dependent manner in neuroblastoma cells when exposed to oxidative stress [433, 473], by modulating amyloid beta (Aβ) peptide production and clearance [433, 438]. DHCR24 also reduces ER stress in neuroblastoma cells via cholesterol elevation mechanisms [469]. Conversely, in W138-TERT fibroblasts and mouse embryonic fibroblasts (MEF), DHCR24 directly

scavenges ROS preventing H_2O_2-induced apoptosis, independent of cholesterol synthesis [140, 423, 437] indicating that the mechanisms of DHCR24's protective effects are cell type-specific.

Increased DHCR24 levels are consistently associated with protective effects in assorted cells. Increased DHCR24 confers resistance against ER stress in neuronal cells and MEF, apoptosis in neuronal cells [421], fibroblasts [469], melanoma cells [420], pituitary adenomas [427], and in adrenal cells [577], and resistance against oxidative stress in neuronal cells [421, 469] and fibroblasts [140, 437]. The mechanisms through which DHCR24 elicits protective effects are emerging as being cell type-specific. Interestingly in MEF, DHCR24's ability to elicit protection against oxidative stress is dependent on its oxidoreductase site albeit independent of its cholesterol biosynthesis role instead serving as a direct ROS-scavenger preventing apoptosis [437]. In neuronal cells, DHCR24 translocates from the ER to the nucleus following inflammatory activation to prevent apoptosis [469].

Given the recent discoveries of DHCR24's cell type-specific multifaceted protective abilities, this study set out to investigate the mechanisms through which DHCR24 elicits suppression against a TNF-α-induced inflammatory response in HCAECs. It was hypothesised that DHCR24 would reduce a TNF-α-induced inflammatory response in an oxidoreductase site-dependent manner, independent of its cholesterol biosynthesis role. The localisation of DHCR24 following TNF-α-activation and the potential role of ER stress control in HCAECs to regulate inflammation were also investigated. The aim of this study was to characterise the mechanisms through which DHCR24 suppresses a TNF-α-induced inflammatory response in HCAECs.

4.2 Methods

4.2.1 Cell culture

HCAECs were cultured in Endothelial Cell Growth Medium (EGM, Cell Applications) at 37 ^{o}C in a 5% CO_2 incubator. For the experiments determining whether DHCR24 overexpression increases cellular cholesterol levels, HCAECs were seeded in 6-well plates at a cell density of $1x10^5$ cells/mL and grown 24 hours to 80% confluency prior to transient transfection (section 2.1). Following the manufacturer's protocol (New England Biolabs), HCAECs were transiently transfected with pDHCR24 (inserted into pcDNA3.1A) or pControl (empty pcDNA3.1A) expression vectors using TransPass HUVEC Transfection Reagent (New England Biolabs) as described in section 2.4.1. Following a 24-hour incubation period, the culture medium was changed and the cells were allowed to recover for a further 24 hours before cholesterol was extracted (section 4.2.3) and quantified (section 4.2.4)

For the experiments exploring the role of DHCR24's oxidoreductase site and DHCR24's effect on ER stress markers, HCAECs were cultured and transiently transfected as above but with the addition of HCAECs transfected with pDHCR24-N294T/K306N plasmid [oxidoreductase mutant – (section 4.2.2)]. Following a 24-hour incubation period, the culture medium was changed and the cells were allowed to recover for a further 24 hours before being treated with 2.5 ng/mL TNF-α for 4 hours. Following treatment, protein and total RNA were extracted and RT-qPCR performed (sections 4.2.5 and 4.2.6 respectively).

To determine whether DHCR24 changes location in HCAECs following TNF-α-activation, HCAECs were cultured in EGM in FD3510 fluorodishes (WPI Europe) at a cell density of $1x10^5$ cells/mL 24 hours prior to being transfected with pDHCR24-EGFP plasmid (section 4.2.2). Following a 24-hour incubation period, the culture medium was changed and the cells were allowed to recover for a further 24 hours in which time DHCR24 expression is increased before being treated with 2.5 ng/mL TNF-α for 4 hours. Following treatment, cells were stained and images obtained (as described in section 2.16).

4.2.2 Site-directed mutagenesis and plasmid constructions

4.2.2.1 pDHCR24-N294T/K306N (oxidoreductase mutant)

Using a DHCR24-pcDNA3.1A clone, a DHCR24 double mutant (N294T/K306N) was generated by Genscript Inc based on [419]. The oxidoreductase mutant was produced from a wild type DHCR24 template using site-directed mutagenesis and cloned into the pcDNA 3.1A plasmid vector to inactivate the known active site. This was followed by two rounds of PCR to introduce the two mutations in sequence. The resulting mutant DNA was then cloned into the pPAL expression vector.

The coding strand primer sequences to generate the mutant are:

N294T: 5'-GAGCCCAGCAAGCTGACTAGCATTGGCAATTAC-3'

K306N: 5'-GCCGTGGTTCTTTAACCATGTGGAGAACTATCTG-3'

4.2.2.2 pDHCR24-EGFP

A DHCR24-EGFP fusion plasmid was produced by Genscript by cloning the entire cloning sequence of human DHCR24 cDNA into the XhoI-EcoRI site of plasmid pEGFP-N1. Using PCR sense primer 5'-CTCGAGGCCACCATGGAGCCCGCCGTGTCGCTGGCC-3' and antisense primer 5'-GAATTCGGTGCCTGGCGGCCTTGCAGATCTTgTC-3', the correct restriction enzyme sites, translation start site, KOZAK sequence, and deleted stop codon were obtained.

4.2.3 Cholesterol extraction

HCAECs were seeded ($1x10^5$ cells/mL) in 6-well plates were transiently transfected with pcDNA3.1A (pControl) or pcDNA3.1A-DHCR24 (pDHCR24) before cholesterol was extracted using hexane/isopropanol (section 2.15.1).

4.2.4 Quantifying cellular cholesterol levels - Amplex Red Cholesterol Assay

Extracted cholesterol was quantified using the Amplex Red Cholesterol assay according to the manufacturer's instructions (Life Technologies) against cholesterol and resorufin fluorescence standards (section 2.15.2).

4.2.5 ELISA

HCAECs were cultured in 96-well plates ($1x10^5$ cells/mL) and transfected with with pcDNA3.1A (pControl), pcDNA3.1A-DHCR24 (pDHCR24), or pDHCR24-N294T/K306N plasmids as described in section 4.2.1. Following transfection, the transfectants were left for 24 hours before the cells were treated with TNF-α (2.5 ng/mL, 4 hours). Following TNF-α-activation, ICAM-1 and VCAM-1 protein levels were measured using ELISA as described in section 2.8.2.1.

4.2.6 Real time PCR

Total RNA was extracted using PureZol (Bio-Rad) and normalised to 200 ng/µL using a UV spectrophotometer at 260/280nm (Nanodrop 1000, Thermo Scientific). For RT-qPCR, cDNA was synthesised using a iScript cDNA Synthesis Kit (Bio-Rad) and iQ SYBR Green I supermix (Bio-Rad) was used to amplify cDNA in a Bio-Rad iQ5 thermocycler. RT-qPCR data was analysed using the $\Delta\Delta C_T$ method [478], using β2M GAPDH, and 18S as reference genes. Primer pair sequences are listed in Table 4.1.

Table 4.1 Primer sequences

Primer	Forward/Reverse primer	Primer Sequence
Human DHCR24	F	5'-CTCGCCGCTCTCGCTTATC-3'
	R	5'-GTCTTGGCTACCCTGCTCCTTCC-3'
VCAM-1	F	5'-GGGACCACATCTACGCTGACA-3'
	R	5'CCTGTCTGCATCCTCCAGAAA-3'
Beta-2 Microglobulin (β2M)	F	5'-CATCCAGCGTACTCCAAAGA-3'
	R	5'-GACAAGTCTGAATGCTCCAC-3'
18S	F	5'-CCAATCACTTCCGACCTGCTG-3'
	R	5'-GCTTTGTATCCCTGCCCTGAG-3'

4.2.7 Immunocytochemistry

HCAECs were seeded as per section 4.2.1 in 4-well Lab-Tek II chamber slides (Lab-Tek) ($1x10^5$ cells/mL). Cells were treated with PBS (control) and TNF-α (1 ng/mL) for 4 hours, and apoA-I rHDL (16 µM/0.45 mg/mL) for 16 hours. As per section 2.16, cells were fixed in 4% (w/v) paraformaldehyde, blocked with a 0.3% (w/v) hydrogen peroxide solution (made up in methanol) for 20 minutes and incubated with anti-DHCR24 rabbit monoclonal IgG (1:200 dilution in 5% (w/v) goat serum) (Cell Signalling Technology) overnight and goat anti-rabbit IgG conjugated to horseradish peroxidase (HRP) (1:200 dilution in 5% (w/v) goat serum) (Cell Signalling Technology) for 30 minutes. Cells were visualised using 3,3'-diaminobenzidine (DAB) (Dako) for 5 minutes, counterstained in haemotoxylin, mounted with DPX (Merck Millipore), and then cover-slipped. Cell images were obtained using a BH-2 Olympus microscope at 20x magnification.

4.2.8 Fluorescent microscopy

HCAECs were seeded in FD3510 fluorodishes (WPI Europe) and transiently transfected with pDHCR24-EGFP as per section 4.2.1. Cells were treated with 2.5 ng/mL for 4% (w/v) paraformaldehyde (20 minutes, room temperature), blocked with 1% (w/v) BSA, 2% (w/v) FBS before being washed. The ER was stained by incubating cells with ER specific anti-GRP78 [578] goat primary antibody (1:1000 dilution in 1% (w/v) BSA, 2% (w/v) FBS) (Invitrogen) for 1 hour and then with anti-goat secondary antibody (1:200 in 1% (w/v) BSA, 2% (w/v) FBS) for 1 hour. The nucleus was stained with 4',6-diamidino-2-phenylindole (Dapi) (1:1000 dilution in PBS) and actin with AlexaFluor488 Phalloidin (1:200 dilution in 1% (w/v) BSA, 2% (w/v) FBS) (20 minutes each). Cells were covered in NPG mounting media and imaged at 60x magnification under oil immersion with a Nikon Ti inverted epifluorescent microscope. NIS elements software was used to collect cell images.

4.2.9 Statistical analysis

Data are expressed as mean ± SEM. Direct comparisons between two treatments were performed using unpaired t-test, while significant differences between multiple treatments were determined by one-way ANOVA with Sidak's *post hoc* test analysis. GraphPad Prism 6.0 was used for analysis. Significance was set at $P<0.05$. To show the effect size, P values lower than $P <0.05$ were specified.

4.3 Results

4.3.1 DHCR24 overexpression does not increase the cholesterol content of HCAECs

To determine whether the mechanism by which DHCR24 facilitates decreasing TNF-α-induced ICAM-1 and VCAM-1 levels is cholesterol-dependent, cultured HCAECs were transfected with pcDNA3.1A (pControl) or pcDNA3.1A-DHCR24 (pDHCR24) expression vectors using TransPass V reagent (New England Biolabs) with the optimised conditions described in section 2.4.1. pcDNA3.1A was the vehicle control for transfection because DHCR24 was cloned into pcDNA3.1A vector for overexpression analysis. Following transfection, the transfectants were left for 24-hours prior to delipidating the cells using hexane/isopropanol and measuring cellular cholesterol levels using the Amplex Red Cholesterol Assay (Life Technologies) as described in section 2.15. Total RNA was then extracted from the delipidated cells as per [579] to verify DHCR24 overexpression.

Figure 4.1 shows that there was no significant increase in cellular cholesterol levels in pDHCR24-overexpressing HCAECs compared to pControl-transfected cells.

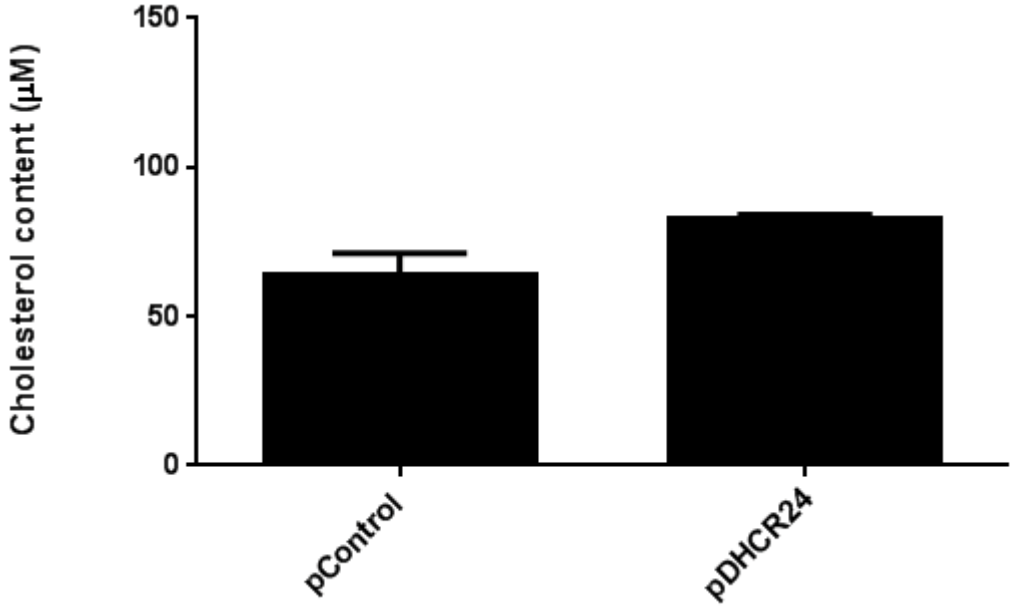

Figure 4.1 DHCR24 overexpression did not increase HCAECs cholesterol content. HCAECs were transfected with pcDNA3.1A (pControl) or pcDNA3.1A-DHCR24 (pDHCR24) plasmids for 4 hours before cholesterol was extracted using hexane/isopropanol. Cholesterol levels were measured using the Amplex Red Cholesterol Assay (Life Technologies). Data are shown as mean ± SEM (n = 3)

4.3.2 Transient transfection of DHCR24 oxidoreductase mutant (pN294T/K306N) increases DHCR24 levels in human coronary artery endothelial cells (HCAECs)

To confirm the transient transfection of the **DHCR24 oxidoreductase mutant (ORM) (**pDHCR24-N294T/K306N**)** increased DHCR24 levels in HCAECs, cultured HCAECs were transfected with pcDNA3.1A (pControl), pDHCR24 or **pN294T/K306N** expression vectors using TransPass V reagent (New England Biolabs) with the optimised conditions described in section 2.4.1. pcDNA3.1A vector (pControl) was the vehicle control for transfection because DHCR24 was cloned into pcDNA3.1A vector for overexpression analysis, and pDHCR24 was the wild type positive control. Following transfection, cells were left for 24 hours prior to extraction of total RNA and subsequent analysis of DHCR24 mRNA levels by real-time RT-qPCR.

From the RT-qPCR results shown in Figure 4.2, transfection of the ORM and wild type DHCR24 using TransPass V (New England Biolabs) was successful with DHCR24 mRNA levels significantly increased ($P<0.0001$ vs pControl), compared to the empty vector control.

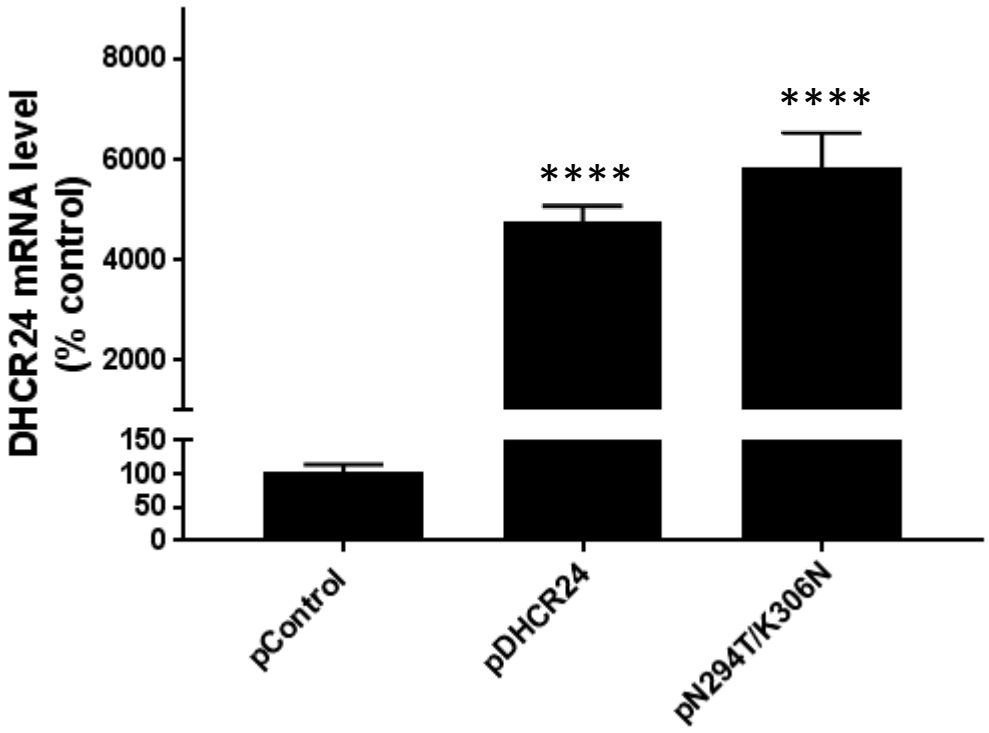

Figure 4.2 Transient transfection of HCAECs with pDHCR24-N294T/K306N successfully increased DHCR24 levels. HCAECs cells were transfected with pcDNA3.1A (pControl), pcDNA3.1A-DHCR24 (pDHCR24), or pN294T/K306N for 24 hours. Total RNA was isolated and RT-qPCR used to measure DHCR24 mRNA levels with GAPDH as a reference gene. Data are shown as mean ± SEM (n = 4) **** P<0.0001 vs pControl.

4.3.3 The DHCR24 oxidoreductase mutant does not suppress TNF-α-induced ICAM-1 or VCAM-1 levels in HCAECs

DHCR24's oxidoreductase site is responsible for catalysing the conversion of desmosterol to cholesterol [419] and is considered the enzyme's active site [580]. To investigate whether DHCR24's effect of reducing TNF-α-induced ICAM-1 and VCAM-1 levels in HCAECs is dependent on the oxidoreductase site, a DHCR24 oxidoreductase mutant (ORM) was produced using site-directed mutagenesis. It was tested whether ORM overexpression could protect against a TNF-α-induced (2.5 ng/mL, 4 hours) inflammatory response as measured by ICAM-1 and VCAM-1 protein levels in HCAECs in a similar fashion to wild type-DHCR24, replicating its effects. The mRNA level of VCAM-1 was also measured to determine if the effect at the protein level was due to an effect on gene expression. Similar to the previous experiment, HCAECs were treated with TNF-α (2.5 ng/mL, 4 hours).

Figures 4.2 and 4.3 show that cytokine activation of HCAECs increased ICAM-1 and VCAM-1 protein levels. Figure 4.4 also shows that VCAM-1 mRNA levels were increased by cytokine activation. pDHCR24-overexpression reduced TNF-α-induced ICAM-1 and VCAM-1 protein (Figures 4.3, 4.4) and mRNA levels (Figure 4.5).

The ORM did not replicate wild type-DHCR24's effects of suppressing TNF-α-induced ICAM-1 and VCAM-1 levels. Figures 4.3 and 4.4 show there was no difference in TNF-α-induced ICAM-1 and VCAM-1 levels between ORM and pControl at the protein level. There was no difference in VCAM-1 mRNA levels between ORM and pControl (Figure 4.5).

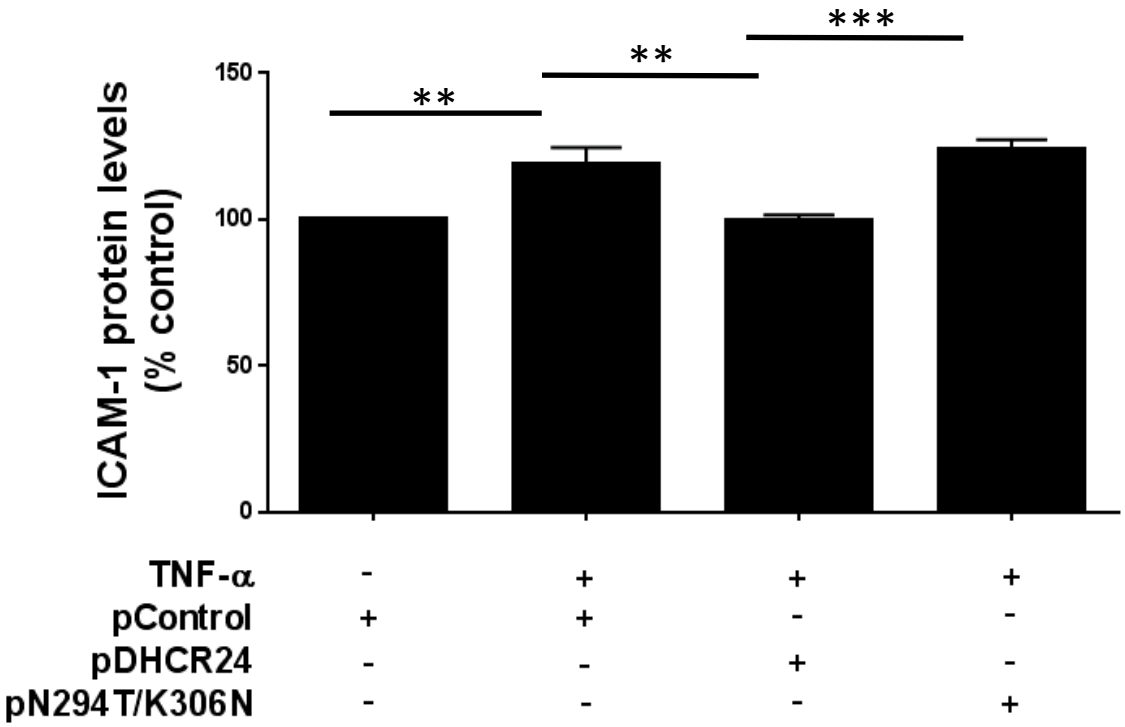

Figure 4.3 DHCR24 oxidoreductase mutant (pN294T/K306N) did not suppress TNF-α-activated ICAM-1 protein levels in HCAECs. pcDNA3.1A-DHCR24 (pDHCR24)-overexpression suppressed ICAM-1 protein levels in TNF-α-activated HCAECs in comparison to pcDNA3.1A (pControl) and pDHCR24-N294T/K306N (pN294T/K306N). HCAECs were transfected with pControl, pDHCR24, or pN294T/K306N plasmids before activation with 2.5 ng/mL TNF-α for 4 hours. ICAM-1 protein levels were measured using the ELISA. Data are shown as mean ± SEM (n = 3) ** P<0.01, *** P<0.001.

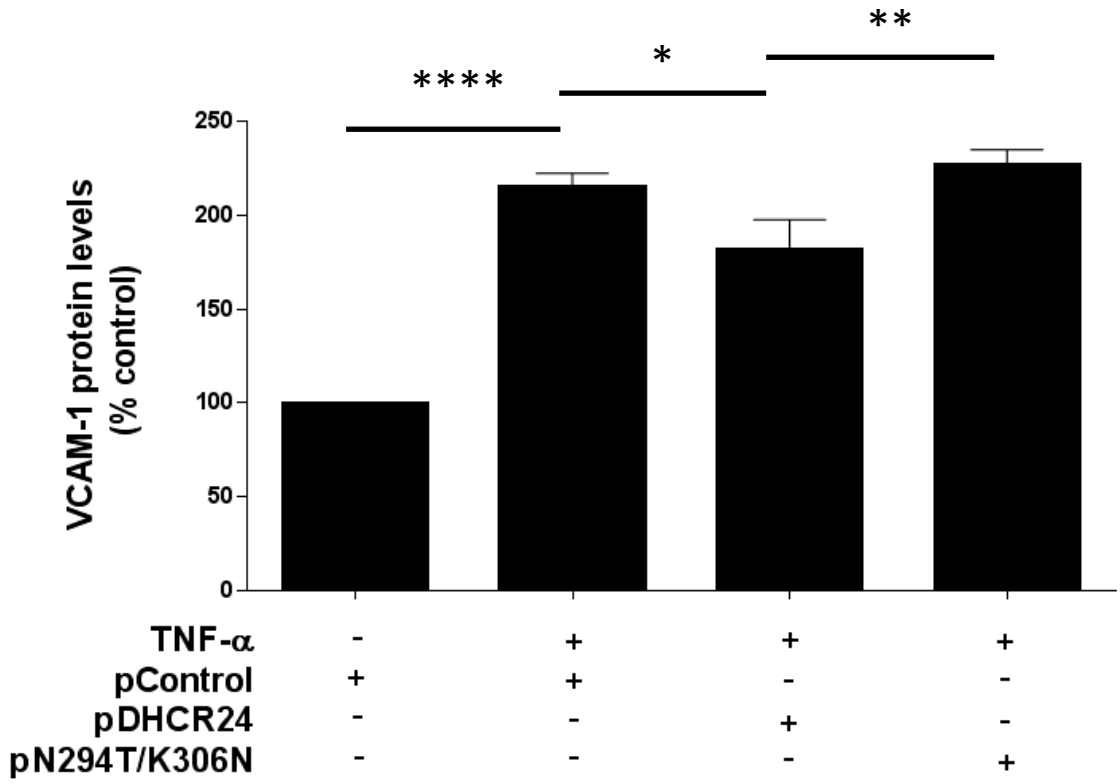

Figure 4.4 DHCR24 oxidoreductase mutant (N294T/K306N) did not suppress TNF-α-activated VCAM-1 protein levels in HCAECs. pcDNA3.1A-DHCR24 (pDHCR24)-overexpression suppressed VCAM-1 protein levels in TNF-α-activated HCAECs in comparison to pcDNA3.1A (pControl) and pDHCR24-N294T/K306N (pN294T/K306N). HCAECs were transfected with pControl, pDHCR24, or pN294T/K306N plasmids before activation with 2.5 ng/mL TNF-α for 4 hours. ICAM-1 protein levels were measured using the ELISA. Data are shown as mean ± SEM (n = 5) * P<0.05, ** P<0.01, **** P<0.0001.

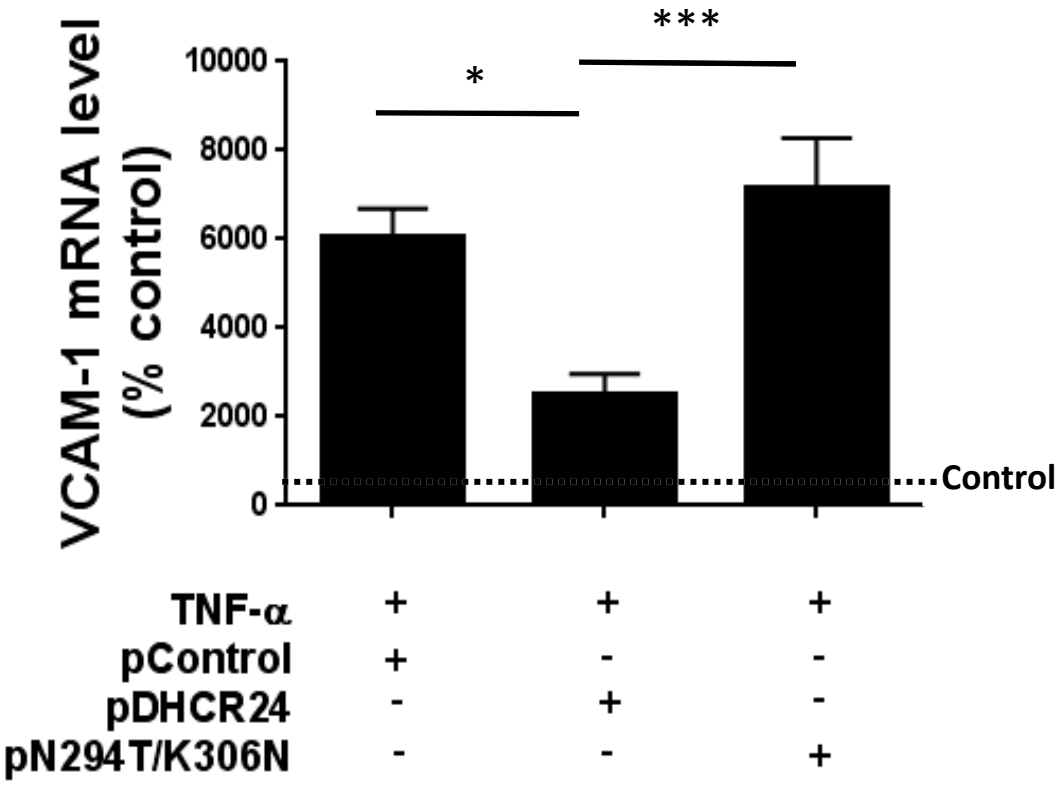

Figure 4.5 DHCR24 oxidoreductase mutant (pN294T/K306N) did not suppress TNF-α-activated VCAM-1 mRNA levels in HCAECs. pcDNA3.1A-DHCR24 (pDHCR24)-overexpression suppressed VCAM-1 mRNA levels in TNF-α-activated HCAECs in comparison to pcDNA3.1A (pControl) and pDHCR24-N294T/K306N (pN294T/K306N). HCAECs were transfected with pControl, pDHCR24, or pN294T/K306N plasmids before activation with 2.5 ng/mL TNF-α for 4 hours. Total RNA was extracted and VCAM-1 mRNA levels were measured using RT-qPCR with β2M as a reference gene. Data are shown as mean ± SEM (n = 3) * $P<0.05$, *** $P<0.001$. Dotted line represents untreated control.

4.3.4 DHCR24 translocates from the ER to the cytoplasm and nucleus in response to TNF-α-activation in HCAECs

DHCR24 is primarily localised and tethered to the ER membrane facing the cytoplasm [140, 581]. The ER localisation of DHCR24 is in keeping with other cholesterol biosynthesis enzymes such as HMG-CoA as *de novo* cholesterol production primarily occurs on the cytoplasmic side of the ER membrane [582]. As DHCR24 catalyses the production of cholesterol, it was originally proposed that DHCR24 would mediate protection in TNF-α-activated HCAECs against the inflammatory response through a cholesterol-mediated process as this mechanism has been demonstrated in other cell types [433, 438]. However, section 4.3.1 shows that DHCR24 overexpression does not increase cholesterol levels and that the protection against TNF-α-activation elicited by DHCR24 in HCAECs does not appear to be cholesterol-dependent. DHCR24 protects fibroblasts (mouse and rat) by translocating from its endogenous, unstimulated location to interact with other proteins and inhibiting stress responses. In MEF, transmembrane domain-deleted DHCR24 translocates from the ER into the cytoplasm following H_2O_2-exposure where it scavenges ROS, consequently preventing apoptosis [140]. Wild type DHCR24 prevents apoptosis in MEF by inhibiting caspase-3 [140], while in rat fasciculata cells, DHCR24 is cleaved by caspase-3 releasing the catalytic domain from the ER membrane preventing apoptosis but also allowing it to translocate to the nucleus. This latter study however did not investigate a role for this translocation subsequent to DHCR24's cleavage by caspase-3 [577]. DHCR24 also inhibits caspase-3 activation by serving as a caspase substrate in neuroglioma H4 cells preventing apoptosis [421]. In rat embryonic fibroblasts, DHCR24 translocates to the nucleus, following H_2O_2 treatment. DHCR24's nuclear translocation in rat embryonic fibroblasts blocks degradation of the tumour suppressor p53 through ubiquitination, leading to accumulation of its active form. p53 is an important tumour suppressor gene which prevents cell proliferation under conditions of cellular stress. DHCR24 displaces E3 ubiquitin ligase Mdm2 from p53 allowing it to accumulate, which in turn enables it to activate DNA repair enzymes, arrest the cell cycle at G1/S and enable DNA repair enzymes to function [423]. These functions of caspase-3 interaction and p53 accumulation both require DHCR24 to translocate to the nucleus. As a first step in exploring DHCR24's multi-functional role and potential interaction with other proteins in HCAECs, it was investigated if it changed localisation following TNF-α-activation.

To investigate the localisation of DHCR24 protein in HCAECs, in quiescent and TNF-α-activated states, HCAECs were treated with PBS or TNF-α and imaged using immunocytochemistry. Detecting DHCR24's localisation and translocation using immunocytochemistry involved treating cells with PBS (control) or TNF-α (1 ng/mL) for 5 hours. Endogenous DHCR24 levels were below the detection sensitivity of the immunocytochemistry used (Figure 4.6 A), and so apoA-I rHDL (16 μM/0.45 mg/mL, 16 hours) was used to increase DHCR24 levels in order to observe DHCR24's localisation in unstressed HCAECs. Following treatment, cells were fixed on slides and stained for immunocytochemistry as described in section 2.16 using rabbit anti-DHCR24 monoclonal antibody (Cell Signalling Technology). Images of the slides were obtained using a BH-2 microscope mounted with a camera.

Figure 4.6 (A) demonstrated that DHCR24 was below detection in HCAECs treated with PBS as a control. However, following apoA-I rHDL pre-incubation for 16 hours DHCR24 levels (as indicated by brown-coloured staining) increased in the cytoplasm (Figure 4.6 B). Moreover, pre-incubation with apoA-I rHDL prior to subsequent TNF-α-activation for 5 hours stimulated increased DHCR24 levels in the cytoplasm (Figure 4.6 C). Additionally, HCAECs treated with only TNF-α for 5 hours showed a mild increase in cytoplasmic DHCR24 protein levels. The increased DHCR24 levels in cells treated with TNF-α alone (Figure 4.6 D), were noticeably lower than the levels induced by cells stimulated with apoA-I rHDL (Figure 4.6 B) or apoA-I rHDL with TNF-α (Figure 4.6 C).

Immunocytochemistry showed that in HCAECs, DHCR24 is localised around the nucleus, possibly on the ER, however this did not provide complete evidence for whether or not DHCR24 was localised to the ER and whether it translocated to the nucleus following TNF-α-activation. Therefore fluorescent microscopy was used to further interrogate DHCR24's localisation using EGFP-tagged DHCR24 (DHCR24-EGFP) transfected HCAECs.

Using EGFP-tagged DHCR24 (pDHCR24-EGFP) transfected HCAECs, fluorescent microscopy was used to investigate DHCR24's localisation in HCAECs, in quiescent and TNF-α activated states. DHCR24-EGFP transfectants were treated with PBS (control) or TNF-α (2.5 ng/mL) for 4 hours. Following treatment, cells were subjected to fluorescent stains colouring the ER, nucleus, and actin - GRP78 with Alexa Fluor 568 for the ER (red), Dapi for the nucleus (cyan), Phalloidin 647 for actin (purple) (section 2.16).

Figure 4.7 shows that in HCAECs, DHCR24 localises to the ER under normal conditions while Figure 4.8 shows that following TNF-α-activation, DHCR24 translocates from the ER throughout the cell to the cytoplasm and nucleus.

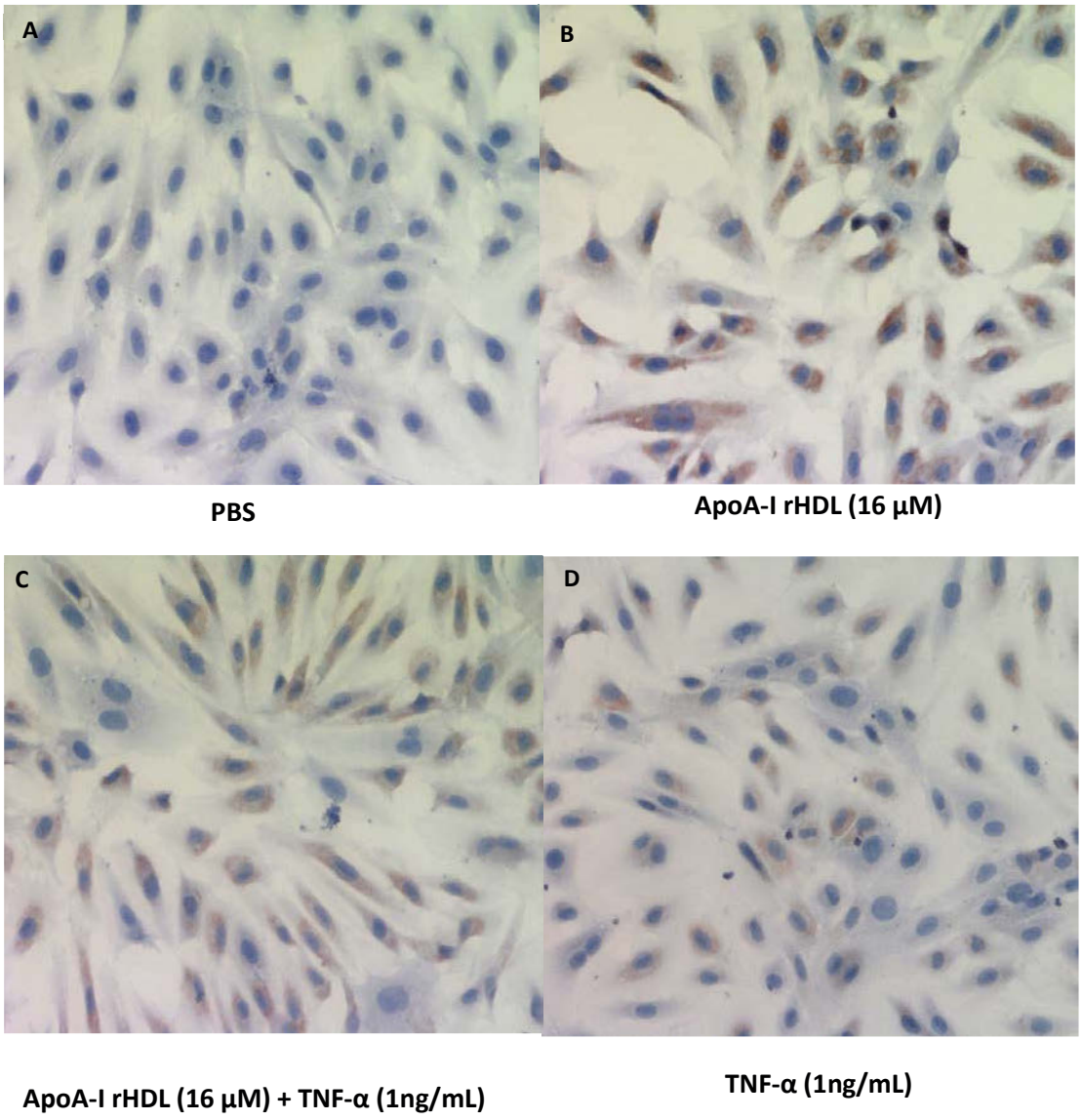

Figure 4.6 Localisation of DHCR24 protein in cultured non-transfected HCAECs by immunocytochemistry staining. Non-transfected HCAECs treated with: (A) PBS for 24 hours; (B) apoA-I rHDL at 16 µM (0.45 mg/mL) for 16 hours; (C) HCAECs pre-incubated with apoA-I rHDL (16 µM) for 16 hours, followed by stimulating with TNF-α at 1 ng/mL for 5 hours; and (D) HCAECs stimulated only with TNF-α (1 ng/mL) for 5 hours. The presence of DHCR24 protein in HCAECs was detected by rabbit anti-DHCR24 monoclonal antibody (Cell Signalling Technology). The slides were stained by haematoxylin and eosin (H&E) with the nucleus stained purple and the cytoplasm stained light blue. DHCR24 proteins (dark brown granules) as shown in B-D were mostly localised in the cytoplasmic region. All images obtained using 20x magnification with a BH-2 Olympus microscope.

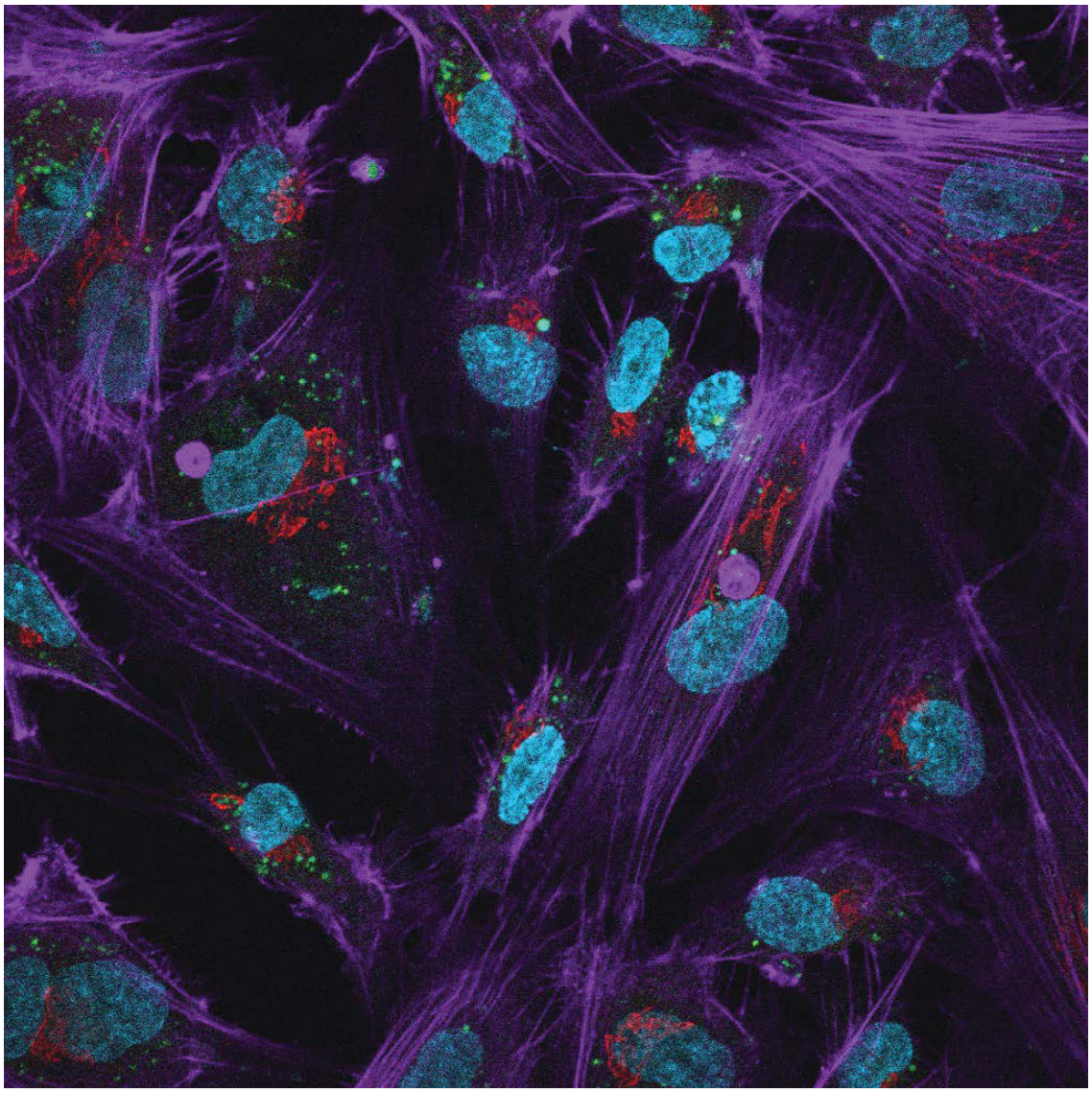

Figure 4.7 DHCR24 localises to the endoplasmic reticulum (ER) in HCAECs. HCAECs were transfected with pDHCR24-EGFP plasmid were fixed with 4% (w/v) paraformaldehyde, and stained with GRP78 with Alexa Fluor 568 for the ER (red), Phalloidin 647 for actin (purple), Dapi for the nucleus (cyan). Images obtained using 60x magnification under oil immersion using a Nikon Confocal microscope.

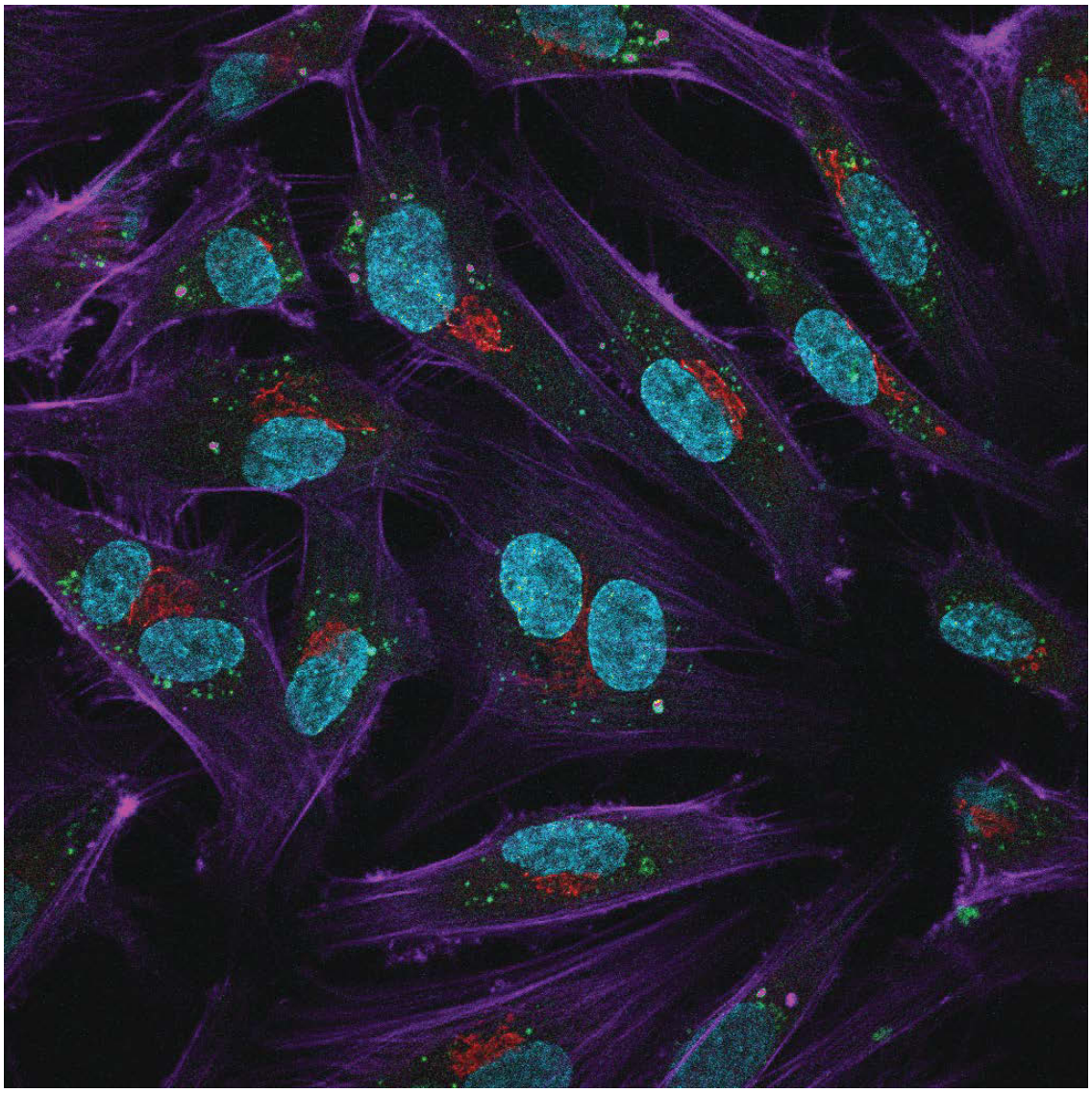

Figure 4.8 DHCR24 translocates from the ER to the cytoplasm and nucleus following TNF-α-activation in HCAECs. HCAECs were transfected with pDHCR24-EGFP plasmid and exposed to TNF-α (2.5 ng/mL) for 4 hours. HCAECs were fixed with 4% (w/v) paraformaldehyde, and stained with GRP78 with Alexa Fluor 568 for the ER (red), Phalloidin 647 for actin (purple), Dapi for the nucleus (cyan). Images obtained using 60x magnification under oil immersion using a Nikon Confocal microscope.

4.3.5. DHCR24 downregulates TNF-α-induced sXBP-1 and ATF-6 levels in HCAECs

The results in section 4.3.4 confirmed that DHCR24 is an ER-resident in HCAECs, however despite this localisation, consistent with other cholesterol biosynthesis enzymes [582], DHCR24 overexpression does not significantly increase cholesterol levels (section 4.3.1). This result indicated that DHCR24's protective effects against a TNF-α-induced inflammatory response in HCAECs are not cholesterol-dependent. In tandem with the observation of DHCR24's localisation to the ER, the hypothesis that DHCR24 may interact with the ER suppressing TNF-α-induced markers of ER stress, in turn facilitating reductions in the associated inflammatory response [86] was formed. To investigate whether DHCR24 suppresses a TNF-α-induced ER stress response and consequently suppresses the inflammatory response, HCAECs were treated with the same conditions used to elicit the inflammatory response in section 4.3.3 (2.5 ng/mL, 4 hours). The DHCR24 oxidoreductase mutant (ORM) was also tested to investigate whether DHCR24's oxidoreductase site is required for protection against TNF-α-induced increases in ER stress marker levels.

Figures 4.9, 4.10, and 4.12 show that as expected in HCAECs, TNF-α-activation leads to significantly increased sXBP-1, XBP-1 and ATF-6 mRNA levels. pDHCR24 overexpression leads to suppression of TNF-α-induced sXBP-1 and ATF-6 mRNA levels (Figure 4.9 and 4.12). The ORM did not replicate wild type DHCR24's ability to suppress TNF-α-induced levels of sXBP-1 (Figure 4.9).

There was no significant difference between the ORM and wild type DHCR24's ability to suppress TNF-α-induced levels of ATF-6 (Figure 4.12) although there was a trend of a reduced suppressive effect exhibited by the ORM.

TNF-α-induced XBP-1 mRNA levels were not significantly suppressed by DHCR24 although a downward trend was observed. The ORM did not follow this trend with a significantly higher level of XBP-1 compared to wild type DHCR24 (Figure 4.10). TNF-α-activation at the inflammatory conditions employed did not significantly increase ATF-4 levels although levels in the TNF-α-activated ORM-transfectants were significantly increased compared to TNF-α-activated wild type DHCR24 (Figure 4.11).

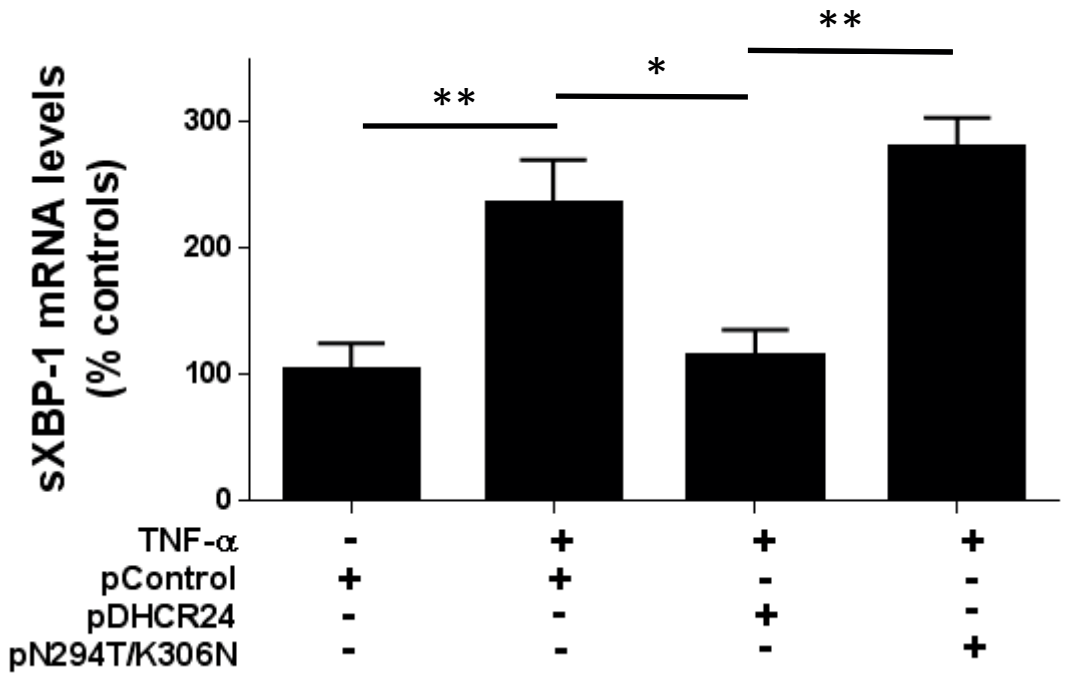

Figure 4.9 pcDNA3.1A-DHCR24 (pDHCR24)-overexpression suppressed sXBP-1 mRNA levels in TNF-α-activated HCAECs in comparison to pcDNA3.1A (pControl) and pDHCR24-N294T/K306N (pN294T/K306N). HCAECs were transfected with pControl, pDHCR24, or pN294T/K306N plasmids before activation with 2.5 ng/mL TNF-α for 4 hours. Total RNA was extracted and sXBP-1 mRNA levels were measured using RT-qPCR with GAPDH as a reference gene. Data are shown as mean ± SEM (n = 4) * P<0.05, ** P<0.01.

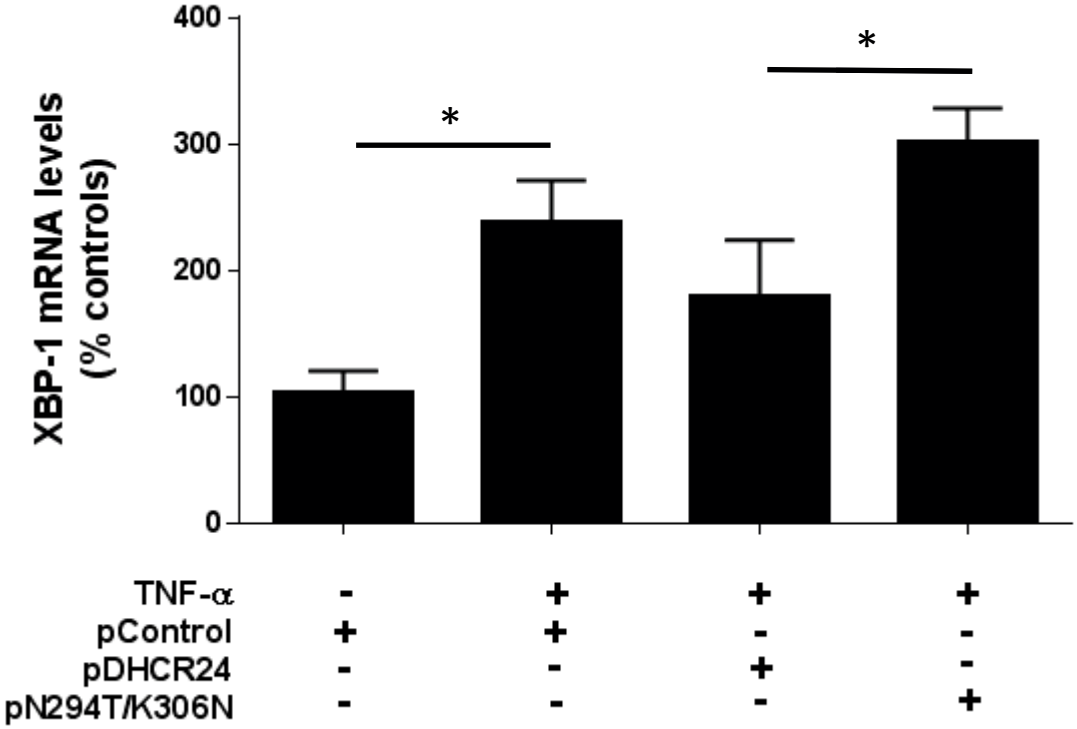

Figure 4.10 pcDNA3.1A-DHCR24 (pDHCR24) and pDHCR24-N294T/K306N (pN294T/K306N) did not suppress XBP-1 mRNA levels in TNF-α-activated HCAECs. XBP-1 mRNA levels were significantly higher in pN294T/K306N cells in comparison to pDHCR24. HCAECs were transfected with pControl, pDHCR24, or pN294T/K306N before activation with 2.5 ng/mL TNF-α for 4 hours. Total RNA was extracted and XBP-1 mRNA levels were measured using RT-qPCR with GAPDH as a reference gene. Data are shown as mean ± SEM (n = 4) * $P<0.05$.

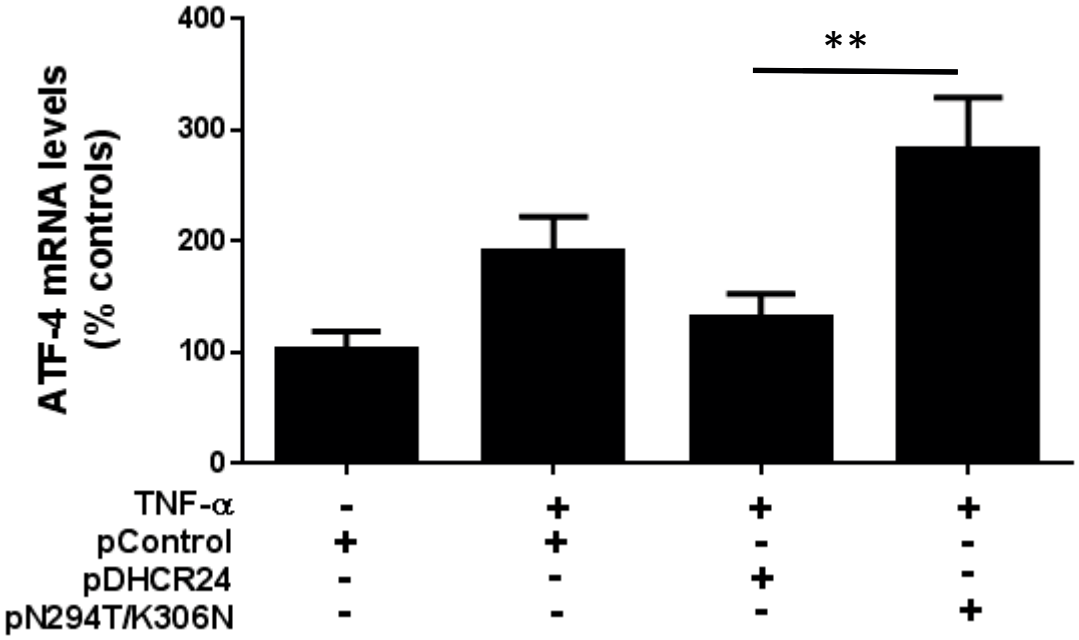

Figure 4.11 ATF-4 mRNA levels were not significantly increased in TNF-α-activated HCAECs. ATF-4 mRNA levels were significantly higher in pDHCR24-N294T/K306N (pN294T/K306N) cells in comparison to pcDNA3.1A-DHCR24. HCAECs were transfected with pcDNA3.1A (pControl), pDHCR24, pN294T/K306N before activation with 2.5 ng/mL TNF-α for 4 hours. Total RNA was extracted and XBP-1 mRNA levels were measured using RT-qPCR with GAPDH as a reference gene. Data are shown as mean ± SEM (n = 4) ** P<0.01.

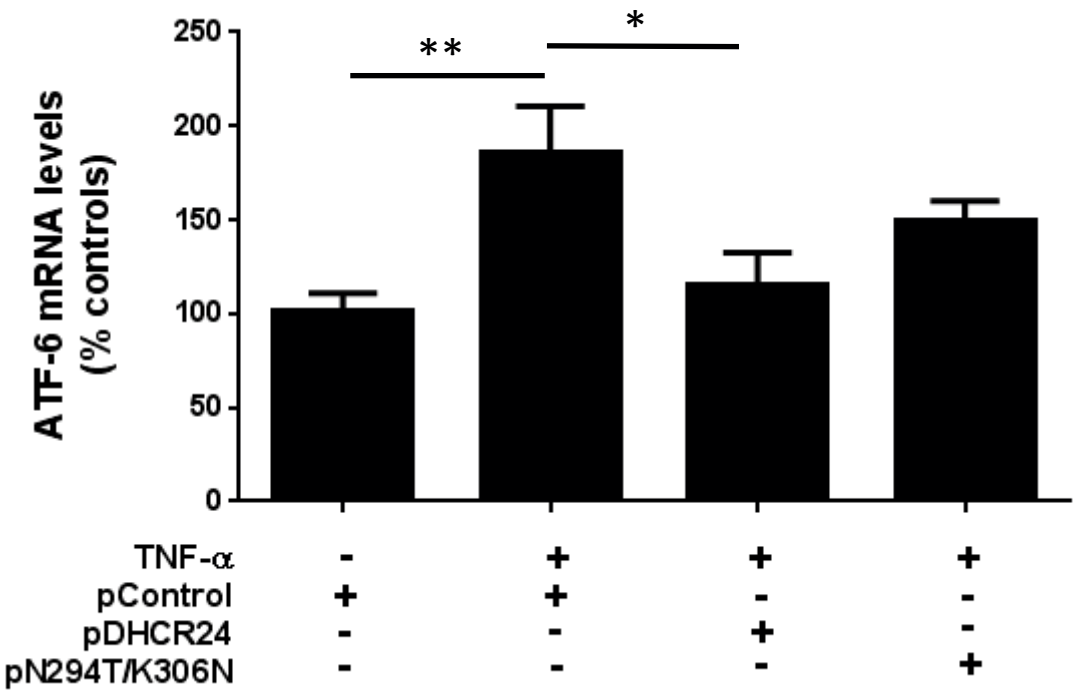

Figure 4.12 pDHCR24 suppressed ATF-6 mRNA levels in TNF-α-activated HCAECs. Oxidoreductase mutant pDHCR24-N294T/K306N (pN294T/K306N) did not significantly suppress ATF-6 mRNA levels. ATF-6 mRNA levels were not significantly suppressed in pcDNA3.1A-DHCR24 (pDHCR24) cells in comparison to pN294T/K306N. HCAECs were transfected with pcDNA3.1A (pControl), pDHCR24, or pN294T/K306N before activation with 2.5 ng/mL TNF-α for 4 hours. Total RNA was extracted and ATF-6 mRNA levels were measured using RT-qPCR with GAPDH as a reference gene. Data are shown as mean ± SEM (n = 4) * P<0.05, ** P<0.01.

4.4 Discussion

Elucidating the mechanisms through which DHCR24 elicits protection against a TNF-α-induced inflammatory response in HCAECs is vital for the understanding of the protein and for the development of potential downstream applications. In this chapter, DHCR24 was demonstrated to suppress a TNF-α-induced inflammatory response as measured by ICAM-1 and VCAM-1 levels independent of cholesterol biosynthesis, but still through the enzyme's oxidoreductase site, and by attenuating mRNA levels of the ER stress markers sXBP-1 and ATF-6 in HCAECs. This work also revealed that DHCR24 translocates from its endogenous localisation of the endoplasmic reticulum freely throughout the cytoplasm and nucleus of HCAECs following TNF-α-activation.

The most novel finding of this study was DHCR24's ability to suppress a TNF-α-induced inflammatory response independent of increased cholesterol levels. It was originally hypothesised that DHCR24 overexpression would lead to increased cholesterol levels, as DHCR24 is an integral cholesterol biosynthesis enzyme in all mammalian organisms [419, 434, 442, 443, 576] and because DHCR24 also facilitates anti-apoptotic activity in human neuroblastoma SH-SY5Y cells (neuronal cells) [433, 438] through a cholesterol-dependent mechanism. In neuroblastoma SH-SY5Y cells DHCR24 also increases cholesterol levels, modulating amyloid beta (Aβ) peptide production and clearance, in addition to reducing pre-fibrillar aggregates and neurotoxicity [433, 438]. Moreover, elevated cholesterol levels are the mechanism through which DHCR24 reduces ER stress in neuroblastoma cells [469]. Conversely, in W138-TERT fibroblasts and mouse embryonic fibroblasts (MEF) DHCR24 directly scavenges ROS, preventing H_2O_2-induced apoptosis, independent of cholesterol biosynthesis [140, 423, 437]. The results presented in this study show that DHCR24-overexpression in HCAECs does not increase cellular cholesterol levels. This may be in part attributed to the availability of sterol precursors and cholesterol requirements of specific cell types [420, 433]. DHCR24 is also not a rate-limiting enzyme, instead catalyses the conversion of desmosterol to cholesterol [419]. Despite the significance of DHCR24's cholesterol biosynthetic role, and published reports of DHCR24 increasing cholesterol levels in response to cellular stress [433, 438, 469], this was surprisingly not the mechanism through which DHCR24 suppresses a TNF-α-induced inflammatory response in HCAECs.

As DHCR24 was not shown to protect against a TNF-α-induced inflammatory response in HCAECs through a cholesterol-dependent mechanism, other mechanisms were investigated. DHCR24 is considered an endoplasmic reticulum (ER) resident protein [437, 581], and so it was hypothesised that in HCAECs it may interact with the ER and consequently mediate reductions in a TNF-α-induced inflammatory response through reductions in (TNF-α-induced)-ER stress markers as ER stress also stimulates inflammation [86]. Further impetus to study this mechanism comes from work reporting that DHCR24 facilitates reductions in tunicamycin-induced ER stress-mediated apoptosis in MEF [469]. The results presented, show that DHCR24 suppresses the mRNA levels of the ER stress markers sXBP-1 and ATF-6 following TNF-α-activation. It is worth noting that while ATF-4 mRNA levels were not significantly increased by TNF-α-activation, an upward trend was observed. Further, there was a downward trend in this marker evident in DHCR24-overexpressing HCAECs. TNF-α-activation increased XBP-1 mRNA levels and revealed that DHCR24 overexpression did not significantly suppress the TNF-α-induced increase but similar to DHCR24's effect on ATF-4 mRNA levels, there was also a downward trend. This lack of significant differences between control-transfectants and DHCR24-overexpressing HCAECs may be attributed to low levels of XBP-1 and ATF-4 mRNA levels, making detecting differences difficult. However, DHCR24-overexpression did lead to a downward trend in each of the ER stress markers. Further as XBP-1 levels are under the control of ATF-6 [583, 584] the suppressive effect of DHCR24 may be evident with a longer treatment time as ATF-6 levels were significantly suppressed and XBP-1 levels exhibited a downward trend. The cytokine treatment conditions selected for this work to induce increases in the ER stress response were the same as those used to induce a TNF-α-driven inflammatory response. Consequently, these results are associated with DHCR24 suppressing a TNF-α-induced inflammatory response, at least in part, by suppressing TNF-α-induced sXBP-1 and ATF-6 mRNA levels. Moreover, with the protective trends exhibited by DHCR24, future experiments solely focusing on the ER stress response rather than the ER stress response as a mediator of the inflammatory response, a greater role for DHCR24 against the ER stress response may be elucidated.

Continuing the study of DHCR24's interaction with the ER, DHCR24's localisation before and after TNF-α-activation in HCAECs was investigated using immunocytochemistry and fluorescent microscopy. Interestingly, immunocytochemistry first revealed that DHCR24 levels were low in unstressed HCAECs as DHCR24 was below detection level. However, following TNF-α-activation DHCR24 levels were increased. This indicates that in HCAECs, TNF-α-

activation leads to an endogenous increase in DHCR24 levels but at these levels it is insufficient to confer protection against TNF-α-activation. This is supported by Chapter 3's results which showed that DHCR24-overexpression was required to significantly suppress a TNF-α-induced inflammatory response. Microscopy showed that pre-incubation of HCAECs with apoA-I rHDL increased DHCR24's protein levels replicating Chapter 3's result, but also provided information about localisation, showing that DHCR24 levels increase throughout the cytoplasm. As DHCR24 levels in untreated HCAECs were below detection level using immunocytochemistry, fluorescence microscopy was used to show that DHCR24's endogenous localisation was to the ER, in keeping with observations in neuronal cells [421], adrenal cells [577] and fibroblasts [140, 437]. DHCR24's translocation from the ER to the cytoplasm and nucleus in TNF-α-activated HCAECs was revealed by fluorescent microscopy and similar to DHCR24's effect in other cell types [140, 423, 577]. DHCR24 translocates from the ER to the nucleus in rat fasciculata cells but not in human fasciculata cells, in response to ACTH-induced ROS production protecting against apoptosis [577] demonstrating the enzyme's cell-specific activity. In MEFs, DHCR24 scavenges H_2O_2-induced ROS while tethered to the ER. However when a DHCR24-transmembrane mutant form of DHCR24 is formed it can also scavenge ROS in the cytoplasm [437]. DHCR24 in MEF can also translocate when cleaved by caspase-3 at DHCR24's caspase cleavage motif sites, releasing it from the ER [140]. Additionally, DHCR24 serves as a caspase death substrate preventing apoptosis with caspase cleavage sites located in its C-terminus [421]. DHCR24's translocation from the ER to the nucleus may suggest activity against apoptosis as seen in rat embryonic fibroblasts [423]. When DHCR24 translocates to the nucleus in rat embryonic fibroblasts following H_2O_2 treatment, it binds to p53, displacing E3 ubiquitin ligase Mdm2 from p53, allowing p53 to accumulate in cells in turn activating DNA repair enzymes and inducing growth arrest by holding the cell cycle at G1/S to enable DNA repair enzymes to function [423]. DHCR24's movement into the cytoplasm may also indicate a role against oxidative stress as reported in MEF cells, in which it directly scavenges tunicamycin-induced H_2O_2 via the enzyme's N-terminal region [437].

The next potential mechanism for facilitating suppression of a TNF-α-induced inflammatory response in HCAECs investigated, was the role of DHCR24's oxidoreductase site. DHCR24's oxidoreductase site is located in the enzyme's N-terminal and considered its active site as it is involved in the reducing the Δ24 bond of desmosterol to produce cholesterol [419]. In addition to this cholesterol biosynthesis role, as mentioned in the previous paragraph, DHCR24's oxidoreductase site has been reported to elicit protection against tunicamycin-induced

oxidative stress in MEF, directly serving as a ROS-scavenger preventing apoptosis, independent of cholesterol biosynthesis [437]. Similarly in HCAECs, it was shown that DHCR24's suppression of a TNF-α-induced inflammatory response was dependent on its oxidoreductase site with suppression of TNF-α-induced ER stress marker sXBP-1 mRNA levels being oxidoreductase site-dependent. While in the previous section it was mentioned that DHCR24 did not significantly suppress XBP-1 and ATF-4 mRNA levels, ORM-overexpression led to significant increases in XBP-1 and ATF-4 levels in comparison to wild type DHCR24. Moreover, TNF-α-activation also led to a trend of increased ATF-6 levels in ORM-transfectants vs wild type DHCR24. These findings show that DHCR24 loses some of its protective ability when its oxidoreductase site is not functional. Following TNF-α-activation, ATF-4 and XBP-1 mRNA levels were also significantly higher in ORM-transfectants than in vector-control transfected HCAECs indicating a loss of protection by DHCR24. This may be a consequence of DHCR24 being unable to compete with the significantly increased ORM levels. Additionally, these ER stress marker levels may also be higher in ORM-transfectants than in control-transfectants as DHCR24 may not be scavenging superoxide due to the loss of the oxidoreductase site functioning in the ORM-transfectants. This work provides support for the significance of DHCR24's oxidoreductase site, adding to the published work in MEF [140] and providing novel information enhancing the understanding of DHCR24's activity in HCAECs. The understanding of DHCR24's oxidoreductase site is particularly valuable for the development of potential downstream therapeutic applications using mimetic forms of the enzyme to suppress inflammation and/or ER stress.

In conclusion, DHCR24 has been shown to suppress TNF-α-induced inflammatory response through suppression of the ER stress markers sXPB-1 and ATF-6 in HCAECs. This work also shows that DHCR24 mediates this activity through its oxidoreductase site, however independent of cholesterol synthesis activity. Endogenous levels of DHCR24 in unstressed HCAECs were shown to be low and localised to the ER. Following TNF-α-activation, DHCR24 translocates to the cytoplasm and nucleus indicating potential roles in H_2O_2-scavenging and the inhibition of apoptosis respectively. The elucidation of these mechanisms provides valuable information about DHCR24's activity in HCAECs, especially given the cell-specific activity of the enzyme, and for the potential development of a DHCR24 mimetic for reducing endothelial cell inflammation if DHCR24 is considered as a novel therapeutic avenue following positive future studies.

Chapter 5 – DHCR24 replicates apoA-I rHDL's suppression of a TNF-α-induced inflammatory response in HuH7 cells

5.1 Introduction

Insulin resistance is a state in which the body is unable to effectively utilise insulin to control circulating blood glucose levels. This is due to insufficient insulin secretion or the body's inadequate response to glucose levels. Initially, this insufficient response leads to the compensatory measure of increased insulin secretion therefore resulting in high levels of insulin within the body (hyperinsulinaemia). However, hyperinsulinaemia creates an inflammatory environment [585] and is not able to be sustained [70, 586]. Following prolonged hyperinsulinaemia, insulin-producing pancreatic β-cells become dysfunctional through a combination of impaired insulin secretion and decreased β-cell mass reducing insulin production [66, 67, 587]. The resultant uncontrolled blood glucose levels or development of insulin resistance leads to the characteristic feature of type 2 diabetes mellitus – hyperglycaemia. Hyperglycaemia is deleterious as it damages tissues and organ systems leading to various pathologies. For example, when endothelial cells that line blood vessels are exposed to high levels of glucose this leads to elevated expression of cell adhesion molecules (CAMs) such as intracellular adhesion molecule-1 (ICAM-1), vascular cell adhesion molecule-1 (VCAM-1), and endothelial-selectin (E-selectin). The combination of these CAMs can lead to the onset of atherosclerosis (as reviewed by [588]). Insulin resistance is therefore considered an inflammatory disease [84].

Hepatic inflammation is one of the primary drivers of insulin resistance [60, 84]. Hepatic inflammation is often caused by obesity precipitated by a sedentary lifestyle and consumption of a high fat diet (HFD) [60, 589]. These factors are implicated in the aetiology of insulin resistance as they increase circulating non-esterified/free fatty acid (FFA) levels which are proinflammatory [84]. Adipose tissue has a role in storing FFAs and triglycerides. However, adipocytes reach a threshold for lipid storage and then lose their FFA uptake capacity. The adipocytes consequently become proinflammatory, releasing FFAs and inflammatory mediators such as TNF-α, IL-6, CRP, IL-8, SAA, and IL-1β [132, 481-486, 590-595]. Consequently, the inhibited FFA storage capacity/activity of the adipocytes leads to increased levels of FFAs, glucose, and proinflammatory mediators in the circulation and in other tissues as they attempt to compensate for the dysfunctional adipose tissue. Liver tissue is one of the FFA storage sites that serve this compensatory role, however, the liver can also become oversaturated with FFA and become inflamed [60, 596].

Hepatic inflammation directly drives insulin resistance pathogenesis through activation of the canonical IκB kinase (IKK)/nuclear factor kappa B (NFκB) signalling pathway [60, 61, 84]. Fat-fed C57BL/6 mice exhibiting raised levels of circulating FFAs, triglycerides, and significantly increased hepatic NFκB activation develop insulin resistance [60]. Further NFκB activation alone (normal chow diet) results in insulin resistance development in these mice [60]. Chronic IKK activity as an aetiological factor for insulin resistance is further supported by the discovery that attenuation of IKK-β activity leads to improved insulin sensitivity – heterozygous IKK-β knockout mice that were fed a HFD showed lower fasting glucose and insulin levels in addition to reduced FFA levels in comparison to IKK-β positive mice littermates [60, 61]. This helps provide a strong link between hepatic inflammation and the onset of insulin resistance [60, 61, 84].

Our laboratory has demonstrated that HDL improves insulin sensitivity in HFD-fed mice, and also reduces TNF-α-induced NFκB activation in HuH7 cells [406]. C57BL/6 mice fed a HFD for 16 weeks to induce insulin resistance, were administered saline or lipid-free apoA-I as a component of reconstituted rHDL for the final 2 or 4 weeks during the HFD regime. Following both the 2 and 4 week apoA-I treatment periods, insulin sensitivity was improved as evidenced by a reduced homeostatic model assessment for insulin resistance (HOMA-IR) score and reduction in associated NFκB-regulated [597, 598] systemic and hepatic inflammatory markers, namely IL-6, TNF-α, IFN-γ, IL-1β, and serum amyloid A1 (SAA-1) [406] – all known drivers of insulin resistance [599]. In TNF-α-activated HuH7 cells, treatment with apoA-I rHDL also suppressed NFκB levels [406]. Similar to HDL's relationship with cardiovascular disease, low levels of HDL are independently related to increased risk of insulin resistance and type 2 diabetes development [600-603], although HDL is not currently used therapeutically for insulin resistance. Further, HDL's apoA-I component is glycated under the hyperglycaemic conditions associated with insulin resistance and type 2 diabetes proportional to blood glucose concentrations, thereby reducing its efficacy [604-606]. Instead of HDL, there are a number of other therapeutics used to treat the disease including salicylates, incretins, and metformin.

Salicylates have long been observed to reduce hyperglycaemia [607] and have been used for the treatment of insulin resistance [274, 608, 609], improving insulin sensitivity while also reducing cardiovascular risk factors [275]. Salicylates suppress inflammation by inhibiting the canonical IKK/NFκB signalling pathway [280]. In the context of insulin resistance, salicylates reduce hepatic inflammation by inhibiting the NFκB signalling pathway, which is directly

implicated in the pathogenesis of insulin resistance [60, 61, 84]. However, while salicylate treatment has been extensively proven to facilitate improvements in insulin resistance [60, 62, 274, 287, 610], its use is associated with adverse effects. The main adverse effects include gastrointestinal (GIT) discomfort [611], which in some patients renders its use intolerable or necessitates reduced dosage, particularly after long term usage as it is associated with a significant increase in the incidence of gastrointestinal haemorrhage [612]; Hepatotoxicity is the other main adverse effect associated with salicylate use, especially at higher doses [287, 613].

Incretins are post-prandially released enteroendocrine hormones secreted from the GIT into the bloodstream by K and L cells [614, 615] which increase insulin secretion by activating β-cells in a dose-response glucose-dependent manner. Glucagon-like peptide 1 (GLP-1) and glucose-dependent insulinotropic polypeptide (GIP) are classified as incretins and are targeted to improve insulin sensitivity. An example of a GLP-1R agonist mimetic is exenatide/exendin-4. From *in vivo* work, in addition to the aforementioned effects, exendin-4 is also able to increase β-cell proliferation and islet mass, prevent β-cell apoptosis, enhance islet neogenesis, and together improve insulin secretion [318, 319, 616]. However, incretins have been noted to cause GIT discomfort as a side effect of the drug's mechanism of action which involves inhibition of gastric emptying, making their administration unsuitable for some patients [327]. The use of incretin mimetics such as exendin-4, also leads to the induction of anti-exenatide antibodies, which leads to reduced efficacy of the drug in patients who develop a high antibody titre [617]. An analysis of data from the FDA adverse event reporting system database alarmingly revealed that administration of exenatide also significantly causes and enhances the severity of pancreatitis, and significantly increases the incidence of pancreatic cancer compared to use of control drugs [328]. However, the specific mechanisms of action and adverse effects of various incretin compounds differ. For example long-acting acting GLP-1 receptor agonists exhibit stronger effects on fasting glucose levels mediated by their insulinotropic and glucagonostatic actions, while short-acting forms elicit postprandial blood glucose-lowering predominately by inhibiting gastric emptying. Work to personalise incretin-based therapeutics for treatment of insulin resistance and type 2 diabetes mellitus is ongoing [618].

Metformin is the main drug used to manage T2D and hyperglycaemia, and belongs to the biguanide class of drugs [619, 620]. Metformin reduces insulin resistance by suppressing hepatic glucose production [331], increasing intestinal glucose use, decreasing fatty-acid

oxidation, and increasing insulin-mediated glucose disposal [349-351]. Metformin also increases AMP-activated protein kinase (AMPK) activity, which limits hepatic fatty acid synthesis through inhibition of acetyl-CoA carboxylase 1 and 2 (ACC1 and ACC2) [348], by increasing AMP levels and preventing mitochondrial respiration [346]. Use of metformin also increases HDL levels [621] and improves glycation impaired-HDL-mediated cholesterol efflux by inhibiting advanced glycation end products [352]. However, as with incretins and salicylates, metformin can cause GIT discomfort, leading to limited dosage or discontinuation of the drug [622]. The primary concern with metformin administration is the development of lactic acidosis in those with impaired renal function as metformin's inhibition of hepatic mitochondrial respiration increases plasma lactate levels (as reviewed by [380]). As a result of this risk, metformin is associated with a number of contraindications including renal impairment, coronary artery diseases, respiratory diseases, hepatic diseases, old age, use of contrast media, and surgery [351, 623]. However, metformin remains a frontline therapy for the treatment of insulin resistance and T2D [620], with its effects on blood glucose-lowering being strong and its positive effects on HDL levels and function also being particularly valuable [620].

Currently, despite HDL's ability to improve insulin sensitivity *in vivo*, and its suppression of TNF-α-induced inflammatory markers in cultured hepatocytes [406], it is not used therapeutically, although it is in development. New approaches are required to treat insulin resistance to provide more therapeutic avenues for a variety of patients. The previous chapters demonstrated that apoA-I rHDL increases DHCR24 levels and that DHCR24 suppresses a TNF-α-induced inflammatory response in HCAECs. In this work it was hypothesised that apoA-I rHDL incubation of HuH7 cells would increase DHCR24 levels.

Additionally to date, there has been no published research on DHCR24's potential role in mediating protection or in mimicking HDL's protective role against a TNF-α-induced inflammatory response in hepatocytes. The work in Chapters 3 and 4, have provided impetus into investigation of DHCR24 in other cell types after demonstrating the enzyme's ability to suppress a TNF-α-induced inflammatory response in HCAECs. To investigate this link, the FFAs (oleic, palmitic, stearic fatty acids) at lipid loading conditions (3:1:1) in combination with TNF-α or a cytokine cocktail (TNF-α, IFN-γ, IL-1β) were used to increase IL-8 (CXCL8) mRNA levels in HuH7 cells. The inflammatory marker IL-8 was investigated in this work as it is an inflammatory mediator which is increased in obese [481], insulin resistant, and diabetic patients [624, 625], as well as in hepatocytes *in vitro* following TNF-α-activation [626]. The aim of this work was to

determine whether apoA-I rHDL increases DHCR24 mRNA levels in HuH7 cells. Silencing experiments were conducted to ascertain whether DHCR24 is involved in the protective effect of apoA-I rHDL against a TNF-α-induced inflammatory response in HuH7 cells. DHCR24 overexpression was also investigated to see if it protected against a TNF-α-induced inflammatory response. The overall aim was to determine if DHCR24 replicates HDL's protective effects in HuH7 cells.

5.2 Methods

5.2.1 Cell culture

HuH7 cells were cultured in Dulbecco's minimum essential medium (DMEM) (Sigma-Aldrich) supplemented with 10% (v/v) Fetal Bovine Serum (FBS) (Sigma-Aldrich) at 37 ^{o}C in a 5% CO_2 incubator (section 2.1.1).

For the experiments determining whether apoA-I rHDL pre-incubation increases DHCR24 mRNA levels, HuH7 cells were seeded in 6-well plates at a cell density of $1.5x10^5$ cells/mL (section 2.1) and grown 24 hours prior to treatment with apoA-I rHDL (section 5.2.3).

To elucidate whether DHCR24 mediates the protective effect of HDL against a TNF-α-induced inflammatory response, HuH7 cells were cultured as described in section 2.1, seeded in 12-well plates at a cell density of $1.5x10^5$ cells/mL and grown 24 hours to 80% confluency prior to transient transfection with siRNA according to the manufacturer's protocol (section 5.2.4) and FFA/cytokine treatment (section 2.6.2.5).

For the experiments determining whether DHCR24 overexpression replicates the suppressive effect of apoA-I rHDL, HuH7 cells were seeded in 12-well plates at a cell density of $1.5x10^5$ cells/mL and grown 24 hours prior to treatment to 80% confluency. Following a 24-hour transfection period, the transfection culture medium was replaced with fresh culture medium. The cells were then allowed to recover for a further 24 hours to increase DHCR24 expression, before total RNA were isolated and RT-qPCR performed (sections 2.10 – 2.14).

5.2.2 ApoA-I isolation method

Using pooled samples of autologously donated human plasma (Gribbles Pathology) ApoA-I was isolated and purified through sequential isopycnic ultracentrifugation (Beckman Coulter), and anion exchange chromatography as described by [627].

5.2.3 ApoA-I rHDL pre-incubation

HuH7 cells were incubated for 16 hours with 0.45 mg/μL apoA-I rHDL (half-physiological concentration) before cell treatment (section 5.2.6). Phosphate buffered saline (PBS) was used as the vehicle control.

5.2.4 DHCR24 knockdown in HuH7 cells

After seeding HuH7 cells at a cell density of $1.5x10^5$ cells/mL into tissue culture plates in DMEM + 10% (v/v) FBS (section 2.1.2), DHCR24 knockdown was performed using siControl/siDHCR24 (Santa Cruz) and HiPerfect transfection reagents (Qiagen) (Table 5.1) according to the manufacturer's instructions (Qiagen) as described in section 2.4.2.

Table 5.1 siDHCR24 in HuH7 cells using HiPerfect Transfection Reagent

Components	Amount in 1 mL of growth medium
siControl/siDHCR24	20 μL
Serum-free DMEM	80 μL
HiPerfect	9 μL
Total transfection volume	109 μL

5.2.5 Transient transfection using TransPass HUVEC Transfection Reagent

HuH7 cells were seeded at a cell density of $1.5x10^5$ cells/mL in Dulbecco's minimum essential medium (DMEM) (Sigma-Aldrich) supplemented with 10% (v/v) Fetal Bovine Serum (FBS) (Sigma-Aldrich) (section 2.1.2). According to the manufacturer's protocol (New England Biolabs), HuH7 cells were transiently transfected with pDHCR24 (inserted into pcDNA3.1A) or pControl (empty pcDNA3.1A) expression vectors using TransPass HUVEC Transfection Reagent (New England Biolabs) as described in section 2.4.1. Following a 24-hour incubation period, the culture medium was changed and the cells were allowed to recover for a further 24 hours.

5.2.6 ELISA

HuH7 cells were cultured in 96-well plates ($1.5x10^5$ cells/mL) and transfected with pcDNA3.1A (pControl) or pcDNA3.1A-DHCR24 (pDHCR24) as described in section 2.1. Following transfection, the transfectants were left for 24 hours before the cells were treated with TNF-α (5 ng/mL, 4 hours). Following TNF-α-activation, supernatant was collected, and IL-8 protein levels were measured according to the manufacturer's protocol (Life Technologies)) using ELISA as described in section 2.8.

5.2.7 Real Time PCR

Total RNA was extracted from HuH7 cells using PureZol (Bio-Rad) and normalised to 200 ng/µL normalised using a UV spectrophotometer at 260/280nm (Nanodrop 1000, Thermo Scientific). Normalised mRNA was reverse transcribed into cDNA using iScript cDNA Synthesis Kit (Bio-Rad). iQ SYBR Green I supermix (Bio-Rad) was used to amplify RT-PCR in a Bio-Rad iQ5 thermocycler. Relative changes in mRNA levels were determined by the $\Delta\Delta C_T$ method [478], using β2-microglobulin (β2M) and glyceraldehyde-3-phosphate dehydrogenase (GAPDH) mRNA levels as reference genes. Primer pair sequences are listed in Table 5.2.

Table 5.2. Primer sequences

Primer	Forward/Reverse primer	Primer Sequence
Human DHCR24	F	5'-CTCGCCGCTCTCGCTTATC-3'
	R	5'-GTCTTGGCTACCCTGCTCCTTCC-3'
Glyceraldehyde-3-phosphate dehydrogenase (GAPDH)	F	5'-CCAATCACTTCCGACCTGCTG-3'
	R	5'-GCTTTGTATCCCTGCCCTGAG-3'
Beta-2 Microglobulin (β2M)	F	5'-CATCCAGCGTACTCCAAAGA-3'
	R	5'-GACAAGTCTGAATGCTCCAC-3'
Interleukin 8 (IL-8)	F	5'-CAGCTCTGTGTGAAGGTGCAGTTT-3'
	R	5'-GTTGGCGCAGTGTGGTCCACTC-3'

5.2.8 Statistical analysis

Data are expressed as mean ± SEM. Direct comparisons between two treatments were performed using unpaired t-test, while significant differences between multiple treatments were determined by one-way ANOVA with Sidak's *post hoc* test analysis. GraphPad Prism 6.0 was used for analysis. Significance was set at $P<0.05$. To show the effect size, P values lower than $P <0.05$ were specified.

5.3 Results

5.3.1 ApoA-I rHDL increases DHCR24 mRNA levels in HuH7 cells

Previously, our laboratory demonstrated that HDL improves insulin sensitivity in mice in addition to inhibiting a TNF-α-induced inflammatory response in HuH7 cells [406]. In Chapter 3 it was shown that incubation with apoA-I rHDL significantly increases DHCR24 levels and that DHCR24 mediates at least in part, the protective effect of apoA-I rHDL against a TNF-α-induced inflammatory response in HCAECs. The following series of experiments aimed to determine whether DHCR24 replicates this effect in HuH7 cells, and mediates HDL's suppression of a TNF-α-induced inflammatory response through apoA-I rHDL-mediated increases in DHCR24 mRNA levels. First, to investigate whether apoA-I rHDL increases DHCR24 mRNA levels in HuH7 cells, cells were treated with apoA-I rHDL (16 µM/0.45 mg/mL) for 16 hours prior to analysis by RT-qPCR. Figure 5.1 shows an increase of DHCR24 mRNA levels following apoA-I rHDL treatment ($P<0.005$).

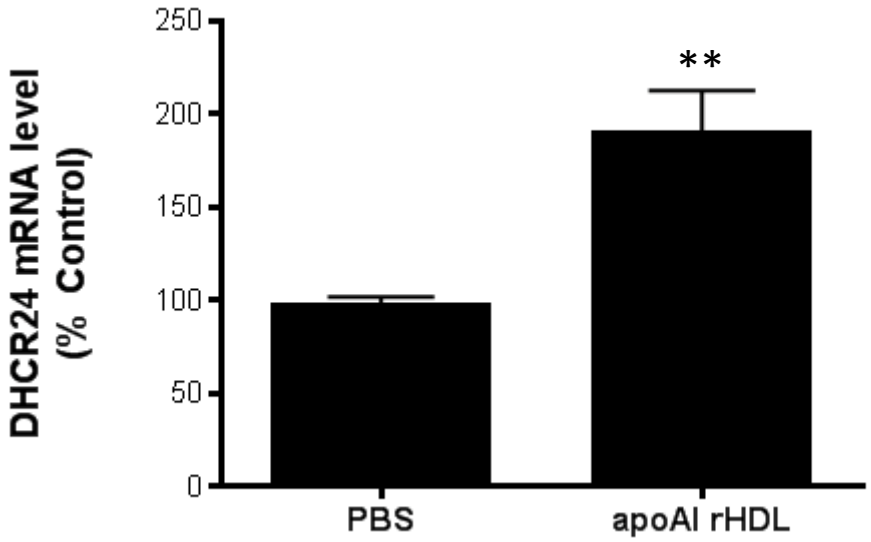

Figure 5.1 DHCR24 mRNA levels are increased in HuH7 cells following 16 hour apoA-I rHDL treatment. HuH7 cells were treated with 16 μmol/L (0.45mg/mL) apoA-I rHDL for 16 hours compared to a PBS control. After treatment, total RNA was isolated and RT-qPCR used to measure DHCR24 mRNA levels using β2M as a reference gene. Data are shown as mean ± SEM (n = 3) ** P<0.01.

5.3.2 Transient transfection with siDHCR24 reduces DHCR24 mRNA levels in HuH7 cells

Section 5.3.1 showed that incubation of HuH7 cells with apoA-I rHDL significantly increased DHCR24 levels. For the next experiments, it was investigated whether apoA-I rHDL's suppressive effect against TNF-α-activation in HuH7 cells was a DHCR24-mediated process. To determine whether DHCR24 mediates apoA-I rHDL's effect of attenuating a TNF-α-induced inflammatory response, HuH7 cells were first transfected using HiPerfect transfection reagents (Qiagen), with siDHCR24 to reduce DHCR24 mRNA levels, and with siControl serving as a control.

The RT-qPCR results shown in Figure 5.2 confirm that transfection using siDHCR24 significantly reduced DHCR24 mRNA levels compared to the siRNA scrambled sequence vector control.

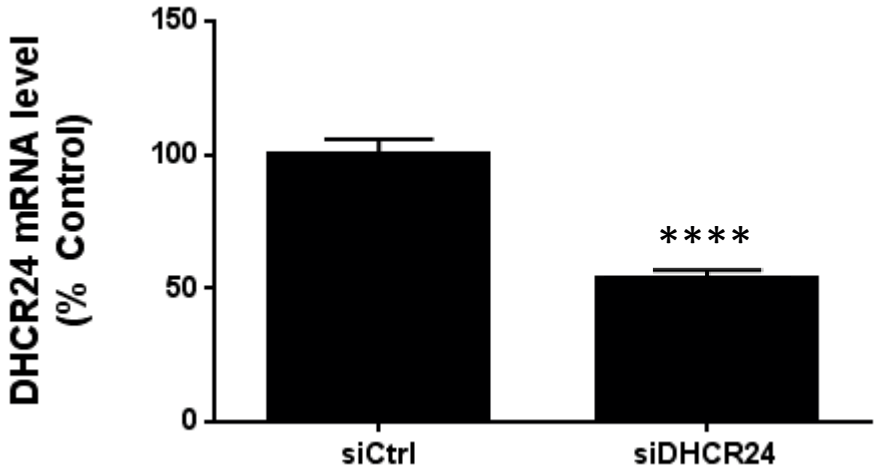

Figure 5.2 DHCR24 mRNA levels are decreased following transfection with siRNA against DHCR24. HuH7 cells were transfected with siControl or siDHCR24. Total RNA was isolated and using RT-qPCR DHCR24 mRNA levels were measured with β2M as a reference gene. Data are shown as mean ± SEM (n = 3) **** P<0.0001.

5.3.3 TNF-α-activation reduces DHCR24 mRNA levels in HuH7 cells

To determine whether the reduction of DHCR24 mRNA levels achieved in section 5.3.2 was similar to the effect of TNF-α-induced inflammatory activation in HuH7 cells, the effect of TNF-α-activation was analysed. HuH7 cells were treated with TNF-α (5 ng/mL) for 4 hours. Figure 5.3 indicates that DHCR24 mRNA levels in HuH7 cells were reduced compared to control following TNF-α-activation.

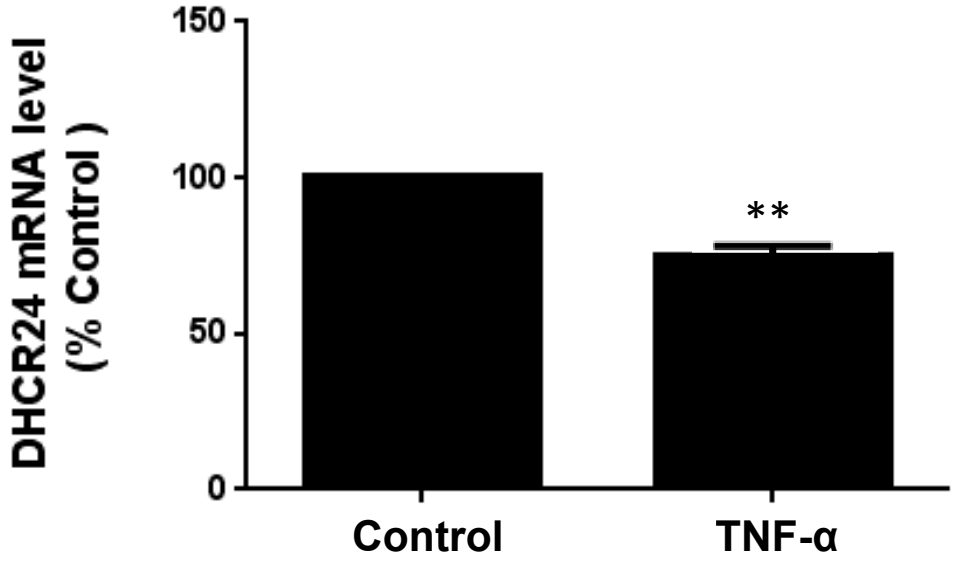

Figure 5.3 DHCR24 mRNA levels are decreased in TNF-α-activated HuH7 cells. HuH7 cells were transfected with pcDNA3.1A-DHCR24 and then activated with 5 ng/mL TNF-α for 4 hours. DHCR24 mRNA levels were measured using RT-qPCR with β2M as a reference gene. Data are shown as mean ± SEM (n = 3) ** P<0.01.

5.3.4 The suppressive effect of apoA-I rHDL against TNF-α-induced IL-8 mRNA levels in HuH7 cells is lost when DHCR24 is knocked down

The inflammatory marker IL-8 was investigated in this study as it is an inflammatory mediator which is increased in obese [481, 483, 486], insulin resistant, and diabetic patients [482, 624, 625]. In this work with HuH7 cells, and previously in human umbilical vein endothelial cells, HDL has been demonstrated to suppress TNF-α-induced IL-8 levels [628]. As apoA-I rHDL incubation of HuH7 cells was demonstrated to significantly increase DHCR24 levels, it was investigated whether apoA-I rHDL's suppressive effect against TNF-α-activation in HuH7 cells was a DHCR24-mediated process. To determine this, HuH7 cells were transfected with siDHCR24 to reduce DHCR24 mRNA levels, and siControl serving as a control, prior to treatment with cytokine cocktail/FFA or TNF-α/FFA compared to treated controls pre-incubated with apoA-I rHDL.

Results in Figures 5.4 A and 5.5 A show that inflammatory activation using cytokine cocktail/FFA or TNF-α/FFA treatments increased IL-8 mRNA levels. Figure 5.4 A shows that the cytokine cocktail/FFA treatment significantly increases IL-8 mRNA levels and that apoA-I pre-incubation significantly suppresses TNF-α-induced IL-8 mRNA levels in siControl-transfected HuH7 cells. Figure 5.5 A demonstrates that activation with TNF-α/FFA raises IL-8 mRNA levels and that apoA-I rHDL pre-incubation suppresses IL-8 mRNA levels siControl HuH7 cells.

The effect of apoA-I rHDL attenuating IL-8 mRNA levels following FFA/cytokine-activation is abrogated in siDHCR24 HuH7 cells. Figure 5.4 B shows that in HuH7 cells pre-incubated with apoA-I rHDL and treated with cytokine cocktail/FFA, IL-8 mRNA levels in siDHCR24-transfected HuH7 cells are significantly increased compared to siControl-transfected HuH7 cells. Figure 5.5 B shows that in HuH7 cells pre-incubated with apoA-I rHDL and treated with TNF-α/FFA, IL-8 mRNA levels in siDHCR24-transfected HuH7 cells are significantly increased compared to siControl-transfected HuH7 cells.

A siControl

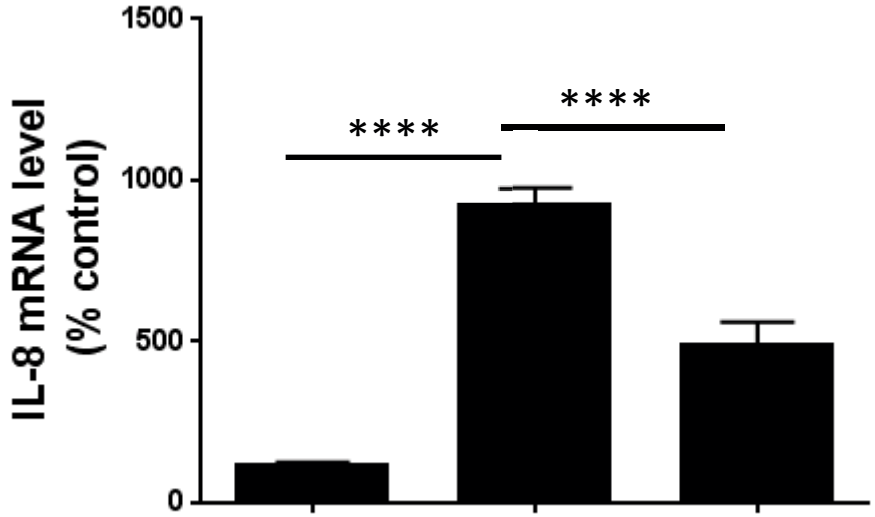

PBS	+	-	-
Cytokine cocktail + FFA	-	+	+
ApoA-I rHDL	-	-	+

B siDHCR24

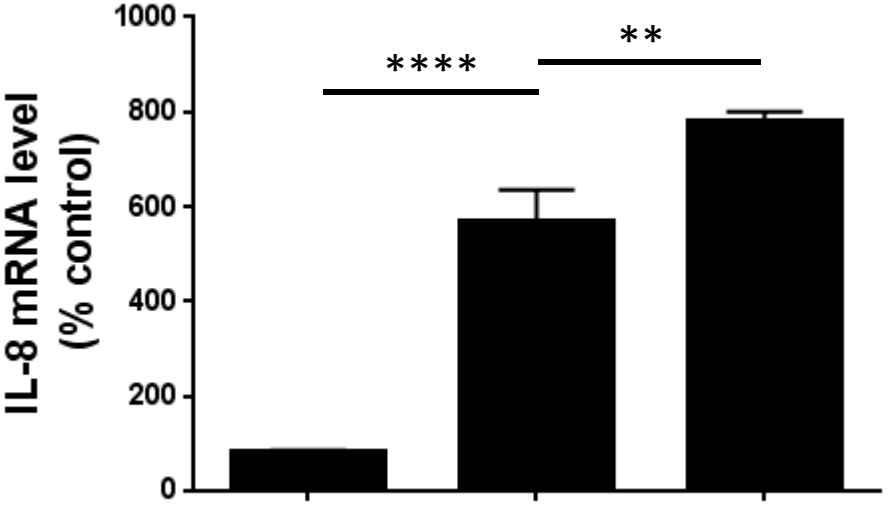

PBS	+	-	-
Cytokine cocktail + FFA	-	+	+
ApoA-I rHDL	-	-	+

Figure 5.4 The suppressive effect of apoA-I rHDL against cytokine cocktail/FFA treatment-induced IL-8 mRNA levels in HuH7 cells is lost when DHCR24 is knocked down (A) IL-8 mRNA levels are suppressed by apoA-I rHDL 16-hour pre-incubation following cytokine cocktail/FFA treatment in siControl HuH7 cells (B) IL-8 mRNA levels are increased following cytokine treatment in apoA-I rHDL 16-hour pre-incubated siDHCR24 HuH7 cells. HuH7 cells were transfected with siControl and siDHCR24 then treated with cytokine cocktail/FFA or apoA-I rHDL/cytokine cocktail/FFA. Total RNA was extracted and IL-8 mRNA levels were measured using RT-qPCR with GAPDH as a reference gene. Data are shown as mean ± SEM (n = 6) ** P<0.01, **** P<0.0001.

A siControl

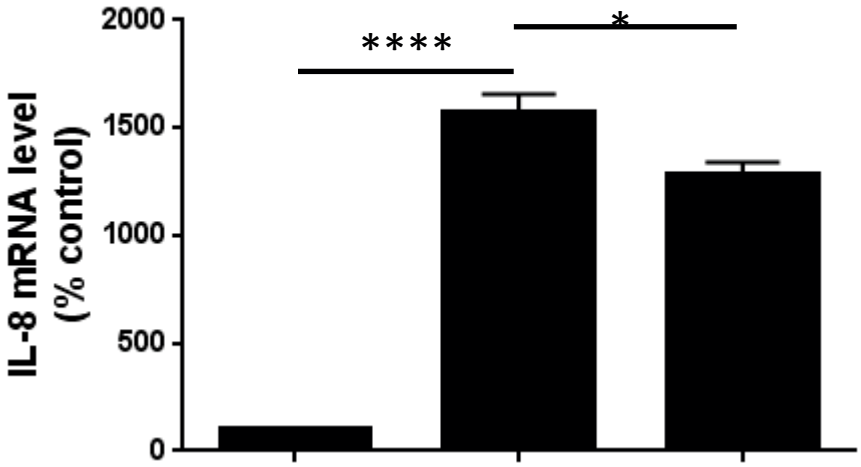

PBS	+	-	-
TNF-α + FFA	-	+	+
ApoA-I rHDL	-	-	+

B siDHCR24

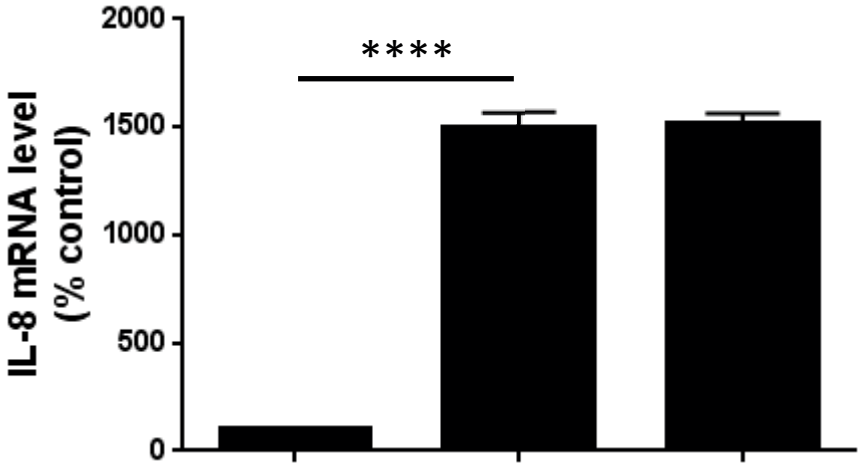

PBS	+	-	-
TNF-α + FFA	-	+	+
ApoA-I rHDL	-	-	+

Figure 5.5 The suppressive effect of apoA-I rHDL against TNF-α/FFA treatment-induced IL-8 mRNA levels in HuH7 cells is lost when DHCR24 is knocked down (A) IL-8 mRNA levels are suppressed by apoA-I rHDL 16-hour pre-incubation following TNF-α/FFA treatment in siControl HuH7 cells (B) IL-8 mRNA levels are not decreased by apoA-I rHDL 16-hour pre-incubation following TNF-α/FFA treatment in siDHCR24 HuH7 cells. HuH7 cells were transfected with siControl and treated TNF-α/FFA or apoA-I rHDL/TNF-α/FFA. Total RNA was extracted and IL-8 mRNA levels were measured using RT-qPCR with GAPDH as a reference gene. Data are shown as mean ± SEM (n = 6) * P<0.05, **** P<0.0001.

5.3.5 Transient transfection of pcDNA3.1A-DHCR24 increases DHCR24 levels in HuH7 cells

In order to determine whether DHCR24-overexpression mimics HDL's ability to suppress TNF-α-induced IL-8 mRNA levels in HuH7 cells, DHCR24 levels were first increased using transient transfection. To confirm that transient transfection of pcDNA3.1A-DHCR24 increased DHCR24 levels in HuH7 cells, cultured HuH7 cells were transfected with pcDNA3.1A (pControl) or pcDNA3.1A-DHCR24 (pDHCR24) expression vectors using TransPass V reagent (New England Biolabs) with the optimised conditions described in section 2.4.1. pcDNA3.1A vector was the vehicle control for transfection because DHCR24 was cloned into pcDNA3.1A vector for overexpression analysis. Following transfection, cells were left for 24-hours prior to extraction of total RNA and subsequent analysis of DHCR24 mRNA levels by real-time RT-qPCR.

From the RT-qPCR results shown in Figure 5.6, transfection using TransPass V was successful with DHCR24 mRNA levels significantly increased compared to the vector control.

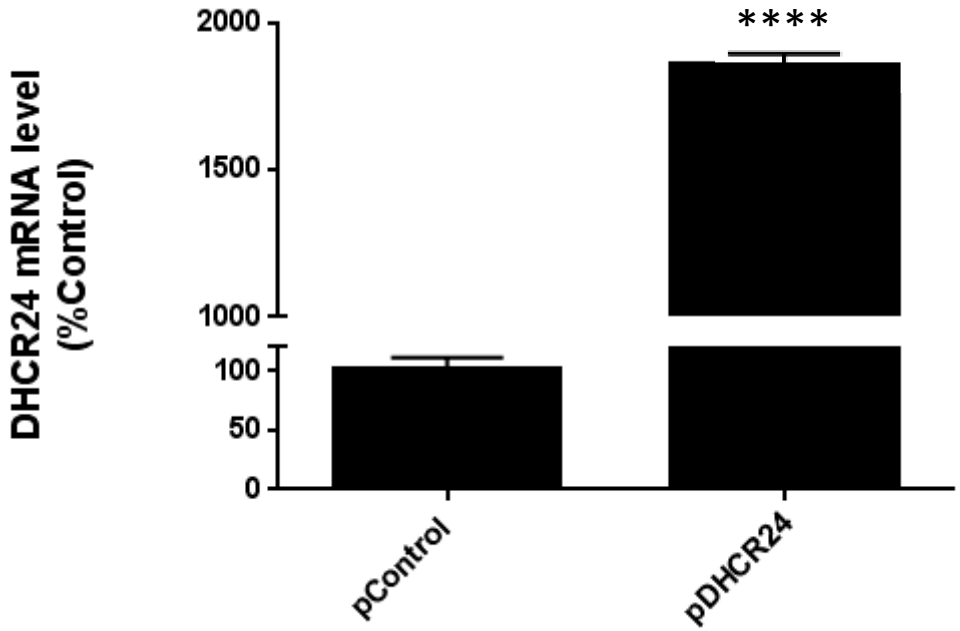

Figure 5.6 Transient transfection of HuH7 cells with pcDNA3.1A-DHCR24 successfully increased DHCR24 levels. HuH7 cells were transfected with pcDNA3.1A or pcDNA3.1A-DHCR24 for 24 hours. Total RNA was isolated and RT-qPCR used to measure DHCR24 mRNA levels with β2M as a reference gene. Data are shown as mean ± SEM (n = 3) **** P<0.0001.

5.3.6 Increased DHCR24 suppresses TNF-α-activated IL-8 levels in HuH7 cells

In the next experiments, it was hypothesised that increasing DHCR24 levels would mimic apoA-I rHDL's effect of suppressing TNF-α-induced Il-8 expression. HuH7 cells were transfected with pcDNA3.1A (pControl) or pcDNA3.1A-DHCR24 (pDHCR24) for 24 hours prior to TNF-α (5 ng/mL) treatment for 4 hours. IL-8 protein levels were measured using ELISA. TNF-α treatment increased IL-8 protein levels compared to vehicle control ($P<0.0001$), a result that was abrogated in pDHCR24-transfected HuH7 cells ($P<0.01$) (Figure 5.7).

It was next assessed whether increased DHCR24 levels also suppressed TNF-α-induced IL-8 mRNA levels, mimicking apoA-I rHDL's effect at the level of gene transcription. HuH7 cells were transfected with pcDNA3.1A vector (pControl) or pcDNA3.1A-DHCR24 prior to TNF-α (5 ng/mL) treatment for 4 hours. IL-8 mRNA levels were measured using RT-qPCR with β2M as a reference gene. TNF-α treatment increased IL-8 mRNA levels compared to vehicle control ($P<0.0001$), and HuH7 cells transfected with pcDNA3.1A-DHCR24 demonstrated suppressed IL-8 mRNA levels compared to TNF-α-activated pcDNA3.1A vector HCAECs ($P<0.01$) (Figure 5.8).

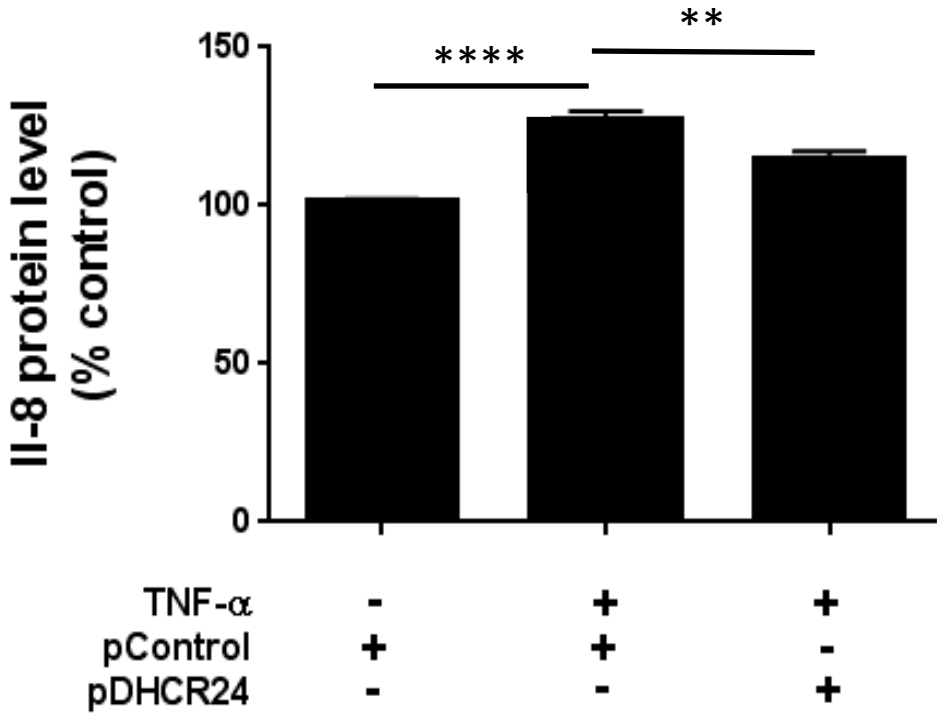

Figure 5.7 DHCR24-overexpression suppressed TNF-α-activated IL-8 protein levels in HuH7 cells. HuH7 cells were transfected with pcDNA3.1A (pControl) or pcDNA3.1A-DHCR24 (pDHCR24) before activation with 5 ng/mL TNF-α for 4 hours. IL-8 protein levels were measured using the ELISA. Data are shown as mean ± SEM (n = 3) ** P<0.01, **** P<0.0001.

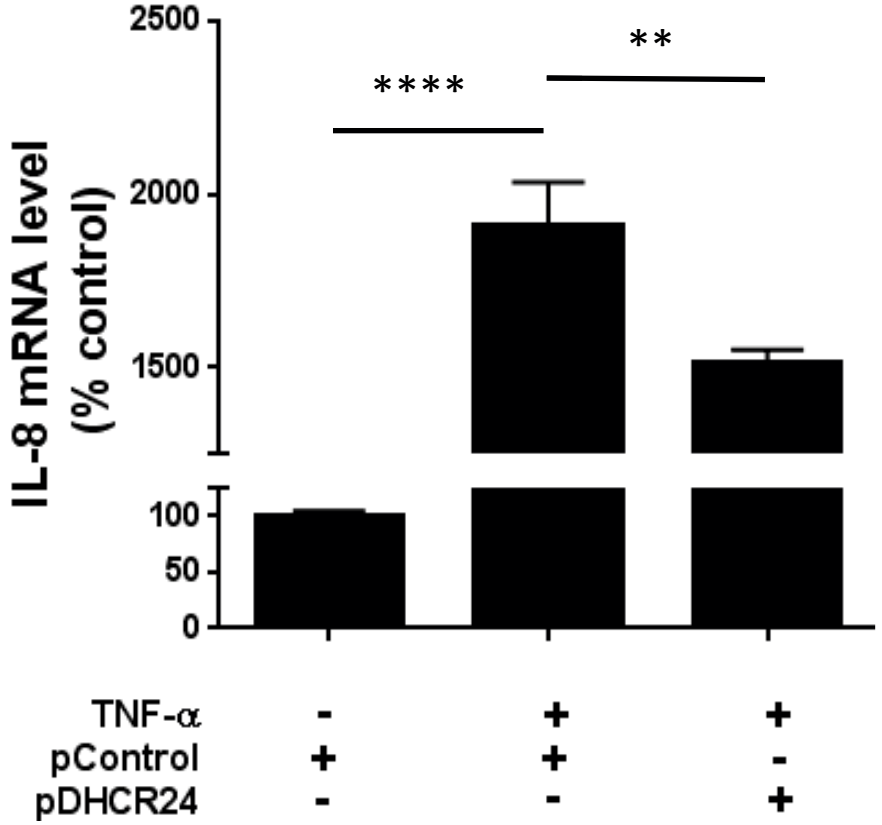

Figure 5.8 DHCR24-overexpression reduced IL-8 mRNA levels in TNF-α-activated HuH7 cells. HuH7 cells were transfected with pcDNA3.1A (pControl) or pcDNA3.1A-DHCR24 (pDHCR24) before activation with 5 ng/mL TNF-α for 4 hours. IL-8 mRNA levels were measured using RT-qPCR with β2M as a reference gene. Data are shown as mean ± SEM (n = 3) ** P<0.01, **** P<0.0001.

5.4 Discussion

The work in this chapter demonstrates the novel discovery that half physiological concentration of apoA-I rHDL increases DHCR24 levels in HuH7 cells. It was also revealed that DHCR24 mediates, at least in part, apoA-I rHDL's suppression of FFA/cytokine-induced IL-8 mRNA levels. Moreover, this study provides proof-of-principal that DHCR24 mimics HDL's effect of suppressing FFA/cytokine-induced IL-8 mRNA levels. HDL has been reported to improve insulin sensitivity and reduce hepatic NFκB levels [406] providing impetus into investigating the ability of DHCR24 to replicate the effects of HDL in HuH7 cells. Further the results in Chapters 3 and 4, which showed that DHCR24 is increased by HDL and that DHCR24 mediates HDL's protective effects against a TNF-α-induced inflammatory response in HCAECs, also stimulated investigation of DHCR24's effect in HuH7 cells.

The effect of apoA-I rHDL treatment on DHCR24 mRNA levels in HuH7 cells was investigated first, elucidating whether HDL increases DHCR24 levels. The data obtained from this study showed that treatment with 0.45 mg/mL (half physiological concentration) apoA-I rHDL for 16 hours produced significant increases in DHCR24 mRNA levels in HuH7 cells (Figure 6.1). The effect of apoA-I rHDL treatment on DHCR24 mRNA levels was investigated in HuH7 cells as our laboratory's previous work showed that HDL treatment in HFD-fed mice improves insulin sensitivity (as demonstrated by glucose tolerance test and HOMA-IR) [406]. The result of increased DHCR24 mRNA levels following apoA-I rHDL treatment in HuH7 cells is also consistent with the effect of HDL on DHCR24 levels in HCAECs presented in Chapter 3. This result of increased DHCR24 levels by apoA-I rHDL treatment in HuH7 cells led to the hypothesis that DHCR24 may be mediating the suppressive effect of apoA-I rHDL in HuH7 cells against the cytokine-induced inflammatory response.

The next experiment led on from the result that apoA-I rHDL increases DHCR24 mRNA levels in HuH7 cells and our laboratory's previous work which determined HDL treatment in HFD-fed mice improves insulin sensitivity [406]. To assess whether DHCR24 mediates regulation of the cytokine-induced inflammatory response, IL-8 mRNA levels were stimulated in HuH7 cells using oleic, palmitic and stearic fatty acids at physiological lipid loading concentrations (3:1:1), and the cytokines TNF-α, IL-1β, and IFN-γ using previously optimised treatment conditions. The FFAs and cytokines utilised in this work were selected to replicate the inflammatory conditions associated with insulin resistance. The FFA used directly induce inflammation leading to insulin

resistance [591, 592]. Reductions in fatty acids and adipose load are also known to improve insulin sensitivity in humans [629, 630], and reduce associated proinflammatory cytokine levels [629-631]. Measurement of IL-8 mRNA levels was selected in this work as it is strongly associated with insulin resistance, diabetes [625], and adiposity [481, 632]. Further, IL-8 levels are reported to be stimulated in hepatocytes *in vitro* in response to inflammatory activation [626]. A silencing experiment was carried out to identify if DHCR24 is involved in the effect of apoA-I rHDL to suppress cytokine-induced IL-8 mRNA levels in hepatocytes. Using an siRNA approach in HuH7 cells, it was shown for the first time that DHCR24 mediates at least in part, suppressive effect of apoA-I rHDL against cytokine-induced IL-8 mRNA levels. While complete DHCR24 silencing was not achieved in these experiments, at the level of DHCR24 reduction achieved (46.7% reduction, $P<0.0001$), the change was sufficient to demonstrate dramatic effects showing that the IL-8 mRNA regulatory role of apoA-I rHDL is at least in part, DHCR24-mediated. Furthermore, the DHCR24 mRNA level decrease achieved using siRNA was also greater than the level of DHCR24 reduction caused by the TNF-α treatment conditions used in these experiments, which significantly increase IL-8 mRNA levels. As a future direction it would be valuable to observe if complete DHCR24 silencing would further augment cytokine-induced IL-8 mRNA levels. However, these results demonstrate that small although significant, decreases in DHCR24 mRNA levels elicit strong effects on cytokine-induced IL-8 mRNA levels, abrogating apoA-I rHDL's IL-8 mRNA regulatory effect.

Following on from the observation that DHCR24 contributes to the suppressive effect of apoA-I rHDL on cytokine-induced IL-8 mRNA levels, the effect of DHCR24 overexpression on the cytokine-induced inflammatory response was investigated. DHCR24 overexpression in HuH7 cells showed that DHCR24 can mimic the suppressive effect of apoA-I rHDL on the cytokine-induced inflammatory response. This protective effect of DHCR24 is in keeping with DHCR24's effect in HCAECs reported in Chapter 3, and further provides proof-of-principle that DHCR24 suppresses the cytokine-induced inflammatory response in HuH7 cells, indicating a potentially protective role of DHCR24 in hepatocytes.

Interestingly, while DHCR24 overexpression is able to suppress the cytokine-induced inflammatory response, incrementally increasing or restoring DHCR24 mRNA levels back to physiological values, rather than overexpressing DHCR24, may be sufficient to significantly suppress IL-8 mRNA levels in activated HuH7 cells. The results presented show that HuH7 cell DHCR24 levels are reduced approximately 20% when activated with TNF-α, and that using this treatment condition, TNF-α significantly increases IL-8 mRNA levels. Further, while TNF-α

treatment decreased DHCR24 mRNA levels, DHCR24 mRNA levels were augmented by apoA-I rHDL incubation by approximately 2-fold. At the half physiological concentrations of apoA-I rHDL used in this experiment, the 2-fold DHCR24 mRNA level increase was sufficient to significantly decrease cytokine-induced IL-8 mRNA levels as demonstrated in the siRNA experiments. Using siRNA against DHCR24, the suppression mediated by apoA-I rHDL against cytokine-induced IL-8 mRNA levels was lost even when DHCR24 mRNA levels were reduced by only approximately 50%. Together this shows that restoring or incrementally increasing DHCR24 levels (using apoA-I rHDL) is sufficient to significantly attenuate cytokine-induced IL-8 mRNA levels in HuH7 cells.

Restoring or incrementally increasing DHCR24 levels in the liver would be particularly valuable as a potential therapeutic avenue for hepatic inflammation or insulin resistance, as DHCR24-overexpression has been associated with (hepatitis C virus-associated) hepatic tumour development [462, 633, 634]. The approach for treating hepatic inflammation to attenuate inflammation and potentially improve insulin sensitivity would therefore be to restore normal physiological DHCR24 levels rather than to create potentially pathological overexpression. This would eliminate concerns associated with the formation of hepatic tumours which occurs at supra-physiological DHCR24 levels [462, 633]. As the results presented indicate, small increases in DHCR24 mRNA levels significantly suppressed cytokine-induced IL-8 mRNA levels. As a future direction it would also be valuable to determine to what extent DHCR24 levels in the livers of insulin resistant patients are decreased comparing them to the *in vitro* DHCR24 mRNA reductions in HuH7 cells presented in this work and to provide data to ascertain the extent DHCR24 levels would need to be increased to restore DHCR24 to a normal physiological range in humans.

As mentioned previously, TNF-α significantly contributes to the pathogenesis of insulin resistance increasing the inflammatory response in the liver [132, 635, 636]. Increased DHCR24 levels produced suppression of cytokine-induced IL-8 levels in HuH7 cells indicating there may be merit in pursuing DHCR24 as a therapeutic target for the treatment of insulin resistance and hepatic inflammation. HDL has been shown to improve insulin sensitivity [406] although it can become dysfunctional under cellular stress, with effects such as glycation affecting its protective abilities [604-606]. Concordantly, increasing HDL levels may not necessarily reflect their protective properties for improving insulin resistance, especially long term treatments. DHCR24 can perform some of the anti-inflammatory effects of HDL in HuH7 cells and could be used as a therapeutic to replicate ‘healthy HDL’. DHCR24’s ability to inhibit the cytokine-

induced inflammatory response in HuH7 cells creates impetus into its investigation as a therapeutic target and also indicates that DHCR24 serves multifaceted roles in HuH7 cells, being involved in more than just cholesterol biosynthesis.

Before any therapeutic applications for DHCR24 against insulin resistance or hepatic inflammation may be considered, further experimentation including characterisation of DHCR24 in HuH7 cells is required. The work in the next chapter focuses on characterising DHCR24's role in suppressing the cytokine-induced inflammatory response in HuH7 cells, following on from the data presented in this chapter. The work reported here proves for the first time that in HuH7 cells, DHCR24 is increased by apoA-I rHDL and facilitates the regulatory effect of apoA-I rHDL on cytokine-induced IL-8 mRNA levels. Further, these data provide proof-of-principle that DHCR24 replicates the protective effect of HDL in HuH7 cells adding to the current reported knowledge of DHCR24's potentially protective abilities (anti-oxidative [421, 423, 438] and anti-apoptotic effects [421, 425, 437, 471]), adding inflammatory mediator modulation in HuH7 cells to its developing list of multifaceted functions.

Chapter 6 – Characterisation of the mechanisms mediating DHCR24's protective effects in HuH7 cells

6.1 Introduction

In the previous chapter it was established for the first time, that increasing DHCR24 levels in HuH7 cells mimics HDL's protective effect of suppressing TNF-α-induced IL-8 levels. These observations are significant and provided proof-of-principal that DHCR24 replicates HDL's ability in HuH7 cells although they do not identify the mechanism by which DHCR24 mediates its protective effects. DHCR24 possesses multiple roles in various cell types, however, it is unknown which of these roles DHCR24 serves in HuH7 cells. This study focuses on investigating the mechanisms by which DHCR24 mediates the effect of suppressing TNF-α-induced IL-8 levels in HuH7 cells, building upon the novel discoveries of the work in the previous chapter. This study set out to characterise in HuH7 cells, DHCR24's cholesterol biosynthesis role, the significance of its oxidoreductase site, and its potential ability to suppress ER stress markers and prevent apoptosis.

DHCR24's initial discovery and the role it is primarily recognised for, is its activity as a cholesterol biosynthesis enzyme. DHCR24's cholesterol biosynthesis activity involves catalysing the conversion of desmosterol to cholesterol, the final step of cholesterol biosynthesis [419]. Cholesterol is integral to the correct functioning and survival of all mammalian organisms, with an absence of cholesterol being fatal [419, 440, 443]. In keeping with this, patients demonstrating the multiple-congenital-anomaly syndrome, desmosterolosis that is caused by the accumulation of desmosterol, show mutations in the *dhcr24* gene [419, 440-443, 574]. Desmosterolosis also leads to a deficiency in plasma membrane cholesterol. This leads to death shortly after birth in humans [443] and in mice [434, 575, 576]. In addition to DHCR24's essential cholesterol biosynthesis role for the correct development and functioning of the body, it also mediates protection against cellular stressors. For example, in neuroblastoma cells the protection effected by DHCR24 against oxidative stress occurs in a cholesterol-dependent manner [433, 473] by modulating amyloid beta (Aβ) peptide production and clearance [433, 438]. DHCR24 also reduces ER stress in neuroblastoma cells via cholesterol elevations mechanism [469]. Conversely, in W138-TERT fibroblasts and mouse embryonic fibroblasts (MEF) DHCR24 directly scavenges ROS preventing H_2O_2-induced apoptosis, independent of cholesterol synthesis [140, 423, 437] indicating that the mechanisms of DHCR24's protective effects are cell type-specific.

Increased DHCR24 levels are consistently associated with protective effects in assorted cells. Increased DHCR24 confers resistance against ER stress in neuronal cells and MEF. DHCR24 also prevents apoptosis in neuronal cells [421], fibroblasts [469], melanoma cells [420], pituitary adenomas [427], and in adrenal cells [577]. Moreover resistance against oxidative stress in facilitated by DHCR24 in neuronal cells [421, 469] and fibroblasts [140, 437]. The mechanisms through which DHCR24 elicits protective effects are emerging as being cell type-specific. Interestingly in MEF, DHCR24's ability to elicit protection against oxidative stress is dependent on its oxidoreductase site. DHCR24's oxidoreductase site is responsible for cholesterol biosynthesis, however, in MEF independent of cholesterol biosynthesis, this region is serves to directly scavenge ROS thereby preventing apoptosis [437]. In neuronal cells, DHCR24 translocates from the ER to the nucleus following inflammatory activation to prevent apoptosis [469].

Given the recent discoveries of DHCR24's cell type-specific multifaceted abilities, this project set out to investigate the mechanisms through which DHCR24 elicits protection against TNF-α-induced inflammatory mediator increases in HuH7 cells. It was hypothesised that DHCR24 would protect against TNF-α-induced inflammation in an oxidoreductase site-dependent manner, independent of its cholesterol biosynthesis role. The role of DHCR24 in the control of ER stress as a mechanism to regulate inflammation, DHCR24's localisation, and its effect on apoptosis in HuH7 cells were also investigated. The aim of this study was to characterise the mechanisms through which DHCR24 suppresses against a TNF-α-induced inflammation in HuH7 cells.

6.2 Methods

6.2.1 Cell culture

HuH7 cells were cultured in Dulbecco's minimum essential medium (DMEM) (Sigma-Aldrich) supplemented with 10% (v/v) Fetal Bovine Serum (FBS) (Sigma-Aldrich) at 37 ^{o}C in a 5% CO_2 incubator (section 2.1.1).

For the experiments determining whether DHCR24 overexpression increases cholesterol levels, HuH7 cells were seeded in 6-well plates at a cell density of $1.5x10^5$ cells/mL and grown for 24 hours prior to transient transfection, to 80% confluency. According to the manufacturer's protocol (New England Biolabs), HuH7 cells were transiently transfected with pDHCR24 (inserted into pcDNA 3.1A) or pControl (empty pcDNA 3.1A) expression vectors using TransPass HUVEC Transfection Reagent (New England Biolabs) as described in section 2.1.1. Following a 24-hour incubation period, the culture medium was changed and the cells were allowed to recover for a further 24 hours before cholesterol was extracted (section 6.2.3) and quantified (section 6.2.4)

To explore the role of DHCR24's oxidoreductase site and DHCR24's effect on ER stress markers, HuH7 cells were cultured and transiently transfected as above but with the addition of HuH7 cells transfected with pDHCR24-N294T/K306N plasmid [oxidoreductase mutant – (section 6.2.2)]. Following a 24-hour incubation period, the culture medium was changed and the cells were allowed to recover for a further 24 hours before being treated with 5 ng/mL TNF-α for 4 hours. Following treatment, supernatant was collected to quantify secreted protein (section 6.2.5) while RT-qPCR was performed following extraction of total RNA (section 6.2.6).

To determine whether DHCR24 changes localisation in HuH7 cells following TNF-α-activation, HuH7 cells were cultured in 6-well plates at a cell density of $1.5x10^5$ cells/mL 24 hours prior to being treated with 5 ng/mL TNF-α for 4 hours. Following treatment, cells were stained using immunocytochemistry and images obtained (section 6.2.7).

For the experiment elucidating DHCR24's role against TNF-α-induced apoptosis, HuH7 cells were seeded in 96-well plates at a cell density of $1.5x10^5$ cells/mL and grown for 24 hours prior to transient transfection, to 80% confluency. HuH7 cells were transiently transfected according to the manufacturer's protocol (New England Biolabs) as above with pControl, pDHCR24, or pDHCR24-N294T/K306N plasmids. Following a 24-hour incubation period, the culture medium

was changed and the cells were allowed to recover for a further 24 hours before being treated with 15 ng/mL TNF-α for 18 hours and apoptosis was measured (section 6.2.8)

6.2.2 Site-directed mutagenesis and plasmid constructions

Using a DHCR24-pcDNA3.1A clone, double mutant (N294T/K306N) (oxidoreductase mutant) was generated by Genescript Inc based on [419]. The oxidoreductase mutant was produced from a wild type DHCR24 template using site-directed mutagenesis and cloned into the pcDNA3.1A plasmid vector to inactivate the known active site. This was followed by two rounds of PCR to introduce the two mutations in sequence. The resulting mutant DNA was then cloned into the pPAL expression vector.

The coding strand primer sequences to generate the mutant are:

N294T: 5'-GAGCCCAGCAAGCTGACTAGCATTGGCAATTAC-3'

K306N: 5'-GCCGTGGTTCTTTAACCATGTGGAGAACTATCTG-3'

6.2.3 Cholesterol extraction

HuH7 cells ($1.5x10^5$ cells/mL) in 6-well plates were transiently transfected with pcDNA3.1A (pControl) or pcDNA3.1A-DHCR24 (pDHCR24) before cholesterol was extracted using hexane/isopropanol (section 2.15.1).

6.2.4 Quantifying cellular cholesterol levels - Amplex Red Cholesterol Assay

Extracted cholesterol was quantified according to the manufacturer's instructions (Life Technologies) against cholesterol and resorufin fluorescence standards (section 2.15.2).

6.2.5 ELISA

HuH7 cells were cultured in 96-well plates ($1.5x10^5$ cells/mL) and transfected with with pcDNA3.1A (pControl), pcDNA3.1A-DHCR24 (pDHCR24), or pDHCR24-N294T/K306N plasmids as described in section 6.2.2. Following transfection, the transfectants were left for 24 hours before the cells were treated with TNF-α (5 ng/mL, 4 hours). Following TNF-α-activation, supernatant was collected and IL-8 protein levels were measured using ELISA as described in section 2.8.2.2.

6.2.6 Real time PCR

Total RNA was extracted using PureZol (Bio-Rad) and normalised to 200 ng/µL using a UV spectrophotometer at 260/280nm (Nanodrop 1000, Thermo Scientific). For RT-qPCR, cDNA was synthesised using iScript cDNA Synthesis Kit (Bio-Rad) and using iQ SYBR Green I supermix (Bio-Rad) was used to amplify in a Bio-Rad iQ5 thermocycler. RT-qPCR data was analysed using the $\Delta\Delta C_T$ method [478], using β2M and GAPDH as reference genes. Primer pair sequences are listed in Table 6.1.

Table 6.1 Primer sequences

Primer	Forward/Reverse primer	Primer Sequence
Human DHCR24	F	5'-CTCGCCGCTCTCGCTTATC-3'
	R	5'-GTCTTGGCTACCCTGCTCCTTCC-3'
Glyceraldehyde-3-phosphate dehydrogenase (GAPDH)	F	5'-CCAATCACTTCCGACCTGCTG-3'
	R	5'-GCTTTGTATCCCTGCCCTGAG-3'
Beta-2 Microglobulin (β2M)	F	5'-CATCCAGCGTACTCCAAAGA-3'
	R	5'-GACAAGTCTGAATGCTCCAC-3'
Interleukin 8 (IL-8)	F	5'-CAGCTCTGTGTGAAGGTGCAGTTT-3'
	R	5'-GTTGGCGCAGTGTGGTCCACTC-3'

6.2.7 Immunocytochemistry

HuH7 cells were seeded as per section 6.2.1 in 4-well Lab-Tek II chamber slides (Lab-Tek). Cells were treated with PBS (control) or TNF-α (5 ng/mL) for 4 hours. As per section 2.16, cells were fixed in 4% (w/v) paraformaldehyde, blocked with methanol:hydrogen peroxide solution (30%) for 20 minutes and incubated with anti-DHCR24 rabbit monoclonal IgG (1:200 dilution in 5% (w/v) goat serum) (Cell Signalling Technology) overnight and goat anti-rabbit IgG conjugated to horseradish peroxidase (HRP) (1:200 dilution in 5% (w/v) goat serum) (Cell Signalling Technology) for 30 minutes. Cells were visualised using 3,3'-diaminobenzidine (DAB) (Dako) for 5 minutes, counterstained in haemotoxylin, mounted with DPX (Merck Millipore), and then cover-slipped. Cell images were obtained using a BH-2 Olympus microscope at 20x magnification.

6.2.8 Apoptosis assay

Apoptosis was measured using the Cell Death Detection ELISA Plus (Roche) according to the manufacturer's instructions (section 2.18).

6.2.9 Statistical analysis

Data are expressed as mean ± SEM. Direct comparisons between two treatments were performed using unpaired t-test, while significant differences between multiple treatments were determined by one-way ANOVA with Sidak's *post hoc* test analysis. GraphPad Prism 6.0 was used for analysis. Significance was set at $P<0.05$. To show the effect size, P values lower than $P <0.05$ were specified.

6.3 Results

6.3.1 The cholesterol content of HuH7 cells was not increased by DHCR24 overexpression

Cultured HuH7 cells were transfected with with pcDNA3.1A (pControl) or pcDNA3.1A-DHCR24 (pDHCR24) expression vectors using TransPass V reagent (New England Biolabs) with the optimised conditions described in section 2.4.1 in order to elucidate if DHCR24 mediates decreases in TNF-α-induced IL-8 levels via a cholesterol-dependent mechanism. For these experiments, pcDNA3.1A plasmid vector was used as the vehicle control for transfection because DHCR24 was cloned into pcDNA3.1A plasmid vector for overexpression analysis. Transfectants were subsequently incubated for 24-hours prior to delipidating the cells using hexane/isopropanol and measuring cellular cholesterol levels using the Amplex Red Cholesterol Assay (Life Technologies) as described in section 2.15. To verify DHCR24 overexpression, total RNA was extracted from the delipidated cells as per [579].

Figure 6.1 shows that in pDHCR24-overexpressing HuH7 cells there was no significant increase in cellular cholesterol levels compared to pControl-transfected HuH7 cells.

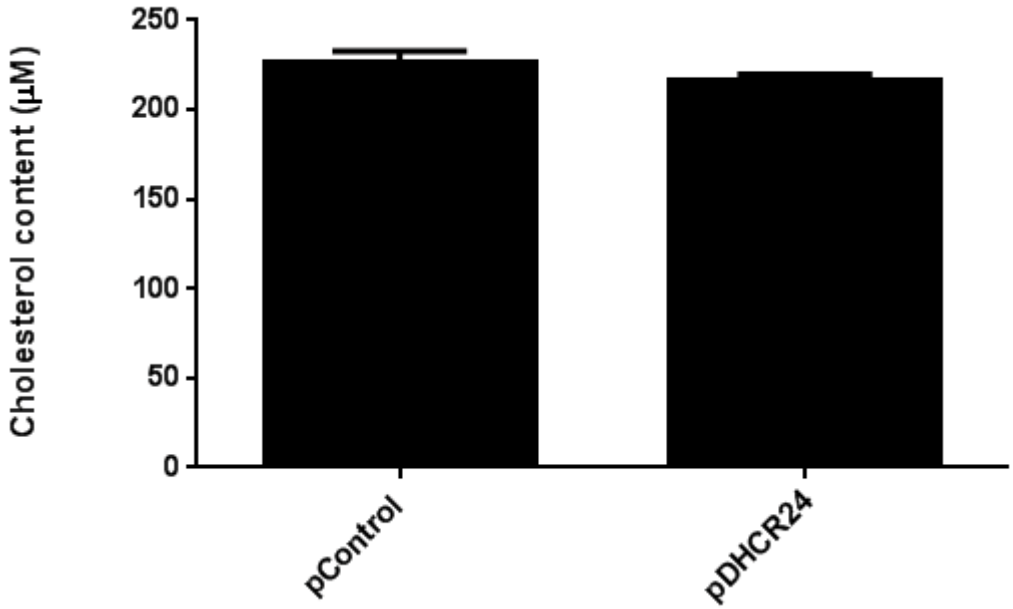

Figure 6.1 DHCR24 overexpression does not increase HuH7 cell cellular cholesterol content. HuH7 cells were transfected with pcDNA3.1A (pControl) or pcDNA3.1A-DHCR24 (pDHCR24) for 24 hours before cholesterol was extracted using hexane/isopropanol. Cholesterol levels were measured using the Amplex Red Cholesterol Assay (Life Technologies). Data are shown as mean ± SEM (n = 3).

6.3.2 Transient transfection of pDHCR24-N294T/K306N increases DHCR24 levels in HuH7 cells

To confirm that transient transfection of the DHCR24 oxidoreductase mutant (ORM) pDHCR24-N294T/K306N increased DHCR24 levels in HuH7 cells, cultured HuH7 cells were transfected with pcDNA3.1A (pControl), pcDNA3.1A-DHCR24 (pDHCR24), or pDHCR24-N294T/K306N (pN294T/K306N) expression vectors using TransPass V reagent (New England Biolabs) with the optimised conditions described in section 2.4.1. pcDNA3.1A vector was the vehicle control for transfection because DHCR24 was cloned into pcDNA3.1A vector for overexpression analysis, while pDHCR24 was the wild type positive control. Following transfection, cells were left for 24-hours prior to extraction of total RNA and subsequent analysis of DHCR24 mRNA levels by real-time RT-qPCR.

From the RT-qPCR results shown in Figure 6.2, transfection using TransPass V was successful with DHCR24 mRNA levels significantly increased compared to the vector control.

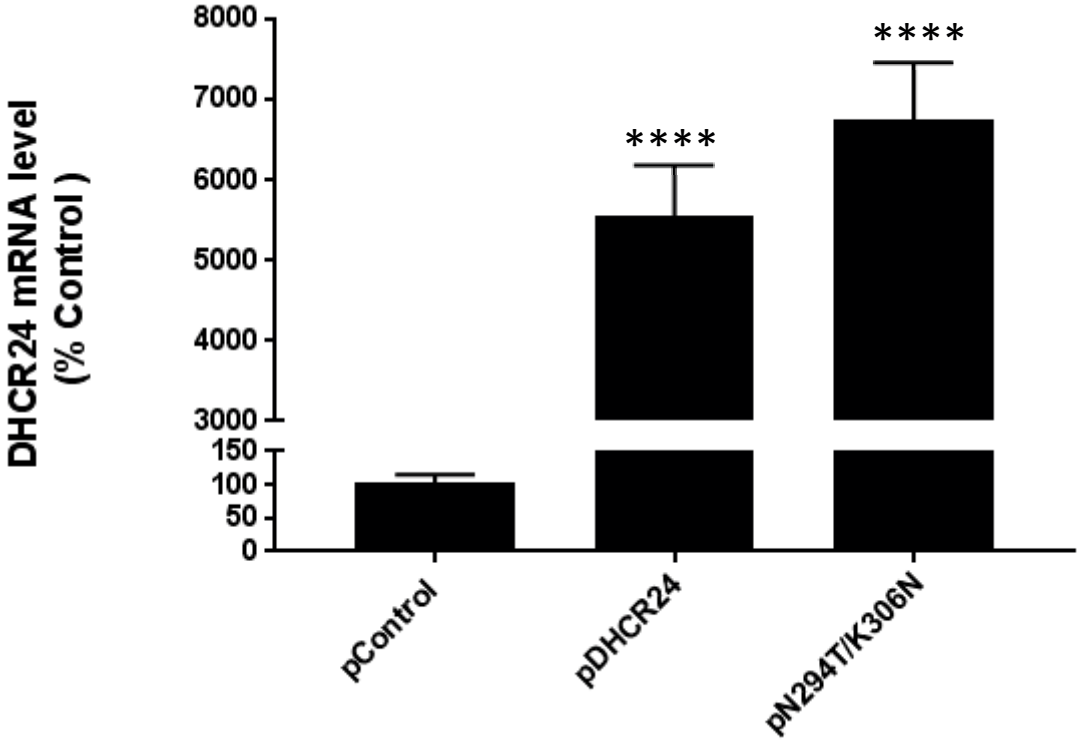

Figure 6.2 Transient transfection of HuH7 cells with pDHCR24-N294T/K306N successfully increased DHCR24 levels. HuH7 cells were transfected with pcDNA3.1A, pcDNA3.1A-DHCR24, or pN294T/K306N for 24 hours. Total RNA was isolated and RT-qPCR used to measure DHCR24 mRNA levels with β2M as a reference gene. Data are shown as mean ± SEM (n = 3) **** P<0.0001 vs pControl.

6.3.3 TNF-α-induced IL-8 levels in HuH7 cells were not suppressed DHCR24 by the DHCR24 oxidoreductase mutant.

DHCR24 catalyses the conversation of desmosterol to cholesterol via its oxidoreductase site [419] and is also considered the enzyme's active site [473, 580]. To elucidate whether DHCR24 oxidoreductase site is facilitates DHCR24's reduction of TNF-α-induced IL-8 levels in HuH7 cells, a DHCR24 oxidoreductase mutant (ORM) was produced using site-directed mutagenesis.

Investigation of whether ORM overexpression could protect against a TNF-α-induced (5 ng/mL, 4 hours) IL-8 protein levels in HuH7 cells in a manner comparable to wild type-DHCR24, replicating its effects. To test whether if the effect at the protein level was due to an effect on gene expression the mRNA level of IL-8 was also measured. As in the previous experiment, HuH7 cells were treated with TNF-α (5 ng/mL, 4 hours).

Figure 6.3 shows that cytokine activation increased IL-8 protein levels in HuH7 cells. Figure 6.4 also shows that cytokine activation increased IL-8 mRNA levels, while pDHCR24-overexpression reduced TNF-α-induced IL-8 protein (Figures 6.3) and mRNA levels (Figure 6.4).

Overexpression of the ORM did not replicate wild type-DHCR24's effects of suppressing TNF-α-IL-8 levels in HuH7 cells. Figure 6.3 shows that at the protein level there was no difference in TNF-α-induced IL-8 levels between ORM and pControl. There was no difference in IL-8 mRNA levels between ORM and pControl, although IL-8 mRNA levels were significantly higher in ORM than in wild type-DHCR24 (Figure 6.4).

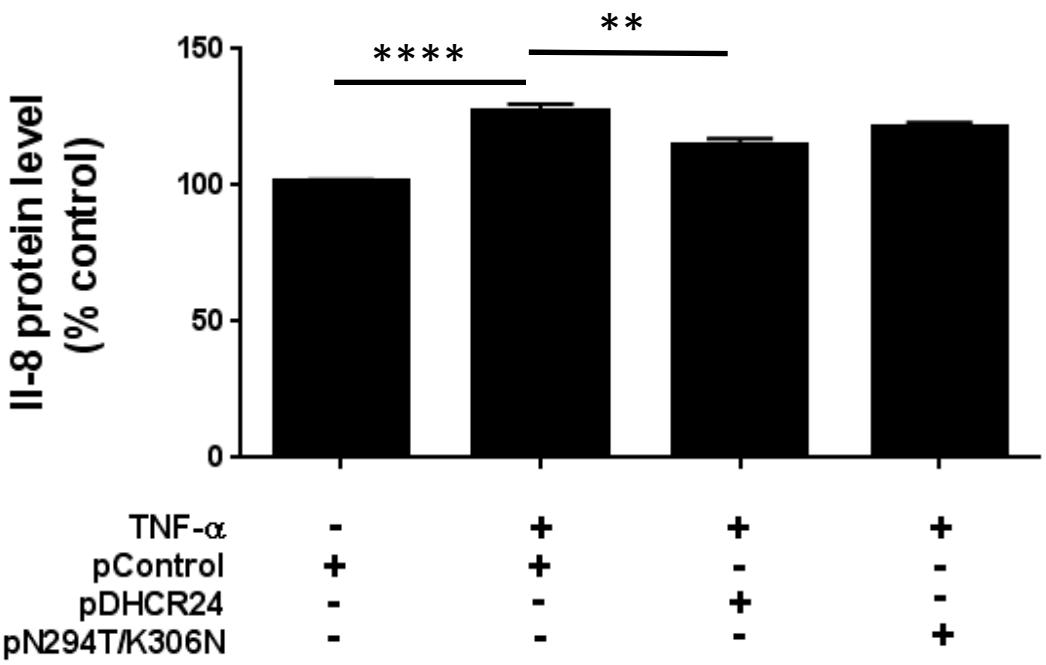

Figure 6.3 DHCR24 oxidoreductase mutant (N294T/K306N) did not suppress TNF-α-activated IL-8 protein levels in HuH7 cells. pcDNA3.1A-DHCR24 (pDHCR24)-overexpression suppressed IL-8 protein levels in TNF-α-activated HuH7 cells in comparison to pcDNA3.1A (pControl). HuH7 cells were transfected with pControl, pDHCR24, or pDHCR24-N294T/K306N plasmids before activation with 5 ng/mL TNF-α for 4 hours. Supernatant was collected and IL-8 protein levels were measured using ELISA. Data are shown as mean ± SEM (n = 4) ** P<0.01, **** P<0.0001.

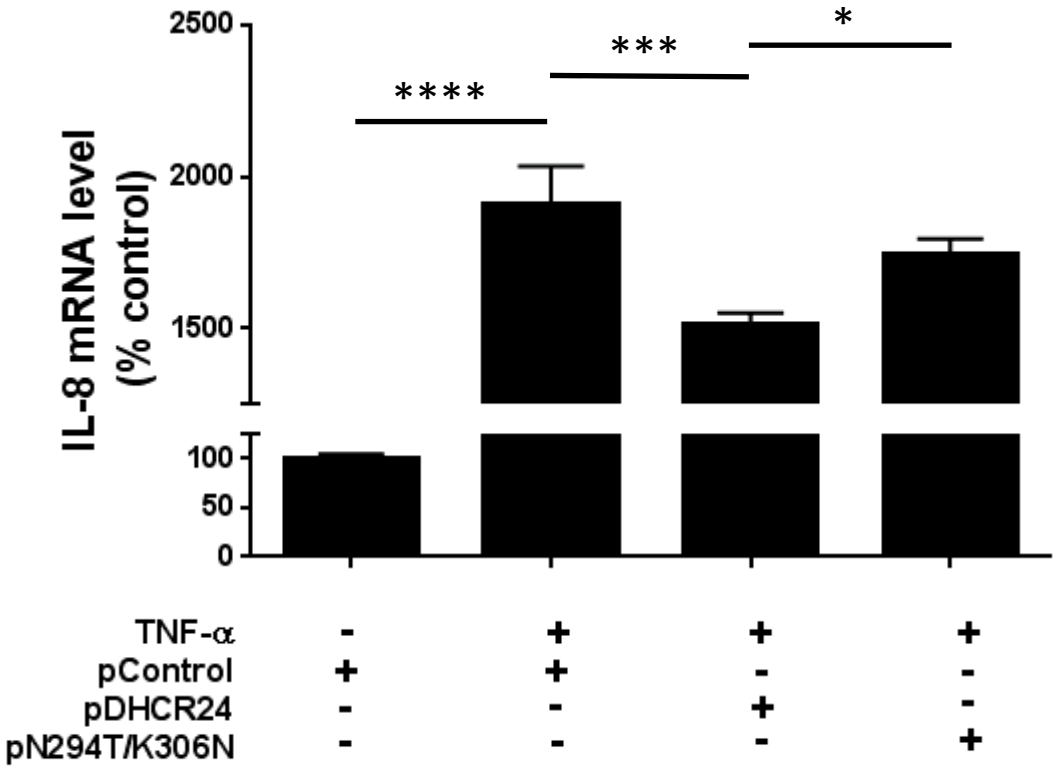

Figure 6.4 DHCR24 oxidoreductase mutant (pN294T/K306N) did not suppress TNF-α-activated IL-8 mRNA levels in HuH7 cells. pcDNA3.1A-DHCR24 (pDHCR24)-overexpression suppressed IL-8 mRNA levels in TNF-α-activated HuH7 cells in comparison to pcDNA3.1A (pControl) and pN294T/K306N. HuH7 cells were transfected with pControl, pDHCR24, or pDHCR24-N294T/K306N plasmids before activation with 5 ng/mL TNF-α for 4 hours. Total RNA was extracted and IL-8 mRNA levels were measured using RT-qPCR with β2M as a reference gene. Data are shown as mean ± SEM (n = 4) * P<0.05, *** P<0.001, **** P<0.0001.

6.3.4 DHCR24's localisation does not change but its levels are reduced by cytokine activation in HuH7 cells

DHCR24's localisation is primarily at the ER membrane facing the cytoplasm [140, 581]. Localisation of DHCR24 at the ER membrane, is consistent with other cholesterol biosynthesis enzymes such as HMG-CoA, as *de novo* cholesterol biosynthesis predominantly takes place on the cytoplasmic side of the ER membrane [582]. As DHCR24 is a cholesterol synthesis enzyme, it was originally proposed that DHCR24 would mediate protection in TNF-α-activated HuH7 cells against the inflammatory response through a cholesterol-mediated process as this mechanism has been demonstrated in other cell types [433, 438]. However, section 6.3.1 shows that DHCR24 overexpression does not increase cholesterol levels and that the protection against TNF-α-activation elicited by DHCR24 in HuH7 cells does not appear to be cholesterol-dependent. DHCR24 protects fibroblasts (mouse and rat) by translocating from its endogenous, unstimulated location to interact with other proteins and inhibiting stress responses. Transmembrane domain-deleted DHCR24 translocates from the ER into the cytoplasm following H_2O_2-exposure where it scavenges ROS, consequently preventing apoptosis in MEF [140]. In MEF, wild type DHCR24 also prevents apoptosis by inhibiting caspase-3 [140], while in rat fasciculata cells, DHCR24 is cleaved by caspase-3 releasing the catalytic domain from the ER membrane preventing apoptosis but also allowing it to translocate to the nucleus. This latter study however did not investigate a role for this translocation subsequent to DHCR24's cleavage by caspase-3 [577]. DHCR24 also inhibits caspase-3 activation by serving as a caspase substrate in neuroglioma H4 cells preventing apoptosis [421]. In rat embryonic fibroblasts, DHCR24 translocates to the nucleus, following H_2O_2 treatment. This nuclear translocation of DHCR24 in rat embryonic fibroblasts blocks degradation of the tumour suppressor p53 through ubiquitination, resulting in accumulation of its active form. p53 is an important tumour suppressor gene which prevents cell proliferation under conditions of cellular stress. DHCR24 enables p53 to accumulate by displacing E3 ubiquitin ligase Mdm2, which thereby enables it to activate DNA repair enzymes, arrest the cell cycle at G1/S and enable DNA repair enzymes to function [423]. These functions of caspase-3 interaction and p53 accumulation both require DHCR24 to translocate to the nucleus. Chapter 4 showed that following TNF-α-activation in HCAECs, DHCR24 translocates from the ER to the nucleus. As a first step in exploring DHCR24's multi-functional role and potential interaction with other proteins in HuH7 cells, it was investigated if DHCR24 changed localisation following activation with TNF-α.

To investigate the localisation of DHCR24 protein in HuH7 cells, in both quiescent and TNF-α-activated states, HuH7 cells were treated with PBS or TNF-α and imaged using immunocytochemistry. Detecting DHCR24's localisation and translocation using immunocytochemistry involved treating cells with PBS (control) or TNF-α (5 ng/mL) for 4 hours. Following treatment, cells were fixed with methanol and stained by immunocytochemistry as described in section 2.16 using rabbit anti-DHCR24 monoclonal antibody (Cell Signalling Technology). Images of the slides were obtained using an Olympus BH-2 microscope.

Figure 6.5 (A) shows that in HuH7 cells, DHCR24 levels are highly expressed located peri-nuclearly, nuclearly, and throughout the cytoplasm. Following TNF-α-activation, DHCR24 levels markedly decrease as evidenced by a noticeably lower intensity of (brown) staining and remain mainly in a peri-nuclear and nuclear localisation.

To further explore DHCR24 localisation after TNF-α exposure, fluorescent microscopy was used to further elucidate DHCR24's localisation using EGFP-tagged DHCR24 (DHCR24-EGFP) transfected HuH7 cells. Unfortunately, the auto-fluorescent nature of hepatocytes precluded usable images from being obtained [637, 638].

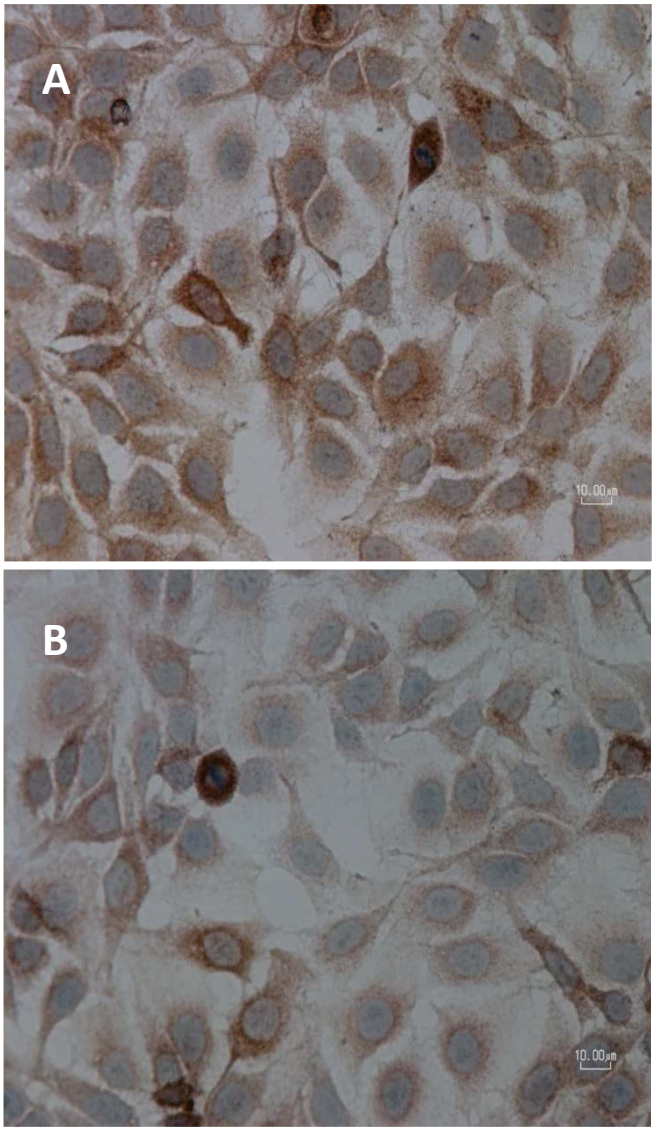

Figure 6.5 Localisation of DHCR24 protein in cultured non-transfected HuH7 cells by immunocytochemistry staining. Non-transfected HuH7 cells: (A) PBS 4 hours (control); (B) Stimulated with TNF-α (5 ng/mL) for 4 hours. The presence of DHCR24 protein in HuH7 cells was detected by rabbit anti-DHCR24 monoclonal antibody (Cell Signalling Technology). The cells were stained by haematoxylin and eosin (H&E) with the nucleus stained purple and the cytoplasm stained light blue. DHCR24 proteins (dark brown granules) as shown in A and B were mostly localised in the cytoplasmic region. Figure B shows DHCR24 staining was reduced following TNF-α-activation. All images obtained using 40x magnification with an Olympus BH-2 microscope.

6.3.5 DHCR24 overexpression inhibits apoptosis in HuH7 cells and requires the oxidoreductase site

Inflammation can culminate in apoptosis [639] and accumulating evidence shows that DHCR24 serves anti-apoptotic roles in various cell types [140, 421, 423, 433, 437, 438, 577]. For example, in neuronal cells DHCR24 interacts with caspase-3 and blocks p53 degradation subsequently preventing apoptosis [423], while in W138-TERT fibroblasts and MEF, DHCR24 scavenges H_2O_2 in the cytoplasm preventing ROS-induced apoptosis [140, 423, 437]. The result in 6.3.4 also shows that DHCR24 is localised to the nucleus in HuH7 cells following TNF-α-activation suggesting a potential nuclear interaction which may culminate in inhibition of apoptosis. Therefore it was investigated whether DHCR24 would protect against TNF-α-induced apoptosis in HuH7 cells.

This experiment investigated whether DHCR24 can suppress TNF-α-induced apoptosis in HuH7 cells. Secondary to this, it was also determined if DHCR24 did protect against apoptosis, whether the oxidoreductase site was important for the effect. HuH7 cells were transfected with pcDNA3.1A (pControl), pcDNA3.1A-DHCR24 (pDHCR24), or pDHCR24-N294T/K306N (pN294T/K306N) before being treated with TNF-α (15 ng/µL 18 hours) to induce apoptosis. Using ELISA [Cell Death Detection ELISA^{PLUS} (Roche)] apoptosis was quantified (using enrichment factor of mono- and oligonucleosomes as a measurement for apoptosis measurement) [640-642].

Figure 6.6 shows that TNF-α-activation induced apoptosis compared to untreated control while wild type DHCR24 prevented apoptosis compared to TNF-α-activated pControl. The ORM did not protect against TNF-α-induced apoptosis with a significantly higher level of apoptosis detected compared to compared to wild type DHCR24 ($P<0.05$).

Thus far it has been shown that increasing DHCR24 suppresses a TNF-α-induced inflammatory response and apoptosis. DHCR24 has also been shown to be localised to the ER and consequentially, DHCR24 may control a TNF-α-induced ER stress response.

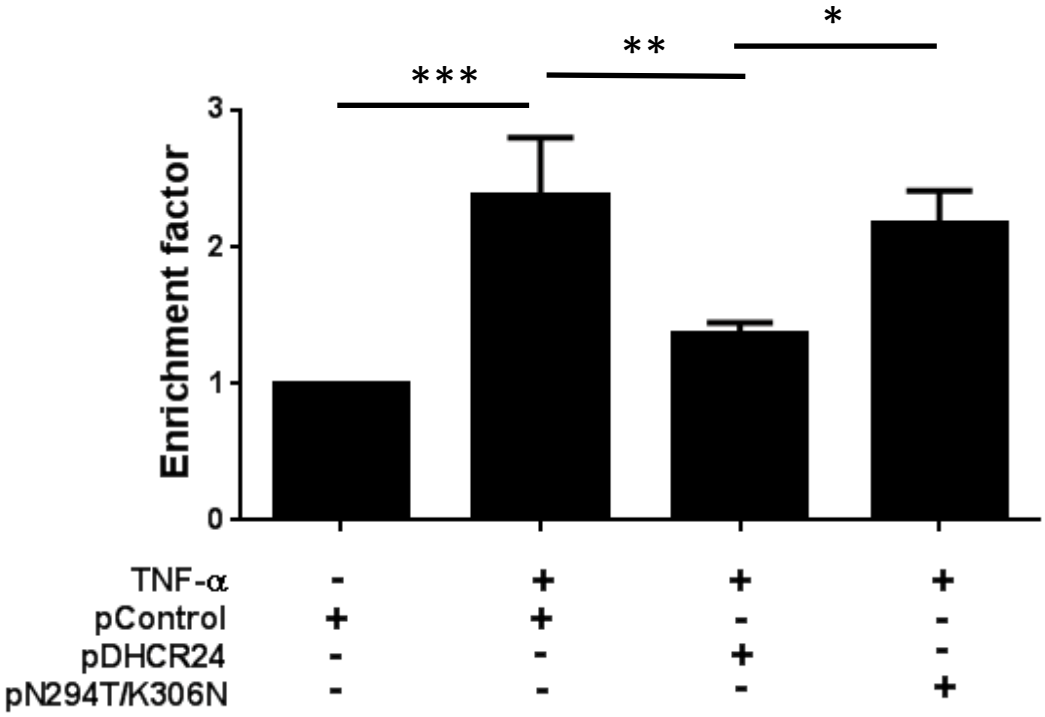

Figure 6.6 Apoptosis levels are significantly decreased by wild type DHCR24 but not the DHCR24 oxidoreductase mutant (N294T/K306N) in TNF-α-activated HuH7 cells. HuH7 cells were transfected with pcDNA3.1A (pControl), pcDNA3.1A-DHCR24 (pDHCR24), or pDHCR24-N294T/K306N (pN294T/K306N) before activation with 15 ng/mL TNF-α for 18 hours. Following cell treatment, HuH7 cell apoptosis levels were measured using ELISA [Cell Death Detection ELISA^{PLUS} (Roche)]. Data are shown as mean ± SEM (n = 6) * P<0.05, ** P<0.01, *** P<0.001.

6.3.6 Cytokine activation does not increase ER stress markers in HuH7 cells

DHCR24 was shown to be localised peri-nuclearly and potentially the ER in HuH7 cells however, despite this localisation which is consistent with other cholesterol biosynthesis enzymes [582], increasing DHCR24 levels does not significantly increase cholesterol levels (section 6.3.1). Therefore, it is unlikely that DHCR24's protective effects against a TNF-α-induced inflammatory response in HuH7 cells are cholesterol-dependent. It was next hypothesised that in HuH7 cells, DHCR24 may have a role in controlling ER stress and that in turn facilitates a reduced inflammatory response [86]. To investigate whether DHCR24 suppresses a TNF-α-induced ER stress response, HuH7 cells were treated with 5 ng/mL TNF-α for 4 hours.

Surprisingly, Figures 6.7 to 6.10 show that TNF-α-activation at the inflammatory conditions used did not significantly increase sXBP-1, XBP-1, ATF-4 or ATF-6 mRNA levels. Consequently, there were no significant differences in sXBP-1, XBP-1, ATF-4 or ATF-6 mRNA levels between the HuH7 cells transfectants.

Induction of ER stress using TNF-α was attempted in the same fashion as for HCAECs (Chapter 4) however in the case of HuH7 cells, this was unsuccessful. Therefore the involvement of DHCR24 in ER stress was not further investigated.

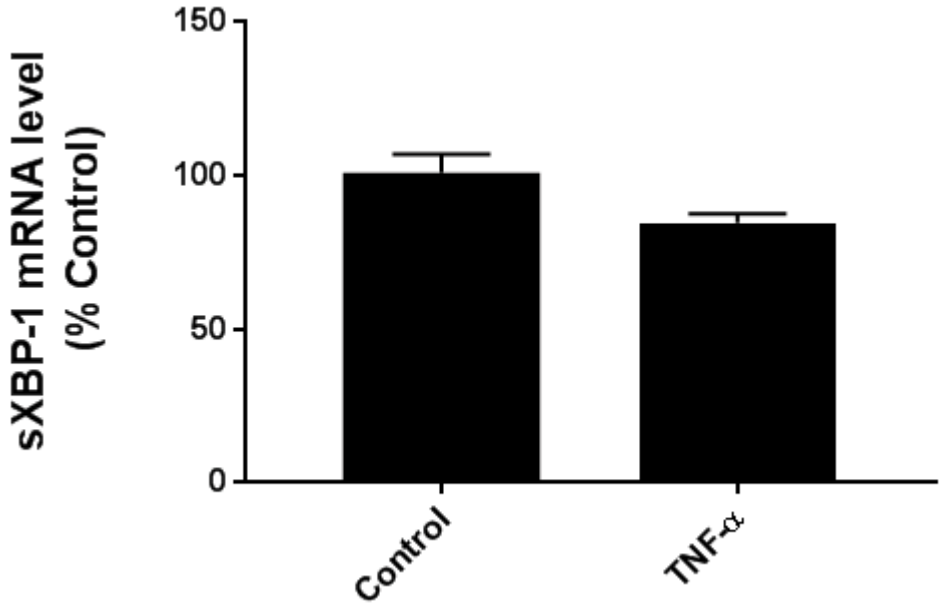

Figure 6.7 sXBP-1 mRNA levels were not increased in TNF-α activated HuH7 cells. HuH7 cells were transfected with pcDNA3.1A before activation with 5 ng/mL TNF-α for 4 hours. Total RNA was extracted and sXBP-1 mRNA levels were measured using RT-qPCR with GAPDH as a reference gene. Data are shown as mean ± SEM (n = 6).

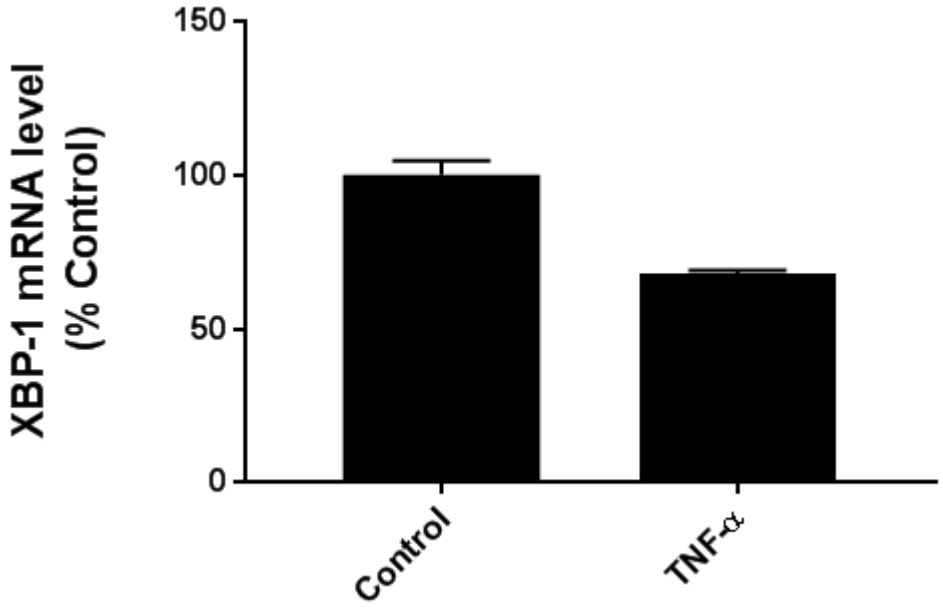

Figure 6.8 XBP-1 mRNA levels were not increased in TNF-α-activated HuH7 cells. HuH7 cells were transfected with pcDNA3.1A before activation with 5 ng/mL TNF-α for 4 hours. Total RNA was extracted and XBP-1 mRNA levels were measured using RT-qPCR with GAPDH as a reference gene. Data are shown as mean ± SEM (n = 3).

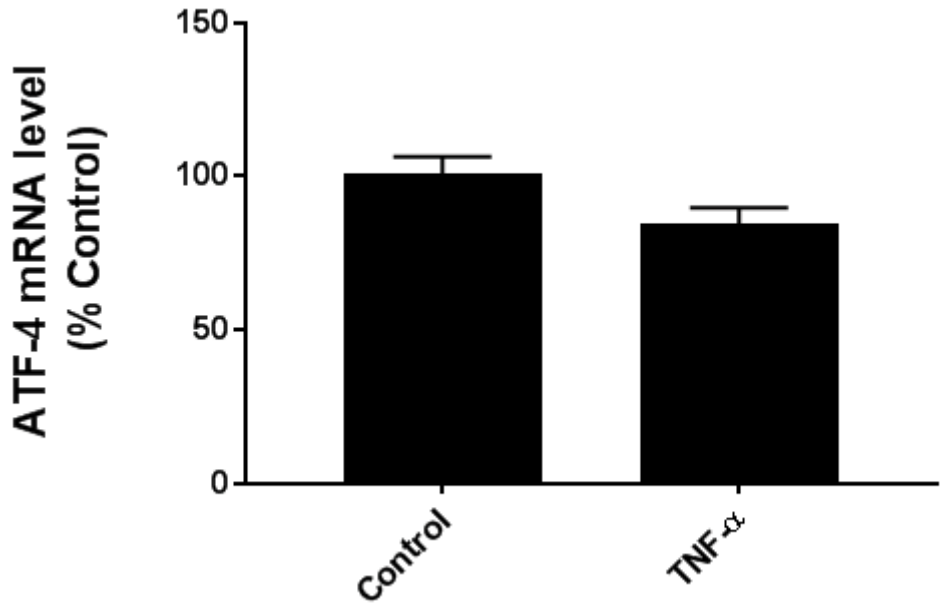

Figure 6.9 ATF-4 mRNA levels were not increased in TNF-α-activated HuH7 cells. HuH7 cells were transfected with pcDNA3.1A before activation with 5 ng/mL TNF-α for 4 hours. Total RNA was extracted and ATF-4 mRNA levels were measured using RT-qPCR with GAPDH as a reference gene. Data are shown as mean ± SEM (n = 6).

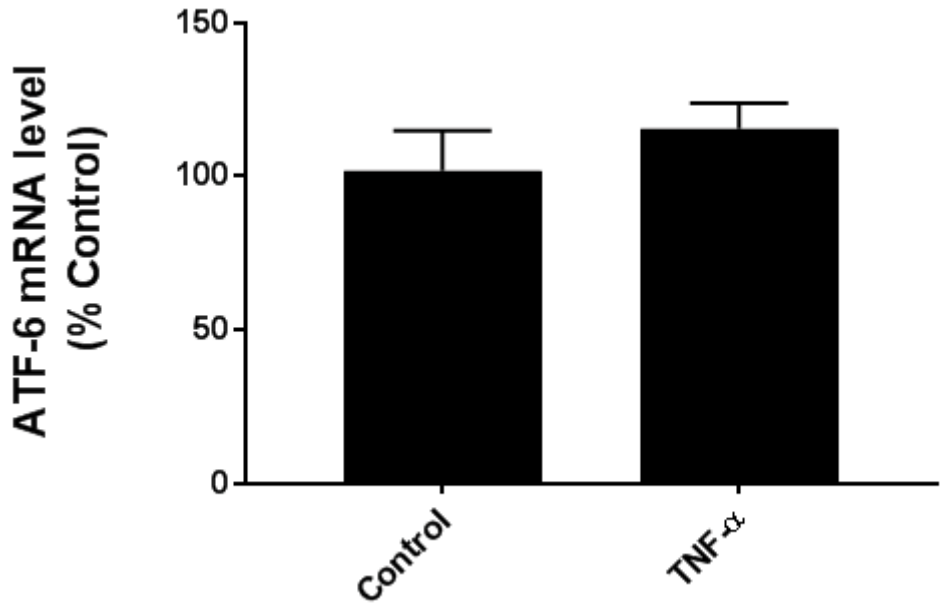

Figure 6.10 ATF-6 mRNA levels were not increased in TNF-α-activated HuH7 cells. HuH7 cells were transfected with pcDNA3.1A before activation with 5 ng/mL TNF-α for 4 hours. Total RNA was extracted and ATF-6 mRNA levels were measured using RT-qPCR with GAPDH as a reference gene. Data are shown as mean ± SEM (n = 3).

6.4 Discussion

This chapter focused on elucidating the mechanisms through which DHCR24 affords protection against a TNF-α-induced inflammatory response in HuH7 cells. In this study, DHCR24 was demonstrated to suppress a TNF-α-induced inflammatory response as measured by IL-8 levels. This suppressive effect was shown to be independent of cholesterol levels although dependent on the enzyme's oxidoreductase-site. Suppression of a TNF-α-induced inflammatory response by DHCR24 also did not occur through suppression of the ER stress markers sXBP-1, XBP-1, ATF-4, or ATF-6 despite peri-nuclear localisation in HuH7 cells. This work also revealed that in HuH7 cells, increased DHCR24 levels prevent TNF-α-induced apoptosis.

The most striking finding of this study was DHCR24's ability to suppress a TNF-α-induced inflammatory response that was independent of increased cholesterol levels in HuH7 cells. This was in contrast to the original hypothesis which suggested that DHCR24 overexpression would lead to increased cholesterol levels, as DHCR24 is an integral cholesterol biosynthesis enzyme [419, 434, 442, 443, 576]. Moreover, this hypothesis also stemmed from DHCR24 facilitating anti-apoptotic activity in human neuroblastoma SH-SY5Y cells (neuronal cells) through a cholesterol-dependent mechanism [433, 438]. In neuroblastoma SH-SY5Y cells, increasing cholesterol levels is also the mechanism by which DHCR24 modulates amyloid beta (Aβ) peptide production and clearance, as well as reducing pre-fibrillar aggregates and neurotoxicity [433, 438]. This hypothesis was also strengthened by DHCR24 suppressing ER stress levels in neuroblastoma cells through augmentation of cholesterol levels [469]. The results presented now show that DHCR24's suppression of a TNF-α-induced inflammatory response in HuH7 cells is independent of increasing cholesterol levels. This is similar to what was found in Chapter 4 whereby DHCR24-overexpression did not increase cholesterol levels in HCAECs. This is also in keeping with DHCR24's effect in W138-TERT fibroblasts and mouse embryonic fibroblasts (MEF). In these cell types, DHCR24 directly scavenges ROS, preventing H_2O_2-induced apoptosis, independent of cholesterol biosynthesis [140, 423].

The lack of increased cholesterol levels following DHCR24 overexpression may be part due to an insufficiency of sterol precursors for cholesterol biosynthesis. DHCR24 is also not a rate-limiting enzyme in the conversion of desmosterol to cholesterol [419]. Further the cholesterol-independent suppression of a TNF-α-induced inflammatory response may be attributed to the cell type-specific activity of DHCR24. As mentioned, DHCR24 protects against cellular stress

through increased cholesterol levels in some cell types [433, 438, 469] but not in all [140, 420, 423].

Another surprising negative finding is that DHCR24 did not control a TNF-α-induced ER stress response in these cells. As DHCR24 is primarily endoplasmic reticulum (ER) resident protein [437, 581], it was hypothesised that in HuH7 cells it may control ER stress. It has been previously reported that DHCR24 reduces tunicamycin-induced ER stress activity preventing apoptosis in MEF [469]. To investigate whether DHCR24 controls a TNF-α-induced ER stress response it was first necessary to show TNF-α-induced ER stress in these cells. Surprisingly, the conditions used did not induce an ER stress response as evidenced by no significant increases in sXBP-1, XBP-1, ATF-4, or ATF-6 mRNA levels. This is interesting because it shows that a TNF-α-induced inflammatory response in HuH7 cells is not stimulating an ER stress response. Therefore ER stress is unlikely to be driving apoptosis. The lack of an ER stress response following TNF-α-activation may be due to the relatively high endogenous cholesterol content of HuH7 cells. Cholesterol is known to protect against cellular stress. In cell types where cholesterol is protective against cellular stress, increasing DHCR24 levels also increases levels of cholesterol [433, 438, 469]. The current work has highlighted that the cholesterol content in HuH7 cells is much higher than in HCAECs (compared Figure 4.1 vs Figure 6.1). This is not too surprising given hepatocytes are the primary cholesterol biosynthesis cells in the body. Consequently, the high cholesterol content of HuH7 cells may innately resist a TNF-α-induced ER-stress response.

The localisation and potential nuclear translocation of DHCR24 in HuH7 cells was next investigated. DHCR24 translocates from the ER to the nucleus in other cell types [423, 577], including HCAECs (Chapter 4). Importantly is has been reported that DHCR24 translocates from the ER to the nucleus in rat fasciculata cells in response to ACTH-induced ROS production protecting against apoptosis. However, under the same ACTH treatment conditions, DHCR24 does not translocate from the ER in human fasciculata cells [577]. DHCR24 in MEF is released from the ER, allowing it to translocate throughout the cell when cleaved by caspase-3 at DHCR24's caspase cleavage motif sites [140]. In rat embryonic fibroblasts, DHCR24 also translocates from the ER to the nucleus [423]. DHCR24 also serves as a caspase death substrate preventing apoptosis with caspase cleavage sites located in its C-terminus [421]. Together, this demonstrates the enzyme's cell-specific activity and its ability to facilitate protection against assorted cellular stressors by translocating through the cell. In this work, IHC was utilised to determine that DHCR24 was localised peri-nuclearly. Further interrogation

using fluorescence microscopy was attempted but auto-fluorescence of HuH7 cells [637, 638] stopped any meaningful investigations. However, DHCR24's perinuclear localisation is consistent with its ER-location as a cholesterol synthesising enzyme [582].

DHCR24 serves an anti-apoptotic role in a variety of cell types [140, 421, 433, 437, 438, 469]. In some cell types DHCR24 protects against apoptosis following translocation to the nucleus. For example, DHCR24's H_2O_2-induced-translocation to the nucleus in rat embryonic fibroblasts, allows it to bind to p53, in turn displacing E3 ubiquitin ligase Mdm2 from p53, which frees p53 to activate DNA repair enzymes. This induces growth arrest by holding the cell cycle at G1/S to enable DNA repair enzymes to function [423]. Together with the observation that DHCR24 is located in the nucleus in HuH7 cells before and after TNF-α-activation, DHCR24's direct role against TNF-α-induced apoptosis was investigated. Further chronic inflammation, characteristic of insulin resistance, can lead to apoptosis [643, 644]. In this work, as measured by enrichment of mono- and oligo-nucleosomes as a marker for DNA fragmentation and apoptosis, DHCR24 was shown for the first time to protect against TNF-α-induced apoptosis in HuH7 cells. DHCR24 is a caspase death substrate, with caspase cleavage sites located in its C-terminus which enables it to prevent apoptosis [421]. Future work will require elucidation of the specific mechanism(s) through which DHCR24 protects against TNF-α-induced apoptosis in HuH7 cells. However, from this work it is clear that in HuH7 cells DHCR24 serves an anti-apoptotic role against TNF-α-induced apoptosis. This is significant in the context of insulin resistance and type 2 diabetes, in addition to other disease states which are characterised by hepatic inflammation such as non-alcoholic steatohepatitis [645] as chronic inflammation can lead to apoptosis, in turn causing the liver to become necrotic, culminating in potentially fatal liver failure [646].

To further investigate the potential mechanisms for DHCR24's suppression of a TNF-α-induced inflammatory response in HuH7 cells, the role of DHCR24's oxidoreductase site was investigated using a DHCR24 oxidoreductase mutant (ORM). DHCR24's oxidoreductase site was a target of interest as it is the reported active site of the enzyme [419, 473, 580]. Further, the enzyme's oxidoreductase site is located in the N-terminal region. This is significant, as in MEF DHCR24 scavenges tunicamycin-induced H_2O_2 via the N-terminal [437]. Similar to this observation and in keeping with the effect observed in HCAECs (Chapter 4), DHCR24's suppression of a TNF-α-induced inflammatory response in HuH7 cells was dependent on its oxidoreductase site. DHCR24 was also shown for the first time to protect against TNF-α-induced apoptosis in HuH7 cells and that this was mediated via the oxidoreductase region.

Together this supplements the existing work in MEF [140] and HCAECs (Chapter 4), and provides novel information which builds upon the current understanding of DHCR24's activity in HuH7 cells. This is particularly valuable as an understanding of DHCR24's oxidoreductase site is vital for the development of potential downstream therapeutic applications. Potentially mimetic forms of DHCR24 or its oxidoreductase site may be produced to suppress inflammation and apoptosis.

In summation, DHCR24 has been demonstrated to suppress a TNF-α-induced inflammatory response. DHCR24 also prevents TNF-α-induced apoptosis. Moreover, this work shows that DHCR24 mediates suppression of a TNF-α-induced inflammatory response and prevents apoptosis through its oxidoreductase site, albeit independent of cholesterol synthesis activity. Following TNF-α-activation DHCR24 levels in HuH7 cells were shown to be decreased. DHCR24 was also determined to be located around and in the nucleus before and after TNF-α-activation nucleus indicating potential roles in H_2O_2-scavenging and the inhibition of apoptosis respectively. The elucidation of these mechanisms provides valuable information about DHCR24's activity in HuH7 cells, especially given the emerging understanding of the cell-specific activity of the enzyme, and for the potential development of a DHCR24 mimetic for reducing hepatocyte inflammation if DHCR24 is considered as a novel therapeutic avenue following positive future studies.

Chapter 7 – Summary, Conclusions, and Limitations

DHCR24 is primarily known as a cholesterol biosynthesis enzyme, catalysing the conversion of desmosterol to cholesterol [419]. However, recent work shows that DHCR24 also inhibits cellular stress in a range of cell types [1, 420-427]. These effects, paired with the upregulation of DHCR24 by HDL, in HCAECs [1], provided impetus to investigate whether DHCR24 had a protective effect in HCAECs. The preliminary work, which paved the way for the study presented in this thesis, indicated that by silencing DHCR24, HDL's protective effect against cytokine-activation was abrogated [1]. The work in this thesis extends these findings by showing that DHCR24 knockdown attenuates the suppressive effect of apoA-I rHDL against TNF-α-induced IL-8 levels in HuH7 cells. This indicated that DHCR24 mediates, at least in part, HDL's protective effect against a TNF-α-induced inflammatory response in both HCAECs and HuH7 cells.

This study provides proof-of-principle that DHCR24 replicates HDL's effect of suppressing a TNF-α-induced inflammatory response. This works adds to the existing knowledge of DHCR24's protective effect, and shows the effect of DHCR24 overexpression in HCAECs and HuH7 cells. Stemming from the novel observation that DHCR24 alone suppresses a TNF-α-induced inflammatory response in HCAECs and HuH7 cells, the mechanism underlying these effects was investigated. Elucidating the mechanisms through which DHCR24 elicits this protection is vital for an understanding of the protein's function and for the development of potential therapeutic applications.

The investigation of DHCR24's mechanisms of suppressing a TNF-α-induced inflammatory response revealed that the enzyme's effect is dependent on its oxidoreductase site in HCAECs and HuH7 cells. DHCR24's oxidoreductase region is considered its active site, catalysing the reduction reaction of desmosterol to cholesterol [419]. The DHCR24 double mutation was selected as it ensures complete abrogation of DHCR24's cholesterol synthesis activity [419]. Further, DHCR24's oxidoreductase site elicits protection against tunicamycin-induced oxidative stress in MEF. In MEF DHCR24's oxidoreductase region has been shown to facilitate DHCR24's scavenging of tunicamycin-induced H_2O_2 while independent of cholesterol biosynthesis [437]. The results in this study show that the effect of DHCR24's oxidoreductase site in HCAECs and HuH7 cells is similar to the work reported in mouse embryonic fibroblasts (MEF).

An intriguing observation associated with the investigation of DHCR24's oxidoreductase site was that transfection levels varied. Transfection levels were determined using the sensitive measure of RT-qPCR. The disparity in transfection levels of DHCR24 and the DHCR24 oxidoreductase mutant (ORM) in HCAECs can be observed in Figure 3.1 compared to Figure 4.2 and in HuH7 cells by Figure 5.6 compared to Figure 6.2. Interestingly, the ORM consistently transfected at higher levels than the wild type DHCR24, potentially reflecting a higher transfection efficiency. However, despite higher ORM transfection levels than wild type DHCR24, the ORM did not suppress TNF-α-induced cellular stress while the wild type DHCR24 consistently did. This, in turn, further validates the results investigating the effect of DHCR24's oxidoreductase site obtained in this thesis. In the results where a slight downward trend in cellular stress markers was observed in the ORM-transfectants (e.g. Figure 4.12 and Figure 6.3) in comparison to the negative control, endogenous wild type DHCR24 may be attributed to the effect as endogenous levels of DHCR24 were present in the ORM-transfectants. In future work, it would be valuable to increase the transfection efficiency to determine whether the effects reported in this work would be more significant. Additionally, it would be valuable to repeat these experiments in a DHCR24 negative background. The results showed that DHCR24's oxidoreductase site is required in HCAECs and HuH7 cells to suppress a TNF-α-induced inflammatory response. Moreover, DHCR24's oxidoreductase site's is also involved in the conversion of desmosterol to cholesterol activity, and therefore led to the investigation of a cholesterol-mediated mechanism for DHCR24's suppression of a TNF-α-induced inflammatory response in HCAECs and HuH7 cells.

The most striking finding of this study was that DHCR24's ability to suppress a TNF-α-induced inflammatory response was independent of increased total cellular cholesterol levels in both HCAECs and HuH7 cells. This was in contrast to the original hypothesis which suggested that DHCR24 overexpression would lead to increased cholesterol levels, as DHCR24 is an integral cholesterol biosynthesis enzyme [419, 434, 442, 443, 576]. Further, DHCR24 facilitates anti-apoptotic activity in human neuroblastoma SH-SY5Y cells (neuronal cells) through a cholesterol-dependent mechanism [433, 438]. In neuroblastoma SH-SY5Y cells, increasing cholesterol levels is also the mechanism by which DHCR24 modulates amyloid beta (Aβ) peptide production and clearance, as well as reducing pre-fibrillar aggregates and neurotoxicity [433, 438]. Moreover, ER stress levels in neuroblastoma cells are also reduced by augmentation of cholesterol levels by DHCR24 [469]. The finding that DHCR24's suppression of a TNF-α-induced inflammatory response in HCAECs and HuH7 cells is independent of increased

total cellular cholesterol levels is consistent with DHCR24's effect in W138-TERT fibroblasts and MEF. In these cell types, ROS are directly scavenged by DHCR24, thereby preventing H_2O_2-induced apoptosis, independent of cholesterol biosynthesis [140, 423]. Moreover, our laboratory's previous work confirmed that suppression of a TNF-α-induced inflammatory response by HDL increasing DHCR24 levels in HCAECs was independent of cholesterol synthesis. The experiment showed by using cyclodextrin to deplete cells of cholesterol, that neither DHCR24 nor VCAM-1 levels were increased. Simvastatin was also used to inhibit cholesterol synthesis, which decreased DHCR24 levels but similarly, did not increase VCAM-1 levels. This indicated that cholesterol was not involved in the regulation of VCAM-1 by HDL's increase of DHCR24 levels [1]. The work presented builds upon these previous observations, and shows that DHCR24 overexpression does not influence total cellular cholesterol levels in HCAECs or HuH7 cells.

DHCR24 overexpression may not increase total cellular cholesterol levels in HCAECs and HuH7 cells, in part, due to the availability of sterol precursors and the cholesterol requirements of specific cell types [420, 433, 437]. Additionally, DHCR24 is not a rate-limiting enzyme in its catalysis of the conversion of desmosterol to cholesterol [419]. Another possible mechanism precluding increased total cellular cholesterol levels following DHCR24 overexpression, is increased levels of the cholesterol synthesis regulator 24(S),25-epoxycholesterol (24,25EC) [647]. In future directions, investigating whether DHCR24 overexpression leads to increased levels of 24,25EC in HCAECs and HuH7 cells may elucidate whether this regulator is responsible for preventing increases in cholesterol.

Cholesterol protects against cellular stress and DHCR24 has been demonstrated to elicit protective effects by increasing cholesterol levels in some cell types [433, 438, 469]. A limitation of this work was restricting analysis of cellular cholesterol levels, to measurements from unstressed DHCR24-overexpressing cells. Cholesterol depletion can lead to induction of apoptosis [648-650]. In future studies, it would be valuable to identify whether changes in cholesterol content occur following TNF-α-treatment. This would determine if under the treatment conditions used in these experiments, DHCR24 returns cholesterol to physiological levels in HCAECs and HuH7 cells. The inflammatory response has also been associated with cholesterol accumulation rather than depletion, as a consequence of disrupted cellular cholesterol efflux pathways [651]. However, most studies reporting cholesterol depletion-induced apoptosis involve artificially depleting cholesterol (e.g. using methyl-cylodextrin) [648-650]. Experimentally-induced cholesterol overload in SH-SY5Y human neuroblastoma cells

disturbs cholesterol homeostasis. This, in turn, induces apoptosis through increased ROS-generation and conversion of cholesterol to 24-OHC [652], a brain cholesterol oxidation metabolite unable to reduce ROS (as reviewed by [653]). Oxidative stress also increases cholesterol levels in tissue samples from normal aging and Alzheimer's disease patient brains. This is due to dysfunctional cholesterol metabolism, and in this context increased cholesterol is not protective [654]. Therefore, uncontrolled cellular cholesterol levels would induce further cellular stress rather than be protective. DHCR24 may ameliorate the cellular stress responsible for perturbing cholesterol metabolism preventing cholesterol accumulation, and directly suppress TNF-α-induced ER stress and inflammatory stress responses in HCAECs and HuH7 cells. Consequently, this may further support that DHCR24 does not suppress a TNF-α-induced inflammatory response in HCAECs and HuH7 cells through cholesterol biosynthesis mechanisms but through more direct mechanisms. However, further work in this area is required to validate these hypotheses, especially given the cell type-specific functions of DHCR24. Cholesterol depletion studies using cyclodextrin would be valuable in future work to elucidate whether the disparity between DHCR24's effects in HCAECs and HuH7 cells is affected by their varying cholesterol content.

Another limitation of this work was that the method used to quantify cholesterol levels following DHCR24 overexpression only measured total cellular cholesterol. It is possible that while the change in total cellular cholesterol was not significant, that changes in cholesterol levels may be detected when subcellular cholesterol pools are individually investigated. This possibility is supported by the results which indicate an upward trend of increased cholesterol levels following DHCR24 overexpression. Future work should focus on following up this work with investigation of cholesterol content of individual subcellular regions such as the plasma membrane, the ER, caveolae, and other lipid raft-like domains following DHCR24 overexpression in HCAECs and HuH7 cells. A difference in cholesterol content in one of these subcellular regions following DHCR24 overexpression, would elucidate a mechanism of DHCR24's activity. Moreover, concerns of cholesterol-induced cellular stress as mentioned in the preceding paragraph, from this mechanism would be unlikely as the total cellular cholesterol increase would not be significant as shown in this study.

The mechanisms of DHCR24's suppression of a TNF-α-induced inflammatory response described to this point were similar in HCAECs and HuH7 cells. However, DHCR24's translocation following TNF-α-activation was shown to be cell type-specific. In HCAECs, TNF-α-activation stimulates DHCR24 to move from its endogenous, unstimulated location in the ER

into the cytoplasm and nucleus. This work is supported by unpublished Western Blot findings from our laboratory which showed that DHCR24 is located in the cytoplasm. In contrast to HCAECs, DHCR24 in HuH7 cells remains predominately localised peri-nuclearly before and after TNF-α-activation. More specific investigation of DHCR24's endogenous localisation in HuH7 cells was precluded by the auto-fluorescent nature of the cells [637, 638]. The less sensitive method of using immunohistochemistry staining with light microscopy (this method has previously been used by our laboratory - data unpublished) could only reveal a peri-nuclear localisation for DHCR24 in HuH7 cells. However, these observations support the cell type-specific activity of DHCR24. In keeping with this translocation effect in HCAECs, DHCR24 mediates protection in rat fibroblasts [423], and adrenal cells [577] by translocating from its ER localisation to interact with other proteins and inhibiting stress responses. In MEF, transmembrane domain-deleted DHCR24, when exposed to H_2O_2, translocates from its endogenous ER localisation freely throughout the cytoplasm and nucleus, scavenging ROS, thereby precluding apoptosis [140]. Wild type DHCR24 also prevents apoptosis in MEF through caspase-3 interaction inhibiting apoptosis [140]. Moreover, DHCR24 is cleaved by caspase-3, in rat fasciculata cells, releasing the catalytic domain from the ER membrane preventing apoptosis by also allowing it to translocate to the nucleus [472]. In neuroglioma H4 cells, DHCR24 inhibits caspase-3 activation by serving as a caspase substrate preventing apoptosis [421]. Additionally, in rat embryonic fibroblasts, DHCR24 translocates to the nucleus, following H_2O_2 treatment. DHCR24's nuclear translocation in rat embryonic fibroblasts blocks degradation of the tumour suppressor p53 through ubiquitination, leading to accumulation of its active form, consequently preventing apoptosis [423]. These functions of caspase-3 interaction and p53 accumulation are both dependent on DHCR24 translocating to the nucleus. In this study, in both HCAECs and HuH7 cells, DHCR24 localised to and around the nucleus, and in HuH7 cells protected against TNF-α-induced apoptosis. The translocation of DHCR24 to the cytoplasm in HCAECs and its cytoplasm-adjacent localisation in HuH7 cells also merits investigation into a potential ROS-scavenging mechanism, a feature of DHCR24 reported in neuronal cells [421, 469] and fibroblasts [140, 423, 437]. Moreover, future studies investigating DHCR24 and its translocalisation to the nucleus, and probing of its specific activity against apoptosis in HCAECs and HuH7 cells, may also reveal additional cell type-specific mechanisms.

The cell type-specific nature of DHCR24 was also evident with the regulation of ER stress markers. DHCR24's suppression of a TNF-α-induced inflammatory response occurred through

control of ER stress markers in HCAECs but not in HuH7 cells. DHCR24 is primarily an ER-resident protein as was shown in this study in HCAECs and has been shown by others [437, 581]. Therefore, in combination with the known mechanism of ER stress stimulating inflammation [86], ER modulation by DHCR24 was investigated. Additionally, previous work reports that DHCR24 facilitates reductions in tunicamycin-induced ER stress activity thereby preventing apoptosis in MEF [469] and protects against ER stress-induced apoptosis in neuronal cells [469]. The same cytokine treatment conditions that were used to induce the inflammatory response were used to investigate whether DHCR24 controls a TNF-α-induced ER stress response to suppress an inflammatory response. This work showed that a TNF-α-induced inflammatory response is regulated by suppression of an ER stress response in HCAECs, but not in HuH7 cells. The ER stress response in HuH7 cells was not activated following TNF-α-activation which may have been as a result of the relatively high endogenous cholesterol content of HuH7 cells. This work supports DHCR24's previously reported cell type-specific activity, with the interplay between suppression of a TNF-α-induced inflammatory response and the ER stress response being divergent in HCAECs and HuH7 cells. A limitation of this work was that DHCR24's effect on a TNF-α-induced ER stress response was performed with the aim to determine whether regulation of a TNF-α-induced ER stress response was responsible for modulating the TNF-α-induced inflammatory response rather than directly analysing DHCR24's suppression of a TNF-α-induced ER stress response. Consequently, the effect of DHCR24 against a TNF-α-induced ER stress response in HuH7 cells could not be determined, as the TNF-α-induced inflammatory response conditions did not elicit a TNF-α-induced ER stress response. In future work DHCR24's effect on the ER stress response should be investigated using optimised ER stress conditions separate from the inflammatory response. This would determine DHCR24's effect on TNF-α-induced ER stress response conditions in HuH7 cells, and may show more of an effect in HCAECs.

The endogenous level and change in DHCR24 levels following TNF-α-activation also varied in the two cell types. Firstly, the HuH7 cells contained higher levels of DHCR24 than HCAECs. This increased endogenous DHCR24 level may account for the effect of the ORM being more pronounced in HCAECs than in HuH7 cells. The higher endogenous levels of DHCR24 in HuH7 cells could have partially but not significantly, suppressed a TNF-α-induced inflammatory response despite transfection of the ORM which is why IL-8 levels were not increased to the level of the treated control-transfected cells. Interestingly, DHCR24 levels increased in HCAECs in response to TNF-α-activation, yet decreased in HuH7 cells. However, despite the increase in

DHCR24 levels reported in HCAECs following TNF-α-activation, it was not sufficient to elicit a protective effect. This work showed DHCR24 overexpression facilitates a potent suppressive effect against a TNF-α-induced inflammatory response. This also indicates that should further studies validate a therapeutic potential for DHCR24 against inflammation in endothelial cells, an approach of substantially increasing DHCR24 levels by approximately 17-fold through localised delivery of DHCR24 would be required. Localised delivery of DHCR24 or a DHCR24 oxidoreductase site-based mimetic to select regions of the endothelium could potentially be facilitated through gene transfer or localised mimetic delivery. Use of advanced drug delivery systems such as liposomes, protein chemical conjugates, polymeric carriers, and recombinant fusion constructs could be considered to ensure localised and contained delivery of DHCR24. The advanced drug delivery systems listed also have greater utility drug delivery to the endothelium than drugs circulating in blood, which often have no endothelial cell affinity (as reviewed by [655]).

The effect of TNF-α-activation on DHCR24 levels in HuH7 cells was the opposite of HCAECs, with DHCR24 levels decreasing. An approach for treatment could therefore be restoring DHCR24 expression to physiological values. ApoA-I rHDL incubation of HuH7 cells augmented DHCR24 mRNA levels by approximately 2-fold. The half-physiological concentration of apoA-I rHDL (16 μM/0.45 mg/mL) used in this experiment also significantly decreased TNF-α-induced IL-8 mRNA levels. Moreover, in the experiments using siRNA, decreased DHCR24 levels stopped apoA-I rHDL from protecting against increases in TNF-α-induced IL-8 mRNA levels, even when DHCR24 mRNA levels were reduced by only approximately 50%. Together this shows that restoring or incrementally increasing DHCR24 levels is sufficient to significantly attenuate TNF-α-induced IL-8 mRNA levels in HuH7 cells, while overexpressing DHCR24 levels is required to suppress ICAM-1 and VCAM-1 levels in HCAECs. Potential avenues of restoring DHCR24 levels in hepatocytes may include gene therapy. The fenestrated structure of hepatic endothelium enables viral diffusion and subsequent hepatocyte transduction. Therefore using DHCR24-based gene therapy to reduce hepatic inflammation in insulin resistance may be viable [656]. Localised mimetic delivery with advanced drug delivery systems is another potential drug-delivery option (as reviewed by [655]). However, with all of the DHCR24-based therapies, ensuring that DHCR24 levels are localised and controlled, and specifically in hepatocytes remain close to physiological levels, would be necessary in the treatment of hepatic inflammation.

DHCR24-overexpression has been associated with (hepatitis C virus-associated) hepatic tumour development [462, 633, 634]. In light of this, the work shown here in HuH7 cells which indicates DHCR24's suppression of a TNF-α-induced inflammatory response can be achieved with incremental increases of DHCR24, or with its restoration to physiological levels, is positive. Future work is required to determine the merit of perusing DHCR24 to treat hepatic inflammation to potentially improve insulin sensitivity. However, based on this work, the small increases in DHCR24 levels required for such a treatment would eliminate concerns associated with the formation hepatic tumours, as this occurs at supra-physiological DHCR24 levels [462, 633]. In future work, determining to what extent DHCR24 levels in the livers of insulin resistant patients are decreased would be valuable. Comparing *in vivo* DHCR24 levels to the *in vitro* DHCR24 mRNA reductions in HuH7 cells presented in this work may help ascertain the extent DHCR24 levels would need to be increased to restore DHCR24 to a normal physiological range in humans. This study was limited by investigation of DHCR24's effects against a TNF-α-induced inflammatory response *in vitro.* However, the positive work from this study merits further investigation of DHCR24's activity against cellular stressors such as oxidative stress and apoptosis, and *in vivo* work. Ascertaining the DHCR24 levels required to suppress inflammatory conditions and determining the *in vivo* practicality of DHCR24, would determine if DHCR24 translational applications are feasible for development. DHCR24's utility as a biomarker for early atherosclerosis or insulin resistance development would be limited due to the invasive nature of obtaining sample. Further, DHCR24 levels may vary significantly between patients (see DHCR24 as a biomarker Section 1.10.2), making changes difficult to detect. Therefore DHCR24's main potential translational application would be to develop a mimetic to restore or increase DHCR24 levels in specific tissues to abrogate the inflammatory responses that drive endothelial and/or hepatic cell inflammatory diseases and disorders. However, further basic science research is required to further elucidate DHCR24's mechanisms and effects, in addition to *in vivo* studies before development of downstream therapeutic applications can be considered.

Together, the results presented in this study strongly propose the potential for DHCR24 to be used as the foundation for a therapeutic agent against endothelial and hepatic inflammation - a previously unexplored potential therapeutic approach. The data also extends general science building upon the current literature revealing the mechanisms for DHCR24's suppression of a TNF-α-induced inflammatory response in HCAECs and HuH7 cells. More work is now required, to elucidate in further detail these mechanisms, and to discover further roles for DHCR24 in

HCAECs and HuH7 cells. The results from this study are novel and highlight that the development of DHCR24 or DHCR24 oxidoreductase site-derived mimetics to prevent or treat the onset of inflammatory disorders driven by endothelial cell and hepatic inflammation, is promising.

Chapter 8 – References

1. McGrath, K.C., X.H. Li, R. Puranik, E.C. Liong, J.T. Tan, V.M. Dy, B.A. DiBartolo, P.J. Barter, K.A. Rye, and A.K. Heather, *Role of 3beta-hydroxysteroid-delta 24 reductase in mediating antiinflammatory effects of high-density lipoproteins in endothelial cells.* Arterioscler Thromb Vasc Biol, 2009. **29**(6): p. 877-82.
2. Glass, C.K. and J.L. Witztum, *Atherosclerosis. the road ahead.* Cell, 2001. **104**(4): p. 503-16.
3. Castelli, W.P., R.J. Garrison, P.W. Wilson, R.D. Abbott, S. Kalousdian, and W.B. Kannel, *Incidence of coronary heart disease and lipoprotein cholesterol levels. The Framingham Study.* JAMA, 1986. **256**(20): p. 2835-8.
4. Berry, J.D., A. Dyer, X. Cai, D.B. Garside, H. Ning, A. Thomas, P. Greenland, L. Van Horn, R.P. Tracy, and D.M. Lloyd-Jones, *Lifetime Risks of Cardiovascular Disease.* New England Journal of Medicine, 2012. **366**(4): p. 321-329.
5. Avery, C.L., L.R. Loehr, C. Baggett, P.P. Chang, A.M. Kucharska-Newton, K. Matsushita, W.D. Rosamond, and G. Heiss, *The Population Burden of Heart Failure Attributable to Modifiable Risk Factors: The ARIC (Atherosclerosis Risk in Communities) Study.* Journal of the American College of Cardiology, 2012. **60**(17): p. 1640-1646.
6. Yusuf, S., S. Hawken, S. Ôunpuu, T. Dans, A. Avezum, F. Lanas, M. McQueen, A. Budaj, P. Pais, J. Varigos, and L. Lisheng, *Effect of potentially modifiable risk factors associated with myocardial infarction in 52 countries (the INTERHEART study): case-control study.* The Lancet, 2004. **364**(9438): p. 937-952.
7. Ross, R., *Atherosclerosis--an inflammatory disease.* N Engl J Med, 1999. **340**(2): p. 115-26.
8. Bai, N., T. Kido, H. Suzuki, G. Yang, T.J. Kavanagh, J.D. Kaufman, M.E. Rosenfeld, C. van Breemen, and S.F.v. Eeden, *Changes in atherosclerotic plaques induced by inhalation of diesel exhaust.* Atherosclerosis, 2011. **216**(2): p. 299-306.
9. Leon-Latre, M., B. Moreno-Franco, E.M. Andres-Esteban, M. Ledesma, M. Laclaustra, V. Alcalde, J.L. Penalvo, J.M. Ordovas, J.A. Casasnovas, and i. Aragon Workers' Health Study, *Sedentary lifestyle and its relation to cardiovascular risk factors, insulin resistance and inflammatory profile.* Rev Esp Cardiol (Engl Ed), 2014. **67**(6): p. 449-55.
10. Fujii, C. and H. Sakakibara, *Association between insulin resistance, cardiovascular risk factors and overweight in Japanese schoolchildren.* Obes Res Clin Pract, 2012. **6**(1): p. e1-e90.
11. Won, S., R.A. Hong, R.V. Shohet, T.B. Seto, and N.I. Parikh, *Methamphetamine-associated cardiomyopathy.* Clin Cardiol, 2013. **36**(12): p. 737-42.
12. Lambert, G., *Depression, the bete noire of cardiology?* Mol Psychiatry, 2002. **7**(1): p. 17.
13. Hubert, H.B., M. Feinleib, P.M. McNamara, and W.P. Castelli, *Obesity as an independent risk factor for cardiovascular disease: a 26-year follow-up of participants in the Framingham Heart Study.* Circulation, 1983. **67**(5): p. 968-77.
14. Kim, K.S., W.L. Owen, D. Williams, and L.L. Adams-Campbell, *A comparison between BMI and Conicity index on predicting coronary heart disease: the Framingham Heart Study.* Ann Epidemiol, 2000. **10**(7): p. 424-31.
15. Kim, J.H., J.J. Cho, and Y.S. Park, *Relationship between sarcopenic obesity and cardiovascular disease risk as estimated by the Framingham risk score.* J Korean Med Sci, 2015. **30**(3): p. 264-71.
16. Grundy, S.M., *Atherosclerosis imaging and the future of lipid management.* Circulation, 2004. **110**(23): p. 3509-11.

17. Davies, P.F. and S.C. Tripathi, *Mechanical stress mechanisms and the cell. An endothelial paradigm.* Circ Res, 1993. **72**(2): p. 239-45.
18. Stocker, R. and J.F. Keaney, Jr., *Role of oxidative modifications in atherosclerosis.* Physiol Rev, 2004. **84**(4): p. 1381-478.
19. Ross, R., *The pathogenesis of atherosclerosis: a perspective for the 1990s.* Nature, 1993. **362**(6423): p. 801-9.
20. Ross, R. and J.A. Glomset, *Atherosclerosis and the arterial smooth muscle cell: Proliferation of smooth muscle is a key event in the genesis of the lesions of atherosclerosis.* Science, 1973. **180**(4093): p. 1332-9.
21. American Diabetes, A., *Diagnosis and classification of diabetes mellitus.* Diabetes Care, 2008. **31 Suppl 1**: p. S55-60.
22. American Diabetes, A., *(2) Classification and diagnosis of diabetes.* Diabetes Care, 2015. **38 Suppl**: p. S8-S16.
23. Inzucchi, S.E., *Diagnosis of diabetes.* N Engl J Med, 2013. **368**(2): p. 193.
24. Mortel, K.F., J.S. Meyer, P.A. Sims, and K. McClintic, *Diabetes mellitus as a risk factor for stroke.* South Med J, 1990. **83**(8): p. 904-11.
25. Hayden, M.R. and S.C. Tyagi, *Intimal redox stress: Accelerated atherosclerosis in metabolic syndrome and type 2 diabetes mellitus. Atheroscleropathy.* Cardiovascular Diabetology, 2002. **1**(1): p. 1-27.
26. Huxley, R., A. Ansary-Moghaddam, A. Berrington de Gonzalez, F. Barzi, and M. Woodward, *Type-II diabetes and pancreatic cancer: a meta-analysis of 36 studies.* Br J Cancer, 2005. **92**(11): p. 2076-2083.
27. Chari, S.T., C.L. Leibson, K.G. Rabe, L.J. Timmons, J. Ransom, M. de Andrade, and G.M. Petersen, *Pancreatic Cancer–Associated Diabetes Mellitus: Prevalence and Temporal Association With Diagnosis of Cancer.* Gastroenterology, 2008. **134**(1): p. 95-101.
28. Boulton, A.J.M., A.I. Vinik, J.C. Arezzo, V. Bril, E.L. Feldman, R. Freeman, R.A. Malik, R.E. Maser, J.M. Sosenko, and D. Ziegler, *Diabetic Neuropathies.* A statement by the American Diabetes Association, 2005. **28**(4): p. 956-962.
29. Martin, C.L., J.W. Albers, and R. Pop-Busui, *Neuropathy and Related Findings in the Diabetes Control and Complications Trial/Epidemiology of Diabetes Interventions and Complications Study.* Diabetes Care, 2014. **37**(1): p. 31-38.
30. Haffner, S.M., S. Lehto, T. Ronnemaa, K. Pyorala, and M. Laakso, *Mortality from coronary heart disease in subjects with type 2 diabetes and in nondiabetic subjects with and without prior myocardial infarction.* N Engl J Med, 1998. **339**.
31. Ritz, E., I. Rychlík, F. Locatelli, and S. Halimi, *End-stage renal failure in type 2 diabetes: A medical catastrophe of worldwide dimensions.* American Journal of Kidney Diseases, 1999. **34**(5): p. 795-808.
32. King, H., R.E. Aubert, and W.H. Herman, *Global Burden of Diabetes, 1995–2025: Prevalence, numerical estimates, and projections.* Diabetes Care, 1998. **21**(9): p. 1414-1431.
33. Zimmet, P., K.G. Alberti, and J. Shaw, *Global and societal implications of the diabetes epidemic.* Nature, 2001. **414**(6865): p. 782-7.
34. Wild, S., G. Roglic, A. Green, R. Sicree, and H. King, *Global prevalence of diabetes. Estimates for the year 2000 and projections for 2030.* Diabetes Care, 2004. **27**.
35. Wild, S., G. Roglic, A. Green, R. Sicree, and H. King, *Global Prevalence of Diabetes.* Estimates for the year 2000 and projections for 2030, 2004. **27**(5): p. 1047-1053.
36. Fox, C.S., S. Coady, P.D. Sorlie, R.B. D'Agostino, Sr., M.J. Pencina, R.S. Vasan, J.B. Meigs, D. Levy, and P.J. Savage, *Increasing cardiovascular disease burden due to diabetes mellitus: the Framingham Heart Study.* Circulation, 2007. **115**(12): p. 1544-50.

37. Zaccardi, F., D.R. Webb, T. Yates, and M.J. Davies, *Pathophysiology of type 1 and type 2 diabetes mellitus: a 90-year perspective.* Postgrad Med J, 2016. **92**(1084): p. 63-9.
38. Hu , F.B., J.E. Manson , M.J. Stampfer , G. Colditz , S. Liu , C.G. Solomon , and W.C. Willett *Diet, Lifestyle, and the Risk of Type 2 Diabetes Mellitus in Women.* New England Journal of Medicine, 2001. **345**(11): p. 790-797.
39. Mollica, M.P., L. Lionetti, R. Putti, G. Cavaliere, M. Gaita, and A. Barletta, *From chronic overfeeding to hepatic injury: role of endoplasmic reticulum stress and inflammation.* Nutr Metab Cardiovasc Dis, 2011. **21**(3): p. 222-30.
40. Sese, M.A., D. Jimenez-Pavon, C.C. Gilbert, M. Gonzalez-Gross, F. Gottrand, S. de Henauw, C. Breidenassel, J. Warnberg, K. Widhalm, D. Molnar, Y. Manios, M. Cuenca-Garcia, A. Kafatos, L.A. Moreno, and H.S. Group, *Eating behaviour, insulin resistance and cluster of metabolic risk factors in European adolescents. The HELENA study.* Appetite, 2012. **59**(1): p. 140-7.
41. Alexander, K.E., E.E. Ventura, D. Spruijt-Metz, M.J. Weigensberg, M.I. Goran, and J.N. Davis, *Association of breakfast skipping with visceral fat and insulin indices in overweight Latino youth.* Obesity (Silver Spring), 2009. **17**(8): p. 1528-33.
42. Li, Y., H. Zhang, C. Jiang, M. Xu, Y. Pang, J. Feng, X. Xiang, W. Kong, G. Xu, Y. Li, and X. Wang, *Hyperhomocysteinemia promotes insulin resistance by inducing endoplasmic reticulum stress in adipose tissue.* J Biol Chem, 2013. **288**(14): p. 9583-92.
43. Chen, M., R.N. Bergman, G. Pacini, and J. D. Porte, *Pathogenesis of Age-Related Glucose Intolerance in Man: Insulin Resistance and Decreased β-Cell Function.* The Journal of Clinical Endocrinology & Metabolism, 1985. **60**(1): p. 13-20.
44. Facchini, F.S., N. Hua, F. Abbasi, and G.M. Reaven, *Insulin Resistance as a Predictor of Age-Related Diseases.* The Journal of Clinical Endocrinology & Metabolism, 2001. **86**(8): p. 3574-3578.
45. Moran, A., D.R. Jacobs, J. Steinberger, L.M. Steffen, J.S. Pankow, C.-P. Hong, and A.R. Sinaiko, *Changes in Insulin Resistance and Cardiovascular Risk During Adolescence.* Establishment of Differential Risk in Males and Females, 2008. **117**(18): p. 2361-2368.
46. Ding, E.L., Y. Song, V.S. Malik, and S. Liu, *Sex differences of endogenous sex hormones and risk of type 2 diabetes: A systematic review and meta-analysis.* JAMA, 2006. **295**(11): p. 1288-1299.
47. Martos, R., M. Valle, R. Morales, R. Cañete, M.I. Gavilan, and V. Sánchez-Margalet, *Hyperhomocysteinemia correlates with insulin resistance and low-grade systemic inflammation in obese prepubertal children.* Metabolism, 2006. **55**(1): p. 72-77.
48. Ford, E.S., W.H. Giles, and A.H. Mokdad, *Increasing Prevalence of the Metabolic Syndrome Among U.S. Adults.* Diabetes Care, 2004. **27**(10): p. 2444-2449.
49. Mokdad, A.H., B.A. Bowman, E.S. Ford, F. Vinicor, J.S. Marks, and J.P. Koplan, *THe continuing epidemics of obesity and diabetes in the united states.* JAMA, 2001. **286**(10): p. 1195-1200.
50. Mokdad, A.H., E.S. Ford, B.A. Bowman, and et al., *PRevalence of obesity, diabetes, and obesity-related health risk factors, 2001.* JAMA, 2003. **289**(1): p. 76-79.
51. Muscelli, E., G. Mingrone, S. Camastra, M. Manco, J.A. Pereira, J.C. Pareja, and E. Ferrannini, *Differential effect of weight loss on insulin resistance in surgically treated obese patients.* Am J Med, 2005. **118**(1): p. 51-7.
52. Wicksteed, B., C. Alarcon, I. Briaud, M.K. Lingohr, and C.J. Rhodes, *Glucose-induced translational control of proinsulin biosynthesis is proportional to preproinsulin mRNA levels in islet beta-cells but not regulated via a positive feedback of secreted insulin.* J Biol Chem, 2003. **278**(43): p. 42080-90.

53. Polonsky, K.S., B.D. Given, L. Hirsch, E.T. Shapiro, H. Tillil, C. Beebe, J.A. Galloway, B.H. Frank, T. Karrison, and E. Van Cauter, *Quantitative study of insulin secretion and clearance in normal and obese subjects.* J Clin Invest, 1988. **81**(2): p. 435-41.
54. Seidell, J.C., *Obesity, insulin resistance and diabetes--a worldwide epidemic.* Br J Nutr, 2000. **83 Suppl 1**: p. S5-8.
55. Sturm, R., J.S. Ringel, and T. Andreyeva, *Increasing Obesity Rates And Disability Trends.* Health Affairs, 2004. **23**(2): p. 199-205.
56. Mingrone , G., S. Panunzi , A. De Gaetano , C. Guidone , A. Iaconelli , L. Leccesi , G. Nanni , A. Pomp , M. Castagneto , G. Ghirlanda , and F. Rubino *Bariatric Surgery versus Conventional Medical Therapy for Type 2 Diabetes.* New England Journal of Medicine, 2012. **366**(17): p. 1577-1585.
57. George, S., J.J. Rochford, C. Wolfrum, S.L. Gray, S. Schinner, J.C. Wilson, M.A. Soos, P.R. Murgatroyd, R.M. Williams, C.L. Acerini, D.B. Dunger, D. Barford, A.M. Umpleby, N.J. Wareham, H.A. Davies, A.J. Schafer, M. Stoffel, S. O'Rahilly, and I. Barroso, *A Family with Severe Insulin Resistance and Diabetes Due to a Mutation in AKT2.* Science, 2004. **304**(5675): p. 1325-1328.
58. Matthews, D.R., C.A. Cull, I.M. Stratton, R.R. Holman, and R.C. Turner, *UKPDS 26: Sulphonylurea failure in non-insulin-dependent diabetic patients over six years. UK Prospective Diabetes Study (UKPDS) Group.* Diabet Med, 1998. **15**(4): p. 297-303.
59. Holman, R.R., *Assessing the potential for α-glucosidase inhibitors in prediabetic states.* Diabetes Research and Clinical Practice, 1998. **40, Supplement 1**: p. S21-S25.
60. Cai, D., M. Yuan, D.F. Frantz, P.A. Melendez, L. Hansen, J. Lee, and S.E. Shoelson, *Local and systemic insulin resistance resulting from hepatic activation of IKK-beta and NF-kappaB.* Nat Med, 2005. **11**(2): p. 183-90.
61. Arkan, M.C., A.L. Hevener, F.R. Greten, S. Maeda, Z.W. Li, J.M. Long, A. Wynshaw-Boris, G. Poli, J. Olefsky, and M. Karin, *IKK-beta links inflammation to obesity-induced insulin resistance.* Nat Med, 2005. **11**(2): p. 191-8.
62. Shoelson, S.E., J. Lee, and M. Yuan, *Inflammation and the IKK beta/I kappa B/NF-kappa B axis in obesity- and diet-induced insulin resistance.* Int J Obes Relat Metab Disord, 2003. **27 Suppl 3**: p. S49-52.
63. Knoch, K.P., H. Bergert, B. Borgonovo, H.D. Saeger, A. Altkruger, P. Verkade, and M. Solimena, *Polypyrimidine tract-binding protein promotes insulin secretory granule biogenesis.* Nat Cell Biol, 2004. **6**(3): p. 207-14.
64. Tillmar, L., C. Carlsson, and N. Welsh, *Control of insulin mRNA stability in rat pancreatic islets. Regulatory role of a 3'-untranslated region pyrimidine-rich sequence.* J Biol Chem, 2002. **277**(2): p. 1099-106.
65. Kloppel, G., M. Lohr, K. Habich, M. Oberholzer, and P.U. Heitz, *Islet pathology and the pathogenesis of type 1 and type 2 diabetes mellitus revisited.* Surv Synth Pathol Res, 1985. **4**(2): p. 110-25.
66. Yoon, K.H., S.H. Ko, J.H. Cho, J.M. Lee, Y.B. Ahn, K.H. Song, S.J. Yoo, M.I. Kang, B.Y. Cha, K.W. Lee, H.Y. Son, S.K. Kang, H.S. Kim, I.K. Lee, and S. Bonner-Weir, *Selective β-Cell Loss and α-Cell Expansion in Patients with Type 2 Diabetes Mellitus in Korea.* The Journal of Clinical Endocrinology & Metabolism, 2003. **88**(5): p. 2300-2308.
67. Butler, A.E., J. Janson, S. Bonner-Weir, R. Ritzel, R.A. Rizza, and P.C. Butler, *β-Cell Deficit and Increased β-Cell Apoptosis in Humans With Type 2 Diabetes.* Diabetes, 2003. **52**(1): p. 102-110.
68. Martin, C., K.S. Desai, and G. Steiner, *Receptor and postreceptor insulin resistance induced by in vivo hyperinsuiinemia.* Canadian Journal of Physiology and Pharmacology, 1983. **61**(8): p. 802-807.

69. Leibowitz, G., G. Üçkaya, A.I. Oprescu, E. Cerasi, D.J. Gross, and N. Kaiser, *Glucose-Regulated Proinsulin Gene Expression Is Required for Adequate Insulin Production during Chronic Glucose Exposure.* Endocrinology, 2002. **143**(9): p. 3214-3220.
70. Reaven, G.M., *Role of Insulin Resistance in Human Disease.* Diabetes, 1988. **37**(12): p. 1595-1607.
71. Sonmez, B., B. Bozkurt, A. Atmaca, M. Irkec, M. Orhan, and U. Aslan, *Effect of Glycemic Control on Refractive Changes in Diabetic Patients With Hyperglycemia.* Cornea, 2005. **24**(5): p. 531-537.
72. Nakamura, M., A. Kanamori, and A. Negi, *Diabetes mellitus as a risk factor for glaucomatous optic neuropathy.* Ophthalmologica, 2005. **219**(1): p. 1-10.
73. Mitchell, P., W. Smith, T. Chey, and P.R. Healey, *Open-angle glaucoma and diabetes: the Blue Mountains eye study, Australia.* Ophthalmology, 1997. **104**(4): p. 712-8.
74. Kramer, H.J., Q. Nguyen, G. Curhan, and C. Hsu, *REnal insufficiency in the absence of albuminuria and retinopathy among adults with type 2 diabetes mellitus.* JAMA, 2003. **289**(24): p. 3273-3277.
75. Smith, L.L., S.P. Burnet, and J.D. McNeil, *Musculoskeletal manifestations of diabetes mellitus.* Br J Sports Med, 2003. **37**(1): p. 30-5.
76. Fowler, M.J., *Microvascular and Macrovascular Complications of Diabetes.* Clinical Diabetes, 2008. **26**(2): p. 77-82.
77. Janghorbani, M., R.M. Van Dam, W.C. Willett, and F.B. Hu, *Systematic review of type 1 and type 2 diabetes mellitus and risk of fracture.* Am J Epidemiol, 2007. **166**(5): p. 495-505.
78. Danaei, G., M.M. Finucane, Y. Lu, G.M. Singh, M.J. Cowan, C.J. Paciorek, J.K. Lin, F. Farzadfar, Y.H. Khang, G.A. Stevens, M. Rao, M.K. Ali, L.M. Riley, C.A. Robinson, M. Ezzati, and G. Global Burden of Metabolic Risk Factors of Chronic Diseases Collaborating, *National, regional, and global trends in fasting plasma glucose and diabetes prevalence since 1980: systematic analysis of health examination surveys and epidemiological studies with 370 country-years and 2.7 million participants.* Lancet, 2011. **378**(9785): p. 31-40.
79. Özcan, U., E. Yilmaz, L. Özcan, M. Furuhashi, E. Vaillancourt, R.O. Smith, C.Z. Görgün, and G.S. Hotamisligil, *Chemical Chaperones Reduce ER Stress and Restore Glucose Homeostasis in a Mouse Model of Type 2 Diabetes.* Science, 2006. **313**(5790): p. 1137-1140.
80. Ozcan, U., Q. Cao, E. Yilmaz, A.H. Lee, N.N. Iwakoshi, E. Ozdelen, G. Tuncman, C. Gorgun, L.H. Glimcher, and G.S. Hotamisligil, *Endoplasmic reticulum stress links obesity, insulin action, and type 2 diabetes.* Science, 2004. **306**(5695): p. 457-61.
81. Medzhitov, R., *Origin and physiological roles of inflammation.* Nature, 2008. **454**(7203): p. 428-35.
82. Coussens, L.M. and Z. Werb, *Inflammation and cancer.* Nature, 2002. **420**(6917): p. 860-867.
83. Ross, R., *Atherosclerosis — An Inflammatory Disease.* New England Journal of Medicine, 1999. **340**(2): p. 115-126.
84. Shoelson, S.E., J. Lee, and A.B. Goldfine, *Inflammation and insulin resistance.* J Clin Invest, 2006. **116**(7): p. 1793-801.
85. Maeda, S., L. Chang, Z.W. Li, J.L. Luo, H. Leffert, and M. Karin, *IKKbeta is required for prevention of apoptosis mediated by cell-bound but not by circulating TNFalpha.* Immunity, 2003. **19**(5): p. 725-37.
86. Zhang, K. and R.J. Kaufman, *From endoplasmic-reticulum stress to the inflammatory response.* Nature, 2008. **454**(7203): p. 455-62.

87. Gilmore, T. and M. Herscovitch, *Inhibitors of NF-κB signaling: 785 and counting.* Oncogene, 2006. **25**(51): p. 6887-6899.
88. Libby, P., *Inflammation in atherosclerosis.* Nature, 2002. **420**(6917): p. 868-74.
89. Berliner, J.A. and J.W. Heinecke, *The role of oxidized lipoproteins in atherogenesis.* Free Radical Biology and Medicine, 1996. **20**(5): p. 707-727.
90. Nigro, J., N. Osman, A.M. Dart, and P.J. Little, *Insulin resistance and atherosclerosis.* Endocr Rev, 2006. **27**(3): p. 242-59.
91. Davies, P.F., A. Robotewskyj, M.L. Griem, R.O. Dull, and D.C. Polacek, *Hemodynamic forces and vascular cell communication in arteries.* Arch Pathol Lab Med, 1992. **116**(12): p. 1301-6.
92. Fry, D.L., E.E. Herderick, and D.K. Johnson, *Local intimal-medial uptakes of 125I-albumin, 125I-LDL, and parenteral Evans blue dye protein complex along the aortas of normocholesterolemic minipigs as predictors of subsequent hypercholesterolemic atherogenesis.* Arterioscler Thromb, 1993. **13**(8): p. 1193-204.
93. Stary, H.C., *Composition and classification of human atherosclerotic lesions.* Virchows Arch A Pathol Anat Histopathol, 1992. **421**(4): p. 277-90.
94. van der Wal, A.C., P.K. Das, A.J. Tigges, and A.E. Becker, *Adhesion molecules on the endothelium and mononuclear cells in human atherosclerotic lesions.* Am J Pathol, 1992. **141**(6): p. 1427-33.
95. Poston, R.N., D.O. Haskard, J.R. Coucher, N.P. Gall, and R.R. Johnson-Tidey, *Expression of intercellular adhesion molecule-1 in atherosclerotic plaques.* Am J Pathol, 1992. **140**(3): p. 665-73.
96. Wood, K.M., M.D. Cadogan, A.L. Ramshaw, and D.V. Parums, *The distribution of adhesion molecules in human atherosclerosis.* Histopathology, 1993. **22**(5): p. 437-44.
97. Butcher, E.C., *Leukocyte-endothelial cell recognition: three (or more) steps to specificity and diversity.* Cell, 1991. **67**(6): p. 1033-6.
98. Springer, T.A., *Traffic signals for lymphocyte recirculation and leukocyte emigration: the multistep paradigm.* Cell, 1994. **76**(2): p. 301-14.
99. Huo, Y., A. Hafezi-Moghadam, and K. Ley, *Role of vascular cell adhesion molecule-1 and fibronectin connecting segment-1 in monocyte rolling and adhesion on early atherosclerotic lesions.* Circ Res, 2000. **87**(2): p. 153-9.
100. Ley, K. and Y. Huo, *VCAM-1 is critical in atherosclerosis.* The Journal of Clinical Investigation, 2001. **107**(10): p. 1209-1210.
101. Ramos, C.L., Y. Huo, U. Jung, S. Ghosh, D.R. Manka, I.J. Sarembock, and K. Ley, *Direct Demonstration of P-Selectin– and VCAM-1–Dependent Mononuclear Cell Rolling in Early Atherosclerotic Lesions of Apolipoprotein E–Deficient Mice.* Circulation Research, 1999. **84**(11): p. 1237-1244.
102. Cushing, S.D., J.A. Berliner, A.J. Valente, M.C. Territo, M. Navab, F. Parhami, R. Gerrity, C.J. Schwartz, and A.M. Fogelman, *Minimally modified low density lipoprotein induces monocyte chemotactic protein 1 in human endothelial cells and smooth muscle cells.* Proc Natl Acad Sci U S A, 1990. **87**(13): p. 5134-8.
103. Rajavashisth, T.B., A. Andalibi, M.C. Territo, J.A. Berliner, M. Navab, A.M. Fogelman, and A.J. Lusis, *Induction of endothelial cell expression of granulocyte and macrophage colony-stimulating factors by modified low-density lipoproteins.* Nature, 1990. **344**(6263): p. 254-7.
104. Beekhuizen, H. and R. van Furth, *Monocyte adherence to human vascular endothelium.* J Leukoc Biol, 1993. **54**(4): p. 363-78.
105. Weissberg, P.L., *Atherogenesis: current understanding of the causes of atheroma.* Heart, 2000. **83**(2): p. 247-52.

106. Fogelman, A.M., M.E. Haberland, J. Seager, M. Hokom, and P.A. Edwards, *Factors regulating the activities of the low density lipoprotein receptor and the scavenger receptor on human monocyte-macrophages.* J Lipid Res, 1981. **22**(7): p. 1131-41.
107. Quinn, M.T., S. Parthasarathy, L.G. Fong, and D. Steinberg, *Oxidatively modified low density lipoproteins: a potential role in recruitment and retention of monocyte/macrophages during atherogenesis.* Proc Natl Acad Sci U S A, 1987. **84**(9): p. 2995-8.
108. Steinberg, D., S. Parthasarathy, T.E. Carew, J.C. Khoo, and J.L. Witztum, *Beyond cholesterol. Modifications of low-density lipoprotein that increase its atherogenicity.* N Engl J Med, 1989. **320**(14): p. 915-24.
109. Ross, R., *Atherosclerosis is an inflammatory disease.* Am Heart J, 1999. **138**(5 Pt 2): p. S419-20.
110. Morla, A.O. and J.E. Mogford, *Control of smooth muscle cell proliferation and phenotype by integrin signaling through focal adhesion kinase.* Biochem Biophys Res Commun, 2000. **272**(1): p. 298-302.
111. Thyberg, J., *Differentiated properties and proliferation of arterial smooth muscle cells in culture.* Int Rev Cytol, 1996. **169**: p. 183-265.
112. Grainger, D.J., C.M. Witchell, P.L. Weissberg, and J.C. Metcalfe, *Mitogens for adult rat aortic vascular smooth muscle cells in serum-free primary culture.* Cardiovasc Res, 1994. **28**(8): p. 1238-42.
113. Jawien, A., D.F. Bowen-Pope, V. Lindner, S.M. Schwartz, and A.W. Clowes, *Platelet-derived growth factor promotes smooth muscle migration and intimal thickening in a rat model of balloon angioplasty.* J Clin Invest, 1992. **89**(2): p. 507-11.
114. Stary, H.C., *Changes in components and structure of atherosclerotic lesions developing from childhood to middle age in coronary arteries.* Basic Res Cardiol, 1994. **89 Suppl 1**: p. 17-32.
115. Akima, T., K. Nakanishi, K. Suzuki, M. Katayama, F. Ohsuzu, and T. Kawai, *Soluble elastin decreases in the progress of atheroma formation in human aorta.* Circ J, 2009. **73**(11): p. 2154-62.
116. Davies, M.J., *A macro and micro view of coronary vascular insult in ischemic heart disease.* Circulation, 1990. **82**(3 Suppl): p. II38-46.
117. Williams, K.J. and I. Tabas, *The Response-to-Retention Hypothesis of Early Atherogenesis.* Arteriosclerosis, Thrombosis, and Vascular Biology, 1995. **15**(5): p. 551-561.
118. Skalen, K., M. Gustafsson, E.K. Rydberg, L.M. Hulten, O. Wiklund, T.L. Innerarity, and J. Boren, *Subendothelial retention of atherogenic lipoproteins in early atherosclerosis.* Nature, 2002. **417**(6890): p. 750-754.
119. Srinivasan, S.R., P. Vijayagopal, E.R. Dalferes, Jr., B. Abbate, B. Radhakrishnamurthy, and G.S. Berenson, *Low density lipoprotein retention by aortic tissue. Contribution of extracellular matrix.* Atherosclerosis, 1986. **62**(3): p. 201-8.
120. Schwenke, D.C. and T.E. Carew, *Initiation of atherosclerotic lesions in cholesterol-fed rabbits. II. Selective retention of LDL vs. selective increases in LDL permeability in susceptible sites of arteries.* Arteriosclerosis, 1989. **9**(6): p. 908-18.
121. Ismail, N.A., M.Z. Alavi, and S. Moore, *Lipoprotein-proteoglycan complexes from injured rabbit aortas accelerate lipoprotein uptake by arterial smooth muscle cells.* Atherosclerosis, 1994. **105**(1): p. 79-87.
122. Vijayagopal, P., S.R. Srinivasan, B. Radhakrishnamurthy, and G.S. Berenson, *Lipoprotein-proteoglycan complexes from atherosclerotic lesions promote cholesteryl ester accumulation in human monocytes/macrophages.* Arterioscler Thromb, 1992. **12**(2): p. 237-49.

123. Hurt, E., G. Bondjers, and G. Camejo, *Interaction of LDL with human arterial proteoglycans stimulates its uptake by human monocyte-derived macrophages.* J Lipid Res, 1990. **31**(3): p. 443-54.
124. Riserus, U., W.C. Willett, and F.B. Hu, *Dietary fats and prevention of type 2 diabetes.* Prog Lipid Res, 2009. **48**(1): p. 44-51.
125. Miwa, I., N. Ichimura, M. Sugiura, Y. Hamada, and S. Taniguchi, *Inhibition of glucose-induced insulin secretion by 4-hydroxy-2-nonenal and other lipid peroxidation products.* Endocrinology, 2000. **141**(8): p. 2767-72.
126. Richardson, M., S.J. Hadcock, M. DeReske, and M.I. Cybulsky, *Increased expression in vivo of VCAM-1 and E-selectin by the aortic endothelium of normolipemic and hyperlipemic diabetic rabbits.* Arterioscler Thromb, 1994. **14**(5): p. 760-9.
127. Ceriello, A., L. Quagliaro, L. Piconi, R. Assaloni, R. Da Ros, A. Maier, K. Esposito, and D. Giugliano, *Effect of Postprandial Hypertriglyceridemia and Hyperglycemia on Circulating Adhesion Molecules and Oxidative Stress Generation and the Possible Role of Simvastatin Treatment.* Diabetes, 2004. **53**(3): p. 701-710.
128. Piconi, L., L. Quagliaro, R. Da Ros, R. Assaloni, D. Giugliano, K. Esposito, C. Szabo, and A. Ceriello, *Intermittent high glucose enhances ICAM-1, VCAM-1, E-selectin and interleukin-6 expression in human umbilical endothelial cells in culture: the role of poly(ADP-ribose) polymerase.* J Thromb Haemost, 2004. **2**(8): p. 1453-9.
129. Quagliaro, L., L. Piconi, R. Assaloni, R. Da Ros, A. Maier, G. Zuodar, and A. Ceriello, *Intermittent high glucose enhances ICAM-1, VCAM-1 and E-selectin expression in human umbilical vein endothelial cells in culture: The distinct role of protein kinase C and mitochondrial superoxide production.* Atherosclerosis, 2005. **183**(2): p. 259-267.
130. Haubner, F., K. Lehle, D. Münzel, C. Schmid, D.E. Birnbaum, and J.G. Preuner, *Hyperglycemia increases the levels of vascular cellular adhesion molecule-1 and monocyte-chemoattractant-protein-1 in the diabetic endothelial cell.* Biochemical and Biophysical Research Communications, 2007. **360**(3): p. 560-565.
131. Gustavsson, C., C.-D. Agardh, A.V. Zetterqvist, J. Nilsson, E. Agardh, and M.F. Gomez, *Vascular Cellular Adhesion Molecule-1 (VCAM-1) Expression in Mice Retinal Vessels Is Affected by Both Hyperglycemia and Hyperlipidemia.* PLoS ONE, 2010. **5**(9): p. e12699.
132. Hotamisligil, G.S., N.S. Shargill, and B.M. Spiegelman, *Adipose expression of tumor necrosis factor-alpha: direct role in obesity-linked insulin resistance.* Science, 1993. **259**(5091): p. 87-91.
133. Hamann, A., H. Benecke, Y. Le Marchand-Brustel, V.S. Susulic, B.B. Lowell, and J.S. Flier, *Characterization of insulin resistance and NIDDM in transgenic mice with reduced brown fat.* Diabetes, 1995. **44**(11): p. 1266-73.
134. Uysal, K.T., S.M. Wiesbrock, M.W. Marino, and G.S. Hotamisligil, *Protection from obesity-induced insulin resistance in mice lacking TNF-alpha function.* Nature, 1997. **389**(6651): p. 610-4.
135. Schroder, M., *Endoplasmic reticulum stress responses.* Cell Mol Life Sci, 2008. **65**(6): p. 862-94.
136. Ou, W.-J., J.J.M. Bergeron, Y. Li, C.Y. Kang, and D.Y. Thomas, *Conformational Changes Induced in the Endoplasmic Reticulum Luminal Domain of Calnexin by Mg-ATP and Ca.* Journal of Biological Chemistry, 1995. **270**(30): p. 18051-18059.
137. Vassilakos, A., M. Michalak, M.A. Lehrman, and D.B. Williams, *Oligosaccharide Binding Characteristics of the Molecular Chaperones Calnexin and Calreticulin†.* Biochemistry, 1998. **37**(10): p. 3480-3490.
138. Beckers, C.J. and W.E. Balch, *Calcium and GTP: essential components in vesicular trafficking between the endoplasmic reticulum and Golgi apparatus.* J Cell Biol, 1989. **108**(4): p. 1245-56.

139. Schmitt, H.D., M. Puzicha, and D. Gallwitz, *Study of a temperature-sensitive mutant of the ras-related YPT1 gene product in yeast suggests a role in the regulation of intracellular calcium.* Cell, 1988. **53**(4): p. 635-47.
140. Lu, X., Y. Li, J. Liu, X. Cao, X. Wang, D. Wang, H. Seo, and B. Gao, *The membrane topological analysis of 3beta-hydroxysteroid-Delta24 reductase (DHCR24) on endoplasmic reticulum.* J Mol Endocrinol, 2012. **48**(1): p. 1-9.
141. Suckling, K.E. and E.F. Stange, *Role of acyl-CoA: cholesterol acyltransferase in cellular cholesterol metabolism.* Journal of Lipid Research, 1985. **26**(6): p. 647-71.
142. Tabas, I., *Consequences of cellular cholesterol accumulation: basic concepts and physiological implications.* J Clin Invest, 2002. **110**(7): p. 905-11.
143. Kedi, X., Y. Ming, W. Yongping, Y. Yi, and Z. Xiaoxiang, *Free cholesterol overloading induced smooth muscle cells death and activated both ER- and mitochondrial-dependent death pathway.* Atherosclerosis, 2009. **207**(1): p. 123-130.
144. Bretscher, M.S. and S. Munro, *Cholesterol and the Golgi apparatus.* Science, 1993. **261**(5126): p. 1280-1.
145. Schröder, M. and R.J. Kaufman, *THE MAMMALIAN UNFOLDED PROTEIN RESPONSE.* Annual Review of Biochemistry, 2005. **74**(1): p. 739-789.
146. Tabas, I., *The role of endoplasmic reticulum stress in the progression of atherosclerosis.* Circ Res, 2010. **107**(7): p. 839-50.
147. Dorner, A.J., L.C. Wasley, and R.J. Kaufman, *Increased synthesis of secreted proteins induces expression of glucose-regulated proteins in butyrate-treated Chinese hamster ovary cells.* J Biol Chem, 1989. **264**(34): p. 20602-7.
148. Walter, P. and D. Ron, *The Unfolded Protein Response: From Stress Pathway to Homeostatic Regulation.* Science, 2011. **334**(6059): p. 1081-1086.
149. Kaufman, R.J., *Orchestrating the unfolded protein response in health and disease.* J Clin Invest, 2002. **110**(10): p. 1389-98.
150. Travers, K.J., C.K. Patil, L. Wodicka, D.J. Lockhart, J.S. Weissman, and P. Walter, *Functional and genomic analyses reveal an essential coordination between the unfolded protein response and ER-associated degradation.* Cell, 2000. **101**(3): p. 249-58.
151. Feng, B., P.M. Yao, Y. Li, C.M. Devlin, D. Zhang, H.P. Harding, M. Sweeney, J.X. Rong, G. Kuriakose, E.A. Fisher, A.R. Marks, D. Ron, and I. Tabas, *The endoplasmic reticulum is the site of cholesterol-induced cytotoxicity in macrophages.* Nat Cell Biol, 2003. **5**(9): p. 781-792.
152. Yao, P.M. and I. Tabas, *Free Cholesterol Loading of Macrophages Induces Apoptosis Involving the Fas Pathway.* Journal of Biological Chemistry, 2000. **275**(31): p. 23807-23813.
153. Wang, X.Z. and D. Ron, *Stress-induced phosphorylation and activation of the transcription factor CHOP (GADD153) by p38 MAP Kinase.* Science, 1996. **272**(5266): p. 1347-9.
154. Schindler, A.J. and R. Schekman, *In vitro reconstitution of ER-stress induced ATF6 transport in COPII vesicles.* Proc Natl Acad Sci U S A, 2009. **106**(42): p. 17775-80.
155. Oyadomari, S. and M. Mori, *Roles of CHOP/GADD153 in endoplasmic reticulum stress.* Cell Death Differ, 2004. **11**(4): p. 381-9.
156. Harding, H.P., I. Novoa, Y. Zhang, H. Zeng, R. Wek, M. Schapira, and D. Ron, *Regulated Translation Initiation Controls Stress-Induced Gene Expression in Mammalian Cells.* Molecular Cell, 2000. **6**(5): p. 1099-1108.
157. Haze, K., H. Yoshida, H. Yanagi, T. Yura, and K. Mori, *Mammalian Transcription Factor ATF6 Is Synthesized as a Transmembrane Protein and Activated by Proteolysis in*

Response to Endoplasmic Reticulum Stress. Molecular Biology of the Cell, 1999. **10**(11): p. 3787-3799.

158. Ye, J., R.B. Rawson, R. Komuro, X. Chen, U.P. Davé, R. Prywes, M.S. Brown, and J.L. Goldstein, *ER Stress Induces Cleavage of Membrane-Bound ATF6 by the Same Proteases that Process SREBPs.* Molecular Cell, 2000. **6**(6): p. 1355-1364.
159. van Huizen, R., J.L. Martindale, M. Gorospe, and N.J. Holbrook, *P58IPK, a novel endoplasmic reticulum stress-inducible protein and potential negative regulator of eIF2alpha signaling.* J Biol Chem, 2003. **278**(18): p. 15558-64.
160. Yoshida, H., T. Okada, K. Haze, H. Yanagi, T. Yura, M. Negishi, and K. Mori, *ATF6 Activated by Proteolysis Binds in the Presence of NF-Y (CBF) Directly to the cis-Acting Element Responsible for the Mammalian Unfolded Protein Response.* Molecular and Cellular Biology, 2000. **20**(18): p. 6755-6767.
161. Haze, K., T. Okada, H. Yoshida, H. Yanagi, T. Yura, M. Negishi, and K. Mori, *Identification of the G13 (cAMP-response-element-binding protein-related protein) gene product related to activating transcription factor 6 as a transcriptional activator of the mammalian unfolded protein response.* Biochem. J., 2001. **355**(1): p. 19-28.
162. Iwakoshi, N.N., M. Pypaert, and L.H. Glimcher, *The transcription factor XBP-1 is essential for the development and survival of dendritic cells.* J Exp Med, 2007. **204**(10): p. 2267-75.
163. Martinon, F., X. Chen, A.H. Lee, and L.H. Glimcher, *TLR activation of the transcription factor XBP1 regulates innate immune responses in macrophages.* Nat Immunol, 2010. **11**(5): p. 411-8.
164. Lin, J.H., H. Li, D. Yasumura, H.R. Cohen, C. Zhang, B. Panning, K.M. Shokat, M.M. LaVail, and P. Walter, *IRE1 Signaling Affects Cell Fate During the Unfolded Protein Response.* Science, 2007. **318**(5852): p. 944-949.
165. Thorp, E., G. Li, T.A. Seimon, G. Kuriakose, D. Ron, and I. Tabas, *Reduced apoptosis and plaque necrosis in advanced atherosclerotic lesions of Apoe-/- and Ldlr-/- mice lacking CHOP.* Cell Metab, 2009. **9**(5): p. 474-81.
166. Okada, T., H. Yoshida, R. Akazawa, M. Negishi, and K. Mori, *Distinct roles of activating transcription factor 6 (ATF6) and double-stranded RNA-activated protein kinase-like endoplasmic reticulum kinase (PERK) in transcription during the mammalian unfolded protein response.* Biochem. J., 2002. **366**(2): p. 585-594.
167. Ma, Y., J.W. Brewer, J.A. Diehl, and L.M. Hendershot, *Two distinct stress signaling pathways converge upon the CHOP promoter during the mammalian unfolded protein response.* J Mol Biol, 2002. **318**(5): p. 1351-65.
168. Yoshida, H., T. Matsui, A. Yamamoto, T. Okada, and K. Mori, *XBP1 mRNA is induced by ATF6 and spliced by IRE1 in response to ER stress to produce a highly active transcription factor.* Cell, 2001. **107**(7): p. 881-91.
169. Marciniak, S.J., C.Y. Yun, S. Oyadomari, I. Novoa, Y. Zhang, R. Jungreis, K. Nagata, H.P. Harding, and D. Ron, *CHOP induces death by promoting protein synthesis and oxidation in the stressed endoplasmic reticulum.* Genes Dev, 2004. **18**(24): p. 3066-77.
170. Li, G., M. Mongillo, K.-T. Chin, H. Harding, D. Ron, A.R. Marks, and I. Tabas, *Role of ERO1-α–mediated stimulation of inositol 1,4,5-triphosphate receptor activity in endoplasmic reticulum stress–induced apoptosis.* The Journal of Cell Biology, 2009. **186**(6): p. 783-792.
171. Timmins, J.M., L. Ozcan, T.A. Seimon, G. Li, C. Malagelada, J. Backs, T. Backs, R. Bassel-Duby, E.N. Olson, M.E. Anderson, and I. Tabas, *Calcium/calmodulin-dependent protein kinase II links ER stress with Fas and mitochondrial apoptosis pathways.* J Clin Invest, 2009. **119**(10): p. 2925-41.

172. Karst, A.M. and G. Li, *BH3-only proteins in tumorigenesis and malignant melanoma.* Cell Mol Life Sci, 2007. **64**(3): p. 318-30.
173. Hacker, G. and A. Weber, *BH3-only proteins trigger cytochrome c release, but how?* Arch Biochem Biophys, 2007. **462**(2): p. 150-5.
174. Puthalakath, H., L.A. O'Reilly, P. Gunn, L. Lee, P.N. Kelly, N.D. Huntington, P.D. Hughes, E.M. Michalak, J. McKimm-Breschkin, N. Motoyama, T. Gotoh, S. Akira, P. Bouillet, and A. Strasser, *ER stress triggers apoptosis by activating BH3-only protein Bim.* Cell, 2007. **129**(7): p. 1337-49.
175. Scorrano, L., S.A. Oakes, J.T. Opferman, E.H. Cheng, M.D. Sorcinelli, T. Pozzan, and S.J. Korsmeyer, *BAX and BAK regulation of endoplasmic reticulum Ca2+: a control point for apoptosis.* Science, 2003. **300**(5616): p. 135-9.
176. Zong, W.X., C. Li, G. Hatzivassiliou, T. Lindsten, Q.C. Yu, J. Yuan, and C.B. Thompson, *Bax and Bak can localize to the endoplasmic reticulum to initiate apoptosis.* J Cell Biol, 2003. **162**(1): p. 59-69.
177. Wang, S. and R.J. Kaufman, *The impact of the unfolded protein response on human disease.* The Journal of Cell Biology, 2012. **197**(7): p. 857-867.
178. Erbay, E., V.R. Babaev, J.R. Mayers, L. Makowski, K.N. Charles, M.E. Snitow, S. Fazio, M.M. Wiest, S.M. Watkins, M.F. Linton, and G.S. Hotamisligil, *Reducing endoplasmic reticulum stress through a macrophage lipid chaperone alleviates atherosclerosis.* Nat Med, 2009. **15**(12): p. 1383-1391.
179. Zeng, L., A. Zampetaki, A. Margariti, A.E. Pepe, S. Alam, D. Martin, Q. Xiao, W. Wang, Z.G. Jin, G. Cockerill, K. Mori, Y.S. Li, Y. Hu, S. Chien, and Q. Xu, *Sustained activation of XBP1 splicing leads to endothelial apoptosis and atherosclerosis development in response to disturbed flow.* Proc Natl Acad Sci U S A, 2009. **106**(20): p. 8326-31.
180. Gargalovic, P.S., N.M. Gharavi, M.J. Clark, J. Pagnon, W.P. Yang, A. He, A. Truong, T. Baruch-Oren, J.A. Berliner, T.G. Kirchgessner, and A.J. Lusis, *The unfolded protein response is an important regulator of inflammatory genes in endothelial cells.* Arterioscler Thromb Vasc Biol, 2006. **26**(11): p. 2490-6.
181. Nakatani, Y., H. Kaneto, D. Kawamori, K. Yoshiuchi, M. Hatazaki, T.A. Matsuoka, K. Ozawa, S. Ogawa, M. Hori, Y. Yamasaki, and M. Matsuhisa, *Involvement of endoplasmic reticulum stress in insulin resistance and diabetes.* J Biol Chem, 2005. **280**(1): p. 847-51.
182. Özcan, U., Q. Cao, E. Yilmaz, A.-H. Lee, N.N. Iwakoshi, E. Özdelen, G. Tuncman, C. Görgün, L.H. Glimcher, and G.S. Hotamisligil, *Endoplasmic Reticulum Stress Links Obesity, Insulin Action, and Type 2 Diabetes.* Science, 2004. **306**(5695): p. 457-461.
183. Wang, D., Y. Wei, D. Schmoll, K.N. Maclean, and M.J. Pagliassotti, *Endoplasmic reticulum stress increases glucose-6-phosphatase and glucose cycling in liver cells.* Endocrinology, 2006. **147**(1): p. 350-8.
184. Lu, P.D., C. Jousse, S.J. Marciniak, Y. Zhang, I. Novoa, D. Scheuner, R.J. Kaufman, D. Ron, and H.P. Harding, *Cytoprotection by pre-emptive conditional phosphorylation of translation initiation factor 2.* EMBO J, 2004. **23**(1): p. 169-79.
185. Scheuner, D., D.V. Mierde, B. Song, D. Flamez, J.W.M. Creemers, K. Tsukamoto, M. Ribick, F.C. Schuit, and R.J. Kaufman, *Control of mRNA translation preserves endoplasmic reticulum function in beta cells and maintains glucose homeostasis.* Nat Med, 2005. **11**(7): p. 757-764.
186. Tsutsumi, A., H. Motoshima, T. Kondo, S. Kawasaki, T. Matsumura, S. Hanatani, M. Igata, N. Ishii, H. Kinoshita, J. Kawashima, K. Taketa, N. Furukawa, K. Tsuruzoe, T. Nishikawa, and E. Araki, *Caloric restriction decreases ER stress in liver and adipose tissue in ob/ob mice.* Biochem Biophys Res Commun, 2011. **404**(1): p. 339-44.

187. Urano, F., X. Wang, A. Bertolotti, Y. Zhang, P. Chung, H.P. Harding, and D. Ron, *Coupling of Stress in the ER to Activation of JNK Protein Kinases by Transmembrane Protein Kinase IRE1.* Science, 2000. **287**(5453): p. 664-666.
188. Ozawa, K., M. Miyazaki, M. Matsuhisa, K. Takano, Y. Nakatani, M. Hatazaki, T. Tamatani, K. Yamagata, J.-i. Miyagawa, Y. Kitao, O. Hori, Y. Yamasaki, and S. Ogawa, *The Endoplasmic Reticulum Chaperone Improves Insulin Resistance in Type 2 Diabetes.* Diabetes, 2005. **54**(3): p. 657-663.
189. Boden, G., X. Duan, C. Homko, E.J. Molina, W. Song, O. Perez, P. Cheung, and S. Merali, *Increase in Endoplasmic Reticulum Stress–Related Proteins and Genes in Adipose Tissue of Obese, Insulin-Resistant Individuals.* Diabetes, 2008. **57**(9): p. 2438-2444.
190. Sharma, N.K., S.K. Das, A.K. Mondal, O.G. Hackney, W.S. Chu, P.A. Kern, N. Rasouli, H.J. Spencer, A. Yao-Borengasser, and S.C. Elbein, *Endoplasmic Reticulum Stress Markers Are Associated with Obesity in Nondiabetic Subjects.* The Journal of Clinical Endocrinology & Metabolism, 2008. **93**(11): p. 4532-4541.
191. Gregor, M.F., L. Yang, E. Fabbrini, B.S. Mohammed, J.C. Eagon, G.S. Hotamisligil, and S. Klein, *Endoplasmic reticulum stress is reduced in tissues of obese subjects after weight loss.* Diabetes, 2009. **58**(3): p. 693-700.
192. Preiss, D. and N. Sattar, *Lipids, lipid modifying agents and cardiovascular risk: a review of the evidence.* Clinical Endocrinology, 2009. **70**(6): p. 815-828.
193. LaRosa, J.C., J. He, and S. Vupputuri, *Effect of statins on risk of coronary disease: a meta-analysis of randomized controlled trials.* JAMA, 1999. **282**(24): p. 2340-6.
194. *Randomised trial of cholesterol lowering in 4444 patients with coronary heart disease: the Scandinavian Simvastatin Survival Study (4S).* Lancet, 1994. **344**(8934): p. 1383-9.
195. Downs, J.R., M. Clearfield, S. Weis, E. Whitney, D.R. Shapiro, P.A. Beere, A. Langendorfer, E.A. Stein, W. Kruyer, and A.M. Gotto, Jr., *Primary prevention of acute coronary events with lovastatin in men and women with average cholesterol levels: results of AFCAPS/TexCAPS. Air Force/Texas Coronary Atherosclerosis Prevention Study.* JAMA, 1998. **279**(20): p. 1615-22.
196. Sacks, F.M., M.A. Pfeffer, L.A. Moye, J.L. Rouleau, J.D. Rutherford, T.G. Cole, L. Brown, J.W. Warnica, J.M. Arnold, C.C. Wun, B.R. Davis, and E. Braunwald, *The effect of pravastatin on coronary events after myocardial infarction in patients with average cholesterol levels. Cholesterol and Recurrent Events Trial investigators.* N Engl J Med, 1996. **335**(14): p. 1001-9.
197. *Prevention of cardiovascular events and death with pravastatin in patients with coronary heart disease and a broad range of initial cholesterol levels. The Long-Term Intervention with Pravastatin in Ischaemic Disease (LIPID) Study Group.* N Engl J Med, 1998. **339**(19): p. 1349-57.
198. Shepherd, J., S.M. Cobbe, I. Ford, C.G. Isles, A.R. Lorimer, P.W. MacFarlane, J.H. McKillop, and C.J. Packard, *Prevention of coronary heart disease with pravastatin in men with hypercholesterolemia. West of Scotland Coronary Prevention Study Group.* N Engl J Med, 1995. **333**(20): p. 1301-7.
199. Spann, Nathanael J., Lana X. Garmire, Jeffrey G. McDonald, David S. Myers, Stephen B. Milne, N. Shibata, D. Reichart, Jesse N. Fox, I. Shaked, D. Heudobler, Christian R.H. Raetz, Elaine W. Wang, Samuel L. Kelly, M.C. Sullards, Robert C. Murphy, Alfred H. Merrill Jr, H.A. Brown, Edward A. Dennis, Andrew C. Li, K. Ley, S. Tsimikas, E. Fahy, S. Subramaniam, O. Quehenberger, David W. Russell, and Christopher K. Glass, *Regulated Accumulation of Desmosterol Integrates Macrophage Lipid Metabolism and Inflammatory Responses.* Cell, 2012. **151**(1): p. 138-152.
200. Istvan, E.S. and J. Deisenhofer, *Structural mechanism for statin inhibition of HMG-CoA reductase.* Science, 2001. **292**(5519): p. 1160-4.

201. Ridker, P.M., N. Rifai, M. Clearfield, J.R. Downs, S.E. Weis, J.S. Miles, A.M. Gotto, Jr., and I. Air Force/Texas Coronary Atherosclerosis Prevention Study, *Measurement of C-reactive protein for the targeting of statin therapy in the primary prevention of acute coronary events.* N Engl J Med, 2001. **344**(26): p. 1959-65.
202. Rattazzi, M., M. Puato, E. Faggin, B. Bertipaglia, A. Zambon, and P. Pauletto, *C-reactive protein and interleukin-6 in vascular disease: culprits or passive bystanders?* J Hypertens, 2003. **21**(10): p. 1787-803.
203. Verma, S., S.H. Li, M.V. Badiwala, R.D. Weisel, P.W. Fedak, R.K. Li, B. Dhillon, and D.A. Mickle, *Endothelin antagonism and interleukin-6 inhibition attenuate the proatherogenic effects of C-reactive protein.* Circulation, 2002. **105**(16): p. 1890-6.
204. Baumann, H. and J. Gauldie, *The acute phase response.* Immunol Today, 1994. **15**(2): p. 74-80.
205. Venugopal, S.K., S. Devaraj, I. Yuhanna, P. Shaul, and I. Jialal, *Demonstration that C-reactive protein decreases eNOS expression and bioactivity in human aortic endothelial cells.* Circulation, 2002. **106**(12): p. 1439-41.
206. Pasceri, V., J.T. Willerson, and E.T. Yeh, *Direct proinflammatory effect of C-reactive protein on human endothelial cells.* Circulation, 2000. **102**(18): p. 2165-8.
207. Pasceri, V., J.S. Cheng, J.T. Willerson, and E.T. Yeh, *Modulation of C-reactive protein-mediated monocyte chemoattractant protein-1 induction in human endothelial cells by anti-atherosclerosis drugs.* Circulation, 2001. **103**(21): p. 2531-4.
208. Zwaka, T.P., V. Hombach, and J. Torzewski, *C-reactive protein-mediated low density lipoprotein uptake by macrophages: implications for atherosclerosis.* Circulation, 2001. **103**(9): p. 1194-7.
209. Laufs, U., V. La Fata, J. Plutzky, and J.K. Liao, *Upregulation of endothelial nitric oxide synthase by HMG CoA reductase inhibitors.* Circulation, 1998. **97**(12): p. 1129-35.
210. Kureishi, Y., Z. Luo, I. Shiojima, A. Bialik, D. Fulton, D.J. Lefer, W.C. Sessa, and K. Walsh, *The HMG-CoA reductase inhibitor simvastatin activates the protein kinase Akt and promotes angiogenesis in normocholesterolemic animals.* Nat Med, 2000. **6**(9): p. 1004-10.
211. Laufs, U., V.L. Fata, and J.K. Liao, *Inhibition of 3-hydroxy-3-methylglutaryl (HMG)-CoA reductase blocks hypoxia-mediated down-regulation of endothelial nitric oxide synthase.* J Biol Chem, 1997. **272**(50): p. 31725-9.
212. Laufs, U. and J.K. Liao, *Post-transcriptional regulation of endothelial nitric oxide synthase mRNA stability by Rho GTPase.* J Biol Chem, 1998. **273**(37): p. 24266-71.
213. Lefer, A.M., B. Campbell, Y.-K. Shin, R. Scalia, R. Hayward, and D.J. Lefer, *Simvastatin Preserves the Ischemic-Reperfused Myocardium in Normocholesterolemic Rat Hearts.* Circulation, 1999. **100**(2): p. 178-184.
214. Scalia, R., M.E. Gooszen, S.P. Jones, M. Hoffmeyer, D.M. Rimmer, 3rd, S.D. Trocha, P.L. Huang, M.B. Smith, A.M. Lefer, and D.J. Lefer, *Simvastatin exerts both anti-inflammatory and cardioprotective effects in apolipoprotein E-deficient mice.* Circulation, 2001. **103**(21): p. 2598-603.
215. Stalker, T.J., A.M. Lefer, and R. Scalia, *A new HMG-CoA reductase inhibitor, rosuvastatin, exerts anti-inflammatory effects on the microvascular endothelium: the role of mevalonic acid.* Br J Pharmacol, 2001. **133**(3): p. 406-12.
216. Rikitake, Y., S. Kawashima, S. Takeshita, T. Yamashita, H. Azumi, M. Yasuhara, H. Nishi, N. Inoue, and M. Yokoyama, *Anti-oxidative properties of fluvastatin, an HMG-CoA reductase inhibitor, contribute to prevention of atherosclerosis in cholesterol-fed rabbits.* Atherosclerosis, 2001. **154**(1): p. 87-96.
217. Cai, H. and D.G. Harrison, *Endothelial dysfunction in cardiovascular diseases: the role of oxidant stress.* Circ Res, 2000. **87**(10): p. 840-4.

218. Liao, J.K., *Effects of statins on 3-hydroxy-3-methylglutaryl coenzyme a reductase inhibition beyond low-density lipoprotein cholesterol.* Am J Cardiol, 2005. **96**(5A): p. 24F-33F.
219. Wassmann, S., U. Laufs, A.T. Bäumer, K. Müller, K. Ahlbory, W. Linz, G. Itter, R. Rösen, M. Böhm, and G. Nickenig, *HMG-CoA Reductase Inhibitors Improve Endothelial Dysfunction in Normocholesterolemic Hypertension via Reduced Production of Reactive Oxygen Species.* Hypertension, 2001. **37**(6): p. 1450-1457.
220. Fromigue, O., E. Hay, D. Modrowski, S. Bouvet, A. Jacquel, P. Auberger, and P.J. Marie, *RhoA GTPase inactivation by statins induces osteosarcoma cell apoptosis by inhibiting p42/p44-MAPKs-Bcl-2 signaling independently of BMP-2 and cell differentiation.* Cell Death Differ, 2006. **13**(11): p. 1845-56.
221. Graaf, M.R., A.B. Beiderbeck, A.C.G. Egberts, D.J. Richel, and H.-J. Guchelaar, *The Risk of Cancer in Users of Statins.* Journal of Clinical Oncology, 2004. **22**(12): p. 2388-2394.
222. Poynter , J.N., S.B. Gruber , P.D.R. Higgins , R. Almog , J.D. Bonner , H.S. Rennert , M. Low , J.K. Greenson , and G. Rennert *Statins and the Risk of Colorectal Cancer.* New England Journal of Medicine, 2005. **352**(21): p. 2184-2192.
223. Campbell, M.J., L.J. Esserman, Y. Zhou, M. Shoemaker, M. Lobo, E. Borman, F. Baehner, A.S. Kumar, K. Adduci, C. Marx, E.F. Petricoin, L.A. Liotta, M. Winters, S. Benz, and C.C. Benz, *Breast Cancer Growth Prevention by Statins.* Cancer Research, 2006. **66**(17): p. 8707-8714.
224. Nielsen , S.F., B.G. Nordestgaard , and S.E. Bojesen *Statin Use and Reduced Cancer-Related Mortality.* New England Journal of Medicine, 2012. **367**(19): p. 1792-1802.
225. Zhang, Y. and T. Zang, *Association between statin usage and prostate cancer prevention: a refined meta-analysis based on literature from the years 2005-2010.* Urol Int, 2013. **90**(3): p. 259-62.
226. Morote, J., A. Celma, J. Planas, J. Placer, I. de Torres, M. Olivan, J. Carles, J. Reventos, and A. Doll, *Role of serum cholesterol and statin use in the risk of prostate cancer detection and tumor aggressiveness.* Int J Mol Sci, 2014. **15**(8): p. 13615-23.
227. Demyanets, S., C. Kaun, S. Pfaffenberger, P.J. Hohensinner, G. Rega, J. Pammer, G. Maurer, K. Huber, and J. Wojta, *Hydroxymethylglutaryl-coenzyme A reductase inhibitors induce apoptosis in human cardiac myocytes in vitro.* Biochem Pharmacol, 2006. **71**(9): p. 1324-30.
228. Chen, J.C., M.L. Wu, K.C. Huang, and W.W. Lin, *HMG-CoA reductase inhibitors activate the unfolded protein response and induce cytoprotective GRP78 expression.* Cardiovasc Res, 2008. **80**(1): p. 138-50.
229. Breder, I., A. Coope, A.P. Arruda, D. Razolli, M. Milanski, G.d.G. Dorighello, H.C.F. de Oliveira, and L.A. Velloso, *Reduction of endoplasmic reticulum stress—A novel mechanism of action of statins in the protection against atherosclerosis.* Atherosclerosis, 2010. **212**(1): p. 30-31.
230. Fukumoto, Y., P. Libby, E. Rabkin, C.C. Hill, M. Enomoto, Y. Hirouchi, M. Shiomi, and M. Aikawa, *Statins alter smooth muscle cell accumulation and collagen content in established atheroma of watanabe heritable hyperlipidemic rabbits.* Circulation, 2001. **103**(7): p. 993-9.
231. Koh, K.K., *Effects of statins on vascular wall: vasomotor function, inflammation, and plaque stability.* Cardiovasc Res, 2000. **47**(4): p. 648-57.
232. Aikawa, M., E. Rabkin, S. Sugiyama, S.J. Voglic, Y. Fukumoto, Y. Furukawa, M. Shiomi, F.J. Schoen, and P. Libby, *An HMG-CoA reductase inhibitor, cerivastatin, suppresses growth of macrophages expressing matrix metalloproteinases and tissue factor in vivo and in vitro.* Circulation, 2001. **103**(2): p. 276-83.

233. Crisby, M., G. Nordin-Fredriksson, P.K. Shah, J. Yano, J. Zhu, and J. Nilsson, *Pravastatin treatment increases collagen content and decreases lipid content, inflammation, metalloproteinases, and cell death in human carotid plaques: implications for plaque stabilization.* Circulation, 2001. **103**(7): p. 926-33.
234. Ness, G.C., S. Eales, D. Lopez, and Z. Zhao, *Regulation of 3-hydroxy-3-methylglutaryl coenzyme A reductase gene expression by sterols and nonsterols in rat liver.* Arch Biochem Biophys, 1994. **308**(2): p. 420-5.
235. Ness, G.C., Z. Zhao, and D. Lopez, *Inhibitors of cholesterol biosynthesis increase hepatic low-density lipoprotein receptor protein degradation.* Arch Biochem Biophys, 1996. **325**(2): p. 242-8.
236. Conde, K., M. Vergara-Jimenez, B.R. Krause, R.S. Newton, and M.L. Fernandez, *Hypocholesterolemic actions of atorvastatin are associated with alterations on hepatic cholesterol metabolism and lipoprotein composition in the guinea pig.* J Lipid Res, 1996. **37**(11): p. 2372-82.
237. Naoumova, R.P., S. Dunn, L. Rallidis, O. Abu-Muhana, C. Neuwirth, N.B. Rendell, G.W. Taylor, and G.R. Thompson, *Prolonged inhibition of cholesterol synthesis explains the efficacy of atorvastatin.* J Lipid Res, 1997. **38**(7): p. 1496-500.
238. Ness, G.C., C.M. Chambers, and D. Lopez, *Atorvastatin action involves diminished recovery of hepatic HMG-CoA reductase activity.* Journal of Lipid Research, 1998. **39**(1): p. 75-84.
239. Armitage, J., *The safety of statins in clinical practice.* The Lancet, 2007. **370**(9601): p. 1781-1790.
240. Pasternak, R.C., S.C. Smith, Jr., C.N. Bairey-Merz, S.M. Grundy, J.I. Cleeman, C. Lenfant, C. American College of, A. American Heart, L. National Heart, and I. Blood, *ACC/AHA/NHLBI Clinical Advisory on the Use and Safety of Statins.* Circulation, 2002. **106**(8): p. 1024-8.
241. Thompson, P.D., P. Clarkson, and R.H. Karas, *Statin-associated myopathy.* JAMA, 2003. **289**(13): p. 1681-1690.
242. Davidson, M.H., J.A. Clark, L.M. Glass, and A. Kanumalla, *Statin safety: an appraisal from the adverse event reporting system.* Am J Cardiol, 2006. **97**(8A): p. 32C-43C.
243. McKenney, J.M., M.H. Davidson, T.A. Jacobson, J.R. Guyton, and F. National Lipid Association Statin Safety Assessment Task, *Final conclusions and recommendations of the National Lipid Association Statin Safety Assessment Task Force.* Am J Cardiol, 2006. **97**(8A): p. 89C-94C.
244. Johnson, T.E., X. Zhang, K.B. Bleicher, G. Dysart, A.F. Loughlin, W.H. Schaefer, and D.R. Umbenhauer, *Statins induce apoptosis in rat and human myotube cultures by inhibiting protein geranylgeranylation but not ubiquinone.* Toxicol Appl Pharmacol, 2004. **200**(3): p. 237-50.
245. Sacher, J., L. Weigl, M. Werner, C. Szegedi, and M. Hohenegger, *Delineation of myotoxicity induced by 3-hydroxy-3-methylglutaryl CoA reductase inhibitors in human skeletal muscle cells.* J Pharmacol Exp Ther, 2005. **314**(3): p. 1032-41.
246. Omar, M.A. and J.P. Wilson, *FDA Adverse Event Reports on Statin-Associated Rhabdomyolysis.* Annals of Pharmacotherapy, 2002. **36**(2): p. 288-295.
247. Furberg, C.D. and B. Pitt, *Withdrawal of cerivastatin from the world market.* Curr Control Trials Cardiovasc Med, 2001. **2**(5): p. 205-207.
248. Staffa, J.A., J. Chang, and L. Green, *Cerivastatin and Reports of Fatal Rhabdomyolysis.* New England Journal of Medicine, 2002. **346**(7): p. 539-540.
249. Harper, C.R. and T.A. Jacobson, *The broad spectrum of statin myopathy: from myalgia to rhabdomyolysis.* Curr Opin Lipidol, 2007. **18**(4): p. 401-8.

250. Bellosta, S., R. Paoletti, and A. Corsini, *Safety of statins: focus on clinical pharmacokinetics and drug interactions.* Circulation, 2004. **109**(23 Suppl 1): p. III50-7.
251. Ridker, P.M., E. Danielson, F.A. Fonseca, J. Genest, A.M. Gotto, Jr., J.J. Kastelein, W. Koenig, P. Libby, A.J. Lorenzatti, J.G. MacFadyen, B.G. Nordestgaard, J. Shepherd, J.T. Willerson, R.J. Glynn, and J.S. Group, *Rosuvastatin to prevent vascular events in men and women with elevated C-reactive protein.* N Engl J Med, 2008. **359**(21): p. 2195-207.
252. Sattar, N., D. Preiss, H.M. Murray, P. Welsh, B.M. Buckley, A.J. de Craen, S.R. Seshasai, J.J. McMurray, D.J. Freeman, J.W. Jukema, P.W. Macfarlane, C.J. Packard, D.J. Stott, R.G. Westendorp, J. Shepherd, B.R. Davis, S.L. Pressel, R. Marchioli, R.M. Marfisi, A.P. Maggioni, L. Tavazzi, G. Tognoni, J. Kjekshus, T.R. Pedersen, T.J. Cook, A.M. Gotto, M.B. Clearfield, J.R. Downs, H. Nakamura, Y. Ohashi, K. Mizuno, K.K. Ray, and I. Ford, *Statins and risk of incident diabetes: a collaborative meta-analysis of randomised statin trials.* Lancet, 2010. **375**(9716): p. 735-42.
253. Preiss, D., S.R. Seshasai, P. Welsh, S.A. Murphy, J.E. Ho, D.D. Waters, D.A. DeMicco, P. Barter, C.P. Cannon, M.S. Sabatine, E. Braunwald, J.J. Kastelein, J.A. de Lemos, M.A. Blazing, T.R. Pedersen, M.J. Tikkanen, N. Sattar, and K.K. Ray, *Risk of incident diabetes with intensive-dose compared with moderate-dose statin therapy: a meta-analysis.* JAMA, 2011. **305**(24): p. 2556-64.
254. Carter, A.A., T. Gomes, X. Camacho, D.N. Juurlink, B.R. Shah, and M.M. Mamdani, *Risk of incident diabetes among patients treated with statins: population based study.* BMJ, 2013. **346**.
255. Brownlee, M., *Biochemistry and molecular cell biology of diabetic complications.* Nature, 2001. **414**(6865): p. 813-820.
256. Banach, M., M. Malodobra-Mazur, A. Gluba, N. Katsiki, J. Rysz, and A. Dobrzyn, *Statin Therapy and New-onset Diabetes: Molecular Mechanisms and Clinical Relevance.* Current Pharmaceutical Design, 2013. **19**(27): p. 4904-4912.
257. Kitazawa, E., N. Tamura, H. Iwabuchi, M. Uchiyama, S. Muramatsu, H. Takahagi, and M. Tanaka, *Biotransformation of Pravastatin Sodium(I).* Biochemical and Biophysical Research Communications, 1993. **192**(2): p. 597-602.
258. Corsini, A., S. Bellosta, R. Baetta, R. Fumagalli, R. Paoletti, and F. Bernini, *New insights into the pharmacodynamic and pharmacokinetic properties of statins.* Pharmacol Ther, 1999. **84**(3): p. 413-28.
259. White, C.M., *A review of the pharmacologic and pharmacokinetic aspects of rosuvastatin.* J Clin Pharmacol, 2002. **42**(9): p. 963-70.
260. Rowan, C., A.D. Brinker, P. Nourjah, J. Chang, A. Mosholder, J.S. Barrett, and M. Avigan, *Rhabdomyolysis reports show interaction between simvastatin and CYP3A4 inhibitors.* Pharmacoepidemiol Drug Saf, 2009. **18**(4): p. 301-9.
261. Bottorff, M. and P. Hansten, *Long-term safety of hepatic hydroxymethyl glutaryl coenzyme A reductase inhibitors: the role of metabolism-monograph for physicians.* Arch Intern Med, 2000. **160**(15): p. 2273-80.
262. Bolego, C., R. Baetta, S. Bellosta, A. Corsini, and R. Paoletti, *Safety considerations for statins.* Curr Opin Lipidol, 2002. **13**(6): p. 637-44.
263. Keskitalo, J.E., O. Zolk, M.F. Fromm, K.J. Kurkinen, P.J. Neuvonen, and M. Niemi, *ABCG2 polymorphism markedly affects the pharmacokinetics of atorvastatin and rosuvastatin.* Clin Pharmacol Ther, 2009. **86**(2): p. 197-203.
264. Keskitalo, J.E., M.K. Pasanen, P.J. Neuvonen, and M. Niemi, *Different effects of the ABCG2 c.421C>A SNP on the pharmacokinetics of fluvastatin, pravastatin and simvastatin.* Pharmacogenomics, 2009. **10**(10): p. 1617-24.

265. Group, S.C., E. Link, S. Parish, J. Armitage, L. Bowman, S. Heath, F. Matsuda, I. Gut, M. Lathrop, and R. Collins, *SLCO1B1 variants and statin-induced myopathy--a genomewide study.* N Engl J Med, 2008. **359**(8): p. 789-99.
266. Niemi, M., M.K. Pasanen, and P.J. Neuvonen, *SLCO1B1 polymorphism and sex affect the pharmacokinetics of pravastatin but not fluvastatin.* Clinical Pharmacology & Therapeutics, 2006. **80**(4): p. 356-366.
267. Pasanen, M.K., M. Neuvonen, P.J. Neuvonen, and M. Niemi, *SLCO1B1 polymorphism markedly affects the pharmacokinetics of simvastatin acid.* Pharmacogenet Genomics, 2006. **16**(12): p. 873-9.
268. Pasanen, M.K., H. Fredrikson, P.J. Neuvonen, and M. Niemi, *Different effects of SLCO1B1 polymorphism on the pharmacokinetics of atorvastatin and rosuvastatin.* Clin Pharmacol Ther, 2007. **82**(6): p. 726-33.
269. McClure, D.L., R.J. Valuck, M. Glanz, J.R. Murphy, and J.E. Hokanson, *Statin and statin-fibrate use was significantly associated with increased myositis risk in a managed care population.* J Clin Epidemiol, 2007. **60**(8): p. 812-8.
270. Omar, M.A., J.P. Wilson, and T.S. Cox, *Rhabdomyolysis and HMG-CoA reductase inhibitors.* Ann Pharmacother, 2001. **35**(9): p. 1096-107.
271. Husain, S., N.P. Andrews, D. Mulcahy, J.A. Panza, and A.A. Quyyumi, *Aspirin Improves Endothelial Dysfunction in Atherosclerosis.* Circulation, 1998. **97**(8): p. 716-720.
272. Ridker , P.M., M. Cushman , M.J. Stampfer , R.P. Tracy , and C.H. Hennekens *Inflammation, Aspirin, and the Risk of Cardiovascular Disease in Apparently Healthy Men.* New England Journal of Medicine, 1997. **336**(14): p. 973-979.
273. Faghihimani, E., A. Aminorroaya, H. Rezvanian, P. Adibi, F. Ismail-Beigi, and M. Amini, *Salsalate improves glycemic control in patients with newly diagnosed type 2 diabetes.* Acta Diabetologica, 2013. **50**(4): p. 537-543.
274. Goldfine, A.B., V. Fonseca, K.A. Jablonski, L. Pyle, M.A. Staten, and S.E. Shoelson, *The Effects of Salsalate on Glycemic Control in Patients With Type 2 DiabetesA Randomized Trial.* Annals of Internal Medicine, 2010. **152**(6): p. 346-357.
275. Goldfine, A.B., P.R. Conlin, F. Halperin, J. Koska, P. Permana, D. Schwenke, S.E. Shoelson, and P.D. Reaven, *A randomised trial of salsalate for insulin resistance and cardiovascular risk factors in persons with abnormal glucose tolerance.* Diabetologia, 2013. **56**(4): p. 714-723.
276. Goldfine, A.B., R. Silver, W. Aldhahi, D. Cai, E. Tatro, J. Lee, and S.E. Shoelson, *Use of Salsalate to Target Inflammation in the Treatment of Insulin Resistance and Type 2 Diabetes.* Clinical and Translational Science, 2008. **1**(1): p. 36-43.
277. Fleischman, A., S.E. Shoelson, R. Bernier, and A.B. Goldfine, *Salsalate Improves Glycemia and Inflammatory Parameters in Obese Young Adults.* Diabetes Care, 2008. **31**(2): p. 289-294.
278. Pierce, J.W., M.A. Read, H. Ding, F.W. Luscinskas, and T. Collins, *Salicylates inhibit I kappa B-alpha phosphorylation, endothelial-leukocyte adhesion molecule expression, and neutrophil transmigration.* J Immunol, 1996. **156**(10): p. 3961-9.
279. Weber, C., W. Erl, A. Pietsch, and P.C. Weber, *Aspirin inhibits nuclear factor-kappa B mobilization and monocyte adhesion in stimulated human endothelial cells.* Circulation, 1995. **91**(7): p. 1914-7.
280. Yin, M.J., Y. Yamamoto, and R.B. Gaynor, *The anti-inflammatory agents aspirin and salicylate inhibit the activity of I(kappa)B kinase-beta.* Nature, 1998. **396**(6706): p. 77-80.
281. Clarke, R.J., G. Mayo, P. Price, and G.A. FitzGerald, *Suppression of thromboxane A2 but not of systemic prostacyclin by controlled-release aspirin.* New England Journal of Medicine, 1991. **325**(16): p. 1137-1141.

282. Preston , F.E., S. Whipps , C.A. Jackson , A.J. French , P.J. Wyld , and C.J. Stoddard *Inhibition of Prostacyclin and Platelet Thromboxane A2 after Low-Dose Aspirin.* New England Journal of Medicine, 1981. **304**(2): p. 76-79.
283. Diener, H.C., L. Cunha, C. Forbes, J. Sivenius, P. Smets, and A. Lowenthal, *European Stroke Prevention Study 2. Dipyridamole and acetylsalicylic acid in the secondary prevention of stroke.* Journal of the Neurological Sciences, 1996. **143**(1–2): p. 1-13.
284. Baigent, C., R. Collins, P. Appleby, S. Parish, P. Sleight, and R. Peto, *ISIS-2: 10 year survival among patients with suspected acute myocardial infarction in randomised comparison of intravenous streptokinase, oral aspirin, both, or neither.* BMJ, 1998. **316**(7141): p. 1337.
285. Farrell, B., J. Godwin, S. Richards, and C. Warlow, *The United Kingdom transient ischaemic attack (UK-TIA) aspirin trial: final results.* J Neurol Neurosurg Psychiatry, 1991. **54**(12): p. 1044-54.
286. *Swedish Aspirin Low-Dose Trial (SALT) of 75 mg aspirin as secondary prophylaxis after cerebrovascular ischaemic events. The SALT Collaborative Group.* Lancet, 1991. **338**(8779): p. 1345-9.
287. Yuan, M., N. Konstantopoulos, J. Lee, L. Hansen, Z.W. Li, M. Karin, and S.E. Shoelson, *Reversal of obesity- and diet-induced insulin resistance with salicylates or targeted disruption of Ikkbeta.* Science, 2001. **293**(5535): p. 1673-7.
288. Hundal, R.S., K.F. Petersen, A.B. Mayerson, P.S. Randhawa, S. Inzucchi, S.E. Shoelson, and G.I. Shulman, *Mechanism by which high-dose aspirin improves glucose metabolism in type 2 diabetes.* The Journal of Clinical Investigation, 2002. **109**(10): p. 1321-1326.
289. Kharbanda, R.K., B. Walton, M. Allen, N. Klein, A.D. Hingorani, R.J. MacAllister, and P. Vallance, *Prevention of Inflammation-Induced Endothelial Dysfunction.* A Novel Vasculo-Protective Action of Aspirin, 2002. **105**(22): p. 2600-2604.
290. Tohgi, H., S. Konno, K. Tamura, B. Kimura, and K. Kawano, *Effects of low-to-high doses of aspirin on platelet aggregability and metabolites of thromboxane A2 and prostacyclin.* Stroke, 1992. **23**(10): p. 1400-3.
291. Patrono, C., B. Coller, J.E. Dalen, G.A. FitzGerald, V. Fuster, M. Gent, J. Hirsh, and G. Roth, *Platelet-active drugs : The relationships among dose, effectiveness, and side effects.* Chest, 2001. **119**(1_suppl): p. 39S-63S.
292. Sørensen, H.T., L. Mellemkjær, W.J. Blot, G.L. Nielsen, F.H. Steffensen, J.K. McLaughlin, and J.H. Olsen, *Risk of upper gastrointestinal bleeding associated with use of low-dose aspirin.* The American journal of gastroenterology, 2000. **95**(9): p. 2218-2224.
293. De Berardis, G., G. Lucisano, A. D'Ettorre, and et al., *Association of aspirin use with major bleeding in patients with and without diabetes.* JAMA, 2012. **307**(21): p. 2286-2294.
294. Hernández-Díaz, S. and L.A. García Rodríguez, *Cardioprotective aspirin users and their excess risk of upper gastrointestinal complications.* BMC Medicine, 2006. **4**(1): p. 1-9.
295. Laster, J. and R. Satoskar, *Aspirin-Induced Acute Liver Injury.* ACG Case Reports Journal, 2014. **2**(1): p. 48-49.
296. Strassburg, C.P., *Nonimmune-mediated drug-induced hepatotoxicity*, in *Liver Immunology*. 2014, Springer. p. 389-399.
297. Helgason, C.M., K.M. Bolin, J.A. Hoff, S.R. Winkler, A. Mangat, K.L. Tortorice, and L.D. Brace, *Development of aspirin resistance in persons with previous ischemic stroke.* Stroke, 1994. **25**(12): p. 2331-2336.
298. Gum, P.A., K. Kottke-Marchant, E.D. Poggio, H. Gurm, P.A. Welsh, L. Brooks, S.K. Sapp, and E.J. Topol, *Profile and prevalence of aspirin resistance in patients with cardiovascular disease.* The American Journal of Cardiology, 2001. **88**(3): p. 230-235.

299. Poulsen, T.S., B. Jorgensen, L. Korsholm, P.B. Licht, T. Haghfelt, and H. Mickley, *Prevalence of aspirin resistance in patients with an evolving acute myocardial infarction.* Thromb Res, 2007. **119**(5): p. 555-62.
300. Fateh-Moghadam, S., U. Plöckinger, N. Cabeza, P. Htun, T. Reuter, S. Ersel, M. Gawaz, R. Dietz, and W. Bocksch, *Prevalence of aspirin resistance in patients with type 2 diabetes.* Acta Diabetologica, 2005. **42**(2): p. 99-103.
301. Chen, W.-H., X. Cheng, P.-Y. Lee, W. Ng, J.Y.-Y. Kwok, H.-F. Tse, and C.-P. Lau, *Aspirin Resistance and Adverse Clinical Events in Patients with Coronary Artery Disease.* The American Journal of Medicine, 2007. **120**(7): p. 631-635.
302. Pulcinelli, F.M., P. Pignatelli, A. Celestini, S. Riondino, P.P. Gazzaniga, and F. Violi, *Inhibition of platelet aggregation by aspirin progressively decreases in long-term treated patients.* Journal of the American College of Cardiology, 2004. **43**(6): p. 979-984.
303. Mortensen, K., L.L. Christensen, J.J. Holst, and C. Orskov, *GLP-1 and GIP are colocalized in a subset of endocrine cells in the small intestine.* Regul Pept, 2003. **114**(2-3): p. 189-96.
304. Kauth, T. and J. Metz, *Immunohistochemical localization of glucagon-like peptide 1.* Histochemistry, 1987. **86**(5): p. 509-515.
305. Mojsov, S., G. Heinrich, I.B. Wilson, M. Ravazzola, L. Orci, and J.F. Habener, *Preproglucagon gene expression in pancreas and intestine diversifies at the level of post-translational processing.* Journal of Biological Chemistry, 1986. **261**(25): p. 11880-11889.
306. Wheeler, M.B., R.W. Gelling, C.H. McIntosh, J. Georgiou, J.C. Brown, and R.A. Pederson, *Functional expression of the rat pancreatic islet glucose-dependent insulinotropic polypeptide receptor: ligand binding and intracellular signaling properties.* Endocrinology, 1995. **136**(10): p. 4629-39.
307. Ding, W.G. and J. Gromada, *Protein kinase A-dependent stimulation of exocytosis in mouse pancreatic beta-cells by glucose-dependent insulinotropic polypeptide.* Diabetes, 1997. **46**(4): p. 615-21.
308. Wettergren, A., B. Schjoldager, P.E. Mortensen, J. Myhre, J. Christiansen, and J.J. Holst, *Truncated GLP-1 (proglucagon 78-107-amide) inhibits gastric and pancreatic functions in man.* Dig Dis Sci, 1993. **38**(4): p. 665-73.
309. Willms, B., J. Werner, J.J. Holst, C. Orskov, W. Creutzfeldt, and M.A. Nauck, *Gastric emptying, glucose responses, and insulin secretion after a liquid test meal: effects of exogenous glucagon-like peptide-1 (GLP-1)-(7-36) amide in type 2 (noninsulin-dependent) diabetic patients.* J Clin Endocrinol Metab, 1996. **81**(1): p. 327-32.
310. Nauck, M., F. Stockmann, R. Ebert, and W. Creutzfeldt, *Reduced incretin effect in type 2 (non-insulin-dependent) diabetes.* Diabetologia, 1986. **29**(1): p. 46-52.
311. Kolterman, O.G., D.D. Kim, L. Shen, J.A. Ruggles, L.L. Nielsen, M.S. Fineman, and A.D. Baron, *Pharmacokinetics, pharmacodynamics, and safety of exenatide in patients with type 2 diabetes mellitus.* Am J Health Syst Pharm, 2005. **62**(2): p. 173-81.
312. Imeryuz, N., B.C. Yegen, A. Bozkurt, T. Coskun, M.L. Villanueva-Penacarrillo, and N.B. Ulusoy, *Glucagon-like peptide-1 inhibits gastric emptying via vagal afferent-mediated central mechanisms.* Am J Physiol, 1997. **273**(4 Pt 1): p. G920-7.
313. Degn, K.B., B. Brock, C.B. Juhl, C.B. Djurhuus, J. Grubert, D. Kim, J. Han, K. Taylor, M. Fineman, and O. Schmitz, *Effect of intravenous infusion of exenatide (synthetic exendin-4) on glucose-dependent insulin secretion and counterregulation during hypoglycemia.* Diabetes, 2004. **53**(9): p. 2397-403.
314. Bhavsar, S., S. Mudaliar, and A. Cherrington, *Evolution of exenatide as a diabetes therapeutic.* Curr Diabetes Rev, 2013. **9**(2): p. 161-93.

315. Deacon, C.F., M.A. Nauck, M. Toft-Nielsen, L. Pridal, B. Willms, and J.J. Holst, *Both subcutaneously and intravenously administered glucagon-like peptide I are rapidly degraded from the NH2-terminus in type II diabetic patients and in healthy subjects.* Diabetes, 1995. **44**(9): p. 1126-31.
316. Kieffer, T.J., C.H. McIntosh, and R.A. Pederson, *Degradation of glucose-dependent insulinotropic polypeptide and truncated glucagon-like peptide 1 in vitro and in vivo by dipeptidyl peptidase IV.* Endocrinology, 1995. **136**(8): p. 3585-96.
317. Chen, J., F.M. Couto, A.H. Minn, and A. Shalev, *Exenatide inhibits β-cell apoptosis by decreasing thioredoxin-interacting protein.* Biochemical and Biophysical Research Communications, 2006. **346**(3): p. 1067-1074.
318. Xu, G., D.A. Stoffers, J.F. Habener, and S. Bonner-Weir, *Exendin-4 stimulates both beta-cell replication and neogenesis, resulting in increased beta-cell mass and improved glucose tolerance in diabetic rats.* Diabetes, 1999. **48**(12): p. 2270-6.
319. Tourrel, C., D. Bailbé, M.-J. Meile, M. Kergoat, and B. Portha, *Glucagon-Like Peptide-1 and Exendin-4 Stimulate β-Cell Neogenesis in Streptozotocin-Treated Newborn Rats Resulting in Persistently Improved Glucose Homeostasis at Adult Age.* Diabetes, 2001. **50**(7): p. 1562-1570.
320. Fineman, M.S., T.A. Bicsak, L.Z. Shen, K. Taylor, E. Gaines, A. Varns, D. Kim, and A.D. Baron, *Effect on Glycemic Control of Exenatide (Synthetic Exendin-4) Additive to Existing Metformin and/or Sulfonylurea Treatment in Patients With Type 2 Diabetes.* Diabetes Care, 2003. **26**(8): p. 2370-2377.
321. Kendall, D.M., M.C. Riddle, J. Rosenstock, D. Zhuang, D.D. Kim, M.S. Fineman, and A.D. Baron, *Effects of Exenatide (Exendin-4) on Glycemic Control Over 30 Weeks in Patients With Type 2 Diabetes Treated With Metformin and a Sulfonylurea.* Diabetes Care, 2005. **28**(5): p. 1083-1091.
322. Bergenstal, R.M., Y. Li, T.K. Porter, C. Weaver, and J. Han, *Exenatide once weekly improved glycaemic control, cardiometabolic risk factors and a composite index of an HbA1c < 7%, without weight gain or hypoglycaemia, over 52 weeks.* Diabetes Obes Metab, 2013. **15**(3): p. 264-71.
323. Greig, N.H., H.W. Holloway, K.A. De Ore, D. Jani, Y. Wang, J. Zhou, M.J. Garant, and J.M. Egan, *Once daily injection of exendin-4 to diabetic mice achieves long-term beneficial effects on blood glucose concentrations.* Diabetologia, 1999. **42**(1): p. 45-50.
324. Parkes, D.G., R. Pittner, C. Jodka, P. Smith, and A. Young, *Insulinotropic actions of exendin-4 and glucagon-like peptide-1 in vivo and in vitro.* Metabolism, 2001. **50**(5): p. 583-9.
325. Ritzel, R., C. Orskov, J.J. Holst, and M.A. Nauck, *Pharmacokinetic, insulinotropic, and glucagonostatic properties of GLP-1 [7-36 amide] after subcutaneous injection in healthy volunteers. Dose-response-relationships.* Diabetologia, 1995. **38**(6): p. 720-5.
326. Meier, J.J., B. Gallwitz, S. Salmen, O. Goetze, J.J. Holst, W.E. Schmidt, and M.A. Nauck, *Normalization of Glucose Concentrations and Deceleration of Gastric Emptying after Solid Meals during Intravenous Glucagon-Like Peptide 1 in Patients with Type 2 Diabetes.* The Journal of Clinical Endocrinology & Metabolism, 2003. **88**(6): p. 2719-2725.
327. Lovshin, J.A. and D.J. Drucker, *Incretin-based therapies for type 2 diabetes mellitus.* Nat Rev Endocrinol, 2009. **5**(5): p. 262-9.
328. Elashoff, M., A.V. Matveyenko, B. Gier, R. Elashoff, and P.C. Butler, *Pancreatitis, pancreatic, and thyroid cancer with glucagon-like peptide-1-based therapies.* Gastroenterology, 2011. **141**(1): p. 150-6.
329. American Diabetes, A., *Standards of medical care in diabetes--2014.* Diabetes Care, 2014. **37 Suppl 1**: p. S14-80.

330. Inzucchi, S.E., R.M. Bergenstal, J.B. Buse, M. Diamant, E. Ferrannini, M. Nauck, A.L. Peters, A. Tsapas, R. Wender, and D.R. Matthews, *Management of hyperglycaemia in type 2 diabetes: a patient-centered approach. Position statement of the American Diabetes Association (ADA) and the European Association for the Study of Diabetes (EASD).* Diabetologia, 2012. **55**(6): p. 1577-96.
331. Hundal, R.S., M. Krssak, S. Dufour, D. Laurent, V. Lebon, V. Chandramouli, S.E. Inzucchi, W.C. Schumann, K.F. Petersen, B.R. Landau, and G.I. Shulman, *Mechanism by which metformin reduces glucose production in type 2 diabetes.* Diabetes, 2000. **49**(12): p. 2063-2069.
332. Jeng, C.-Y., W.H.-H. Sheu, M.M.-T. Fuh, Y.-D.I. Chen, and G.M. Reaven, *Relationship Between Hepatic Glucose Production and Fasting Plasma Glucose Concentration in Patients With NIDDM.* Diabetes, 1994. **43**(12): p. 1440-1444.
333. El-Mir, M.Y., V. Nogueira, and E. Fontaine, *Dimethylbiguanide inhibits cell respiration via an indirect effect targeted on the respiratory chain complex I.* J Biol Chem, 2000. **275**.
334. Owen, M.R., E. Doran, and A.P. Halestrap, *Evidence that metformin exerts its anti-diabetic effects through inhibition of complex 1 of the mitochondrial respiratory chain.* Biochem J, 2000. **348**.
335. Guigas, B., D. Detaille, C. Chauvin, C. Batandier, F. De Oliveira, E. Fontaine, and X. Leverve, *Metformin inhibits mitochondrial permeability transition and cell death: a pharmacological in vitro study.* Biochem J, 2004. **382**(Pt 3): p. 877-84.
336. Detaille, D., B. Guigas, and C. Chauvin, *Metformin prevents high glucose-induced endothelial cell death through a mitochondrial permeability transition-dependent process.* Diabetes, 2005. **54**.
337. Hirsch, A., D. Hahn, P. Kempna, G. Hofer, J.M. Nuoffer, P.E. Mullis, and C.E. Fluck, *Metformin inhibits human androgen production by regulating steroidogenic enzymes HSD3B2 and CYP17A1 and complex I activity of the respiratory chain.* Endocrinology, 2012. **153**(9): p. 4354-66.
338. Kim, K.H., Y.T. Jeong, S.H. Kim, H.S. Jung, K.S. Park, H.Y. Lee, and M.S. Lee, *Metformin-induced inhibition of the mitochondrial respiratory chain increases FGF21 expression via ATF4 activation.* Biochem Biophys Res Commun, 2013. **440**(1): p. 76-81.
339. Stephenne, X., M. Foretz, N. Taleux, G.C. van der Zon, E. Sokal, L. Hue, B. Viollet, and B. Guigas, *Metformin activates AMP-activated protein kinase in primary human hepatocytes by decreasing cellular energy status.* Diabetologia, 2011. **54**(12): p. 3101-10.
340. El-Mir, M.Y., D. Detaille, and G. Villanueva, *Neuroprotective Role of Antidiabetic Drug Metformin Against Apoptotic Cell Death in Primary Cortical Neurons.* J Mol Neurosci, 2008. **34**.
341. Brunmair, B., K. Staniek, F. Gras, N. Scharf, A. Althaym, R. Clara, M. Roden, E. Gnaiger, H. Nohl, W. Waldhausl, and C. Furnsinn, *Thiazolidinediones, like metformin, inhibit respiratory complex I: a common mechanism contributing to their antidiabetic actions?* Diabetes, 2004. **53**(4): p. 1052-9.
342. Hinke, S.A., G.A. Martens, Y. Cai, J. Finsi, H. Heimberg, D. Pipeleers, and M. Van de Casteele, *Methyl succinate antagonises biguanide-induced AMPK-activation and death of pancreatic beta-cells through restoration of mitochondrial electron transfer.* Br J Pharmacol, 2007. **150**(8): p. 1031-43.
343. Bridges, H.R., A.J. Jones, M.N. Pollak, and J. Hirst, *Effects of metformin and other biguanides on oxidative phosphorylation in mitochondria.* Biochem J, 2014. **462**(3): p. 475-87.

344. Wheaton, W.W., S.E. Weinberg, R.B. Hamanaka, S. Soberanes, L.B. Sullivan, E. Anso, A. Glasauer, E. Dufour, G.M. Mutlu, G.S. Budigner, and N.S. Chandel, *Metformin inhibits mitochondrial complex I of cancer cells to reduce tumorigenesis.* Elife, 2014. **3**: p. e02242.
345. Piel, S., J.K. Ehinger, E. Elmer, and M.J. Hansson, *Metformin induces lactate production in peripheral blood mononuclear cells and platelets through specific mitochondrial complex I inhibition.* Acta Physiol (Oxf), 2015. **213**(1): p. 171-80.
346. Zhou, G., R. Myers, Y. Li, Y. Chen, X. Shen, J. Fenyk-Melody, M. Wu, J. Ventre, T. Doebber, N. Fujii, N. Musi, M.F. Hirshman, L.J. Goodyear, and D.E. Moller, *Role of AMP-activated protein kinase in mechanism of metformin action.* J Clin Invest, 2001. **108**(8): p. 1167-74.
347. Hawley, S.A., F.A. Ross, C. Chevtzoff, K.A. Green, A. Evans, S. Fogarty, M.C. Towler, L.J. Brown, O.A. Ogunbayo, A.M. Evans, and D.G. Hardie, *Use of cells expressing gamma subunit variants to identify diverse mechanisms of AMPK activation.* Cell Metab, 2010. **11**(6): p. 554-65.
348. Ruderman, N.B., D. Carling, M. Prentki, and J.M. Cacicedo, *AMPK, insulin resistance, and the metabolic syndrome.* J Clin Invest, 2013. **123**(7): p. 2764-72.
349. Bailey, C.J., *Biguanides and NIDDM.* Diabetes Care, 1992. **15**(6): p. 755-72.
350. Bailey, C.J., *Metformin--an update.* Gen Pharmacol, 1993. **24**(6): p. 1299-309.
351. Bailey, C.J. and R.C. Turner, *Metformin.* New England Journal of Medicine, 1996. **334**(9): p. 574-579.
352. Matsuki, K., N. Tamasawa, M. Yamashita, J. Tanabe, H. Murakami, J. Matsui, T. Imaizumi, K. Satoh, and T. Suda, *Metformin restores impaired HDL-mediated cholesterol efflux due to glycation.* Atherosclerosis, 2009. **206**(2): p. 434-8.
353. Perez, A., M. Khan, T. Johnson, and M. Karunaratne, *Pioglitazone plus a sulphonylurea or metformin is associated with increased lipoprotein particle size in patients with type 2 diabetes.* Diab Vasc Dis Res, 2004. **1**(1): p. 44-50.
354. Hanefeld, M., P. Brunetti, G.H. Schernthaner, D.R. Matthews, and B.H. Charbonnel, *One-Year Glycemic Control With a Sulfonylurea Plus Pioglitazone Versus a Sulfonylurea Plus Metformin in Patients With Type 2 Diabetes.* Diabetes Care, 2004. **27**(1): p. 141-147.
355. Karavia, E.A., A. Hatziri, C. Kalogeropoulou, N.I. Papachristou, E. Xepapadaki, C. Constantinou, A. Natsos, P.I. Petropoulou, S. Sasson, D.J. Papachristou, and K.E. Kypreos, *Deficiency in apolipoprotein A-I ablates the pharmacological effects of metformin on plasma glucose homeostasis and hepatic lipid deposition.* Eur J Pharmacol, 2015.
356. Holman, R.R., S.K. Paul, M.A. Bethel, D.R. Matthews, and H.A. Neil, *10-year follow up of intensive glucose control in type 2 diabetes.* N Engl J Med, 2008. **359**.
357. Ong, C.R., L.M. Molyneaux, M.I. Constantino, S.M. Twigg, and D.K. Yue, *Long-Term Efficacy of Metformin Therapy in Nonobese Individuals With Type 2 Diabetes.* Diabetes Care, 2006. **29**(11): p. 2361-2364.
358. Campbell, I.W. and H.C. Howlett, *Worldwide experience of metformin as an effective glucose-lowering agent: a meta-analysis.* Diabetes Metab Rev, 1995. **11 Suppl 1**: p. S57-62.
359. Hirst, J.A., A.J. Farmer, R. Ali, N.W. Roberts, and R.J. Stevens, *Quantifying the effect of metformin treatment and dose on glycemic control.* Diabetes Care, 2012. **35**(2): p. 446-54.
360. DeFronzo, R.A. and A.M. Goodman, *Efficacy of Metformin in Patients with Non-Insulin-Dependent Diabetes Mellitus.* New England Journal of Medicine, 1995. **333**(9): p. 541-549.

361. Garber Md, P.A.J., T.G. Duncan Md, A.M. Goodman Md, B.S.N.D.J. Mills Rn, and J.L. Rohlf Md, *Efficacy of Metformin in Type II Diabetes: Results of a Double-Blind, Placebo-controlled, Dose-Response Trialfn1.* The American Journal of Medicine, 1997. **103**(6): p. 491-497.
362. *Effect of intensive blood glucose control with metformin on complications in overweight patients with type 2 diabetes (UKPDS 34).* Lancet, 1998. **352**.
363. Stumvoll, M., N. Nurjhan, G. Perriello, G. Dailey, and J.E. Gerich, *Metabolic effects of metformin in non-insulin-dependent diabetes mellitus.* N Engl J Med, 1995. **333**(9): p. 550-4.
364. DeFronzo, R.A. and A.M. Goodman, *Efficacy of metformin in patients with non-insulin-dependent diabetes mellitus. The Multicenter Metformin Study Group.* N Engl J Med, 1995. **333**(9): p. 541-9.
365. Ford, Rebecca J., Morgan D. Fullerton, Stephen L. Pinkosky, Emily A. Day, John W. Scott, Jonathan S. Oakhill, Adam L. Bujak, Brennan K. Smith, Justin D. Crane, Regje M. Blümer, K. Marcinko, Bruce E. Kemp, Hertzel C. Gerstein, and Gregory R. Steinberg, *Metformin and salicylate synergistically activate liver AMPK, inhibit lipogenesis and improve insulin sensitivity.* Biochemical Journal, 2015. **468**(1): p. 125-132.
366. Hirsch, H.A., D. Iliopoulos, P.N. Tsichlis, and K. Struhl, *Metformin Selectively Targets Cancer Stem Cells, and Acts Together with Chemotherapy to Block Tumor Growth and Prolong Remission.* Cancer Research, 2009. **69**(19): p. 7507-7511.
367. Ben Sahra, I., K. Laurent, S. Giuliano, F. Larbret, G. Ponzio, P. Gounon, Y. Le Marchand-Brustel, S. Giorgetti-Peraldi, M. Cormont, C. Bertolotto, M. Deckert, P. Auberger, J.F. Tanti, and F. Bost, *Targeting cancer cell metabolism: the combination of metformin and 2-deoxyglucose induces p53-dependent apoptosis in prostate cancer cells.* Cancer Res, 2010. **70**(6): p. 2465-75.
368. Ben Sahra, I., J.F. Tanti, and F. Bost, *The combination of metformin and 2-deoxyglucose inhibits autophagy and induces AMPK-dependent apoptosis in prostate cancer cells.* Autophagy, 2010. **6**(5): p. 670-1.
369. Evans, J.M., L.A. Donnelly, A.M. Emslie-Smith, D.R. Alessi, and A.D. Morris, *Metformin and reduced risk of cancer in diabetic patients.* BMJ, 2005. **330**(7503): p. 1304-5.
370. Lalau, J.-D., *Lactic Acidosis Induced by Metformin.* Drug Safety, 2010. **33**(9): p. 727-740.
371. Peters, N., N. Jay, D. Barraud, A. Cravoisy, L. Nace, P.-E. Bollaert, and S. Gibot, *Metformin-associated lactic acidosis in an intensive care unit.* Critical Care, 2008. **12**(6): p. 1-5.
372. Bakris, G.L. and M.E. Molitch, *Should Restrictions Be Relaxed for Metformin Use in Chronic Kidney Disease? Yes, They Should Be Relaxed! What's the Fuss?* Diabetes Care, 2016. **39**(7): p. 1287-91.
373. Kalantar-Zadeh, K. and C.P. Kovesdy, *Should Restrictions Be Relaxed for Metformin Use in Chronic Kidney Disease? No, We Should Never Again Compromise Safety!* Diabetes Care, 2016. **39**(7): p. 1281-6.
374. Lipska, K.J., C.J. Bailey, and S.E. Inzucchi, *Use of Metformin in the Setting of Mild-to-Moderate Renal Insufficiency.* Diabetes Care, 2011. **34**(6): p. 1431-1437.
375. Stades, A.M., J.T. Heikens, D.W. Erkelens, F. Holleman, and J.B. Hoekstra, *Metformin and lactic acidosis: cause or coincidence? A review of case reports.* J Intern Med, 2004. **255**(2): p. 179-87.
376. Salpeter, S.R., E. Greyber, G.A. Pasternak, and E.E. Salpeter, *Risk of fatal and nonfatal lactic acidosis with metformin use in type 2 diabetes mellitus.* Cochrane Database Syst Rev, 2010. **1**.

377. Kajbaf, F., P. Arnouts, M. de Broe, and J.D. Lalau, *Metformin therapy and kidney disease: a review of guidelines and proposals for metformin withdrawal around the world.* Pharmacoepidemiol Drug Saf, 2013. **22**(10): p. 1027-35.
378. Wills, B.K., S.M. Bryant, P. Buckley, and B. Seo, *Can acute overdose of metformin lead to lactic acidosis?* The American Journal of Emergency Medicine, 2010. **28**(8): p. 857-861.
379. Scheen, A.J., *Clinical pharmacokinetics of metformin.* Clin Pharmacokinet, 1996. **30**(5): p. 359-71.
380. DeFronzo, R., G.A. Fleming, K. Chen, and T.A. Bicsak, *Metformin-associated lactic acidosis: Current perspectives on causes and risk.* Metabolism, 2016. **65**(2): p. 20-29.
381. Lalau, J.D. and J.M. Race, *Lactic acidosis in metformin-treated patients. Prognostic value of arterial lactate levels and plasma metformin concentrations.* Drug Saf, 1999. **20**(4): p. 377-84.
382. Davidson, M.B. and A.L. Peters, *An overview of metformin in the treatment of type 2 diabetes mellitus.* Am J Med, 1997. **102**(1): p. 99-110.
383. Baigent, C., A. Keech, P.M. Kearney, L. Blackwell, G. Buck, C. Pollicino, A. Kirby, T. Sourjina, R. Peto, R. Collins, R. Simes, and C. Cholesterol Treatment Trialists, *Efficacy and safety of cholesterol-lowering treatment: prospective meta-analysis of data from 90,056 participants in 14 randomised trials of statins.* Lancet, 2005. **366**(9493): p. 1267-78.
384. LaRosa, J.C., S.M. Grundy, D.D. Waters, C. Shear, P. Barter, J.C. Fruchart, A.M. Gotto, H. Greten, J.J. Kastelein, J. Shepherd, and N.K. Wenger, *Intensive lipid lowering with atorvastatin in patients with stable coronary disease.* N Engl J Med, 2005. **352**(14): p. 1425-35.
385. Pedersen, T.R., O. Faergeman, J.J. Kastelein, A.G. Olsson, M.J. Tikkanen, I. Holme, M.L. Larsen, F.S. Bendiksen, C. Lindahl, M. Szarek, and J. Tsai, *High-dose atorvastatin vs usual-dose simvastatin for secondary prevention after myocardial infarction: the IDEAL study: a randomized controlled trial.* JAMA, 2005. **294**(19): p. 2437-45.
386. Gordon, D.J., J.L. Probstfield, R.J. Garrison, J.D. Neaton, W.P. Castelli, J.D. Knoke, D.R. Jacobs, S. Bangdiwala, and H.A. Tyroler, *High-density lipoprotein cholesterol and cardiovascular disease. Four prospective American studies.* Circulation, 1989. **79**(1): p. 8-15.
387. Assmann, G., H. Schulte, A. von Eckardstein, and Y. Huang, *High-density lipoprotein cholesterol as a predictor of coronary heart disease risk. The PROCAM experience and pathophysiological implications for reverse cholesterol transport.* Atherosclerosis, 1996. **124 Suppl**: p. S11-20.
388. Cockerill, G.W., K.A. Rye, J.R. Gamble, M.A. Vadas, and P.J. Barter, *High-density lipoproteins inhibit cytokine-induced expression of endothelial cell adhesion molecules.* Arterioscler Thromb Vasc Biol, 1995. **15**(11): p. 1987-94.
389. Wadham, C., N. Albanese, J. Roberts, L. Wang, C.J. Bagley, J.R. Gamble, K.A. Rye, P.J. Barter, M.A. Vadas, and P. Xia, *High-density lipoproteins neutralize C-reactive protein proinflammatory activity.* Circulation, 2004. **109**(17): p. 2116-22.
390. Theilmeier, G., B. De Geest, P.P. Van Veldhoven, D. Stengel, C. Michiels, M. Lox, M. Landeloos, M.J. Chapman, E. Ninio, D. Collen, B. Himpens, and P. Holvoet, *HDL-associated PAF-AH reduces endothelial adhesiveness in apoE-/- mice.* FASEB J, 2000. **14**(13): p. 2032-9.
391. Hwang, S.J., C.M. Ballantyne, A.R. Sharrett, L.C. Smith, C.E. Davis, A.M. Gotto, Jr., and E. Boerwinkle, *Circulating adhesion molecules VCAM-1, ICAM-1, and E-selectin in carotid atherosclerosis and incident coronary heart disease cases: the Atherosclerosis Risk In Communities (ARIC) study.* Circulation, 1997. **96**(12): p. 4219-25.

392. de Lemos, J.A., D.A. Morrow, M.S. Sabatine, S.A. Murphy, C.M. Gibson, E.M. Antman, C.H. McCabe, C.P. Cannon, and E. Braunwald, *Association Between Plasma Levels of Monocyte Chemoattractant Protein-1 and Long-Term Clinical Outcomes in Patients With Acute Coronary Syndromes.* Circulation, 2003. **107**(5): p. 690-695.
393. Calabresi, L., M. Gomaraschi, B. Villa, L. Omoboni, C. Dmitrieff, and G. Franceschini, *Elevated Soluble Cellular Adhesion Molecules in Subjects With Low HDL-Cholesterol.* Arteriosclerosis, Thrombosis, and Vascular Biology, 2002. **22**(4): p. 656-661.
394. Ridker, P.M., C.H. Hennekens, B. Roitman-Johnson, M.J. Stampfer, and J. Allen, *Plasma concentration of soluble intercellular adhesion molecule 1 and risks of future myocardial infarction in apparently healthy men.* The Lancet, 1998. **351**(9096): p. 88-92.
395. Rong, J.X., J. Li, E.D. Reis, R.P. Choudhury, H.M. Dansky, V.I. Elmalem, J.T. Fallon, J.L. Breslow, and E.A. Fisher, *Elevating high-density lipoprotein cholesterol in apolipoprotein E-deficient mice remodels advanced atherosclerotic lesions by decreasing macrophage and increasing smooth muscle cell content.* Circulation, 2001. **104**(20): p. 2447-52.
396. Cockerill, G.W., T.Y. Huehns, A. Weerasinghe, C. Stocker, P.G. Lerch, N.E. Miller, and D.O. Haskard, *Elevation of plasma high-density lipoprotein concentration reduces interleukin-1-induced expression of E-selectin in an in vivo model of acute inflammation.* Circulation, 2001. **103**(1): p. 108-12.
397. Ibanez, B., C. Giannarelli, G. Cimmino, C.G. Santos-Gallego, M. Alique, A. Pinero, G. Vilahur, V. Fuster, L. Badimon, and J.J. Badimon, *Recombinant HDLMilano exerts greater anti-inflammatory and plaque stabilizing properties than HDLwild-type.* Atherosclerosis, 2012. **220**(1): p. 72-77.
398. Joy, T. and R.A. Hegele, *Is raising HDL a futile strategy for atheroprotection?* Nat Rev Drug Discov, 2008. **7**(2): p. 143-55.
399. Xia, P., M.A. Vadas, K.A. Rye, P.J. Barter, and J.R. Gamble, *High density lipoproteins (HDL) interrupt the sphingosine kinase signaling pathway. A possible mechanism for protection against atherosclerosis by HDL.* J Biol Chem, 1999. **274**(46): p. 33143-7.
400. Clay, M.A., D.H. Pyle, K.A. Rye, M.A. Vadas, J.R. Gamble, and P.J. Barter, *Time sequence of the inhibition of endothelial adhesion molecule expression by reconstituted high density lipoproteins.* Atherosclerosis, 2001. **157**(1): p. 23-9.
401. Ebron, K., C.J. Andersen, D. Aguilar, C.N. Blesso, J. Barona, C.E. Dugan, J.L. Jones, T. Al-Sarraj, and M.L. Fernandez, *A Larger Body Mass Index is Associated with Increased Atherogenic Dyslipidemia, Insulin Resistance, and Low-Grade Inflammation in Individuals with Metabolic Syndrome.* Metab Syndr Relat Disord, 2015.
402. Do, H.D., V. Lohsoonthorn, W. Jiamjarasrangsi, S. Lertmaharit, and M.A. Williams, *Prevalence of insulin resistance and its relationship with cardiovascular disease risk factors among Thai adults over 35 years old.* Diabetes Res Clin Pract, 2010. **89**(3): p. 303-8.
403. Griffo, E., M. Cotugno, G. Nosso, G. Saldalamacchia, A. Mangione, L. Angrisani, A.A. Rivellese, and B. Capaldo, *Effects of Sleeve Gastrectomy and Gastric Bypass on Postprandial Lipid Profile in Obese Type 2 Diabetic Patients: a 2-Year Follow-up.* Obes Surg, 2015.
404. IP, M.S.M., B. LAM, M.M.T. NG, W.K. LAM, K.W.T. TSANG, and K.S.L. LAM, *Obstructive Sleep Apnea Is Independently Associated with Insulin Resistance.* American Journal of Respiratory and Critical Care Medicine, 2002. **165**(5): p. 670-676.
405. Koren, D., D. Gozal, R. Bhattacharjee, M. Philby, and L. Kheirandish-Gozal, *Impact of Adenotonsillectomy On Insulin Resistance And Lipoprotein Profile In Nonobese And Obese Children.* Chest, 2015.

406. McGrath, K.C., X.H. Li, P.T. Whitworth, R. Kasz, J.T. Tan, S.V. McLennan, D.S. Celermajer, P.J. Barter, K.-A. Rye, and A.K. Heather, *High density lipoproteins improve insulin sensitivity in high-fat diet-fed mice by suppressing hepatic inflammation.* Journal of Lipid Research, 2014. **55**(3): p. 421-430.
407. Drayna, D., A.S. Jarnagin, J. McLean, W. Henzel, W. Kohr, C. Fielding, and R. Lawn, *Cloning and sequencing of human cholesteryl ester transfer protein cDNA.* Nature, 1987. **327**(6123): p. 632-4.
408. Hesler, C.B., T.L. Swenson, and A.R. Tall, *Purification and characterization of a human plasma cholesteryl ester transfer protein.* J Biol Chem, 1987. **262**(5): p. 2275-82.
409. Barter, P.J. and K.A. Rye, *Cholesteryl ester transfer protein inhibition as a strategy to reduce cardiovascular risk.* J Lipid Res, 2012. **53**(9): p. 1755-66.
410. Barter, P., *Lessons learned from the Investigation of Lipid Level Management to Understand its Impact in Atherosclerotic Events (ILLUMINATE) trial.* Am J Cardiol, 2009. **104**(10 Suppl): p. 10E-5E.
411. Schwartz, G.G., A.G. Olsson, M. Abt, C.M. Ballantyne, P.J. Barter, J. Brumm, B.R. Chaitman, I.M. Holme, D. Kallend, L.A. Leiter, E. Leitersdorf, J.J. McMurray, H. Mundl, S.J. Nicholls, P.K. Shah, J.C. Tardif, R.S. Wright, and O.I. dal, *Effects of dalcetrapib in patients with a recent acute coronary syndrome.* N Engl J Med, 2012. **367**(22): p. 2089-99.
412. Nicholls, S.J., H.B. Brewer, J.J. Kastelein, K.A. Krueger, M.D. Wang, M. Shao, B. Hu, E. McErlean, and S.E. Nissen, *Effects of the CETP inhibitor evacetrapib administered as monotherapy or in combination with statins on HDL and LDL cholesterol: a randomized controlled trial.* JAMA, 2011. **306**(19): p. 2099-109.
413. Di Bartolo, B., K. Takata, M. Duong, and S.J. Nicholls, *CETP Inhibition in CVD Prevention: an Actual Appraisal.* Current Cardiology Reports, 2016. **18**(5): p. 1-6.
414. Navab, M., S.Y. Hama, G.P. Hough, G. Subbanagounder, S.T. Reddy, and A.M. Fogelman, *A cell-free assay for detecting HDL that is dysfunctional in preventing the formation of or inactivating oxidized phospholipids.* Journal of Lipid Research, 2001. **42**(8): p. 1308-1317.
415. Khovidhunkit, W., M.S. Kim, R.A. Memon, J.K. Shigenaga, A.H. Moser, K.R. Feingold, and C. Grunfeld, *Effects of infection and inflammation on lipid and lipoprotein metabolism: mechanisms and consequences to the host.* J Lipid Res, 2004. **45**(7): p. 1169-96.
416. Esteve, E., W. Ricart, and J.M. Fernández-Real, *Dyslipidemia and inflammation: an evolutionary conserved mechanism.* Clinical Nutrition, 2005. **24**(1): p. 16-31.
417. Balstad, T.R., K.B. Holven, I.O. Ottestad, K. Otterdal, B. Halvorsen, A.M. Myhre, L. Ose, and M.S. Nenseter, *Altered composition of HDL3 in FH subjects causing a HDL subfraction with less atheroprotective function.* Clinica Chimica Acta, 2005. **359**(1–2): p. 171-178.
418. Holzer, M., R. Birner-Gruenberger, T. Stojakovic, D. El-Gamal, V. Binder, C. Wadsack, A. Heinemann, and G. Marsche, *Uremia Alters HDL Composition and Function.* Journal of the American Society of Nephrology, 2011. **22**(9): p. 1631-1641.
419. Waterham, H.R., J. Koster, G.J. Romeijn, R.C. Hennekam, P. Vreken, H.C. Andersson, D.R. FitzPatrick, R.I. Kelley, and R.J. Wanders, *Mutations in the 3beta-hydroxysterol Delta24-reductase gene cause desmosterolosis, an autosomal recessive disorder of cholesterol biosynthesis.* Am J Hum Genet, 2001. **69**(4): p. 685-94.
420. Di Stasi, D., V. Vallacchi, V. Campi, T. Ranzani, M. Daniotti, E. Chiodini, S. Fiorentini, I. Greeve, A. Prinetti, L. Rivoltini, M.A. Pierotti, and M. Rodolfo, *DHCR24 gene expression is upregulated in melanoma metastases and associated to resistance to oxidative stress-induced apoptosis.* Int J Cancer, 2005. **115**(2): p. 224-30.

421. Greeve, I., I. Hermans-Borgmeyer, C. Brellinger, D. Kasper, T. Gomez-Isla, C. Behl, B. Levkau, and R.M. Nitsch, *The human DIMINUTO/DWARF1 homolog seladin-1 confers resistance to Alzheimer's disease-associated neurodegeneration and oxidative stress.* J Neurosci, 2000. **20**(19): p. 7345-52.
422. Wu, B.J., K. Chen, S. Shrestha, K.L. Ong, P.J. Barter, and K.A. Rye, *High Density Lipoproteins Inhibit Vascular Endothelial Inflammation by Increasing 3beta-Hydroxysteroid-{Delta}24 Reductase Expression and Inducing Heme Oxygenase-1.* Circ Res, 2012.
423. Wu, C., I. Miloslavskaya, S. Demontis, R. Maestro, and K. Galaktionov, *Regulation of cellular response to oncogenic and oxidative stress by Seladin-1.* Nature, 2004. **432**(7017): p. 640-5.
424. Motoyama, K., K. Kameyama, R. Onodera, N. Araki, F. Hirayama, K. Uekama, and H. Arima, *Involvement of PI3K-Akt-Bad pathway in apoptosis induced by 2,6-di-O-methyl-beta-cyclodextrin, not 2,6-di-O-methyl-alpha-cyclodextrin, through cholesterol depletion from lipid rafts on plasma membranes in cells.* Eur J Pharm Sci, 2009. **38**(3): p. 249-61.
425. Benvenuti, S., P. Luciani, G.B. Vannelli, S. Gelmini, E. Franceschi, M. Serio, and A. Peri, *Estrogen and selective estrogen receptor modulators exert neuroprotective effects and stimulate the expression of selective Alzheimer's disease indicator-1, a recently discovered antiapoptotic gene, in human neuroblast long-term cell cultures.* J Clin Endocrinol Metab, 2005. **90**(3): p. 1775-82.
426. Luciani, P., C. Deledda, F. Rosati, S. Benvenuti, I. Cellai, F. Dichiara, M. Morello, G.B. Vannelli, G. Danza, M. Serio, and A. Peri, *Seladin-1 is a fundamental mediator of the neuroprotective effects of estrogen in human neuroblast long-term cell cultures.* Endocrinology, 2008. **149**(9): p. 4256-66.
427. Luciani, P., S. Gelmini, E. Ferrante, A. Lania, S. Benvenuti, S. Baglioni, G. Mantovani, I. Cellai, F. Ammannati, A. Spada, M. Serio, and A. Peri, *Expression of the antiapoptotic gene seladin-1 and octreotide-induced apoptosis in growth hormone-secreting and nonfunctioning pituitary adenomas.* J Clin Endocrinol Metab, 2005. **90**(11): p. 6156-61.
428. Iivonen, S., M. Hiltunen, I. Alafuzoff, A. Mannermaa, P. Kerokoski, J. Puoliväli, A. Salminen, S. Helisalmi, and H. Soininen, *Seladin-1 transcription is linked to neuronal degeneration in Alzheimer's disease.* Neuroscience, 2002. **113**(2): p. 301-310.
429. Mushegian, A.R. and E.V. Koonin, *A putative FAD-binding domain in a distinct group of oxidases including a protein involved in plant development.* Protein Sci, 1995. **4**(6): p. 1243-4.
430. Klahre, U., T. Noguchi, S. Fujioka, S. Takatsuto, T. Yokota, T. Nomura, S. Yoshida, and N.H. Chua, *The Arabidopsis DIMINUTO/DWARF1 gene encodes a protein involved in steroid synthesis.* Plant Cell, 1998. **10**(10): p. 1677-90.
431. Arnold, S.E., B.T. Hyman, J. Flory, A.R. Damasio, and G.W. Van Hoesen, *The topographical and neuroanatomical distribution of neurofibrillary tangles and neuritic plaques in the cerebral cortex of patients with Alzheimer's disease.* Cereb Cortex, 1991. **1**(1): p. 103-16.
432. Van Hoesen, G.W., B.T. Hyman, and A.R. Damasio, *Entorhinal cortex pathology in Alzheimer's disease.* Hippocampus, 1991. **1**(1): p. 1-8.
433. Crameri, A., E. Biondi, K. Kuehnle, D. Lutjohann, K.M. Thelen, S. Perga, C.G. Dotti, R.M. Nitsch, M.D. Ledesma, and M.H. Mohajeri, *The role of seladin-1/DHCR24 in cholesterol biosynthesis, APP processing and Abeta generation in vivo.* EMBO J, 2006. **25**(2): p. 432-43.
434. Mirza, R., S. Hayasaka, Y. Takagishi, F. Kambe, S. Ohmori, K. Maki, M. Yamamoto, K. Murakami, T. Kaji, D. Zadworny, Y. Murata, and H. Seo, *DHCR24 gene knockout mice*

demonstrate lethal dermopathy with differentiation and maturation defects in the epidermis. J Invest Dermatol, 2006. **126**(3): p. 638-47.

435. Waterham, H.R., J. Koster, G.J. Romeijn, R.C.M. Hennekam, P. Vreken, H.C. Andersson, D.R. FitzPatrick, R.I. Kelley, and R.J.A. Wanders, *Mutations in the 3β-Hydroxysterol Δ24-Reductase Gene Cause Desmosterolosis, an Autosomal Recessive Disorder of Cholesterol Biosynthesis.* The American Journal of Human Genetics, 2001. **69**(4): p. 685-694.
436. van Himbergen, T.M., S. Otokozawa, N.R. Matthan, E.J. Schaefer, A. Buchsbaum, M. Ai, L.J. van Tits, J. de Graaf, and A.F. Stalenhoef, *Familial combined hyperlipidemia is associated with alterations in the cholesterol synthesis pathway.* Arterioscler Thromb Vasc Biol, 2010. **30**(1): p. 113-20.
437. Lu, X., F. Kambe, X. Cao, Y. Kozaki, T. Kaji, T. Ishii, and H. Seo, *3beta-Hydroxysteroid-delta24 reductase is a hydrogen peroxide scavenger, protecting cells from oxidative stress-induced apoptosis.* Endocrinology, 2008. **149**(7): p. 3267-73.
438. Cecchi, C., F. Rosati, A. Pensalfini, L. Formigli, D. Nosi, G. Liguri, F. Dichiara, M. Morello, G. Danza, G. Pieraccini, A. Peri, M. Serio, and M. Stefani, *Seladin-1/DHCR24 protects neuroblastoma cells against Abeta toxicity by increasing membrane cholesterol content.* J Cell Mol Med, 2008. **12**(5B): p. 1990-2002.
439. Olender, E.H. and R.D. Simon, *The intracellular targeting and membrane topology of 3-hydroxy-3-methylglutaryl-CoA reductase.* J Biol Chem, 1992. **267**(6): p. 4223-35.
440. Clayton, P., K. Mills, J. Keeling, and D. FitzPatrick, *Desmosterolosis: a new inborn error of cholesterol biosynthesis.* Lancet, 1996. **348**(9024): p. 404.
441. Schaaf, C.P., J. Koster, P. Katsonis, L. Kratz, O.A. Shchelochkov, F. Scaglia, R.I. Kelley, O. Lichtarge, H.R. Waterham, and M. Shinawi, *Desmosterolosis-phenotypic and molecular characterization of a third case and review of the literature.* Am J Med Genet A, 2011. **155A**(7): p. 1597-604.
442. Andersson, H.C., L. Kratz, and R. Kelley, *Desmosterolosis presenting with multiple congenital anomalies and profound developmental delay.* Am J Med Genet, 2002. **113**(4): p. 315-9.
443. FitzPatrick, D.R., J.W. Keeling, M.J. Evans, A.E. Kan, J.E. Bell, M.E. Porteous, K. Mills, R.M. Winter, and P.T. Clayton, *Clinical phenotype of desmosterolosis.* Am J Med Genet, 1998. **75**(2): p. 145-52.
444. Dias, C., R. Rupps, B. Millar, K. Choi, M. Marra, M. Demos, L.E. Kratz, and C.F. Boerkoel, *Desmosterolosis: an illustration of diagnostic ambiguity of cholesterol synthesis disorders.* Orphanet J Rare Dis, 2014. **9**: p. 94.
445. Dias, C., R. Rupps, B. Millar, K. Choi, M. Marra, M. Demos, L. Kratz, and C. Boerkoel, *Desmosterolosis: an illustration of diagnostic ambiguity of cholesterol synthesis disorders.* Orphanet Journal of Rare Diseases, 2014. **9**(1): p. 94.
446. Waterham, H.R., *Defects of cholesterol biosynthesis.* FEBS Lett, 2006. **580**(23): p. 5442-9.
447. Wechsler, A., A. Brafman, M. Shafir, M. Heverin, H. Gottlieb, G. Damari, S. Gozlan-Kelner, I. Spivak, O. Moshkin, E. Fridman, Y. Becker, R. Skaliter, P. Einat, A. Faerman, I. Bjorkhem, and E. Feinstein, *Generation of viable cholesterol-free mice.* Science, 2003. **302**(5653): p. 2087.
448. Witsch-Baumgartner, M., B.U. Fitzky, M. Ogorelkova, H.G. Kraft, F.F. Moebius, H. Glossmann, U. Seedorf, G. Gillessen-Kaesbach, G.F. Hoffmann, P. Clayton, R.I. Kelley, and G. Utermann, *Mutational spectrum in the Delta7-sterol reductase gene and genotype-phenotype correlation in 84 patients with Smith-Lemli-Opitz syndrome.* Am J Hum Genet, 2000. **66**(2): p. 402-12.

449. Woollett, L.A., *The origins and roles of cholesterol and fatty acids in the fetus.* Curr Opin Lipidol, 2001. **12**(3): p. 305-12.
450. Witsch-Baumgartner, M., M. Gruber, H.G. Kraft, M. Rossi, P. Clayton, M. Giros, D. Haas, R.I. Kelley, M. Krajewska-Walasek, and G. Utermann, *Maternal apo E genotype is a modifier of the Smith-Lemli-Opitz syndrome.* J Med Genet, 2004. **41**(8): p. 577-84.
451. Hernandez-Jimenez, M., D. Martinez-Lopez, E. Gabande-Rodriguez, A. Martin-Segura, I. Lizasoain, M.D. Ledesma, C.G. Dotti, and M.A. Moro, *Seladin-1/DHCR24 Is Neuroprotective by Associating EAAT2 Glutamate Transporter to Lipid Rafts in Experimental Stroke.* Stroke, 2016. **47**(1): p. 206-13.
452. Samara, A., M. Galbiati, P. Luciani, C. Deledda, E. Messi, A. Peri, and R. Maggi, *Altered expression of 3-betahydroxysterol delta-24-reductase/selective Alzheimer's disease indicator-1 gene in Huntington's disease models.* Journal of Endocrinological Investigation, 2014. **37**(8): p. 729-737.
453. Kreilaus, F., A.S. Spiro, C.A. McLean, B. Garner, and A.M. Jenner, *Evidence for altered cholesterol metabolism in Huntington's disease post-mortem brain tissue.* Neuropathology and Applied Neurobiology, 2015: p. n/a-n/a.
454. Simpson, J.E., P.G. Ince, F.E. Matthews, P.J. Shaw, P.R. Heath, C. Brayne, C. Garwood, A. Higginbottom, S.B. Wharton, M.R.C.C. Function, and G. Ageing Neuropathology Study, *A neuronal DNA damage response is detected at the earliest stages of Alzheimer's neuropathology and correlates with cognitive impairment in the Medical Research Council's Cognitive Function and Ageing Study ageing brain cohort.* Neuropathol Appl Neurobiol, 2015. **41**(4): p. 483-96.
455. Benvenuti, S., C. Deledda, P. Luciani, G. Modi, A. Bossio, C. Giuliani, B. Fibbi, and A. Peri, *Low Extracellular Sodium Causes Neuronal Distress Independently of Reduced Osmolality in an Experimental Model of Chronic Hyponatremia.* NeuroMolecular Medicine, 2013. **15**(3): p. 493-503.
456. Benvenuti, S., C. Deledda, P. Luciani, C. Giuliani, B. Fibbi, M. Muratori, and A. Peri, *Neuronal distress induced by low extracellular sodium in vitro is partially reverted by the return to normal sodium.* Journal of Endocrinological Investigation, 2015: p. 1-8.
457. Blalock, E.M., J.W. Geddes, K.C. Chen, N.M. Porter, W.R. Markesbery, and P.W. Landfield, *Incipient Alzheimer's disease: microarray correlation analyses reveal major transcriptional and tumor suppressor responses.* Proc Natl Acad Sci U S A, 2004. **101**(7): p. 2173-8.
458. Sharpe, L.J., J. Wong, B. Garner, G.M. Halliday, and A.J. Brown, *Is seladin-1 really a selective Alzheimer's disease indicator?* J Alzheimers Dis, 2012. **30**(1): p. 35-9.
459. Lamsa, R., S. Helisalmi, M. Hiltunen, S.K. Herukka, T. Tapiola, T. Pirttila, S. Vepsalainen, and H. Soininen, *The association study between DHCR24 polymorphisms and Alzheimer's disease.* Am J Med Genet B Neuropsychiatr Genet, 2007. **144B**(7): p. 906-10.
460. Swaminathan, S., L. Shen, S.L. Risacher, K.K. Yoder, J.D. West, S. Kim, K. Nho, T. Foroud, M. Inlow, S.G. Potkin, M.J. Huentelman, D.W. Craig, W.J. Jagust, R.A. Koeppe, C.A. Mathis, C.R. Jack, Jr., M.W. Weiner, A.J. Saykin, and I. Alzheimer's Disease Neuroimaging, *Amyloid pathway-based candidate gene analysis of [(11)C]PiB-PET in the Alzheimer's Disease Neuroimaging Initiative (ADNI) cohort.* Brain Imaging Behav, 2012. **6**(1): p. 1-15.
461. Tedde, A., E. Cellini, S. Bagnoli, S. Sorbi, and A. Peri, *Mutational screening analysis of DHCR24/seladin-1 gene in Italian familial Alzheimer's disease.* Am J Med Genet B Neuropsychiatr Genet, 2008. **147B**(1): p. 117-9.
462. Saito, M., T. Takano, T. Nishimura, M. Kohara, and K. Tsukiyama-Kohara, *3beta-hydroxysterol delta24-reductase on the surface of hepatitis C virus-related*

hepatocellular carcinoma cells can be a target for molecular targeting therapy. PLoS One, 2015. **10**(4): p. e0124197.

463. Ezzikouri, S., K. Kimura, H. Sunagozaka, S. Kaneko, K. Inoue, T. Nishimura, T. Hishima, M. Kohara, and K. Tsukiyama-Kohara, *Serum DHCR24 Auto-antibody as a new Biomarker for Progression of Hepatitis C.* EBioMedicine, 2015. **2**(6): p. 604-12.
464. Romanuik, T.L., T. Ueda, N. Le, S. Haile, T.M.K. Yong, T. Thomson, R.L. Vessella, and M.D. Sadar, *Novel Biomarkers for Prostate Cancer Including Noncoding Transcripts.* The American Journal of Pathology, 2009. **175**(6): p. 2264-2276.
465. Hendriksen, P.J.M., N.F.J. Dits, K. Kokame, A. Veldhoven, W.M. van Weerden, C.H. Bangma, J. Trapman, and G. Jenster, *Evolution of the Androgen Receptor Pathway during Progression of Prostate Cancer.* Cancer Research, 2006. **66**(10): p. 5012-5020.
466. Battista, M.-C., M.-O. Guimond, C. Roberge, A.A. Doueik, L. Fazli, M. Gleave, R. Sabbagh, and N. Gallo-Payet, *Inhibition of DHCR24/Seladin-1 impairs cellular homeostasis in prostate cancer.* The Prostate, 2010. **70**(9): p. 921-933.
467. Lee, G., Y.-S. Ha, Y. Jung, S.-K. Moon, H. Kang, O.-J. Lee, J. Joung, Y. Choi, S.-J. Yun, W.-J. Kim, and I. Kim, *DHCR24 is an Independent Predictor of Progression in Patients with Non-Muscle-Invasive Urothelial Carcinoma, and Its Functional Role is Involved in the Aggressive Properties of Urothelial Carcinoma Cells.* Annals of Surgical Oncology, 2014. **21**(4): p. 538-545.
468. Frances, D., N. Sharma, R. Pofahl, M. Maneck, K. Behrendt, K. Reuter, T. Krieg, C.A. Klein, I. Haase, and C. Niemann, *A role for Rac1 activity in malignant progression of sebaceous skin tumors.* Oncogene, 2015. **34**(43): p. 5505-12.
469. Lu, X., Y. Li, W. Wang, S. Chen, T. Liu, D. Jia, X. Quan, D. Sun, A.K. Chang, and B. Gao, *3 beta-hydroxysteroid-Delta 24 reductase (DHCR24) protects neuronal cells from apoptotic cell death induced by endoplasmic reticulum (ER) stress.* PLoS One, 2014. **9**(1): p. e86753.
470. Tobiume, K., Matsuzawa Atsushi, Takahashi Takumi, Nishitoh Hideki, Morita Kei-ichi, Takeda Kohsuke, Minowa Osamu, Miyazono Kohei, Noda Tetsuo, Ichijoa Hidenori, *ASK1 is required for sustained activations of JNK/p38 MAP kinases and apoptosis.* EMBO Reports, 2001. **2**(3): p. 222-228.
471. Lu, X., F. Kambe, X. Cao, T. Yoshida, S. Ohmori, K. Murakami, T. Kaji, T. Ishii, D. Zadworny, and H. Seo, *DHCR24-knockout embryonic fibroblasts are susceptible to serum withdrawal-induced apoptosis because of dysfunction of caveolae and insulin-Akt-Bad signaling.* Endocrinology, 2006. **147**(6): p. 3123-32.
472. Battista, M.C., C. Roberge, A. Martinez, and N. Gallo-Payet, *24-dehydrocholesterol reductase/seladin-1: a key protein differentially involved in adrenocorticotropin effects observed in human and rat adrenal cortex.* Endocrinology, 2009. **150**(9): p. 4180-90.
473. Kuehnle, K., A. Crameri, R.E. Kalin, P. Luciani, S. Benvenuti, A. Peri, F. Ratti, M. Rodolfo, L. Kulic, F.L. Heppner, R.M. Nitsch, and M.H. Mohajeri, *Prosurvival effect of DHCR24/Seladin-1 in acute and chronic responses to oxidative stress.* Mol Cell Biol, 2008. **28**(2): p. 539-50.
474. Nofer, J.-R., B. Levkau, I. Wolinska, R. Junker, M. Fobker, A. von Eckardstein, U. Seedorf, and G. Assmann, *Suppression of Endothelial Cell Apoptosis by High Density Lipoproteins (HDL) and HDL-associated Lysosphingolipids.* Journal of Biological Chemistry, 2001. **276**(37): p. 34480-34485.
475. Lu, X., F. Kambe, X. Cao, T. Yoshida, S. Ohmori, K. Murakami, T. Kaji, T. Ishii, D. Zadworny, and H. Seo, *DHCR24-Knockout Embryonic Fibroblasts Are Susceptible to Serum Withdrawal-Induced Apoptosis Because of Dysfunction of Caveolae and Insulin-Akt-Bad Signaling.* Endocrinology, 2006. **147**(6): p. 3123-3132.

476. Osborne, J.C., Jr., *Delipidation of plasma lipoproteins.* Methods Enzymol, 1986. **128**: p. 213-22.
477. Matz, C.E. and A. Jonas, *Micellar complexes of human apolipoprotein AI with phosphatidylcholines and cholesterol prepared from cholate-lipid dispersions.* Journal of Biological Chemistry, 1982. **257**(8): p. 4535-4540.
478. Livak, K.J. and T.D. Schmittgen, *Analysis of relative gene expression data using real-time quantitative PCR and the 2(-Delta Delta C(T)) Method.* Methods, 2001. **25**(4): p. 402-8.
479. Go, A.S., D. Mozaffarian, V.L. Roger, E.J. Benjamin, J.D. Berry, M.J. Blaha, S. Dai, E.S. Ford, C.S. Fox, and S. Franco, *Heart disease and stroke statistics-2014 update.* Circulation, 2014. **129**(3).
480. Hansson, G.K., *Inflammation, atherosclerosis, and coronary artery disease.* N Engl J Med, 2005. **352**(16): p. 1685-95.
481. Kim, C.S., H.S. Park, T. Kawada, J.H. Kim, D. Lim, N.E. Hubbard, B.S. Kwon, K.L. Erickson, and R. Yu, *Circulating levels of MCP-1 and IL-8 are elevated in human obese subjects and associated with obesity-related parameters.* Int J Obes, 2006. **30**(9): p. 1347-1355.
482. Bruun, J., C. Verdich, S. Toubro, A. Astrup, and B. Richelsen, *Association between measures of insulin sensitivity and circulating levels of interleukin-8, interleukin-6 and tumor necrosis factor-alpha. Effect of weight loss in obese men.* European Journal of Endocrinology, 2003. **148**(5): p. 535-542.
483. Straczkowski, M., S. Dzienis-Straczkowska, A. Stêpieñ, I. Kowalska, M. Szelachowska, and I. Kinalska, *Plasma Interleukin-8 Concentrations Are Increased in Obese Subjects and Related to Fat Mass and Tumor Necrosis Factor-α System.* The Journal of Clinical Endocrinology & Metabolism, 2002. **87**(10): p. 4602-4606.
484. Park, H.S., J.Y. Park, and R. Yu, *Relationship of obesity and visceral adiposity with serum concentrations of CRP, TNF-α and IL-6.* Diabetes Research and Clinical Practice, 2005. **69**(1): p. 29-35.
485. Curat, C.A., V. Wegner, C. Sengenès, A. Miranville, C. Tonus, R. Busse, and A. Bouloumié, *Macrophages in human visceral adipose tissue: increased accumulation in obesity and a source of resistin and visfatin.* Diabetologia, 2006. **49**(4): p. 744-747.
486. Głowińska, B. and M. Urban, *[Selected cytokines (Il-6, Il-8, Il-10, MCP-1, TNF-alpha) in children and adolescents with atherosclerosis risk factors: obesity, hypertension, diabetes].* Wiadomosci lekarskie (Warsaw, Poland : 1960), 2003. **56**(3-4): p. 109-116.
487. O'Brien, K.D., M.D. Allen, T.O. McDonald, A. Chait, J.M. Harlan, D. Fishbein, J. McCarty, M. Ferguson, K. Hudkins, C.D. Benjamin, and et al., *Vascular cell adhesion molecule-1 is expressed in human coronary atherosclerotic plaques. Implications for the mode of progression of advanced coronary atherosclerosis.* J Clin Invest, 1993. **92**(2): p. 945-51.
488. Ramos, C.L., Y. Huo, U. Jung, S. Ghosh, D.R. Manka, I.J. Sarembock, and K. Ley, *Direct demonstration of P-selectin- and VCAM-1-dependent mononuclear cell rolling in early atherosclerotic lesions of apolipoprotein E-deficient mice.* Circ Res, 1999. **84**(11): p. 1237-44.
489. Ley, K. and Y. Huo, *VCAM-1 is critical in atherosclerosis.* J Clin Invest, 2001. **107**(10): p. 1209-10.
490. Gordon, D.J. and B.M. Rifkind, *High-Density Lipoprotein — The Clinical Implications of Recent Studies.* New England Journal of Medicine, 1989. **321**(19): p. 1311-1316.
491. Assmann, G. and J.R. Nofer, *Atheroprotective effects of high-density lipoproteins.* Annu Rev Med, 2003. **54**: p. 321-41.
492. Mineo, C., H. Deguchi, J.H. Griffin, and P.W. Shaul, *Endothelial and Antithrombotic Actions of HDL.* Circulation Research, 2006. **98**(11): p. 1352-1364.

493. Duffy, D. and D.J. Rader, *Update on strategies to increase HDL quantity and function.* Nat Rev Cardiol, 2009. **6**(7): p. 455-63.
494. Bursill, C.A., M.L. Castro, D.T. Beattie, S. Nakhla, E. van der Vorst, A.K. Heather, P.J. Barter, and K.A. Rye, *High-density lipoproteins suppress chemokines and chemokine receptors in vitro and in vivo.* Arterioscler Thromb Vasc Biol, 2010. **30**(9): p. 1773-8.
495. Patel, S., B.A. Di Bartolo, S. Nakhla, A.K. Heather, T.W. Mitchell, W. Jessup, D.S. Celermajer, P.J. Barter, and K.-A. Rye, *Anti-inflammatory effects of apolipoprotein A-I in the rabbit.* Atherosclerosis, 2010. **212**(2): p. 392-397.
496. Tabet, F., A.T. Remaley, A.I. Segaliny, J. Millet, L. Yan, S. Nakhla, P.J. Barter, K.-A. Rye, and G. Lambert, *The 5A Apolipoprotein A-I Mimetic Peptide Displays Antiinflammatory and Antioxidant Properties In Vivo and In Vitro.* Arteriosclerosis, Thrombosis, and Vascular Biology, 2010. **30**(2): p. 246-252.
497. Rutledge, J.C., A.E. Mullick, G. Gardner, and I.J. Goldberg, *Direct Visualization of Lipid Deposition and Reverse Lipid Transport in a Perfused Artery: Roles of VLDL and HDL.* Circulation Research, 2000. **86**(7): p. 768-773.
498. Badimon, J.J., L. Badimon, and V. Fuster, *Regression of atherosclerotic lesions by high density lipoprotein plasma fraction in the cholesterol-fed rabbit.* Journal of Clinical Investigation, 1990. **85**(4): p. 1234-1241.
499. Shaw, J.A., A. Bobik, A. Murphy, P. Kanellakis, P. Blombery, N. Mukhamedova, K. Woollard, S. Lyon, D. Sviridov, and A.M. Dart, *Infusion of Reconstituted High-Density Lipoprotein Leads to Acute Changes in Human Atherosclerotic Plaque.* Circulation Research, 2008. **103**(10): p. 1084-1091.
500. Feig, J.E., J.X. Rong, R. Shamir, M. Sanson, Y. Vengrenyuk, J. Liu, K. Rayner, K. Moore, M. Garabedian, and E.A. Fisher, *HDL promotes rapid atherosclerosis regression in mice and alters inflammatory properties of plaque monocyte-derived cells.* Proceedings of the National Academy of Sciences, 2011. **108**(17): p. 7166-7171.
501. Puranik, R., S. Bao, E. Nobecourt, S.J. Nicholls, G.J. Dusting, P.J. Barter, D.S. Celermajer, and K.A. Rye, *Low dose apolipoprotein A-I rescues carotid arteries from inflammation in vivo.* Atherosclerosis, 2008. **196**(1): p. 240-7.
502. Chiesa, G., E. Monteggia, M. Marchesi, P. Lorenzon, M. Laucello, V. Lorusso, C. Di Mario, E. Karvouni, R.S. Newton, C.L. Bisgaier, G. Franceschini, and C.R. Sirtori, *Recombinant Apolipoprotein A-IMilano Infusion Into Rabbit Carotid Artery Rapidly Removes Lipid From Fatty Streaks.* Circulation Research, 2002. **90**(9): p. 974-980.
503. Di Bartolo, B.A., L.Z. Vanags, J.T. Tan, S. Bao, K.-A. Rye, P.J. Barter, and C.A. Bursill, *The apolipoprotein A-I mimetic peptide, ETC-642, reduces chronic vascular inflammation in the rabbit.* Lipids in Health and Disease, 2011. **10**(1): p. 1-8.
504. Tardy, C., M. Goffinet, N. Boubekeur, R. Ackermann, G. Sy, A. Bluteau, G. Cholez, C. Keyserling, N. Lalwani, J.F. Paolini, J.-L. Dasseux, R. Barbaras, and R. Baron, *CER-001, a HDL-mimetic, stimulates the reverse lipid transport and atherosclerosis regression in high cholesterol diet-fed LDL-receptor deficient mice.* Atherosclerosis, 2014. **232**(1): p. 110-118.
505. Ou, J., J. Wang, H. Xu, Z. Ou, M.G. Sorci-Thomas, D.W. Jones, P. Signorino, J.C. Densmore, S. Kaul, K.T. Oldham, and K.A. Pritchard, *Effects of D-4F on Vasodilation and Vessel Wall Thickness in Hypercholesterolemic LDL Receptor–Null and LDL Receptor/Apolipoprotein A-I Double-Knockout Mice on Western Diet.* Circulation Research, 2005. **97**(11): p. 1190-1197.
506. Shah, P.K., J. Nilsson, S. Kaul, M.C. Fishbein, H. Ageland, A. Hamsten, J. Johansson, F. Karpe, and B. Cercek, *Effects of Recombinant Apolipoprotein A-IMilano on Aortic Atherosclerosis in Apolipoprotein E–Deficient Mice.* Circulation, 1998. **97**(8): p. 780-785.

507. Morgantini, C., S. Imaizumi, V. Grijalva, M. Navab, A.M. Fogelman, and S.T. Reddy, *Apolipoprotein A-I Mimetic Peptides Prevent Atherosclerosis Development and Reduce Plaque Inflammation in a Murine Model of Diabetes.* Diabetes, 2010. **59**(12): p. 3223-3228.
508. Uehara, Y., S. Ando, E. Yahiro, K. Oniki, M. Ayaori, S. Abe, E. Kawachi, B. Zhang, S. Shioi, H. Tanigawa, S. Imaizumi, S.-i. Miura, and K. Saku, *FAMP, a Novel ApoA-I Mimetic Peptide, Suppresses Aortic Plaque Formation Through Promotion of Biological HDL Function in ApoE-Deficient Mice.* Journal of the American Heart Association, 2013. **2**(3).
509. Nissen, S.E., T. Tsunoda, E.M. Tuzcu, P. Schoenhagen, C.J. Cooper, M. Yasin, G.M. Eaton, M.A. Lauer, W.S. Sheldon, C.L. Grines, S. Halpern, T. Crowe, J.C. Blankenship, and R. Kerensky, *Effect of recombinant ApoA-I Milano on coronary atherosclerosis in patients with acute coronary syndromes: a randomized controlled trial.* JAMA, 2003. **290**(17): p. 2292-300.
510. Li, X., K.-Y. Chyu, J.R.F. Neto, J. Yano, N. Nathwani, C. Ferreira, P.C. Dimayuga, B. Cercek, S. Kaul, and P.K. Shah, *Differential Effects of Apolipoprotein A-I–Mimetic Peptide on Evolving and Established Atherosclerosis in Apolipoprotein E-Null Mice.* Circulation, 2004. **110**(12): p. 1701-1705.
511. Navab, M., G.M. Anantharamaiah, S. Hama, D.W. Garber, M. Chaddha, G. Hough, R. Lallone, and A.M. Fogelman, *Oral Administration of an Apo A-I Mimetic Peptide Synthesized From D-Amino Acids Dramatically Reduces Atherosclerosis in Mice Independent of Plasma Cholesterol.* Circulation, 2002. **105**(3): p. 290-292.
512. Rader, D.J. and A.R. Tall, *The not-so-simple HDL story: Is it time to revise the HDL cholesterol hypothesis?* Nat Med, 2012. **18**(9): p. 1344-6.
513. Oram, J.F., R.M. Lawn, M.R. Garvin, and D.P. Wade, *ABCA1 is the cAMP-inducible apolipoprotein receptor that mediates cholesterol secretion from macrophages.* J Biol Chem, 2000. **275**(44): p. 34508-11.
514. Santamarina-Fojo, S., K. Peterson, C. Knapper, Y. Qiu, L. Freeman, J.F. Cheng, J. Osorio, A. Remaley, X.P. Yang, C. Haudenschild, C. Prades, G. Chimini, E. Blackmon, T. Francois, N. Duverger, E.M. Rubin, M. Rosier, P. Denefle, D.S. Fredrickson, and H.B. Brewer, Jr., *Complete genomic sequence of the human ABCA1 gene: analysis of the human and mouse ATP-binding cassette A promoter.* Proc Natl Acad Sci U S A, 2000. **97**(14): p. 7987-92.
515. Wang, N., D. Lan, W. Chen, F. Matsuura, and A.R. Tall, *ATP-binding cassette transporters G1 and G4 mediate cellular cholesterol efflux to high-density lipoproteins.* Proc Natl Acad Sci U S A, 2004. **101**(26): p. 9774-9.
516. Nakamura, K., M.A. Kennedy, A. Baldan, D.D. Bojanic, K. Lyons, and P.A. Edwards, *Expression and regulation of multiple murine ATP-binding cassette transporter G1 mRNAs/isoforms that stimulate cellular cholesterol efflux to high density lipoprotein.* J Biol Chem, 2004. **279**(44): p. 45980-9.
517. Acton, S., A. Rigotti, K.T. Landschulz, S. Xu, H.H. Hobbs, and M. Krieger, *Identification of Scavenger Receptor SR-BI as a High Density Lipoprotein Receptor.* Science, 1996. **271**(5248): p. 518-520.
518. Ji, Y., B. Jian, N. Wang, Y. Sun, M.L. Moya, M.C. Phillips, G.H. Rothblat, J.B. Swaney, and A.R. Tall, *Scavenger receptor BI promotes high density lipoprotein-mediated cellular cholesterol efflux.* J Biol Chem, 1997. **272**(34): p. 20982-5.
519. Yancey, P.G., M.A. Kawashiri, R. Moore, J.M. Glick, D.L. Williams, M.A. Connelly, D.J. Rader, and G.H. Rothblat, *In vivo modulation of HDL phospholipid has opposing effects on SR-BI- and ABCA1-mediated cholesterol efflux.* J Lipid Res, 2004. **45**(2): p. 337-46.

520. Mackness, M.I., S. Arrol, C. Abbott, and P.N. Durrington, *Protection of low-density lipoprotein against oxidative modification by high-density lipoprotein associated paraoxonase.* Atherosclerosis, 1993. **104**(1-2): p. 129-35.
521. Yuhanna, I.S., Y. Zhu, B.E. Cox, L.D. Hahner, S. Osborne-Lawrence, P. Lu, Y.L. Marcel, R.G. Anderson, M.E. Mendelsohn, H.H. Hobbs, and P.W. Shaul, *High-density lipoprotein binding to scavenger receptor-BI activates endothelial nitric oxide synthase.* Nat Med, 2001. **7**(7): p. 853-7.
522. Suc, I., I. Escargueil-Blanc, M. Troly, R. Salvayre, and A. Negre-Salvayre, *HDL and ApoA prevent cell death of endothelial cells induced by oxidized LDL.* Arterioscler Thromb Vasc Biol, 1997. **17**(10): p. 2158-66.
523. de Souza, J.A., C. Vindis, A. Negre-Salvayre, K.A. Rye, M. Couturier, P. Therond, S. Chantepie, R. Salvayre, M.J. Chapman, and A. Kontush, *Small, dense HDL 3 particles attenuate apoptosis in endothelial cells: pivotal role of apolipoprotein A-I.* J Cell Mol Med, 2010. **14**(3): p. 608-20.
524. Sugano, M., K. Tsuchida, and N. Makino, *High-Density Lipoproteins Protect Endothelial Cells from Tumor Necrosis Factor-α-Induced Apoptosis.* Biochemical and Biophysical Research Communications, 2000. **272**(3): p. 872-876.
525. Riwanto, M., L. Rohrer, B. Roschitzki, C. Besler, P. Mocharla, M. Mueller, D. Perisa, K. Heinrich, L. Altwegg, A. von Eckardstein, T.F. Lüscher, and U. Landmesser, *Altered Activation of Endothelial Anti- and Pro-Apoptotic Pathways by High-Density Lipoprotein from Patients with Coronary Artery Disease: Role of HDL-Proteome Remodeling.* Circulation, 2013.
526. Rye, K.A., M.A. Clay, and P.J. Barter, *Remodelling of high density lipoproteins by plasma factors.* Atherosclerosis, 1999. **145**(2): p. 227-38.
527. Taylor, F., M.D. Huffman, A.F. Macedo, T.H. Moore, M. Burke, G. Davey Smith, K. Ward, and S. Ebrahim, *Statins for the primary prevention of cardiovascular disease.* Cochrane Database Syst Rev, 2013. **1**: p. CD004816.
528. de Haan, W., C.C. van der Hoogt, M. Westerterp, M. Hoekstra, G.M. Dallinga-Thie, H.M.G. Princen, J.A. Romijn, J.W. Jukema, L.M. Havekes, and P.C.N. Rensen, *Atorvastatin increases HDL cholesterol by reducing CETP expression in cholesterol-fed APOE*3-Leiden.CETP mice.* Atherosclerosis, 2008. **197**(1): p. 57-63.
529. Ballantyne, C.M., J. Houri, A. Notarbartolo, L. Melani, L.J. Lipka, R. Suresh, S. Sun, A.P. LeBeaut, P.T. Sager, E.P. Veltri, and G. Ezetimibe Study, *Effect of ezetimibe coadministered with atorvastatin in 628 patients with primary hypercholesterolemia: a prospective, randomized, double-blind trial.* Circulation, 2003. **107**(19): p. 2409-15.
530. Heart Protection Study Collaborative, G., *MRC/BHF Heart Protection Study of cholesterol lowering with simvastatin in 20,536 high-risk individuals: a randomised placebo-controlled trial.* Lancet, 2002. **360**(9326): p. 7-22.
531. Nissen, S.E., E. Tuzcu, P. Schoenhagen, and et al., *Effect of intensive compared with moderate lipid-lowering therapy on progression of coronary atherosclerosis: A randomized controlled trial.* JAMA, 2004. **291**(9): p. 1071-1080.
532. Davidson, M.H., *Reducing Residual Risk for Patients on Statin Therapy: The Potential Role of Combination Therapy.* The American Journal of Cardiology, 2005. **96**(9, Supplement 1): p. 3-13.
533. Ridker, P.M., J. Genest, S.M. Boekholdt, P. Libby, A.M. Gotto, B.G. Nordestgaard, S. Mora, J.G. MacFadyen, R.J. Glynn, and J.J.P. Kastelein, *HDL cholesterol and residual risk of first cardiovascular events after treatment with potent statin therapy: an analysis from the JUPITER trial.* The Lancet, 2010. **376**(9738): p. 333-339.
534. Baigent, C., L. Blackwell, J. Emberson, L. Holland, C. Reith, N. Bhala, R. Peto, E. Barnes, A. Keech, and J. Simes, *Efficacy and safety of more intensive lowering of LDL*

cholesterol: a meta-analysis of data from 170,000 participants in 26 randomised trials. Lancet (London, England), 2010. **376**(9753): p. 1670-1681.

535. Mora, S., R.J. Glynn, and P.M. Ridker, *HDL Cholesterol, Size, Particle Number, and Residual Vascular Risk after Potent Statin Therapy.* Circulation, 2013.
536. Brown, M.L., A. Inazu, C.B. Hesler, L.B. Agellon, C. Mann, M.E. Whitlock, Y.L. Marcel, R.W. Milne, J. Koizumi, H. Mabuchi, and et al., *Molecular basis of lipid transfer protein deficiency in a family with increased high-density lipoproteins.* Nature, 1989. **342**(6248): p. 448-51.
537. Ritsch, A., H. Drexel, F.W. Amann, C. Pfeifhofer, and J.R. Patsch, *Deficiency of cholesteryl ester transfer protein. Description of the molecular defect and the dissociation of cholesteryl ester and triglyceride transport in plasma.* Arterioscler Thromb Vasc Biol, 1997. **17**(12): p. 3433-41.
538. Maruyama, T., N. Sakai, M. Ishigami, K. Hirano, T. Arai, S. Okada, E. Okuda, A. Ohya, N. Nakajima, K. Kadowaki, E. Fushimi, S. Yamashita, and Y. Matsuzawa, *Prevalence and phenotypic spectrum of cholesteryl ester transfer protein gene mutations in Japanese hyperalphalipoproteinemia.* Atherosclerosis, 2003. **166**(1): p. 177-85.
539. Pirim, D., X. Wang, V. Niemsiri, Z.H. Radwan, C.H. Bunker, J.E. Hokanson, R.F. Hamman, M.M. Barmada, F.Y. Demirci, and M.I. Kamboh, *Resequencing of the CETP gene in American whites and African blacks: Association of rare and common variants with HDL-cholesterol levels.* Metabolism, 2016. **65**(1): p. 36-47.
540. de Grooth, G.J., J.A. Kuivenhoven, A.F. Stalenhoef, J. de Graaf, A.H. Zwinderman, J.L. Posma, A. van Tol, and J.J. Kastelein, *Efficacy and safety of a novel cholesteryl ester transfer protein inhibitor, JTT-705, in humans: a randomized phase II dose-response study.* Circulation, 2002. **105**(18): p. 2159-65.
541. Barter, P.J., M. Caulfield, M. Eriksson, S.M. Grundy, J.J. Kastelein, M. Komajda, J. Lopez-Sendon, L. Mosca, J.C. Tardif, D.D. Waters, C.L. Shear, J.H. Revkin, K.A. Buhr, M.R. Fisher, A.R. Tall, B. Brewer, and I. Investigators, *Effects of torcetrapib in patients at high risk for coronary events.* N Engl J Med, 2007. **357**(21): p. 2109-22.
542. Cannon, C.P., S. Shah, H.M. Dansky, M. Davidson, E.A. Brinton, A.M. Gotto, M. Stepanavage, S.X. Liu, P. Gibbons, T.B. Ashraf, J. Zafarino, Y. Mitchel, P. Barter, E. Determining the, and I. Tolerability, *Safety of anacetrapib in patients with or at high risk for coronary heart disease.* N Engl J Med, 2010. **363**(25): p. 2406-15.
543. Barter, P.J., S.J. Nicholls, J.J. Kastelein, and K.A. Rye, *Is Cholesteryl Ester Transfer Protein Inhibition an Effective Strategy to Reduce Cardiovascular Risk? CETP Inhibition as a Strategy to Reduce Cardiovascular Risk: The Pro Case.* Circulation, 2015. **132**(5): p. 423-32.
544. Wu, B.J., K. Chen, S. Shrestha, K.L. Ong, P.J. Barter, and K.A. Rye, *High-density lipoproteins inhibit vascular endothelial inflammation by increasing 3beta-hydroxysteroid-Delta24 reductase expression and inducing heme oxygenase-1.* Circ Res, 2013. **112**(2): p. 278-88.
545. Iivonen, S., M. Hiltunen, I. Alafuzoff, A. Mannermaa, P. Kerokoski, J. Puolivali, A. Salminen, S. Helisalmi, and H. Soininen, *Seladin-1 transcription is linked to neuronal degeneration in Alzheimer's disease.* Neuroscience, 2002. **113**(2): p. 301-10.
546. Shah, P.K., *Apolipoprotein A-I/HDL Infusion Therapy for Plaque Stabilization-Regression: A Novel Therapeutic Approach.* Current Pharmaceutical Design, 2007. **13**(10): p. 1031-1038.
547. Moudry, R., M.O. Spycher, and J.E. Doran, *RECONSTITUTED HIGH DENSITY LIPOPROTEIN MODULATES ADHERENCE OF POLYMORPHONUCLEAR LEUKOCYTES TO HUMAN ENDOTHELIAL CELLS.* Shock, 1997. **7**(3): p. 175-181.

548. Murphy, A.J., K.J. Woollard, A. Hoang, N. Mukhamedova, R.A. Stirzaker, S.P.A. McCormick, A.T. Remaley, D. Sviridov, and J. Chin-Dusting, *High-Density Lipoprotein Reduces the Human Monocyte Inflammatory Response.* Arteriosclerosis, Thrombosis, and Vascular Biology, 2008. **28**(11): p. 2071-2077.
549. Davies, M.J., J.L. Gordon, A.J.H. Gearing, R. Pigott, N. Woolf, D. Katz, and A. Kyriakopoulos, *The expression of the adhesion molecules ICAM-1, VCAM-1, PECAM, and E-selectin in human atherosclerosis.* The Journal of Pathology, 1993. **171**(3): p. 223-229.
550. Noutsias, M., B. Seeberg, H.-P. Schultheiss, and U. Kühl, *Expression of Cell Adhesion Molecules in Dilated Cardiomyopathy: Evidence for Endothelial Activation in Inflammatory Cardiomyopathy.* Circulation, 1999. **99**(16): p. 2124-2131.
551. Cockerill, G.W., K.-A. Rye, J.R. Gamble, M.A. Vadas, and P.J. Barter, *High-Density Lipoproteins Inhibit Cytokine-Induced Expression of Endothelial Cell Adhesion Molecules.* Arteriosclerosis, Thrombosis, and Vascular Biology, 1995. **15**(11): p. 1987-1994.
552. Nicholls, S.J., G.J. Dusting, B. Cutri, S. Bao, G.R. Drummond, K.A. Rye, and P.J. Barter, *Reconstituted high-density lipoproteins inhibit the acute pro-oxidant and proinflammatory vascular changes induced by a periarterial collar in normocholesterolemic rabbits.* Circulation, 2005. **111**(12): p. 1543-50.
553. Schmidt, A., S. Geigenmuller, W. Volker, and E. Buddecke, *The antiatherogenic and antiinflammatory effect of HDL-associated lysosphingolipids operates via Akt -->NF-kappaB signalling pathways in human vascular endothelial cells.* Basic Res Cardiol, 2006. **101**(2): p. 109-16.
554. Park, S.H., J.H. Park, J.S. Kang, and Y.H. Kang, *Involvement of transcription factors in plasma HDL protection against TNF-alpha-induced vascular cell adhesion molecule-1 expression.* Int J Biochem Cell Biol, 2003. **35**(2): p. 168-82.
555. Navab, M., S.S. Imes, S.Y. Hama, G.P. Hough, L.A. Ross, R.W. Bork, A.J. Valente, J.A. Berliner, D.C. Drinkwater, H. Laks, and et al., *Monocyte transmigration induced by modification of low density lipoprotein in cocultures of human aortic wall cells is due to induction of monocyte chemotactic protein 1 synthesis and is abolished by high density lipoprotein.* J Clin Invest, 1991. **88**(6): p. 2039-46.
556. Diederich, W., E. Orso, W. Drobnik, and G. Schmitz, *Apolipoprotein AI and HDL(3) inhibit spreading of primary human monocytes through a mechanism that involves cholesterol depletion and regulation of CDC42.* Atherosclerosis, 2001. **159**(2): p. 313-24.
557. Baker, P.W., K.A. Rye, J.R. Gamble, M.A. Vadas, and P.J. Barter, *Ability of reconstituted high density lipoproteins to inhibit cytokine-induced expression of vascular cell adhesion molecule-1 in human umbilical vein endothelial cells.* J Lipid Res, 1999. **40**(2): p. 345-53.
558. ØSTERUD, B. and E. BJØRKLID, *Role of Monocytes in Atherogenesis.* Physiological Reviews, 2003. **83**(4): p. 1069-1112.
559. Shih, P.T., M.-L. Brennan, D.K. Vora, M.C. Territo, D. Strahl, M.J. Elices, A.J. Lusis, and J.A. Berliner, *Blocking Very Late Antigen-4 Integrin Decreases Leukocyte Entry and Fatty Streak Formation in Mice Fed an Atherogenic Diet.* Circulation Research, 1999. **84**(3): p. 345-351.
560. Wong, C.W., T. Christen, I. Roth, C.E. Chadjichristos, J.-P. Derouette, B.F. Foglia, M. Chanson, D.A. Goodenough, and B.R. Kwak, *Connexin37 protects against atherosclerosis by regulating monocyte adhesion.* Nat Med, 2006. **12**(8): p. 950-954.
561. Van Lenten, B.J., S.Y. Hama, F.C. de Beer, D.M. Stafforini, T.M. McIntyre, S.M. Prescott, B.N. La Du, A.M. Fogelman, and M. Navab, *Anti-inflammatory HDL becomes pro-*

inflammatory during the acute phase response. Loss of protective effect of HDL against LDL oxidation in aortic wall cell cocultures. J Clin Invest, 1995. **96**(6): p. 2758-67.

562. Ansell, B.J., M. Navab, S. Hama, N. Kamranpour, G. Fonarow, G. Hough, S. Rahmani, R. Mottahedeh, R. Dave, S.T. Reddy, and A.M. Fogelman, *Inflammatory/antiinflammatory properties of high-density lipoprotein distinguish patients from control subjects better than high-density lipoprotein cholesterol levels and are favorably affected by simvastatin treatment.* Circulation, 2003. **108**(22): p. 2751-6.
563. Tacer, K.F., D. Kuzman, M. Seliškar, D. Pompon, and D. Rozman, *TNF-α interferes with lipid homeostasis and activates acute and proatherogenic processes.* Physiological Genomics, 2007. **31**(2): p. 216-227.
564. Brånén, L., L. Hovgaard, M. Nitulescu, E. Bengtsson, J. Nilsson, and S. Jovinge, *Inhibition of Tumor Necrosis Factor-α Reduces Atherosclerosis in Apolipoprotein E Knockout Mice.* Arteriosclerosis, Thrombosis, and Vascular Biology, 2004. **24**(11): p. 2137-2142.
565. McKellar, G.E., D.W. McCarey, N. Sattar, and I.B. McInnes, *Role for TNF in atherosclerosis? Lessons from autoimmune disease.* Nat Rev Cardiol, 2009. **6**(6): p. 410-417.
566. Bruunsgaard, H., P. Skinhøj, A.N. Pedersen, M. Schroll, and B.K. Pedersen, *Ageing, tumour necrosis factor-alpha (TNF-α) and atherosclerosis.* Clinical & Experimental Immunology, 2000. **121**(2): p. 255-260.
567. Hwang, S.-J., C.M. Ballantyne, A.R. Sharrett, L.C. Smith, C.E. Davis, A.M. Gotto, and E. Boerwinkle, *Circulating Adhesion Molecules VCAM-1, ICAM-1, and E-selectin in Carotid Atherosclerosis and Incident Coronary Heart Disease Cases: The Atherosclerosis Risk In Communities (ARIC) Study.* Circulation, 1997. **96**(12): p. 4219-4225.
568. Iiyama, K., L. Hajra, M. Iiyama, H. Li, M. DiChiara, B.D. Medoff, and M.I. Cybulsky, *Patterns of vascular cell adhesion molecule-1 and intercellular adhesion molecule-1 expression in rabbit and mouse atherosclerotic lesions and at sites predisposed to lesion formation.* Circ Res, 1999. **85**(2): p. 199-207.
569. Nakashima, Y., E.W. Raines, A.S. Plump, J.L. Breslow, and R. Ross, *Upregulation of VCAM-1 and ICAM-1 at atherosclerosis-prone sites on the endothelium in the ApoE-deficient mouse.* Arterioscler Thromb Vasc Biol, 1998. **18**(5): p. 842-51.
570. Bourdillon, M.C., R.N. Poston, C. Covacho, E. Chignier, G. Bricca, and J.L. McGregor, *ICAM-1 deficiency reduces atherosclerotic lesions in double-knockout mice (ApoE(-/-)/ICAM-1(-/-)) fed a fat or a chow diet.* Arterioscler Thromb Vasc Biol, 2000. **20**(12): p. 2630-5.
571. Cybulsky, M.I., K. Iiyama, H. Li, S. Zhu, M. Chen, M. Iiyama, V. Davis, J.C. Gutierrez-Ramos, P.W. Connelly, and D.S. Milstone, *A major role for VCAM-1, but not ICAM-1, in early atherosclerosis.* J Clin Invest, 2001. **107**(10): p. 1255-62.
572. Rye, K.A. and P.J. Barter, *Cardioprotective functions of HDLs.* J Lipid Res, 2014. **55**(2): p. 168-79.
573. Benvenuti, S., R. Saccardi, P. Luciani, S. Urbani, C. Deledda, I. Cellai, F. Francini, R. Squecco, F. Rosati, G. Danza, S. Gelmini, I. Greeve, M. Rossi, R. Maggi, M. Serio, and A. Peri, *Neuronal differentiation of human mesenchymal stem cells: changes in the expression of the Alzheimer's disease-related gene seladin-1.* Exp Cell Res, 2006. **312**(13): p. 2592-604.
574. Zolotushko, J., H. Flusser, B. Markus, I. Shelef, Y. Langer, M. Heverin, I. Bjorkhem, S. Sivan, and O.S. Birk, *The desmosterolosis phenotype: spasticity, microcephaly and micrognathia with agenesis of corpus callosum and loss of white matter.* Eur J Hum Genet, 2011. **19**(9): p. 942-6.

575. Mirza, R., S. Hayasaka, F. Kambe, K. Maki, T. Kaji, Y. Murata, and H. Seo, *Increased expression of aquaporin-3 in the epidermis of DHCR24 knockout mice.* Br J Dermatol, 2008. **158**(4): p. 679-84.
576. Mirza, R., S. Qiao, Y. Murata, and H. Seo, *Requirement of DHCR24 for postnatal development of epidermis and hair follicles in mice.* Am J Dermatopathol, 2009. **31**(5): p. 446-52.
577. Battista, M.-C., C. Roberge, A. Martinez, and N. Gallo-Payet, *24-Dehydrocholesterol Reductase/Seladin-1: A Key Protein Differentially Involved in Adrenocorticotropin Effects Observed in Human and Rat Adrenal Cortex.* Endocrinology, 2009. **150**(9): p. 4180-4190.
578. Haas, I.G., *BiP (GRP78), an essential hsp70 resident protein in the endoplasmic reticulum.* Experientia, 1994. **50**(11): p. 1012-1020.
579. Akopian, D. and J.D. Medh, *Simultaneous isolation of total cellular lipids and RNA from cultured cells.* BioTechniques, 2006. **41**(4): p. 426-430.
580. Pedretti, A., E. Bocci, R. Maggi, and G. Vistoli, *Homology modelling of human DHCR24 (seladin-1) and analysis of its binding properties through molecular docking and dynamics simulations.* Steroids, 2008. **73**(7): p. 708-19.
581. Zerenturk, E.J., L.J. Sharpe, and A.J. Brown, *DHCR24 associates strongly with the Endoplasmic Reticulum beyond predicted membrane domains: implications for the activities of this multi-functional enzyme.* Biosci Rep, 2014.
582. Olender, E.H. and R.D. Simon, *The intracellular targeting and membrane topology of 3-hydroxy-3-methylglutaryl-CoA reductase.* Journal of Biological Chemistry, 1992. **267**(6): p. 4223-4235.
583. Yoshida, H., T. Matsui, A. Yamamoto, T. Okada, and K. Mori, *XBP1 mRNA Is Induced by ATF6 and Spliced by IRE1 in Response to ER Stress to Produce a Highly Active Transcription Factor.* Cell, 2001. **107**(7): p. 881-891.
584. Lee, K., W. Tirasophon, X. Shen, M. Michalak, R. Prywes, T. Okada, H. Yoshida, K. Mori, and R.J. Kaufman, *IRE1-mediated unconventional mRNA splicing and S2P-mediated ATF6 cleavage merge to regulate XBP1 in signaling the unfolded protein response.* Genes & Development, 2002. **16**(4): p. 452-466.
585. Krogh-Madsen, R., P. Plomgaard, P. Keller, C. Keller, and B.K. Pedersen, *Insulin stimulates interleukin-6 and tumor necrosis factor-alpha gene expression in human subcutaneous adipose tissue.* Am J Physiol Endocrinol Metab, 2004. **286**(2): p. E234-8.
586. Fishel, M.A., G. Watson, T.J. Montine, and et al., *HYperinsulinemia provokes synchronous increases in central inflammation and β-amyloid in normal adults.* Archives of Neurology, 2005. **62**(10): p. 1539-1544.
587. Clark, A., C.A. Wells, I.D. Buley, J.K. Cruickshank, R.I. Vanhegan, D.R. Matthews, G.J. Cooper, R.R. Holman, and R.C. Turner, *Islet amyloid, increased A-cells, reduced B-cells and exocrine fibrosis: quantitative changes in the pancreas in type 2 diabetes.* Diabetes research (Edinburgh, Scotland), 1988. **9**(4): p. 151-159.
588. Maisch, B., P. Alter, and S. Pankuweit, *Diabetic cardiomyopathy--fact or fiction?* Herz, 2011. **36**(2): p. 102-15.
589. Park, E.J., J.H. Lee, G.-Y. Yu, G. He, S.R. Ali, R.G. Holzer, C.H. Österreicher, H. Takahashi, and M. Karin, *Dietary and Genetic Obesity Promote Liver Inflammation and Tumorigenesis by Enhancing IL-6 and TNF Expression.* Cell, 2010. **140**(2): p. 197-208.
590. Kern, P.A., S. Ranganathan, C. Li, L. Wood, and G. Ranganathan, *Adipose tissue tumor necrosis factor and interleukin-6 expression in human obesity and insulin resistance.* Am J Physiol Endocrinol Metab, 2001. **280**(5): p. E745-51.
591. Gastaldelli, A., K. Cusi, M. Pettiti, J. Hardies, Y. Miyazaki, R. Berria, E. Buzzigoli, A.M. Sironi, E. Cersosimo, E. Ferrannini, and R.A. DeFronzo, *Relationship Between*

Hepatic/Visceral Fat and Hepatic Insulin Resistance in Nondiabetic and Type 2 Diabetic Subjects. Gastroenterology, 2007. **133**(2): p. 496-506.

592. Boden, G., P. She, M. Mozzoli, P. Cheung, K. Gumireddy, P. Reddy, X. Xiang, Z. Luo, and N. Ruderman, *Free fatty acids produce insulin resistance and activate the proinflammatory nuclear factor-kappaB pathway in rat liver.* Diabetes, 2005. **54**(12): p. 3458-65.
593. Bulló, M., P. García-Lorda, I. Megias, and J. Salas-Salvadó, *Systemic Inflammation, Adipose Tissue Tumor Necrosis Factor, and Leptin Expression.* Obesity Research, 2003. **11**(4): p. 525-531.
594. Poitou, C., N. Viguerie, R. Cancello, R. De Matteis, S. Cinti, V. Stich, C. Coussieu, E. Gauthier, M. Courtine, J.D. Zucker, G.S. Barsh, W. Saris, P. Bruneval, A. Basdevant, D. Langin, and K. Clément, *Serum amyloid A: production by human white adipocyte and regulation by obesity and nutrition.* Diabetologia, 2005. **48**(3): p. 519-528.
595. Jernås, M., J. Palming, K. Sjöholm, E. Jennische, P.-A. Svensson, B.G. Gabrielsson, M. Levin, A. Sjögren, M. Rudemo, T.C. Lystig, B. Carlsson, L.M.S. Carlsson, and M. Lönn, *Separation of human adipocytes by size: hypertrophic fat cells display distinct gene expression.* The FASEB Journal, 2006. **20**(9): p. 1540-1542.
596. Korenblat, K.M., E. Fabbrini, B.S. Mohammed, and S. Klein, *Liver, Muscle, and Adipose Tissue Insulin Action Is Directly Related to Intrahepatic Triglyceride Content in Obese Subjects.* Gastroenterology, 2008. **134**(5): p. 1369-1375.
597. Pahl, H.L., *Activators and target genes of Rel/NF-kappaB transcription factors.* Oncogene, 1999. **18**(49): p. 6853-66.
598. Oeckinghaus, A. and S. Ghosh, *The NF-kappaB family of transcription factors and its regulation.* Cold Spring Harb Perspect Biol, 2009. **1**(4): p. a000034.
599. Bastard, J.-P., M. Maachi, J.T.v. Nhieu, C. Jardel, E. Bruckert, A. Grimaldi, J.-J. Robert, J. Capeau, and B. Hainque, *Adipose Tissue IL-6 Content Correlates with Resistance to Insulin Activation of Glucose Uptake both in Vivo and in Vitro.* The Journal of Clinical Endocrinology & Metabolism, 2002. **87**(5): p. 2084-2089.
600. von Eckardstein, A., H. Schulte, and G. Assmann, *Risk for diabetes mellitus in middle-aged Caucasian male participants of the PROCAM study: implications for the definition of impaired fasting glucose by the American Diabetes Association. Prospective Cardiovascular Munster.* J Clin Endocrinol Metab, 2000. **85**(9): p. 3101-8.
601. Wilson, P.W., J.B. Meigs, L. Sullivan, C.S. Fox, D.M. Nathan, and R.B. D'Agostino, Sr., *Prediction of incident diabetes mellitus in middle-aged adults: the Framingham Offspring Study.* Arch Intern Med, 2007. **167**(10): p. 1068-74.
602. Montonen, J., D. Drogan, H.G. Joost, H. Boeing, A. Fritsche, E. Schleicher, M.B. Schulze, and T. Pischon, *Estimation of the contribution of biomarkers of different metabolic pathways to risk of type 2 diabetes.* Eur J Epidemiol, 2011. **26**(1): p. 29-38.
603. Abbasi, A., E. Corpeleijn, R.T. Gansevoort, R.O. Gans, H.L. Hillege, R.P. Stolk, G. Navis, S.J. Bakker, and R.P. Dullaart, *Role of HDL cholesterol and estimates of HDL particle composition in future development of type 2 diabetes in the general population: the PREVEND study.* J Clin Endocrinol Metab, 2013. **98**(8): p. E1352-9.
604. Calvo, C., G. Ponsin, and F. Berthezene, *Characterization of the non enzymatic glycation of high density lipoprotein in diabetic patients.* Diabete Metab, 1988. **14**(3): p. 264-9.
605. Matsunaga, T., K. Iguchi, T. Nakajima, I. Koyama, T. Miyazaki, I. Inoue, S.-i. Kawai, S. Katayama, K. Hirano, S. Hokari, and T. Komoda, *Glycated High-Density Lipoprotein Induces Apoptosis of Endothelial Cells via a Mitochondrial Dysfunction.* Biochemical and Biophysical Research Communications, 2001. **287**(3): p. 714-720.

606. Hedrick, C.C., R.S. Thorpe, M.X. Fu, M.C. Harper, J. Yoo, S.M. Kim, H. Wong, and L.A. Peters, *Glycation impairs high-density lipoprotein function.* Diabetologia, 2000. **43**(3): p. 312-320.
607. Williamson, R.T., *On the Treatment of Glycosuria and Diabetes Mellitus with Sodium Salicylate.* British Medical Journal, 1901. **1**(2100): p. 760-762.
608. Chen, M. and R.P. Robertson, *Restoration of the Acute Insulin Response by Sodium Salicylate: A Glucose Dose-related Phenomenon.* Diabetes, 1978. **27**(7): p. 750-756.
609. Baron, S.H., *Salicylates as hypoglycemic agents.* Diabetes Care, 1982. **5**(1): p. 64-71.
610. Kim, J.K., Y.J. Kim, J.J. Fillmore, Y. Chen, I. Moore, J. Lee, M. Yuan, Z.W. Li, M. Karin, P. Perret, S.E. Shoelson, and G.I. Shulman, *Prevention of fat-induced insulin resistance by salicylate.* J Clin Invest, 2001. **108**(3): p. 437-46.
611. Roderick, P.J., H.C. Wilkes, and T.W. Meade, *The gastrointestinal toxicity of aspirin: an overview of randomised controlled trials.* British Journal of Clinical Pharmacology, 1993. **35**(3): p. 219-226.
612. Derry, S. and Y.K. Loke, *Risk of gastrointestinal haemorrhage with long term use of aspirin: meta-analysis.* BMJ, 2000. **321**(7270): p. 1183-1187.
613. Zimmerman, H.J., *EFfects of aspirin and acetaminophen on the liver.* Archives of Internal Medicine, 1981. **141**(3): p. 333-342.
614. Eissele, R., R. GÖKe, S. Willemer, H.P. Harthus, H. Vermeer, R. Arnold, and B. GÖKe, *Glucagon-like peptide-1 cells in the gastrointestinal tract and pancreas of rat, pig and man.* European Journal of Clinical Investigation, 1992. **22**(4): p. 283-291.
615. Fehmann, H.C., R. Goke, and B. Goke, *Cell and molecular biology of the incretin hormones glucagon-like peptide-I and glucose-dependent insulin releasing polypeptide.* Endocr Rev, 1995. **16**(3): p. 390-410.
616. Perfetti, R., J. Zhou, M.E. Doyle, and J.M. Egan, *Glucagon-Like Peptide-1 Induces Cell Proliferation and Pancreatic-Duodenum Homeobox-1 Expression and Increases Endocrine Cell Mass in the Pancreas of Old, Glucose-Intolerant Rats.* Endocrinology, 2000. **141**(12): p. 4600-4605.
617. Drucker, D.J., J.B. Buse, K. Taylor, D.M. Kendall, M. Trautmann, D. Zhuang, L. Porter, and D.-S. Group, *Exenatide once weekly versus twice daily for the treatment of type 2 diabetes: a randomised, open-label, non-inferiority study.* Lancet, 2008. **372**(9645): p. 1240-50.
618. Meier, J.J., *GLP-1 receptor agonists for individualized treatment of type 2 diabetes mellitus.* Nat Rev Endocrinol, 2012. **8**(12): p. 728-42.
619. Cheng, A.Y. and I.G. Fantus, *Oral antihyperglycemic therapy for type 2 diabetes mellitus.* CMAJ, 2005. **172**(2): p. 213-26.
620. Rojas, L.B.A. and M.B. Gomes, *Metformin: an old but still the best treatment for type 2 diabetes.* Diabetology & Metabolic Syndrome, 2013. **5**(1): p. 1-15.
621. Musi, N., M.F. Hirshman, J. Nygren, M. Svanfeldt, P. Bavenholm, O. Rooyackers, G. Zhou, J.M. Williamson, O. Ljunqvist, S. Efendic, D.E. Moller, A. Thorell, and L.J. Goodyear, *Metformin Increases AMP-Activated Protein Kinase Activity in Skeletal Muscle of Subjects With Type 2 Diabetes.* Diabetes, 2002. **51**(7): p. 2074-2081.
622. Sweileh, W.M., *Contraindications to metformin therapy among patients with type 2 diabetes mellitus.* Pharm World Sci, 2007. **29**(6): p. 587-92.
623. Kirpichnikov, D., S.I. McFarlane, and J.R. Sowers, *Metformin: an update.* Ann Intern Med, 2002. **137**(1): p. 25-33.
624. Rotter, V., I. Nagaev, and U. Smith, *Interleukin-6 (IL-6) Induces Insulin Resistance in 3T3-L1 Adipocytes and Is, Like IL-8 and Tumor Necrosis Factor-α, Overexpressed in Human Fat Cells from Insulin-resistant Subjects.* Journal of Biological Chemistry, 2003. **278**(46): p. 45777-45784.

625. Zozulinska, D., A. Majchrzak, M. Sobieska, K. Wiktorowicz, and B. Wierusz-Wysocka, *Serum interleukin-8 level is increased in diabetic patients.* Diabetologia, 1999. **42**(1): p. 117-8.
626. Thornton, A.J., R.M. Strieter, I. Lindley, M. Baggiolini, and S.L. Kunkel, *Cytokine-induced gene expression of a neutrophil chemotactic factor/IL-8 in human hepatocytes.* J Immunol, 1990. **144**(7): p. 2609-13.
627. Osborne Jr, J.C., *[9] Delipidation of plasma lipoproteins*, in *Methods in Enzymology*. 1986, Academic Press. p. 213-222.
628. Cockerill, G.W., M.C. MCDONALD, H. MOTA-FILIPE, S. CUZZOCREA, N.E. MILLER, and C. THIEMERMANN, *High density lipoproteins reduce organ injury and organ dysfunction in a rat model of hemorrhagic shock.* The FASEB Journal, 2001. **15**(11): p. 1941-1952.
629. Hotamisligil, G.S., P. Arner, J.F. Caro, R.L. Atkinson, and B.M. Spiegelman, *Increased adipose tissue expression of tumor necrosis factor-alpha in human obesity and insulin resistance.* J Clin Invest, 1995. **95**(5): p. 2409-15.
630. Dandona, P., R. Weinstock, K. Thusu, E. Abdel-Rahman, A. Aljada, and T. Wadden, *Tumor Necrosis Factor-α in Sera of Obese Patients: Fall with Weight Loss.* The Journal of Clinical Endocrinology & Metabolism, 1998. **83**(8): p. 2907-2910.
631. Kern, P.A., M. Saghizadeh, J.M. Ong, R.J. Bosch, R. Deem, and R.B. Simsolo, *The expression of tumor necrosis factor in human adipose tissue. Regulation by obesity, weight loss, and relationship to lipoprotein lipase.* J Clin Invest, 1995. **95**(5): p. 2111-9.
632. Trøseid, M., K.T. Lappegård, T. Claudi, J.K. Damås, L. Mørkrid, R. Brendberg, and T.E. Mollnes, *Exercise reduces plasma levels of the chemokines MCP-1 and IL-8 in subjects with the metabolic syndrome.* European Heart Journal, 2004. **25**(4): p. 349-355.
633. Nishimura, T., M. Kohara, K. Izumi, Y. Kasama, Y. Hirata, Y. Huang, M. Shuda, C. Mukaidani, T. Takano, Y. Tokunaga, H. Nuriya, M. Satoh, M. Saito, C. Kai, and K. Tsukiyama-Kohara, *Hepatitis C Virus Impairs p53 via Persistent Overexpression of 3β-Hydroxysterol Δ24-Reductase.* Journal of Biological Chemistry, 2009. **284**(52): p. 36442-36452.
634. Takano, T., K. Tsukiyama-Kohara, M. Hayashi, Y. Hirata, M. Satoh, Y. Tokunaga, C. Tateno, Y. Hayashi, T. Hishima, N. Funata, M. Sudoh, and M. Kohara, *Augmentation of DHCR24 expression by hepatitis C virus infection facilitates viral replication in hepatocytes.* J Hepatol, 2011. **55**(3): p. 512-21.
635. Lang, C.H., C. Dobrescu, and G.J. Bagby, *Tumor necrosis factor impairs insulin action on peripheral glucose disposal and hepatic glucose output.* Endocrinology, 1992. **130**(1): p. 43-52.
636. Feinstein, R., H. Kanety, M.Z. Papa, B. Lunenfeld, and A. Karasik, *Tumor necrosis factor-alpha suppresses insulin-induced tyrosine phosphorylation of insulin receptor and its substrates.* J Biol Chem, 1993. **268**(35): p. 26055-8.
637. Rajwa, B., *Image cytometry goes multiphoton.* Cytometry A, 2007. **71**(12): p. 973-5.
638. Rajwa, B., T. Bernas, H. Acker, J. Dobrucki, and J.P. Robinson, *Single- and two-photon spectral imaging of intrinsic fluorescence of transformed human hepatocytes.* Microsc Res Tech, 2007. **70**(10): p. 869-79.
639. Tsutsumi, S., T. Gotoh, W. Tomisato, S. Mima, T. Hoshino, H.J. Hwang, H. Takenaka, T. Tsuchiya, M. Mori, and T. Mizushima, *Endoplasmic reticulum stress response is involved in nonsteroidal anti-inflammatory drug-induced apoptosis.* Cell Death Differ, 2004. **11**(9): p. 1009-1016.
640. Kulms, D., B. Poppelmann, D. Yarosh, T.A. Luger, J. Krutmann, and T. Schwarz, *Nuclear and cell membrane effects contribute independently to the induction of apoptosis in human cells exposed to UVB radiation.* Proc Natl Acad Sci U S A, 1999. **96**(14): p. 7974-9.

641. Huang, T.T., F.G. Liu, C.F. Wei, C.C. Lu, C.C. Chen, H.C. Lin, D.M. Ojcius, and H.C. Lai, *Activation of multiple apoptotic pathways in human nasopharyngeal carcinoma cells by the prenylated isoflavone, osajin.* PLoS One, 2011. **6**(4): p. e18308.
642. Lunardi, C., M. Dolcino, D. Peterlana, C. Bason, R. Navone, N. Tamassia, E. Tinazzi, R. Beri, R. Corrocher, and A. Puccetti, *Endothelial cells' activation and apoptosis induced by a subset of antibodies against human cytomegalovirus: relevance to the pathogenesis of atherosclerosis.* PLoS One, 2007. **2**(5): p. e473.
643. Van Antwerp, D.J., S.J. Martin, T. Kafri, D.R. Green, and I.M. Verma, *Suppression of TNF-alpha-induced apoptosis by NF-kappaB.* Science, 1996. **274**(5288): p. 787-9.
644. Wiley, S.R., K. Schooley, P.J. Smolak, W.S. Din, C.-P. Huang, J.K. Nicholl, G.R. Sutherland, T.D. Smith, C. Rauch, C.A. Smith, and R.G. Goodwin, *Identification and characterization of a new member of the TNF family that induces apoptosis.* Immunity, 1995. **3**(6): p. 673-682.
645. Powell, E.E., W.G. Cooksley, R. Hanson, J. Searle, J.W. Halliday, and L.W. Powell, *The natural history of nonalcoholic steatohepatitis: a follow-up study of forty-two patients for up to 21 years.* Hepatology, 1990. **11**(1): p. 74-80.
646. Leist, M., F. Gantner, I. Bohlinger, G. Tiegs, P.G. Germann, and A. Wendel, *Tumor necrosis factor-induced hepatocyte apoptosis precedes liver failure in experimental murine shock models.* Am J Pathol, 1995. **146**(5): p. 1220-34.
647. Zerenturk, E.J., I. Kristiana, S. Gill, and A.J. Brown, *The endogenous regulator 24(S),25-epoxycholesterol inhibits cholesterol synthesis at DHCR24 (Seladin-1).* Biochim Biophys Acta, 2012. **1821**(9): p. 1269-77.
648. Li, Y.C., M.J. Park, S.-K. Ye, C.-W. Kim, and Y.-N. Kim, *Elevated Levels of Cholesterol-Rich Lipid Rafts in Cancer Cells Are Correlated with Apoptosis Sensitivity Induced by Cholesterol-Depleting Agents.* The American Journal of Pathology, 2006. **168**(4): p. 1107-1118.
649. Park, E.-K., M.J. Park, S.-H. Lee, Y.C. Li, J. Kim, J.-S. Lee, J.W. Lee, S.-K. Ye, J.-W. Park, C.-W. Kim, B.-K. Park, and Y.-N. Kim, *Cholesterol depletion induces anoikis-like apoptosis via FAK down-regulation and caveolae internalization.* The Journal of Pathology, 2009. **218**(3): p. 337-349.
650. Acquavella, N., M.F. Quiroga, O. Wittig, and J.E. Cardier, *Effect of simvastatin on endothelial cell apoptosis mediated by Fas and TNF-α.* Cytokine, 2010. **49**(1): p. 45-50.
651. Chen, Y., Y. Chen, L. Zhao, Y. Chen, M. Mei, Q. Li, A. Huang, Z. Varghese, J.F. Moorhead, and X.Z. Ruan, *Inflammatory stress exacerbates hepatic cholesterol accumulation via disrupting cellular cholesterol export.* Journal of Gastroenterology and Hepatology, 2012. **27**(5): p. 974-984.
652. Huang, Y.-N., C.-I. Lin, H. Liao, C.-Y. Liu, Y.-H. Chen, W.-C. Chiu, and S.-H. Lin, *Cholesterol overload induces apoptosis in SH-SY5Y human neuroblastoma cells through the up regulation of flotillin-2 in the lipid raft and the activation of BDNF/Trkb signaling.* Neuroscience, 2016. **328**: p. 201-209.
653. Murphy, R.C. and K.M. Johnson, *Cholesterol, Reactive Oxygen Species, and the Formation of Biologically Active Mediators.* Journal of Biological Chemistry, 2008. **283**(23): p. 15521-15525.
654. Cutler, R.G., J. Kelly, K. Storie, W.A. Pedersen, A. Tammara, K. Hatanpaa, J.C. Troncoso, and M.P. Mattson, *Involvement of oxidative stress-induced abnormalities in ceramide and cholesterol metabolism in brain aging and Alzheimer's disease.* Proc Natl Acad Sci U S A, 2004. **101**(7): p. 2070-5.
655. Muzykantov, V.R., *Drug delivery carriers on the fringes: natural red blood cells versus synthetic multilayered capsules.* Expert Opin Drug Deliv, 2013. **10**(1): p. 1-4.

656. Descamps, D. and K. Benihoud, *Two key challenges for effective adenovirus-mediated liver gene therapy: innate immune responses and hepatocyte-specific transduction.* Curr Gene Ther, 2009. **9**(2): p. 115-27.